

**Understanding how Changes in Operation and Design of Urban (Waste)Water
Infrastructure may Impact Connected Microbiomes and Public Health**

by

Isaiah Michael Spencer-Williams, ENV. SP

Bachelor of Science, Civil Engineering, University of Pittsburgh, 2019

Master of Science, Civil Engineering, University of Pittsburgh, 2022

Submitted to the Graduate Faculty of the
Swanson School of Engineering in partial fulfillment
of the requirements for the degree of
Doctor of Philosophy

University of Pittsburgh

2024

UNIVERSITY OF PITTSBURGH
SWANSON SCHOOL OF ENGINEERING

This dissertation was presented

by

Isaiah Michael Spencer-Williams, ENV. SP

It was defended on

February 28, 2024

and approved by

Dr. Leonard Casson, PE, ENV. SP, Associate Professor, Civil and Environmental Engineering

Dr. Carla Ng, Associate Professor, Civil and Environmental Engineering

Dr. Kerry Hamilton, Assistant Professor, School of Sustainable Engineering and the Built Environment, Arizona State University

Dissertation Director: Dr. Sarah Haig, Assistant Professor, Civil and Environmental Engineering

Copyright © by Isaiah Michael Spencer-Williams, ENV SP

2024

Understanding how Changes in Operation and Design of Urban (Waste)Water Infrastructure may Impact Connected Microbiomes and Public Health

Isaiah Spencer-Williams, PhD

University of Pittsburgh, 2024

Water safety and demand are defining issues of our time. Globally, population and water demand are continuously growing at a rate which will strain our current urban water systems¹⁻³. As such, it is imperative that our urban water resources are engineered to meet our growing needs. While necessary for the continued protection of urban water sources, current policy and water treatment systems are focused on monitoring traditional chemical contaminants (e.g., lead) or microorganisms linked to fecal contamination (e.g., *Escherichia coli*) with limited consideration of other potential threats to our water systems. As a result, emerging threats such as drinking water-associated pathogens that cause infection in immunocompromised individuals (DWPIs) which cost the economy billions of dollars annually are often addressed reactively or put on watch lists to be possibly regulated much later (i.e., United States Environmental Protection Agency's Contaminant Candidate Lists). As such, more holistic evaluations of water management – both on the operation and design fronts – are required to revitalize our aging water infrastructure and prepare it for the coming challenges. Starting with wastewater treatment, I evaluated the disinfection efficacy of a more sustainable disinfectant on standard fecal contamination indicator organisms. Secondly, I examined the impacts that changes in Pittsburgh's drinking water distribution system lead corrosion control procedure have on the microbial ecology and DWPI concentrations in hydrologically connected urban streams and in the distribution pipes to determine if public or environmental health impacts occurred due to operational changes. Finally, at the resident level, I identified and assessed the potential risks for gastrointestinal and pulmonary infection from

basement floodwaters, while also exploring implicit racial biases in the location and design of household water infrastructure. Furthermore, considering that household water infrastructure and climate change impacts can influence indoor air quality of confined spaces (e.g., basements), I also modeled resident exposures to common indoor air pollutants in basements that are often impacted by climate change, but rarely explored. Overall, this body of work provides water utilities, public health practitioners and consumers with tangible information that will inform future operational and design choices in our urban water systems, ensuring continued public and environmental health protection as water demand and climate change impacts continue to increase.

Table of Contents

Acknowledgements	xxiv
List of Abbreviations	xxvii
1.0 Introduction.....	1
1.1 Motivation and Scientific Significance	1
1.2 Urban Wastewater Treatment and Management Challenges.....	2
1.3 Urban Drinking Water Treatment and Management Challenges.....	3
1.4 Urban Stormwater Treatment, Management, and Climate Challenges	4
1.5 Thesis Objectives and Hypotheses	5
2.0 Specific Aim 1.0: Assessment of On-Site Generated Peracetic Acid Antimicrobial	
Efficacy in Urban Wastewaters	9
2.1 Introduction	10
2.2 Research Approach	15
2.2.1 Sample Collection.....	15
2.2.2 Water Quality Analysis.....	15
2.2.3 PAA Preparation.....	16
2.2.4 Disinfection Efficacy Experimentation	16
2.2.5 Statistical Analyses.....	17
2.3 Results and Discussion	18
2.3.1 TAED-PAA Efficacy in Urban Wastewaters (Plants A–E).....	18
2.3.2 Comparison of TAED-PAA and Commercial PAA Disinfection Efficacy	
(Plants D–F)	19

2.3.3 TAED-PAA Impacts on Water Quality	21
2.4 Conclusions	24
3.0 Specific Aim 2.0: Examination of the Impacts of Distribution System Phosphate Addition on the Microbial Ecology of Hydrologically Connected Local Urban Streams.....	27
3.1 Introduction	29
3.2 Research Approach	31
3.2.1 Sample Collection.....	31
3.2.2 Water Chemistry Analyses.....	33
3.2.3 Nutrient Addition Bioassay	33
3.2.4 Molecular Analyses	34
3.2.4.1 Droplet Digital PCR	34
3.2.4.2 16S rRNA Amplicon Sequencing	35
3.2.4.3 Phenotypic Prediction using BugBase	35
3.2.5 Statistical Analyses.....	36
3.3 Results and Discussion	37
3.3.1 Impacts of PO ₄ ³⁻ Addition on Urban Stream Phosphorus and Nitrogen Concentrations	37
3.3.2 Impacts of PO ₄ ³⁻ Addition on Urban Stream Microbial Community Composition.....	39
3.3.2.1 Non-Metric Multidimensional Scaling Analysis	39
3.3.2.2 Alpha Diversity and Relative Abundance Analysis.....	40
3.3.2.3 Absolute Abundance Analysis	46

3.3.2.4 Impacts of Environmental Parameters on Urban Stream Microbial Community Composition	47
3.3.3 Predicted Impacts of PO ₄ ³⁻ Addition on Urban Stream Microbial Function	49
3.3.3.1 Default Phenotypes	49
3.3.3.2 Phosphorus Related Functional Traits	49
3.3.3.3 Nitrogen Related Functional Traits	51
3.4 Conclusions	52
4.0 Specific Aim 3.0: Examination of the Impacts of Drinking Water Distribution System Phosphate Corrosion Control Addition on the Distribution System Microbiome.....	54
4.1 Introduction	55
4.2 Research Approach	58
4.2.1 Sample Information and Orthophosphate Addition Details.....	58
4.2.2 Sample Collection.....	59
4.2.3 Water Quality	60
4.2.4 Microbial Analyses.....	60
4.2.4.1 Droplet Digital PCR	60
4.2.4.2 16S rRNA Amplicon Sequencing	61
4.2.4.3 Bench-Scale NTM Reactor Experiments.....	61
4.2.4.4 NTM Aggregation Assays	62
4.2.5 Statistical Analyses.....	62
4.3 Results and Discussion	64

4.3.1 Impacts of PO ₄ ³⁻ Addition on DWDS Microbial Community Composition	64
4.3.1.1 Non-Metric Multidimensional Scaling Analysis	64
4.3.1.2 Alpha Diversity and Relative Abundance Analysis	65
4.3.1.3 Impacts of Environmental Parameters	69
4.3.2 Predicted Impacts of PO ₄ ³⁻ Addition on DWDS Microbial Function	70
4.3.2.1 Default phenotypes	70
4.3.2.2 Phosphate utilization phenotypes	72
4.3.2.3 Nitrogen utilization phenotypes	73
4.3.3 Impacts of PO ₄ ³⁻ on Bacterial density and DWPI density	74
4.3.4 Impacts of PO ₄ ³⁻ on NTM growth and aggregation potential	78
4.4 Conclusions	84
5.0 Specific Aim 4.0: Identification of Basement Floodwater Source and the Links to	
Resident Health	85
5.1 Introduction	86
5.2 Research Approach	89
5.2.1 Participant Recruitment and Survey Data Collection	89
5.2.2 Sample Collection	89
5.2.3 Water Quality	90
5.2.4 Microbial Analyses	91
5.2.4.1 Fecal Coliform Analysis	91
5.2.4.2 Droplet Digital PCR	91
5.3 Results and Discussion	92
5.3.1 Assessment of Racial Disparities through County Health Data	92

5.3.2 Absolute Abundance and Coliform Analysis.....	95
5.3.3 Lessons Learned and Future Considerations.....	99
5.3.3.1 Resident Participation and Recruitment.....	99
5.3.3.2 Sample Collection	100
5.4 Expected Results and Preliminary Conclusions	101
6.0 Specific Aim 5.0: Development of a Basement Indoor Air Quality Modeling Tool	
to Assess Physical, Chemical, and Biological Contaminant Pollution Exposure	102
6.1 Introduction	103
6.2 Research Approach	106
6.2.1 Physical, Chemical, and Biological Pollutant Selection.....	106
6.2.2 CONTAM Multizone IAQ Modeling Overview and Residential Building	
Model.....	107
6.2.2.1 Residential Building Model.....	108
6.2.2.2 Occupancy Schedule and Simulated Scenarios.....	111
6.2.2.3 Contaminant and Exposure Modeling.....	111
6.2.3 Exposure Potential Matrix	112
6.2.4 Statistical Analysis of Exposure Data from CONTAM.....	115
6.3 Results and Discussion	115
6.3.1 Relative Exposure Calculation of Scenarios.....	115
6.3.2 Occupancy Exposure Results for Scenarios	118
6.3.3 Future Considerations and Limitations.....	124
6.4 Conclusions	127
7.0 Concluding Remarks and Recommendations to Stakeholders.....	128

Appendix A Aim 1.0 Supplementary Information	131
Appendix A.1 TAED-PAA Synthesis Information	131
Appendix A.2 Water Quality Figures and Tables	133
Appendix B Aim 2.0 Supplementary Information.....	137
Appendix C Aim 3.0 Supplementary Information	150
Appendix D Aim 4.0 Supplementary Information	161
Appendix E Aim 5.0 Supplementary Information.....	165
8.0 Bibliography	169

List of Tables

Table 1: WWTP locations, Treatment trains, and Plant capacity 15

Table 2: Urban Stream Population Density and Land Development Type..... 32

**Table 3: Urban Stream Nutrient Limitations Before and After PO₄³⁻ Addition into the DWDS
..... 38**

**Table 4: Urban Stream alpha diversity indices before and after PO₄³⁻ addition into the
DWDS..... 41**

**Table 5: Linear effect model for the stream community composition (OTUs) using all the
stream water samples collected (n = 85) over the course of one year 48**

**Table 6: Linear effect models for the whole distribution system community composition, and
absolute density of NTM and *L. pneumophila* using all the distribution system water
samples collected (n=98) over the course of one year 70**

**Table 7: 2016-2018 Incidence of Notifiable non-foodborne GI infection caused by
Cryptosporidium, *Campylobacter*, and *Salmonella* in the City of Pittsburgh 94**

Table 8: Relative Exposure Value (REV) questionnaire..... 114

Table 9: Relative Exposure Value (REV) Bin Sizing..... 115

**Table 10: Total mass of pollutant inhaled per week while in the basement in each scenario
..... 121**

**Appendix A Table 1: Average ± s.d. water quality parameters pre- & post- conventional Ct
PAA treatment 136**

**Appendix A Table 2: Average ± s.d. water quality parameters pre- & post- integral Ct PAA
treatment..... 136**

Appendix B Table 1: Different water quality parameters measured in this study and the method / apparatus	145
Appendix B Table 2: Average \pm standard deviation (s.d.) measured water quality parameters before and after full-scale PO_4^{3-} addition into the DWDS. Dissolved concentrations are in parentheses.	145
Appendix B Table 3: ddPCR target genes, amplicon size, annealing temperature, and primer sequences.....	146
Appendix B Table 4: ddPCR reaction conditions.....	146
Appendix B Table 5: ddPCR assay thresholds, LOD, and LOQ	146
Appendix B Table 6: Module list of functional traits relating to phosphate or nitrogen metabolism.....	147
Appendix B Table 7: Significant responses ($p < 0.05$) of green algae and Cyanobacteria biomass to various nutrient treatments (N as mg N/L and P as mg P/L) before PO_4^{3-} addition, two months, and twelve months after PO_4^{3-} addition in S1	147
Appendix B Table 8: Significant responses ($p < 0.05$) of green algae and Cyanobacteria biomass to various nutrient treatments (N as mg N/L and P as mg P/L) before PO_4^{3-} addition, two months, and twelve months after PO_4^{3-} addition in S2	148
Appendix B Table 9: Significant responses ($p < 0.05$) of green algae and Cyanobacteria biomass to various nutrient treatments (N as mg N/L and P as mg P/L) before PO_4^{3-} addition, two months, and twelve months after PO_4^{3-} addition in S3	148
Appendix B Table 10: Significant responses ($p < 0.05$) of green algae and Cyanobacteria biomass to various nutrient treatments (N as mg N/L and P as mg P/L) before PO_4^{3-} addition, two months, and twelve months after PO_4^{3-} addition in S4	148

Appendix B Table 11: Significant responses ($p < 0.05$) of green algae and Cyanobacteria biomass to various nutrient treatments (N as mg N/L and P as mg P/L) before PO_4^{3-} addition, two months, and twelve months after PO_4^{3-} addition in S5 149

Appendix B Table 12: Significant responses ($p < 0.05$) of green algae and Cyanobacteria biomass to various nutrient treatments (N as mg N/L and P as mg P/L) before PO_4^{3-} addition, two months, and twelve months after PO_4^{3-} addition in tap water (DWDS) 149

Appendix B Table 13: Urban stream TN:TP ratios before and one year after PO_4^{3-} addition into the DWDS..... 149

Appendix C Table 1: Different water quality parameters measured in this study and the method / apparatus used 157

Appendix C Table 2: Average \pm standard deviation (s.d.) measured water quality parameters before and after full-scale PO_4^{3-} addition into the DWDS. Dissolved concentrations are in parentheses. 157

Appendix C Table 3: ddPCR target genes, amplicon size, annealing temperature, and primer sequences..... 158

Appendix C Table 4: ddPCR reaction conditions..... 159

Appendix C Table 5: ddPCR assay thresholds, LOD, and LOQ 160

Appendix D Table 1: Different water quality parameters measured in this study and the method / apparatus used 162

Appendix D Table 2: ddPCR target genes, amplicon size, annealing temperature, and primer sequences..... 162

Appendix D Table 3: ddPCR reaction conditions..... 163

Appendix D Table 4: ddPCR assay thresholds, LOD, and LOQ	164
Appendix E Table 1: Assumed residential structure airflow path leakage areas used in CONTAM model from ASHRAE 62.1.....	165
Appendix E Table 2: Zone design air supply rates.....	165
Appendix E Table 3: Adult occupancy schedule used in the CONTAM simulation for all case scenarios.....	166
Appendix E Table 4: Child occupancy schedule used in the CONTAM simulation for all case scenarios.....	167
Appendix E Table 5: Assumed Ambient and starting zone pollutant concentrations or mass flow rate	168
Appendix E Table 6: Age-based intake factors for children ages 0 – 18 years	168
Appendix E Table 7: Activity-based intake factors from Pleil et al. 2021.....	168

List of Figures

Figure 1: The urban water cycle as mapped to Thesis Specific Aims.....	6
Figure 2: Global PAA Usage in 2022 from Market.US	12
Figure 3: Simulated representation of the a) single point (conventional) and b) integral Ct approaches in wastewater disinfection. The line represents the residual concentration of the disinfectant, and the shaded regions represent the Ct achieved under each Ct approach.	14
Figure 4: Average (n = 9) ± standard deviation a) total coliform and b) <i>E. coli</i> log reductions after TAED-PAA application across five urban WWTPs.....	19
Figure 5: Average (n = 9) total coliform log reductions after PAA application across WWTPs under a) single point residual and b) integral Ct approach. * designates a statistically significant (p-value < 0.05) difference in log reductions between TAED-PAA and Commercial PAA.	21
Figure 6: Map of Urban Stream (green) and Distribution System (blue) sampling locations for Aims 2 and 3. Five urban streams and seven distribution system sites were sampled for the work presented in Objectives #2 and #3.....	32
Figure 7: Average (n = 15) total phosphorus concentration in each urban stream before and after PO₄³⁻ addition into the DWDS. Error bars represent the standard deviation. Significant differences (p-value < 0.05) in concentration are indicated by an asterisk.	39
Figure 8: Nonmetric Multi-Dimensional Scaling plots of Bray-Curtis distances for the five urban stream sites sampled (a) seasonally and (b) before and after PO₄³⁻ corrosion	

control addition. The ellipses represent the 95% confidence interval of the distribution from the centroid of the cluster points..... 40

Figure 9: Top 10 most abundant phyla in all five urban streams before and after PO₄³⁻ addition in the distribution system. Proteobacteria dominated the urban stream microbial communities under both conditions. Significant differences (p-value < 0.05) in phyla after PO₄³⁻ addition in the DWDS are indicated by an asterisk. 42

Figure 10: Total bacteria absolute density in urban streams before and after PO₄³⁻ addition into the DWDS. No significant differences were observed in any stream after PO₄³⁻ addition. 47

Figure 11: Predicted relative abundance of phosphorus- and nitrogen-related phenotypes in urban streams before and after PO₄³⁻ addition into the DWDS. Predicted significant differences in bacterial two-component regulatory systems and nitrogen fixation were observed across three of the five urban streams examined (*, P < 0.05; **, P < 0.01). 50

Figure 12: Non-metric Multi-Dimensional Scaling plots for all DS samples separated by a) season and b) orthophosphate addition into the DS (stress values = 0.26). 65

Figure 13: a) Top 10 most abundant phyla and b) top 10 most abundant genera across all DWDS sites before and 1-year after full-scale PO₄³⁻ addition (n = 14 in each condition). 67

Figure 14: Significant changes in predicted relative abundance of default phenotypes at sites 710 and 773 in the DWDS, significant difference at a p-value < 0.05 are denoted by * 72

Figure 15: Predicted relative abundance of phosphorus & nitrogen related phenotypes in the DWDS, significant difference at a p-value < 0.001 are denoted by * 74**

Figure 16: a) Geometric average (n = 14) of absolute density of DWPIs, total bacteria, *Cyanobacteria*, and *C. Accumulibacter* in the DWDS before and one year after PO₄³⁻ addition. Error bars represent the standard deviation. * signifies a significant difference in measured density at p-value < 0.001. b) Boxplot of NTM absolute density at each DWDS site before and one-year after PO₄³⁻ addition. 75**

Figure 17: a) ATP, b) absolute NTM density and c) total bacterial density in the DWDS throughout the study duration and comparison three years later. 78

Figure 18: Planktonic vs aggregate NTM ratios (ranges in parentheses) for *M. smegmatis* (0 – 245) and *M. abcessus* (0 – 122) at different concentrations of phosphate (each tile is one technical replicate, for a total of n = 9 per species x phosphate concentration x time)..... 81

Figure 19: Average fecal coliform concentration from PA WWTPs in Specific Aim 1.0 and the stormwater samples (n = 2) collected for this study. 96

Figure 20: Boxplots of the log₁₀ transformed viable total bacteria, *L. pneumophila*, NTM, *P. aeruginosa*, *S. enterica*, and norovirus absolute gene copies within bio-respirable aerosols (< 5µm) that could be inhaled during a 10 minute laundry event (n = 5 homes). Samples with no detects had their densities set at half of the limit of detection for the assay prior to normalization. Absolute densities (calculated originally as gene copies / L of air) were normalized to an average time of 10 minutes per visit to the basement to do something like laundry. The average daily inhalation rate of a woman

was used to calculate how much air would be inhaled during 10 minutes due to all the residents I samples from being Black women. 98

Figure 21: Single family residence modeled in CONTAM. The modeled residence was a one—story home with a subgrade basement that is used for laundry (control case scenario) and for a variety of other activities (test case scenarios). 109

Figure 22: Relative Exposure Values (REVs) for each simulated scenario. The REV was calculated using the questionnaire presented in Table 8 and the activity and age of the occupant used in the simulation. 116

Figure 23: Percent contribution to average weekly exposure from the basement, living room, and other spaces in the home for the three pollutants examined under each scenario (a: Control, b: Home Office, c: Home Gym, d: Den / Play room). 119

Figure 24: Average \pm stadard deveiation weekly (n = 7) basement and whole home exposure concentrations to a) radon, b) PM2.5, and c) mold spores for each scenario. Significant differences were observed for all three pollutants between the control and each test scenario, while only a difference in whole home radon exposure was observed (due to basement contributions). * signifies a significant difference at <0.05 p-value and ** signifies a significant difference at a p-value < 0.01. 123

Appendix A Figure 1: TAED-PAA production schematic (provided by Lubrizol)..... 131

Appendix A Figure 2: Average (n = 9) a) total coliform and b) *E. coli* counts before and after TAED-PAA treatment for plants A – E..... 133

Appendix A Figure 3: Conventional Ct average (n = 9) a) TAED-PAA treated total coliform, b) TAED-PAA treated *E. coli*, c) Commercial PAA treated total coliform, d)

Commercial PAA treated <i>E. coli</i> counts before and after treatment; e) <i>E. coli</i> log10 reductions under both PAA treatments.....	134
Appendix A Figure 4: Integral Ct average (n = 9) a) TAED-PAA treated total coliform, b) TAED-PAA treated <i>E. coli</i>, c) Commercial PAA treated total coliform, d) Commercial PAA treated <i>E. coli</i> counts before and after treatment; e) <i>E. coli</i> log10 reductions under both PAA treatments.....	134
Appendix A Figure 5: Average (n = 3) total transition metal concentrations with standard deviation before and after PAA application under conventional Ct approach. a) total copper, b) total iron, and c) total manganese across the three plants studied in section 2.3.2.....	135
Appendix A Figure 6: Average (n = 3) total transition metal concentrations with standard deviation before and after PAA application under integral Ct approach. a) total copper, b) total iron, and c) total manganese across the three plants studied in section 2.3.2.....	135
Appendix B Figure 1: Average (n = 15) total nitrogen concentration in each urban stream before and after PO₄³⁻ addition into the DWDS. Error bars represent the standard deviation.....	137
Appendix B Figure 2: Average (n = 15) total nitrogen concentration in each urban stream before and after PO₄³⁻ addition into the DWDS. Error bars represent the standard deviation.....	138
Appendix B Figure 3: Nonmetric multidimensional scaling (NMDS) plots of Bray-Curtis distances for the five urban stream sites sampled. The ellipses represent the 95% confidence interval of the distribution from the centroid of the cluster points.	139

Appendix B Figure 4: Top 10 most abundant phyla in urban streams a) S1, b) S3, and c) S5 before and after PO₄³⁻ addition in the distribution system. 140

Appendix B Figure 5: Top 10 most abundant phyla in urban streams a) S2 and b) S4 before and after PO₄³⁻ addition in the distribution system. 140

Appendix B Figure 6: Cyanobacteria absolute abundance in urban streams before and after PO₄³⁻ addition into the DWDS . No significant differences were observed in any stream after PO₄³⁻ addition. 141

Appendix B Figure 7: *Candidatus Accumulibacter* absolute abundance in urban streams before and after PO₄³⁻ addition into the DWDS . No significant differences were observed in any stream after PO₄³⁻ addition. 141

Appendix B Figure 8: Average phosphorus and nitrogen functional trait relative abundance of stream S1 before and after PO₄³⁻ addition into the DWDS. * represents a p-value < 0.05, ** represents a p-value < 0.01..... 142

Appendix B Figure 9: Average phosphorus and nitrogen functional trait relative abundance of stream S2 before and after PO₄³⁻ addition into the DWDS..... 142

Appendix B Figure 10: Average phosphorus and nitrogen functional trait relative abundance of stream S3 before and after PO₄³⁻ addition into the DWDS..... 143

Appendix B Figure 11: Average phosphorus and nitrogen functional trait relative abundance of stream S4 before and after PO₄³⁻ addition into the DWDS. * represents a p-value < 0.05, ** represents a p-value < 0.01..... 143

Appendix B Figure 12: Average phosphorus and nitrogen functional trait relative abundance of stream S5 before and after PO₄³⁻ addition into the DWDS. * represents a p-value < 0.05, ** represents a p-value < 0.01..... 144

Appendix C Figure 1: PO₄³⁻ dosing (left scale, in blue) and water temperature (right scale, in orange) over the duration of the one-year study. Water temperature was averaged between the seven distribution sites and error bars represent the standard deviation. 150

Appendix C Figure 2: (a) Total chlorine, (b) total lead, (c) pH, and (d) PO₄³⁻ concentration across the seven distribution system sites over the duration of the one-year study. 151

Appendix C Figure 3: Average ± standard deviation of absolute density of DWPIs, total bacteria, and Cyanobacteria in the DWDS before (n = 21) and after PO₄³⁻ addition (n = 77). The after category contains data from 9 months of sample collection. 152

Appendix C Figure 4: Ratio of NTM (as measured by the *atpE* gene) to total bacteria (as measured by the 16S rRNA gene) across the seven distribution system sites over the course of the study duration and three years later. 153

Appendix C Figure 5: a) NTM concentration over the batch reactor study duration and b) absolute density of NTM species in batch reactors. 154

Appendix C Figure 6: Average densities of *M. abcessus* and *M. avium* in the DWDS at the time of the significant increase in 2019 155

Appendix C Figure 7: Aggregate fraction of *M. abcessus* cultures suspended in phosphate buffered saline mixed with 6% Tween20. As phosphate level increased, the number of suspended aggregates decreased 155

Appendix C Figure 8: Average (n = 9 for each species, at each timepoint, at each phosphorus concentration) ± standard deviation of planktonic vs aggregate NTM ratios for *M. abcessus* (left), *M. avium* (middle), and *M. smegmatis* (right). 156

Appendix C Figure 9: Planktonic vs aggregate NTM ratios (ranges in parentheses) for *M. avium* (0 – 547) at different concentrations of phosphate (each tile is one technical replicate, for a total of n = 9 per species x phosphate concentration x time). 156

Appendix D Figure 1: Boxplots of the log10 transformed viable total bacteria, *L. pneumophila*, NTM, *P. aeruginosa*, *S. enterica*, and norovirus absolute gene copies within floodwaters. Samples with no detects had their densities set at half of the limit of detection for the assay prior to normalization. 161

Acknowledgements

Thanks, and praise goes out to my God Almighty, without whom my life would not be possible and who has blessed me in unimaginable ways.

The work described herein is a culmination of my time at the University of Pittsburgh and I am grateful for all the support I received along my journey. This body of work would not have been possible without the help of my advisor and mentor, Dr. Sarah Haig. I express my sincerest gratitude for her continued support and guidance throughout this journey. I also would like to thank my committee members Dr. Leonard Casson, Dr. Carla Ng, and Dr. Kerry Hamilton. Thank you all for your feedback, guidance, and insights into my work and for taking the time to be on my committee.

It is with great honor that I express my gratitude to and dedicate this body of work to my communities, of whom I would also be nothing without. Specifically, to my mother, Cecelia Spencer, my sister Trinity Spencer, my late grandparents, Hazel and Alexander Spencer Jr., and the rest of my family for being my biggest cheerleaders and my anchors when I needed support. To Drs. Yvette Moore and Sossena Wood for taking a chance and investing in a young 9th grader with a wild dream to be an engineer and for the family bond we have built over the years. To my entire Investing NOW and Pitt EXCEL families, for showing me what it means to be a competent Black engineer and for molding me into the engineer I am today. To all my friends, namely Trenita Finney, Sarah Pitell, Marinda Taliaferro, Maurice Sturdivant, Samuel Copeland, Malik Roberts, and Jahari Mercer, for walking this journey with me as confidantes. To my art communities, both The Coloured Section Black Artists' Collective and my Twitch Streaming Family, for helping me to explore the use of creativity in my work, for helping me keep an open mindset, and for giving

me an outlet to create outside the confines of the academy. To my late mentor, Natiq Jalil, for showing me what it means to be an indomitable spirit and for encouraging me to always push the boundaries of this world. And to the person who has been there through every up and every down, soon to be Dr. Jessica Vaden, thank you for being there continuously and for walking the journey of the PhD with me. I am appreciative of everyone's contributions in pouring into me as I completed this degree and am happy to share the accomplishment with you all. **WE** did it big, y'all!

I would also like to thank and acknowledge the funding sources and research partners throughout my journey: the National Science Foundation, Lubrizol Home Care Corporation (special shout outs to Dr. Christopher Cypcar and Dr. Allister Theobald), the Pittsburgh Water and Sewer Authority, Black and Veatch (special shout out to Dr. Gary Hunter), the Pittsburgh Center for Healthy Environments and Equity Research, the University of Pittsburgh High-Throughput Cluster Computational Services, the Engineering Office of Diversity at the Swanson School of Engineering and the Pitt STRIVE Program, Women for a Healthy Environment, and the Provost's Dissertation Year Fellowship for Historically Underrepresented Students.

Within the university, I want to thank my support systems: the Investing NOW program, the Pitt EXCEL program, the Pitt STRIVE program, and the Department of Civil and Environmental Engineering. I thank you all for allowing me to make a home here since joining as a high school student in 2011 and for providing me with the resources to become a competent civil and environmental engineer. Specific shoutouts go to: Mr. Darryl Wiley and Dr. Jay Oriola for their efforts in developing and priming me for college during my high school years; Mrs. Yetunde Olaore, Dr. Sylvanus Wosu, and Dr. Steve Abramowitch, for providing a pathway to graduate success from my early undergraduate years; Dr. David Malehorn for all the lab training and

management he did to make my lab work as seamless as possible; Dr. Andrew Bunger for the continual support and inclusion in his research even after I had transitioned into another research field; Ms. Cheryl Morand, Ms. Alysia Grogan, Ms. Kira Duncan, and the rest of the front office staff who make the department run like a well-oiled machine; and all of the students that I have had the pleasure and privilege to tutor, teach, or mentor – you all have taught me valuable lessons that I will carry forward with me in my future endeavors.

List of Abbreviations

ARG - Antibiotic resistance genes

ARB - Antibiotic resistant bacteria

CCA – Canonical Correspondence Analysis

CCL – Contaminant Candidate List

CEC - Contaminants of emerging concern

CNP – Carbon:Nitrogen:Phosphorus

CSO – Combined Sewer Overflow

DBPs – Disinfection By-products

ddPCR – Droplet Digital Polymerase Chain Reaction

DO – Dissolved Oxygen

DWDS – Drinking Water Distribution System

DWPI – Drinking Water-Associated Pathogens that Infect the Immunocompromised

EPA – Environmental Protection Agency

HPCs – Heterotrophic Plate Counts

IAQ – Indoor Air Quality

KEGG – Kyoto Encyclopedia of Genes and Genomes

LSLs – Lead service lines

MGEs – Mobile Genetic Elements

NMDS – Non-metric Multidimensional Scaling

NTM – Nontuberculous Mycobacteria

OTUs – Operational Taxonomic Units

PAA – Peracetic Acid

PO_4^{3-} – Orthophosphate

PVC – Planctomycetes-Verrucomicrobia-Chlamydiae

QMRA - Quantitative microbial risk assessment

TAED – Tetraacetythylenediamine

TAED-PAA – PAA generated from granular TAED and sodium percarbonate

WHE – Women for a Healthy Environment

WWTPs – Wastewater Treatment Plants

1.0 Introduction

1.1 Motivation and Scientific Significance

As the world population continues to grow, so will the number of urban areas and systems needed to sustain our current way of life. Previous work has shown that the continuous urbanization is associated with increased water demand, negative impacts to urban water quality, and increased global demand for access to safe water¹⁻³. Particularly, it has been estimated that the global water demand has increased over 600% in the last century and is set to continue to increase significantly in three primary areas – industry, domestic use, and agriculture⁴. Currently, global water demand in all three areas represents about 4,600 km³ per year with this figure expected to increase by 30% in the next two decades⁵. Combined with an approximate 22 to 32% increase in global population, an increase in deteriorating water quality due to rapid urbanization⁶, and mediocre at best water systems as graded by the American Society of Civil Engineers in the 2021 Infrastructure Report Card⁷, the state of water management, infrastructure and treatment as it currently stands is unequipped to effectively continue to provide both adequate water volume and quality.

Because of the increase in need for access to safe and sustainable water, society has increased the availability and advanced the state of water treatment approaches to help augment existing water supplies to meet global demand. However, despite the growth in innovation and understanding of urban water management, infrastructure, and quality impacts, there are still a plethora of challenges that need to be addressed to ensure public and environmental health. Notably, regulation, policy, and treatment design have historically focused on addressing

widespread physical and chemical contaminants (e.g., lead, disinfection by-products) or microorganisms connected to fecal contamination (e.g., fecal coliforms; despite their limited association with pathogenic presence⁸). While necessary for continued public health protection our historical focus on only “physical-chemical-fecal” contamination in water has limited our view on other potential threats to all our urban water systems (wastewater, drinking water, and storm water), such as contaminants of emerging concern (CECs)⁹⁻¹¹ and drinking water-associated pathogens that cause infection in the immunocompromised or otherwise susceptible individuals (DWPIs) such as *Legionella pneumophila* and nontuberculous mycobacteria (NTM)¹².

1.2 Urban Wastewater Treatment and Management Challenges

With a substantial increase in water demand in the coming decades, there will inevitably be increases in the amount of water that will need to be effectively treated for both discharge into the environment and for domestic use. Additionally, with substantial increases in population, there will also be an increase in the number of inputs into our wastewater streams that will need to be treated. Wastewater compositions are variable based on the location and the activities of the surrounding population, but primarily consist of human waste (e.g., sewage, greywaters from human activities), industrial waste (e.g., heavy metals and dyes from production), and in the case of places with combined sewer systems, stormwater runoff from impermeable surfaces¹³. With a large variation in composition, there are often increased demands for current treatment processes to meet regulatory effluent standards, especially when treatments are not fine-tuned to specific waste streams. Ineffective upstream treatment can cause problems for downstream processes such as disinfection and discharge. Conventional wastewater processes (e.g., disinfection by

chlorination) may not always be sufficient to deal with emerging contaminants, microbiological threats and the factors that surround their proliferation. Recent work has highlighted the increase in emerging threats including the persistence of antibiotic resistance genes (ARGs) and antibiotic resistant bacteria (ARB)¹⁴⁻¹⁶, increased nutrient loadings (primarily from agricultural applications)¹⁷, and most recently the presence of viruses and other microorganisms that have devastating impacts on the public health sector (e.g., COVID-19, norovirus)¹⁸⁻²⁰. Moreover, alongside these emergent threats there is still the ever-present concern of the production of toxic halogenated disinfection by-products (DBPs) from the chlorination of wastewaters and the general concerns with transport and delivery of chlorination. To date, most wastewater treatment plants utilize chlorine, ozone, and ultraviolet (UV) light radiation to disinfect secondary effluents, with chlorine and chlorinated alternatives being the most widely used due to their effectiveness²¹. However, due to increasing regulations surrounding DBP concentrations and other effluent quality concerns, many wastewater systems have focused on utilizing advanced oxidation processes and nutrient removal processes to return permit compliant water back to the environment before further use²². Despite advancements in wastewater treatment, the use of the advanced and innovative techniques is not widespread likely due to concerns of cost, lack of data on efficacy and implementation, and strict regulatory guidelines on wastewater effluents.

1.3 Urban Drinking Water Treatment and Management Challenges

In the drinking water sector, there has been great emphasis on the detection and mitigation of DWPIs and CECs. As such, there has been a recent shift in identifying, assessing, and combatting emerging threats particularly in drinking water distribution systems (DWDS). Most

recently, the United States Environmental Protection Agency (EPA) published contaminant candidate list (CCL) 5 that include contaminants of emerging concern (e.g., per- and polyfluoroalkyl substances, Carbamazepine, Sulfamethoxazole) and microorganisms related to public health outcomes (e.g., *L. pneumophila*, *Mycobacterium avium*, *Pseudomonas aeruginosa*) that are not yet regulated under the Safe Drinking Water Act²³⁻²⁵. Furthermore, work in urban water infrastructure assessment has suggested the need for more holistic evaluations of drinking water management throughout the entire water usage cycle (e.g., treatment, distribution, discharge)²⁶. Specifically, evaluating the impacts of full-scale operational changes in treatment is critical to understanding how downstream microbial communities, and in turn public health, will be affected. Previous works have examined variation in microbial communities in drinking water treatment and drinking water distribution systems (DWDS) across differing treatment regimes²⁷⁻³². However, there are still broad knowledge gaps with respect to the impacts on aquatic microbiomes from operational changes made to address emerging permitting requirements and stricter regulations.

1.4 Urban Stormwater Treatment, Management, and Climate Challenges

In addition to better evaluations of current operational and design choices in the built environment, considerations of how to better manage and handle climate change and its impacts on urban water infrastructure are necessary. Historically, as society has urbanized, thousands of miles of pipes (e.g., concrete, iron, lead) were constructed to transport both waste- and stormwater from urban centers. Due to economic constraints and the state of construction technology at the time, many of these pipe systems were often connected^{33,34}, forming what we know as combined

sewer systems. However, as urbanization and technical advances have increased and changes in climate have become more profound (e.g., increased drought and precipitation events), full-scale system changes have not been made at the same rate causing increased consequences such as flooding and possible exposure to pathogenic organisms from combined sewer overflows. Additionally, in areas where the threat of water scarcity is increasing, there has been a push to capture and use stormwaters as alternate water sources. However, due to a lack of information on the presence and risk from microbial contaminants, stormwater use (both potable and non-potable) has seen limited implementation. Generally, monitoring of stormwater microorganisms includes monitoring for standard fecal indicator bacteria (e.g., *Escherichia coli*), although they do not often correlate well with the presence of pathogens in environmental waters³⁵. Without an understanding of the presence of common stormwater pathogens and mechanisms driving how they proliferate in residences impacted by climate change events (e.g., urban flooding), assessments of exposure cannot be made. Furthermore, when considering the impacts of flooding in the built environment, other factors such as air-exchange rates and relative humidity in buildings must be considered to assess exposure. As such, holistic evaluations of the operational and design parameters associated with stormwater treatment and conveyance and their impacts are imperative to advancing urban water quality and management.

1.5 Thesis Objectives and Hypotheses

Given that increased urbanization will expand the potential for the dissemination of waterborne pathogens in the environments³⁶, there is a need for us to better understand how changes in the built environment impact microorganisms that are relevant to public and

environmental health. Information on the concentrations of pathogenic microorganisms, as well as the impacts on the microbiome from changes in the built environment will be needed for further evaluation and assessment to protect the public and environment alike. Understanding these impacts will allow us to inform current and future design and operational choices (e.g., disinfection methods, corrosion control, etc.) in urban water infrastructure (Figure 1) allowing for proactive rather than reactive management of microbial quality issues. Moreover, understanding how operational and design choices influence water system microbiology enables us to optimize the built environment, enhancing the safety, reliability, and usability of our constrained water resources.

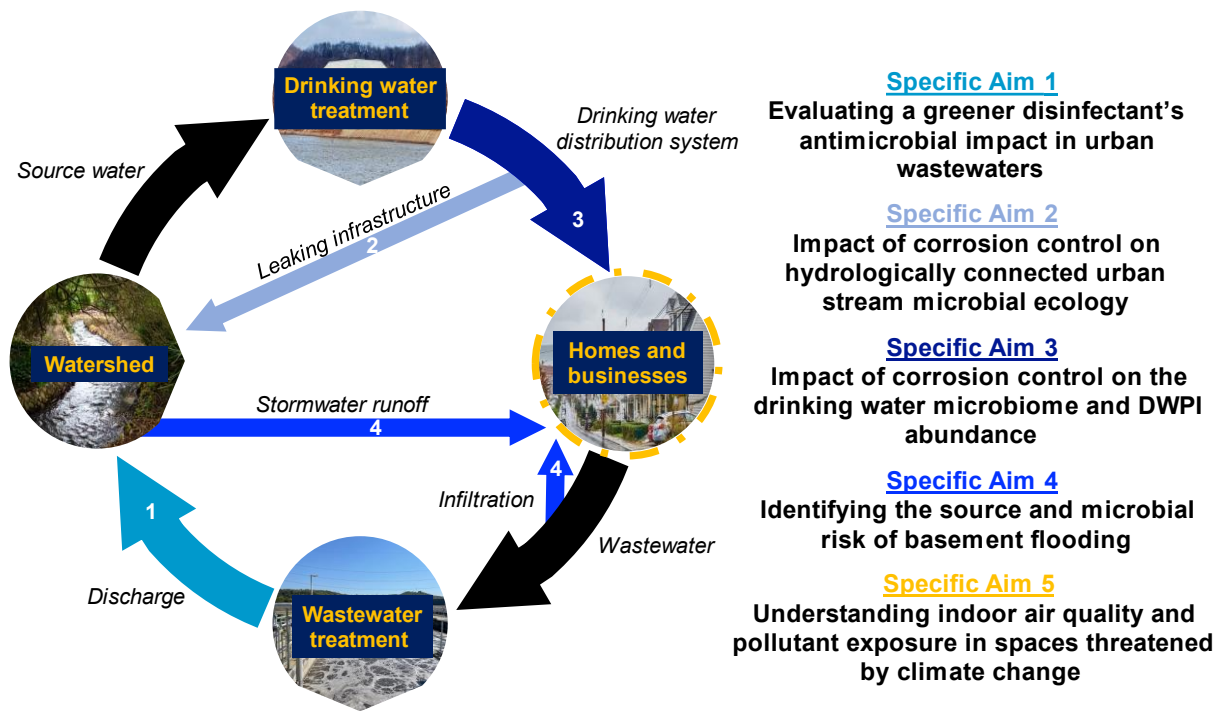


Figure 1: The urban water cycle as mapped to Thesis Specific Aims

The following specific aims were pursued to evaluate and assess the impacts of operational and design changes in urban water infrastructure to provide insight on the impacts to the urban water microbiome:

1. Assess the antimicrobial efficacy of on-site generated peracetic acid (PAA) in urban wastewaters. It was hypothesized that on-site generated PAA would have a comparable antimicrobial efficacy to that of commercially used PAA in wastewater matrices.
2. Examine the impacts of full-scale distribution system orthophosphate addition on the microbial ecology of hydrologically connected urban stream networks. It was hypothesized that the addition of excess orthophosphate into an aging and leaking DWDS would change the microbial community composition and nutrient limitation status of surrounding urban stream networks.
3. Examine the impacts of full-scale distribution system orthophosphate addition on the microbial ecology and abundance of DWPIs in the drinking water distribution system. It was hypothesized that the addition of excess orthophosphate into a phosphorus limited DWDS would change the microbial community composition and increase the density of DWPIs such as NTM, *L. pneumophila*, and *P. aeruginosa* in the drinking water DWDS.
4. Identify and assess the risk of gastrointestinal and pulmonary infection from basement floodwaters. Recent studies have identified stormwater exposure as being associated with an increase in gastrointestinal-infection related hospital visits, however waterborne disease outbreaks are increasingly being attributed to DWPIs without identifying the source of exposure. It was hypothesized that basement

floodwaters (infiltrated stormwaters and sewage backup) was an exposure route to both gastrointestinal (e.g., *Salmonella*, Norovirus) and pulmonary DWPIs.

5. Examine the impacts of pollutant exposure in newly evolving, but often not considered living spaces that are susceptible to climate change. The relationship between water and air is intertwined, with frequent interactions observed between the two. In energy-efficient residences with tight building envelopes, indoor air pollutants can become trapped, leading to elevated concentrations exacerbated by increased moisture infiltration. However, mainstream indoor air quality models typically neglect exposure scenarios occurring in spaces such as basements which are now being used as primary living spaces for various activities and are the first places in a residence to encounter the impacts of climate change (e.g., increased moisture). It was hypothesized that human exposure to pollutants in basements was driven by both the frequency of the occupant activity in the space and the type of activity the occupant performs in the space.

Overall, this body of work assesses changes in the urban water microbiome and potential environmental and public health risks posed by operational and management choices in urban water systems (Figure 1). By examining microbial impacts in multiple water sources (e.g., urban wastewaters, urban streams, DWDS, infiltrated stormwater), more effective design and operational choices can be made to not only preserve the quality of our water, but to also protect the environment and public health better. Understanding the impacts from operational changes will allow water professionals to make more informed and proactive decisions surrounding the design of future treatment schemes, management strategies, and policy or legislation.

2.0 Specific Aim 1.0: Assessment of On-Site Generated Peracetic Acid Antimicrobial Efficacy in Urban Wastewaters

Specific Aim 1.0 was funded by The Lubrizol Corporation, who supplied the tetraacetylenediamine and sodium percarbonate to generate the TAED-PAA and played no role in data collection or interpretation. The results of Specific Aim 1.0 have been published in one journal publication and two conference proceedings. In addition, knowledge gained from this work aided in the creation of a book chapter: Nontraditional Disinfection in Wastewater Treatment Fundamentals III.

Journal Article

Isaiah Spencer-Williams, Allister Theobald, Christopher C. Cypcar, Leonard W. Casson, and Sarah-Jane Haig. (2022). Examining the Antimicrobial Efficacy of Granulated Tetraacetylenediamine Derived Peracetic Acid and Commercial Peracetic Acid in Urban Wastewaters. *Water Environment Research*, 94(2), p.e10688. doi: 10.1002/wer.10688

Book Chapter

Gary Hunter, Leonard Casson, Bernadette Drouhard, **Isaiah Spencer-Williams**. (2022). Nontraditional Disinfection. In Wastewater Treatment Fundamentals III – Advanced Treatment. *Water Environment Federation*, (pp 185 – 203). Virginia.

Peer Reviewer Conference Proceedings

1. **Spencer-Williams, I.**, Theobald, A., Cypcar, C., Casson, L., Haig, S.J. (2020, October 5 - 9). *A Comparative Study on the Antimicrobial Efficacy of Granulated TAED*

(Tetraacetythylenediamine) Derived Peracetic Acid and Commercial Peracetic Acid in Urban Wastewaters. WEFTEC Connect 2020 (Virtual Conference).

2. **Spencer-Williams, I.**, Hunter, G., Theobald, A., Burks, P., Mathews, J., Osta-Ustarroz, P., Hugill, J., Hillock, K.A., Drouhard, B., Casson, L., Haig, S.J. (2019, September 21 – 25). *A New Disinfectant Formulation: Using Granulated TAED Derived Peracetic Acid for Wastewater Disinfection. WEFTEC 2019, Chicago, IL.*

2.1 Introduction

Many wastewater treatment plants (WWTPs) discharge their effluents into the environment via surface waters which may also function as recreational or drinking water sources. As such, the effluents discharged by WWTPs are federally required to be disinfected to reduce microbiological loads³⁷⁻⁴⁰, typically via the use of cost effective powerful disinfectants such as chlorine and chlorinated alternatives^{21,41,42}. However, the use of typical disinfection methods (e.g., chlorination) may produce disinfection by-products (DBPs) that pose carcinogenic and genotoxic environmental concerns (e.g., trihalomethanes, haloacetic acids)⁴³. Due to the health and environmental concerns surrounding DBP production, state and federal regulations mandate the maximum allowable concentrations for these by-products; however, these allowable concentrations continue to decrease, putting pressure on utilities to seek alternative disinfection methodologies that provide low capital and operational costs while ensuring public and environmental safety^{37,43-45}.

Today, there are several emerging alternative disinfectants that are available to disinfect wastewater, however, peracetic acid (PAA) has become more relevant as a wastewater disinfectant

over the last 40 years due to its ease of implementation and relatively low capital costs⁴². Typically sold as a concentrated liquid product, PAA is an organic peroxide that exhibits a wide range of antimicrobial properties, produces limited non-toxic DBPs, and has been widely utilized in a number of industries for sterilization and disinfection⁴⁶⁻⁶⁴ (Figure 2), where it has been effective in reducing fungal and bacterial contamination. Compared with traditional chlorine-containing disinfectants, PAA has a stronger oxidizing ability, higher disinfection efficiency⁶⁵⁻⁶⁷, can directly oxidize organic compounds (e.g., ibuprofen) using its high redox potential^{68,69}, and can also be activated by various methods (e.g., ultraviolet light, transition metal ions) to degrade organic pollutants in urban wastewater⁶⁹⁻⁷². In its municipal wastewater uses, PAA has been used alone and in combination with other water treatment processes (namely UV) to achieve better disinfection efficiency^{73,74}, while it has seen less use in industrial applications likely due to more uniformity in pollutant degradation in low COD waters^{51,75} and the potential for system corrosion with high PAA dosage⁷⁶. Likewise, PAA has seen limited use in drinking water treatment as maintaining a residual for drinking water distribution purposes could be challenging for an exponentially decaying disinfectant. Another reason for PAA's limited use in drinking water is likely due to the potential for enhancing biofilm formation, as biofilms formation can increase in the presence of carboxylic acids (one of the potential PAA DBPs)⁷⁶. However, due to the oxidizing capability of PAA, there has been work done to examine PAA pre-oxidation in chlorinated surface water treatment systems⁷⁷.

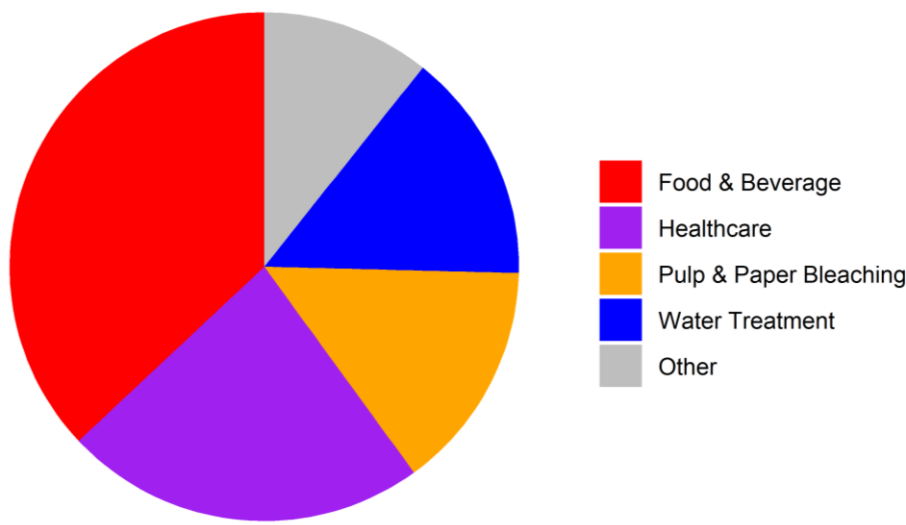


Figure 2: Global PAA Usage in 2022 from Market.US

Despite its use in other sectors and even in the wastewater market, PAA still has been less widely used than common chlorinated options to disinfect wastewater in the United States (~1% of the market in 2020) likely because of physical-chemical constituent interference concerns⁷⁸, implementation and procurement costs, and variability in disinfection permitting requirements for PAA⁴². To address the issue of procurement, it is thought that as PAA usage increases more economical methods of producing and delivering PAA will be explored (i.e., on-site generation). Currently, there are no known WWTPs that produce PAA on-site, likely due to on-site generated PAA stability concerns, and a lack of data on on-site produced PAA disinfection efficacy. As such, it is imperative that on-site generated PAA is examined for differences in disinfection efficacies tested to ensure that adverse changes to microbial loads are not created, thus ensuring public health safety. One method that is under consideration is on-site generation of PAA from granulated tetraacetylenediamine (TAED) and sodium percarbonate (TAED-PAA).

TAED is an important component of laundry and automatic dishwasher detergents, where it is used as an activator for improving bleaching performance when it is reacted with a hydrogen peroxide source in the detergent (Human & Environmental Risk Assessment, 2002). Compared

with commercially available PAA, TAED-PAA generated peracetic acid has a much lower total oxidant concentration (total amount of oxidizing agent in solution i.e., the peracetic acid and hydrogen peroxide level combined). The lower total oxidant concentration is due to the lack of hydrogen peroxide present in solution as it is not needed to stabilize the peracetic acid equilibrium, therefore leading to the needed validation of its performance as a possible wastewater disinfectant. Additionally, traditional comparisons of different disinfectant efficacies are performed by assessing log reductions of fecal water quality indicator organisms with the same disinfectant exposure (disinfectant concentration (C) x time of exposure (t) – Ct). Namely, many practitioners use the conventional end-point disinfectant concentration multiplied by the time of exposure (Figure 3). Unfortunately, this approach may lead to misrepresentations of true Ct values when working with exponentially decaying disinfectants such as PAA (Figure 3). In practice, this may lead to underdosing of PAA, leaving the true dose required to achieve regulatory permits unknown, and ultimately having an impact on operational and capital costs.

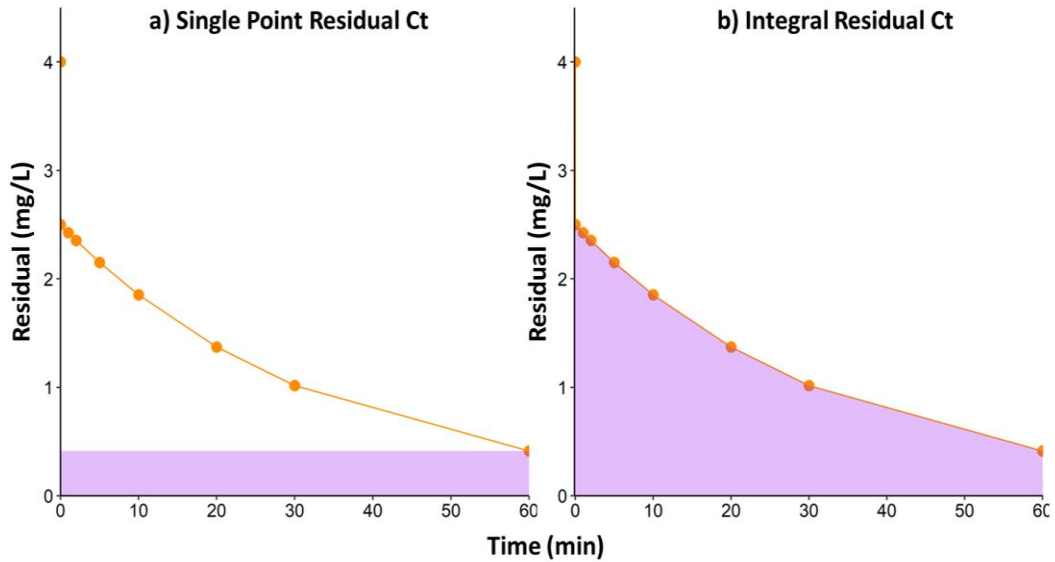


Figure 3: Simulated representation of the a) single point (conventional) and b) integral Ct approaches in wastewater disinfection. The line represents the residual concentration of the disinfectant, and the shaded regions represent the Ct achieved under each Ct approach.

Given the limited used of commercially available PAA as a wastewater disinfectant in the United States likely due to transportation and cost concerns, potential disinfection efficacy interference from physical and chemical parameters, and concerns surrounding misrepresentations of disinfection efficacy, the work done in Specific Aim 1.0 aims to assess the disinfection efficacy of TAED-PAA compared to that of commercially available PAA to ensure no adverse changes to achievable microbial reductions, to identify and confirm the physical and chemical parameters that may interfere with PAA disinfection efficacy, and to compare PAA disinfection efficacy under two distinct Ct approaches in urban wastewater effluents.

2.2 Research Approach

2.2.1 Sample Collection

10 L samples of secondary wastewater effluent (i.e., pre-disinfection) were collected from six wastewater treatment plants with different treatment trains in three different states in the United States of America (Table 1). Once collected, the 10 L samples were stored on ice for up to 24h before being characterized and used in disinfection efficacy experiments.

Table 1: WWTP locations, Treatment trains, and Plant capacity

Plant Name	Plant Location	Treatment Train	Plant Capacity (MGD)
Plant A	KS	Conventional, Trickling Filter	17.0
Plant B	KS	Conventional	1.5
Plant C	MO	Industrial	3.0
Plant D	PA	Activated Sludge	7.0
Plant E	PA	Sequencing Batch Reactor	1
Plant F	PA	Trickling Filter, Nitrification Tower, Anaerobic Digester	4.9

2.2.2 Water Quality Analysis

The water chemistry of all samples was characterized both pre- and post-addition of TAED-PAA and Commercial PAA. Eleven water quality parameters were measured according to standard methods⁷⁹. Temperature and pH were measured using a lab-grade 3-in-1 benchtop pH meter (Fisher Scientific, Waltham, MA, USA). Dissolved oxygen (DO) was measured at both day

zero and day five using a P20 BOD US Pro 20 BOD kit (YSI Inc., Yellow Springs, OH, USA). Total nitrogen and total phosphorous were measured using Test 'N Tube vials (Hach, Loveland, CO, USA) and analyzed using a portable DR900 spectrophotometer (Hach, Loveland, CO, USA). Total and dissolved iron, copper, and manganese concentrations were determined using a Nexion 300x inductively coupled plasma mass spectrometer (PerkinElmer, Waltham, MA, USA) with a limit of detection of 0.002 mg/L for copper and 0.02 mg/L for manganese and iron.

2.2.3 PAA Preparation

A 500 mg/L stock of TAED-PAA (Lubrizol Advanced Materials, Inc, Cleveland, OH, USA) was prepared using granulated TAED and granulated sodium percarbonate with a final pH of 6.0 following Lubrizol laboratory procedures (Appendix A Figure 1) and stored in the dark to prevent light degradation. A 1000 mg/L commercial PAA solution was prepared from an ~15% PAA equilibrium sample (Jet Harvest Solutions, Longwood, FL, USA) on the day the samples were analyzed. Before use in the disinfection efficacy experiments, the concentration of peracetic acid in the TAED-PAA and the commercial PAA stock solutions were measured using the DPD (N,N-diethyl-p-phenylenediamine) colorimetric method for measuring total chlorine in drinking and wastewaters⁸⁰. The final PAA concentration was determined using equation (1-1):

$$\frac{mg}{L} PAA = 1.07 * \frac{mg}{L} Total\ Chlorine * dilution\ factor \quad (1-1)$$

2.2.4 Disinfection Efficacy Experimentation

Wastewater samples from each WWTP (Plants A – E) were treated using the 500 mg/L stock solution of TAED-PAA or the 1000 mg/L stock solution of PAA to achieve a final

concentration 2.5 mg/L PAA for 20 min. (Ct = 50 mg-min/L, not considering PAA demand or decay). For quality assurance, negative controls (no PAA added) were run alongside membrane and media blanks. Both the negative controls and treated samples were diluted using phosphate buffered saline (PBS) (Fisher Scientific, Waltham, MA, USA) and immediately processed using USEPA Method 1604 to determine the concentration of fecal indicator organisms (e.g., *E. coli* and total coliforms)⁸¹. All collected membrane filters were plated on MI agar (Fisher Scientific, Waltham, MA, USA) and incubated for 24 h at 35°C. After 24 h, filters were analyzed under ambient light and 366 nm UV light to differentiate and elicit colonies of *E. coli* and other coliforms.

To evaluate differences in total and fecal coliform removal efficacy between the conventional and integrated Ct approach, experiments were conducted under both conventional and integrated Ct approaches. In the conventional approach, enough PAA was added to each wastewater to achieve a 2.5 mg/L concentration of PAA in solution, not considering demand and decay effects. No further PAA was added during the 20-min experimental period. In the integrated Ct approach, the time (t) until the original dose of PAA was depleted by 40% was calculated using the equation 2 (decay and demand constants were estimated by averaging the range of values from existing literature⁸²) and at that point additional PAA was added to maintain 2.5 mg/L of PAA in each wastewater.

$$\frac{mg}{L} PAA \text{ in } WW = \left(\frac{mg}{L} PAA_0 - D \right) * e^{-kt} \quad (1-2)$$

2.2.5 Statistical Analyses

Significant differences between the log reductions in the control samples, TAED-PAA treated samples, and commercial PAA treated samples under both Ct approaches were determined

using the non-parametric Wilcoxon test. Linear regression models were created to visualize the relationships between the achieved log reductions and the water quality parameters, and MANOVA was used to analyze significance. All statistical analyses and figures were performed and made in R with significance set at a p-value < 0.05.

2.3 Results and Discussion

2.3.1 TAED-PAA Efficacy in Urban Wastewaters (Plants A–E)

Significant differences (p-value < 0.05) in the concentrations of *E. coli* and total coliforms were observed across all samples treated with TAED-PAA. Average reductions across all five WWTPs were 2.1 ± 0.2 log-units and 2.3 ± 0.1 log-units for *E. coli* and total coliforms, respectively (Figure 4). While these results concur with previous studies' success in total coliform and *E. coli* reduction^{46,47,83,84} using commercial PAA, other factors must be considered before a plant would consider switching over to TAED-PAA. Given the increasing need for alternative water sources and innovative water reclamation approaches, the U.S. EPA 2012 Guidelines for Water Reuse state that wastewaters should be disinfected to no detectable fecal coliforms per 100 mL of water for unrestricted usage and less than or equal to 200 fecal coliforms per 100 mL for restricted usages³⁸. Under a 2.5 mg/L TAED-PAA treatment, Plants C and D were unable to reach 200 total coliforms per 100 mL wastewater possibly due to elevated suspended and dissolved solid levels, thus a higher dose of TAED-PAA would be needed to meet regulation (Appendix A Figure 2). Previous studies comment on the impact of elevated suspended and dissolved solid concentrations on PAA disinfection efficacy, showing adverse effects^{85–88}. Overall, across the five urban wastewaters

disinfected, TAED-PAA application did achieve a 2 log-unit reduction for both total coliforms and *E. coli*, making it a viable option for wastewater disinfection that should be fine-tuned for specific applications.

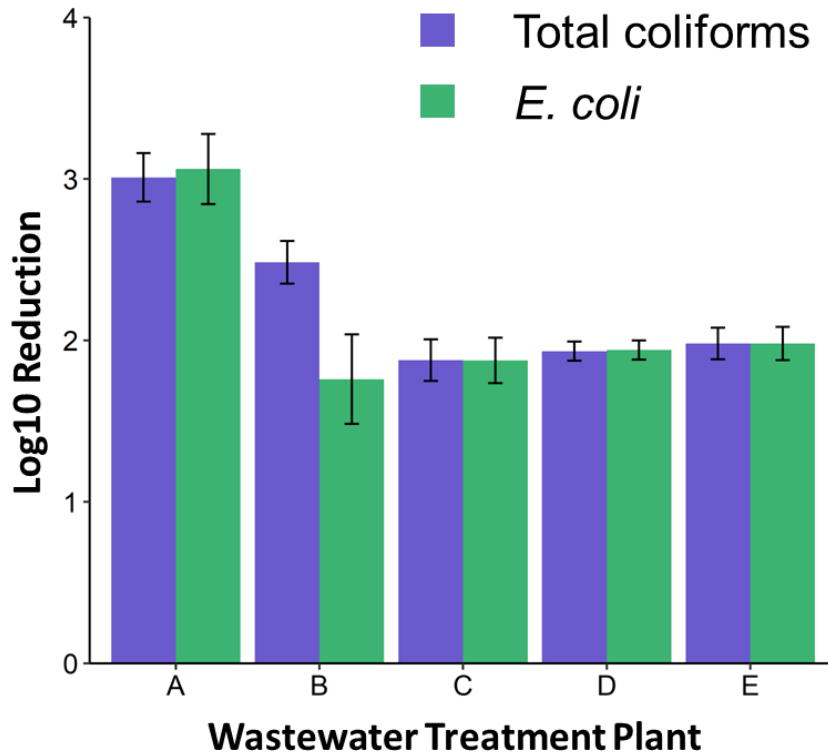


Figure 4: Average ($n = 9$) \pm standard deviation a) total coliform and b) *E. coli* log reductions after TAED-PAA application across five urban WWTPs.

2.3.2 Comparison of TAED-PAA and Commercial PAA Disinfection Efficacy (Plants D–F)

Overall, significant decreases in the concentrations of both *E. coli* and total coliforms were observed in samples treated with TAED-PAA and commercial PAA, respectively. The average *E. coli* log reduction across all three WWTPs were 1.9 ± 0.4 log-units and 2.5 ± 0.6 log units for TAED-PAA and commercial PAA, respectively, while the average total coliform log reductions were calculated to be 2.2 ± 0.5 log-units under both PAA treatments (Appendix A Figure 3).

Individually, disinfection efficacy testing revealed instances where TAED-PAA exhibited higher log removals than the commercial PAA, and vice versa, however only one significant difference was observed between the log removals at Plant D under the conventional Ct approach (Figure 5). Under the integrated Ct approach, significant decreases in both *E. coli* and total coliform concentrations were observed for samples treated with 2.5 mg/L of PAA (either TAED-PAA or Commercial PAA). The average *E. coli* log reductions were 2.5 ± 0.7 and 2.7 ± 0.3 for TAED-PAA and commercial PAA, respectively, while the average total coliform log reductions across all plants were 2.3 ± 0.5 and 2.1 ± 0.2 for TAED-PAA and commercial PAA (Appendix A Figure 4). While an average of at least 2.0 log-unit reduction was achieved under both PAA treatments, it is important to note that no significant differences in performance between the two PAAs were observed in any of the urban wastewater matrices under the integrated Ct approach. However, when comparing the disinfection efficacy between the conventional Ct and the integrated Ct approaches for each disinfectant, significant increases in log reduction were observed for both disinfectants at Plant D. The lack of significant differences in performance could be a factor of PAA-specific and time-dependent demands (D) and decay (k) rates in solution. Both D and k were set at a constant for all wastewaters and were calculated as the average of the range of D and k values found in literature, 0.61 mg/L and 0.00875 min⁻¹, respectively⁸². In practice, mechanistic studies would have to be conducted to properly fit decay and demand coefficients based on each individual wastewater, resulting in a better representation of the true disinfection potential. Under the integrated Ct approach using these values, 0.75 ± 0.76 mL of PAA was added after 14 minutes to experimental reactors to maintain a PAA concentration of 2.5 mg/L. This resulted in a final PAA Ct of 34.67 mg-min /L, as compared to a conventional Ct of 31.73 mg-min/L. The lack of significant differences in disinfection efficacy between the two Ct approaches could also be

explained by the similar Ct, however, it is important to note that this work was done assuming a set value for D and k based off literature. To investigate and better understand the potential impacts D and k have on efficacy further, future work should include conducting mechanistic studies to examine TAED-PAA concentration at different time intervals and properly fit demand and decay coefficients, monitoring TAED-PAA decay and inactivation rate kinetics in solution and should be performed using a continuous stirred-tank reactor to better simulate full-scale operation.

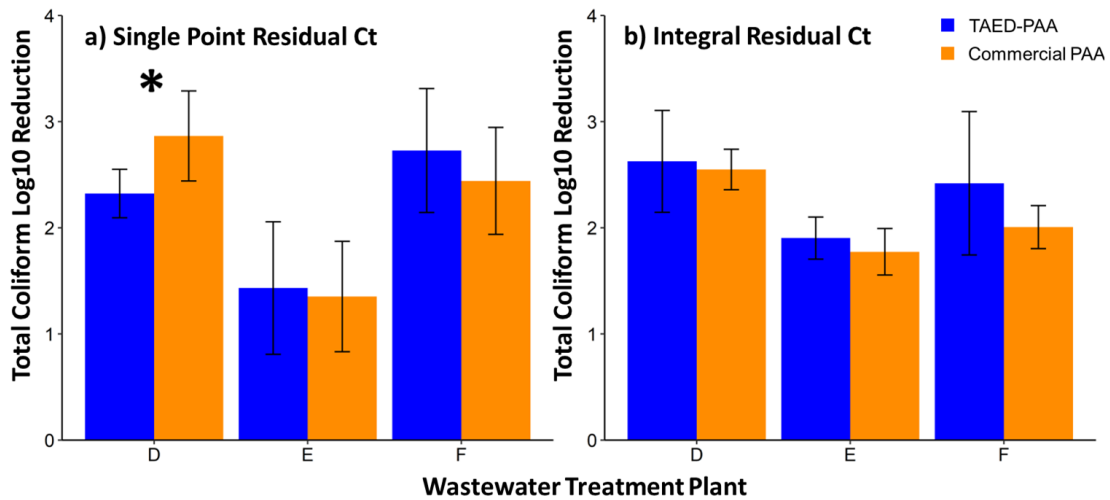


Figure 5: Average (n = 9) total coliform log reductions after PAA application across WWTPs under a) single point residual and b) integral Ct approach. * designates a statistically significant (p-value < 0.05) difference in log reductions between TAED-PAA and Commercial PAA.

2.3.3 TAED-PAA Impacts on Water Quality

Like commercially available PAA, it is hypothesized that TAED-PAA decay rate and disinfection 284 efficacy are strongly tied to standard water quality parameters^{42,46,50,51,87-91}. Previous studies have disagreed on the effects of PAA addition on finished water BOD levels with several reporting a decrease in BOD levels after PAA treatment^{49,51} and others showing no significant change^{86,92}. Under both Ct approaches examined here, BOD₅ measurements varied

between PAA treatment and plant. For example, Plant D exhibited a 15% increase in BOD₅ after TAED-PAA treatment, but a 24% decrease after treatment with the Commercial PAA under the conventional Ct approach (Appendix A Table 1). Conversely, Plant F exhibited a decrease in BOD₅ levels under both Ct calculation methods (Appendix A Table 2). Increases in BOD make sense due to PAA generating a BOD due to the acetic acid in solution⁴². Overall, the variation in BOD observed poses a potential concern when thinking about receiving water quality and permitting violations for WWTPs as increased BOD levels result in decreased oxygen availability for other organisms and can cause microbial regrowth over time. However, it has been suggested that PAA formulations can also generate elevated levels of dissolved oxygen (DO), which could offset any elevation in BOD that it may cause⁴². Thus, further experiments should be conducted to fully elucidate the impacts of PAA addition on BOD and DO concentrations prior to full-scale use and discharge into receiving streams.

With respect to suspended solids and turbidity in wastewaters, previous literature has shown that an elevated presence of TSS can adversely impact the consumption of PAA in wastewater^{46,50,85–88,93–95}. The lack of TSS data in this study makes it difficult to assess the impacts of PAA addition (all wastewaters were characterized for TSS, however, complications in measuring (i.e., filter tears) rendered the data unusable). It has been suggested that the primary two mechanisms by which TSS affects PAA disinfection efficacy is by increasing the oxidative demand (thus reducing the disinfecting dose) and by creating a protective shield for microorganisms⁸⁷. Referring to the microbial data (Figures 4, 5), the plants that had the highest TSS (or turbidity in the cases where TSS data was not available) showed no reduced disinfection efficacy, but further testing would need to be done to confirm these results. In terms of TDS, there was a consistent trend of reduced levels across all WWTPs and between both Ct approaches. The

reduction in TDS levels could be explained by the fact that the decay of PAA is driven by the initial oxidative demand required by dissolved transition metals^{82,96}. Furthermore, no significant difference in reduction of was observed between the two Ct approaches. This could be due to the initial oxidative demand for PAA being satisfied; thus, no further reduction would be achieved in the presence of more disinfectant.

Previous studies have documented the various effects that transition metals in water have on PAA decomposition^{46,76,89,91,97,98}. Metal ions such as iron (Fe^{2+}), manganese (Mn^{2+}), and copper (Cu^{2+}) catalyze PAA decomposition through complex redox reactions. It has also been stated that Cu^{2+} and silver (Ag^+) can also promote the formation of free radicals, thus enhancing PAA disinfection efficiency⁴². Across WWTPs, there were varying results in the concentration of total transition metals pre- and post-disinfection with PAA (Appendix A Figures 5 and 6), however few significant differences were observed. Looking at all WWTPs D-F collectively, total manganese concentrations were found to be significantly increased (11% increase; 0.07 ± 0.04 mg/L to 0.08 ± 0.04 ; p-value < 0.05) after being treated with TAED-PAA. Comparatively, manganese concentrations were not found to be significantly affected after commercial PAA addition. To determine the reason for increase, TAED-PAA was also analyzed via inductively coupled plasma mass spectrometry (ICP-MS) to quantify manganese concentrations in the stock solution; however, results did not indicate any additional manganese in the stock solution. Although manganese concentrations were increased, it is important to note that since manganese is thought to act as a catalyst in solution with PAA, changes in concentration would not be expected. As such, the increase observed in this study could have been an artifact of a previous run on the ICP-MS. Moreover, manganese concentrations were found to have a significant positive correlation with log *E. coli* and total coliform reductions (i.e., as log reduction increases, total manganese

increases) which is expected as manganese is thought to catalyze PAA decomposition in aqueous solutions^{76,91,96,97}. Hypothetically, it is possible that the manganese in solution could be catalyzing PAA to form acetyl(per)oxyl radicals, which may be responsible for disinfection and increased disinfection efficacy^{72,76}. Further examination should be conducted to better understand the role manganese plays in TAED-PAA disinfection of secondary effluents.

2.4 Conclusions

In summary, the work done under Specific Aim 1 demonstrated the antimicrobial efficacy of TAED-PAA in urban wastewater matrices and suggests that TAED-PAA performs comparably to commercially available PAA as a wastewater disinfectant. On average, wastewater samples treated with 2.5 mg/L of TAED-PAA or commercial liquid PAA achieved similar log-unit reductions of *E. coli* (1.9 ± 0.4 , 2.5 ± 0.6 , respectively) and total coliforms (2.2 ± 0.5 , both). Additionally, performance differences were observed between the different disinfection exposure (Ct) methods at Plant D, where an increase in antimicrobial performance and decreases in parameters such as BOD and total phosphorus were noted. The increase in antimicrobial performance coupled with the changes in water quality parameters suggest that water matrix parameters are critical in determining what Ct approach is used and should be investigated further in the future. The similarity between the antimicrobial efficacies of TAED-PAA and commercial PAA provides WWTP operators with a new option for disinfection that has no perceived adverse microbial effects. However, before TAED-PAA could become more widely adopted for wastewater disinfection, further testing should be completed to fully elucidate its efficacy in

different urban water matrices to ensure consistent permitting requirements for standard fecal indicator organisms (126 cfu / 100 mL) ⁹⁹.

Future testing of TAED-PAA should include the determination of the instantaneous demand and decay coefficient in a variety of wastewaters to ensure accurate dosing and antimicrobial efficacy. At pilot and full scale, the averaging of common demand and decay coefficients may not be sufficient in dosing the system correctly, leading to decreased disinfection efficacy in the effluent and receiving stream. Additionally, the microbial inactivation kinetics of TAED-PAA should be elucidated on both standard fecal indicator organisms, but also other pathogenic organisms (e.g., Norovirus, *Clostridium perfringens*) and on the growing threat of antibiotic resistant bacteria (ARBs) in receiving waters. In particular, the minimum dose, time intervals needed to achieve varying regulatory permits and public health requirements, and synergies with other disinfection methods will be required for further consideration at full scale. In practice, it will be necessary to conduct mechanistic studies that collect and fit different water quality parameters into a PAA decay curve to better understand the best case-scenarios for PAA usage. It will be critical for wastewater permit applicants (especially those with no regulation on PAA usage) to collect as much information as possible and conduct site-specific testing to ensure compliance and receiving stream protection. As of 2018, PAA usage in the United States has been regulated for water reclamation purposes in six states, with regulation pending in others¹⁰⁰. Furthermore, with many WWTPs shifting to resource recovery practices, there may also be promise in recovering TAED components from wastewaters to circularly use in TAED-PAA production.

Lastly, cost will also be an important factor in elevating both PAA and TAED-PAA to the forefront of wastewater disinfection. Several key design factors will have significant impact on the

financial viability of PAA at a given WWTP. Namely, the ability to retrofit the existing infrastructure and PAA chemical procurement (chemical procurement for commercial PAA, dry powders for on-site generation) will be determining economic factors. Other factors such as equipment, construction, operation and maintenance, safety and training, and stakeholder buy-in will also be important to consider. Due to the limited use of PAA (and TAED-PAA), it currently is more expensive than chlorinated disinfection options, and will continue to be until it becomes a more established and widely used wastewater disinfectant. Theoretically though, compared to conventional chlorine disinfection PAA and TAED-PAA could potentially have lower capital costs in the long term due to not needing to quench the residual PAA (i.e., no need to procure extra chemicals and storage) and the ability to dose in the exact amount of PAA needed at any given time due to integral Ct. Work done by Manoli et al., has discussed the advantages of using the integral Ct approach at the pilot scale and found that overall PAA usage in kg is halved as compared to conventional Ct approaches¹⁰¹. Additionally, one plant in New Jersey that currently employs PAA as its primary disinfectant recorded a 10 – 12 % reduction in costs in 2018 from using PAA and expected an even bigger savings as they continued to use it⁷⁸. Overall, while PAA may have its limitations as a one-size-fits-all wastewater disinfectant, its upside as a targeted disinfectant should continue to be explored in laboratory, pilot, and full-scale settings. This continued exploration will allow operators to identify primary PAA applications and help them continue to meet their regulatory requirements, while also promoting environmental safety and not causing problems for downstream processes such as drinking water treatment.

3.0 Specific Aim 2.0: Examination of the Impacts of Distribution System Phosphate Addition on the Microbial Ecology of Hydrologically Connected Local Urban Streams

Specific Aim 2.0 was funded by The National Science Foundation (grant number: 1929843). The results of Specific Aim 2.0 have been published in one journal publication, with one additional paper under review and results shared in four conference proceedings:

Journal Article

1. **Isaiah Spencer-Williams,** Anusha Balangoda, Richard Dabundo, Emily Elliott, and Sarah-Jane Haig. (2022). Exploring the Impacts of Full-Scale Distribution System Orthophosphate Corrosion Control Implementation on the Microbial Ecology of Hydrologically Connected Urban Streams. *Microbiology Spectrum*, 10(6). <https://doi.org/10.1128/spectrum.02158-22>.
2. Anusha Balangoda, Emily Elliot, Richard Dabundo, **Isaiah Spencer-Williams,** and Sarah-Jane Haig. (2023). Assessing Nutrient Limitation in Urban Streams Following the Addition of Orthophosphate-Based Corrosion Control to Drinking Water. *In Revision, Biogeochemical Dynamics in Urban Systems: Interactions, Feedbacks, and Cumulative Impacts*.

Conference Proceedings

1. **Spencer-Williams, I.,** Balangoda, A., Dabundo, R., Elliott, E.M, Haig, S.J. Investigating the Impacts of Orthophosphate Lead Corrosion Control on Urban Stream and Distribution System Microbial Ecology. AEEESP Annual Conference 2022. June 28 – 30, 2022.
2. **Spencer-Williams, I.,** Balangoda, A., Dabundo, R., Elliott, E.M, Haig, S.J. From Corrosion Control to Ecological Influence: Examining the Impacts of Orthophosphate

Corrosion Control on Urban Stream and Distribution System Microbial Ecology. Gordon Research Conference: Microbiology of the Built Environment. June 19 – 24, 2022.

Peer Reviewed Conference Proceedings

3. Balangoda, A., Dabundo, R., **Spencer-Williams, I.** Haig, S., Elliott, E.M. Assessing the Impacts of Nutrient Limitation on Algal Growth and Ecosystem Health. AGU Annual Meeting. December 14, 2021
4. Balangoda, A., Dabundo, R., **Spencer-Williams, I.** Haig, S., Elliott, E.M. Effects of large-scale drinking water orthophosphate addition on urban stream nutrient dynamics and eutrophication potential. SFS Annual Meeting. Virtual, May 23-27, 2021.

3.1 Introduction

Many drinking water utilities source their water from large freshwater sources (e.g., surface water, ground water) that receive treated wastewater effluents. As such, typical drinking water treatment is done by a multibarrier approach in which the source water is treated in series through several processes in order to reliably produce drinking water which meets federal and state regulations^{23,24,102,103}. However, once the treated water goes out into the DS and subsequently into building plumbing, it is subject to several interactions with different piping materials. Historically in the United States, lead has been used as a piping material due to its long usable life span and malleability compared with iron^{104,105}. However, concerns about the potential for lead contamination in water and its toxicity were widespread even before lead was a commonly used piping material¹⁰⁴. In 1859, a collection of chemists, engineers, and other public health officials' opinions on the introduction of lead service pipes into drinking water infrastructure was published where objections were raised given the various health concerns¹⁰⁶. Later, an article published in 1889 detailed instances of lead-poisoning from drinking water infrastructure and its relation to sterility in women, while another in 1914 discussed 120 different observations of lead absorption into the body and its effects on human health^{107,108}. Despite efforts from public health officials and engineers, lead use for piping materials continued as plumbing codes for cities still mandated lead pipes be used¹⁰⁴. Then in the early 1980s through the 2000s the use of lead piping was heavily scrutinized, most notably with the 2001 lead crisis in Washington DC, and more recently the 2014 lead crisis in Flint, Michigan¹⁰⁹⁻¹¹¹. Since then, cities across the nation have been required to implement new strategies into their treatment trains to continue to meet regulated levels of contaminants such as lead.

The City of Pittsburgh, like many other cities in the United States, experienced its own lead crisis in its drinking water as lead levels were elevated above the EPA Lead and Copper Rule of 15 ppb in over 10 percent of homes sampled in 2016. However, the problem dates back even earlier, with lead levels consistently on the rise since 1998¹¹². This rise has been attributed to the changing of corrosion control methods from soda ash to caustic soda¹¹² to save money. While this change was beneficial to the utility economically, they did not assess the impacts on the water chemistry, which led to even further increases in lead concentration. To address the elevated lead levels in drinking water, Pittsburgh's drinking water utility opted for lead service line (LSLs) replacement, however, economic and time constraints make complete LSL replacement a slow and expensive process. Given the urgency of lead mitigation, Pittsburgh like many other water utilities chose to introduce orthophosphate (PO_4^{3-}) corrosion control, which forms a protective scale on pipe surfaces, to provide a quicker and more economical solution to control lead release while awaiting completed LSL replacement¹¹⁰. Phosphate-based corrosion inhibitors, namely polyphosphates and orthophosphates, have been widely used by drinking water utilities for decades and have had varied success in inhibiting corrosion from copper, lead, and iron plumbing materials¹¹³⁻¹²⁰. Successful implementations of phosphate-based corrosion inhibitors have considered the system water quality, namely pH and alkalinity, to ensure adherent scales in the pipes. Specifically, in the city of Pittsburgh, success has been observed over the last few years as the pH in the system was adjusted to fall within the target pH range of 8.8 – 10¹²¹ (DWDS tap average of 8.4 before PO_4^{3-} addition into system).

Although orthophosphate is successful in preventing further corrosion in our DWDS, aging pipelines are prone to leaks and breaks that may leach treated drinking water into our natural environment¹²². With many of our DS pipes running underground, the addition of up to 1.8 mg/L

of phosphorus into a system with previously non-detectable phosphorus could potentially have adverse impacts on hydrologically connected (surrounding) water bodies including urban streams and rivers and groundwater sources^{123,124}. In particular, increased phosphorus addition may lead to increased growth of taxa related to eutrophication (e.g., *Cyanobacteria*)^{125,126}, or polyphosphate utilization (e.g., *Candidatus Accumulibacter*, green algae)¹²⁷, and more holistically a shift in nutrient limitation status of aquatic communities which could result in irreversible changes to aquatic food webs^{128–136}. The work presented in Specific Aim 2 aims to assess for the first time if an operational change in the DWDS (e.g., orthophosphate addition) impacts the microbiome of surrounding urban streams that may receive water from pipe breaks, leaks, etc.

3.2 Research Approach

3.2.1 Sample Collection

Urban stream samples were collected monthly from five above-ground urban stream locations in Pittsburgh, PA (Figure 6, Table 2). Under this collection regime, 15 samples (3 time points, 5 urban streams) were collected before PO_4^{3-} addition in the DS and 70 samples (14 time points, 5 urban streams) were collected after PO_4^{3-} addition. Water samples were collected and 1L was filtered within an hour of collection through 0.2 μm polycarbonate filters. DNA was then extracted from the filters the FastDNA Spin Kit (MP Biomedicals, Solon, OH) and used in subsequent microbial analyses.

Table 2: Urban Stream Population Density and Land Development Type

Urban Stream	Population Density (person / km ²)	Land Development Type
Shades Run (S1)	534.3	Mixed Forest
Negley Run (S2)	2604.6	Developed, Medium Intensity
Fern Hollow (S3)	1514.7	Mixed Forest; Developed, Medium Intensity
Panther Hollow (S4)	2822.5	Developed, Medium Intensity
Phipps Run (S5)	0.00	Developed, Open Space

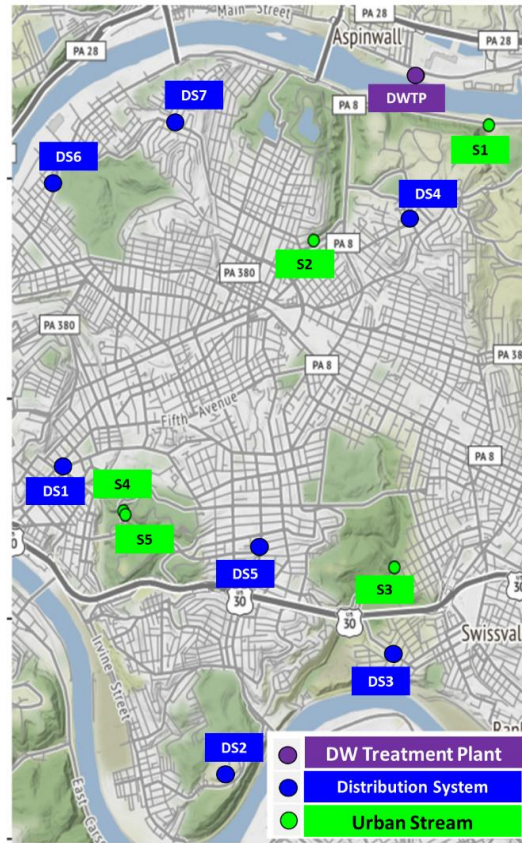


Figure 6: Map of Urban Stream (green) and Distribution System (blue) sampling locations for Aims 2 and 3. Five urban streams and seven distribution system sites were sampled for the work presented in Objectives #2 and #3.

3.2.2 Water Chemistry Analyses

1 L of urban stream water was collected from the surface of each stream and filtered withing 24h of collection through a 0.45 μm polyvinylidene fluoride membrane syringe filter (Thermo Fisher Scientific, Waltham, MA). Filtered water samples were used for the measurements of nitrate, nitrite, ammonium, and soluble reactive phosphorus, while unfiltered samples were used for total nitrogen, total phosphorus, and total reactive phosphorus concentrations (Appendix B Tables 1 and 2). Total nitrogen, total phosphorus, total reactive phosphorus, soluble reactive phosphorus, nitrate, nitrite, and ammonium were all measured using a Lachat QuickChem Analyzer (HACH, Loveland, CO). Silica was found to interfere with phosphate measurements, so a modified version of QuickChem method 10-115-01-1-Y that is equivalent to EPA method 365.1 was used. Temperature and pH were monitored on site using a multiparameter sonde (Yellow Spring Instruments, Yellow Springs, OH, USA).

Nitrate/nitrite nitrogen ($^{15}\text{N}/^{14}\text{N}$) and oxygen ($^{18}\text{O}/^{16}\text{O}$) isotope ratios were measured using the denitrifier method described in Sigman et al. 2001 and Casciotti et al. 2002. Briefly, nitrate and nitrite were converted into nitrous oxide and the N and O isotopic composition was then measured using an IsoPrime isotope ratio mass spectrometer interfaced with a Micromass Trace Gass Pre-concentrator system (Thermo Fisher Scientific, Waltham, MA).

3.2.3 Nutrient Addition Bioassay

Nutrient addition bioassays were also conducted by our colleagues in the Department of Geology and Environmental Science to examine changes in nutrient limitation and the effects on cyanobacterial and algal species. Briefly, 4L of both DS and urban stream water were collected

for the nutrient addition bioassays, with the first bioassay done shortly before PO_4^{3-} addition into the DS, the second three months after PO_4^{3-} addition, and the last twelve months after PO_4^{3-} addition. Samples were inoculated with either green algae or *Cyanobacteria* and treated with varying ratios of phosphorus and nitrogen. Nutrient treatments were administered in triplicate and following treatments, samples were incubated in a fume hood for seven days under a 16h:8h light-dark cycle using grow lights. After incubation, absorbance was measured as a proxy for algal biomass at 678 nm using a spectrophotometer (Thermo Fisher Scientific, Waltham, MA).

3.2.4 Molecular Analyses

3.2.4.1 Droplet Digital PCR

DNA was extracted from the stored filters using the FastDNA Spin Kit (MP Biomedicals, Solon, OH) and stored at -20°C until use. The abundance of total bacteria was determined using droplet digital PCR (ddPCR) targeting the 16S rRNA gene using primers described in ¹³⁷. Absolute quantification of *Cyanobacteria* and the polyphosphate accumulating genus *Candidatus Accumulibacter* were determined using previously published primers targeting their specific 16S rRNA genes ^{138 139} (Appendix B Table 3).

ddPCR reactions were performed for all DNA samples ($n = 90$), alongside negative controls (ddPCR negative controls, filtration controls and extraction controls) and positive controls (gblocks of the target amplicons, Integrated DNA Technologies, Inc., Coralville, IA, USA). Droplets were generated to a 20 μL reaction volume in a 96-well plate that was heat sealed. PCR was then performed on the C1000 TouchTM Thermal Cycler (Bio-Rad Laboratories, Inc., Hercules, CA, USA) within 15 min of droplet generation using the reaction conditions presented in Appendix B Table 4. Plates were run on the droplet reader within 1 h of PCR completion and

thresholds (Appendix B Table 5) were set for each ddPCR assay using Quantasoft v1.0.596 to determine the absolute abundance of the target taxa using the method described by Lievens et al.¹⁴⁰

3.2.4.2 16S rRNA Amplicon Sequencing

16S rRNA gene amplicon library preparation and sequencing were performed on all samples at the Argonne National Laboratory following the Illumina Earth Microbiome Protocol¹⁴¹. Samples were sequenced on an Illumina HiSeq2500 with a total of 5,063,434 raw reads generated from the samples. After quality assurance and control, the average quality score was 94% with a median of 29,000 reads per sample. Microbiome analysis was performed using QIIME2 with quality filtering performed using the method described in Bolyen et al.¹⁴². Reads were assigned to operational taxonomic units (OTUs) using a 97% cutoff using the closed reference OTU-picking protocol in QIIME2 (version 2020.2) using the Silva (version 132.5) and Greengenes (version 13.5) databases. The OTUs generated from the Silva database were used in microbiome analysis while the OTUs from the Greengenes database were used specifically in BugBase¹⁴³ to predict phenotypes present in the samples.

3.2.4.3 Phenotypic Prediction using BugBase

Predicted phenotypes were assigned to all OTUs using BugBase's default nine common traits (aerobic and anaerobic respiration, gram-negative and gram-positive delineation, pathogenic presence, and stress tolerance) and additional traits relating to phosphate and nitrogen metabolism. All traits used with BugBase were compatible Kyoto Encyclopedia of Genes and Genomes (KEGG) pathways (Appendix B Table B6).

3.2.5 Statistical Analyses

Taxonomic and OTU tables generated for the samples were transformed using the Hellinger transformation due to the dataset having many zeros and or low relative abundances¹⁴⁴. The transformed OTU data was then used to calculate pairwise dissimilarities between samples based on the Bray-Curtis dissimilarity index, with the resulting matrices examined for temporal and spatial patterns in the bacterial community structure by Non-metric Multidimensional Scaling as implemented in the Vegan package in R¹⁴⁵. Significant differences in the microbial community compositions of the urban streams before and after PO_4^{3-} addition were determined by nonparametric permutational analysis of variance (PERMANOVA) using adonis as implemented in the Vegan package in R¹⁴⁶. Alpha diversity indices (Shannon diversity index, Chao's richness, Pielou's evenness) were also calculated and examined before and after PO_4^{3-} addition. The relationships between environmental parameters and patterns in bacterial community structure were examined by canonical correspondence analysis (CCA) with significance tested by ANOVA after reducing the overall suite of environmental variables with a stepwise Akaike information criterion model. Additionally, significant differences in the absolute bacterial abundance before and after PO_4^{3-} addition were determined by non-parametric Wilcoxon testing and the functional relationships between water quality parameters and bacterial groups were analyzed by stepwise multivariate forward / reverse regression analysis. All statistical analyses were performed in R (version 4.0.2)¹⁴⁷ with significance set at a p-value < 0.05.

3.3 Results and Discussion

3.3.1 Impacts of PO_4^{3-} Addition on Urban Stream Phosphorus and Nitrogen

Concentrations

After PO_4^{3-} addition into the DWDS, a significant increase in the average total phosphorus concentration in the urban streams was observed (Figure 7) while no significant change was observed in total nitrogen (Appendix B Figure 1). The significant increase in the average total phosphorus concentration was driven by a significant increase in stream S2. Stream S2 exists in an area of medium development intensity (Table 2) and has the highest human population density surrounding it out of all five streams, which would increase the likelihood of a hydrological connection to urban water infrastructure. While there are a range of inputs to urban stream networks (e.g., stormwater runoff, nutrient and metal mobilization from sediments), previous work has looked at the spatial distribution of potential deteriorating water infrastructure in Pittsburgh and documented that 71% of existing streams across the City of Pittsburgh are located in a potential leakage zone¹⁴⁸. Therefore, the increase in average total phosphorus could be indicative that these urban streams are receiving PO_4^{3-} from leaking DWDS infrastructure and are hydrologically connected, but further spatial and sensor analysis would be needed to confirm this. Additional supporting evidence of these urban streams being hydrologically connected to urban water infrastructure comes from the water isotope data examined by Balangoda et al, which found the predominant source of nitrogen in the urban streams is urban wastewater inputs (Appendix B Figure 2).

Further work was also done to examine the impacts of PO_4^{3-} addition on phosphorus and nitrogen limitations in the five urban streams¹⁴⁹ (Table 3, Appendix B Tables 7 – 12). Four of the

five streams (S1, S3, S4, S5) were either phosphorus limited or nitrogen-phosphorus co-limited prior to PO_4^{3-} addition into the DWDS, however two months after PO_4^{3-} addition into the DS four streams shifted completely to phosphorus-nitrogen co-limitation (S1, S3, S5) or nitrogen limitation (S4). Interestingly, twelve months after PO_4^{3-} addition, nutrient limitations had shifted back to phosphorus limited or nitrogen-phosphorus co-limited, suggesting that PO_4^{3-} addition in the DWDS caused a temporary shift in urban stream nutrient limitations, but not a holistic shift. It's worth noting that the temporary shift in nutrient limitations could be indicative of the resilience of stream microbial community as there are many microorganisms that can occupy the same niche and have the same functional roles.

Table 3: Urban Stream Nutrient Limitations Before and After PO_4^{3-} Addition into the DWDS

Urban Stream	Before PO_4^{3-}	Two months After PO_4^{3-}	Twelve months After PO_4^{3-}
Shades Run (S1)	P limitation	PN colimitation	P limitation
Negley Run (S2)	PN colimitation	PN colimitation	PN colimitation
Fern Hollow (S3)	P limitation	PN colimitation	P limitation
Panther Hollow (S4)	P limitation	PN limitation	P limitation
Phipps Run (S5)	P limitation	PN colimitation	P limitation

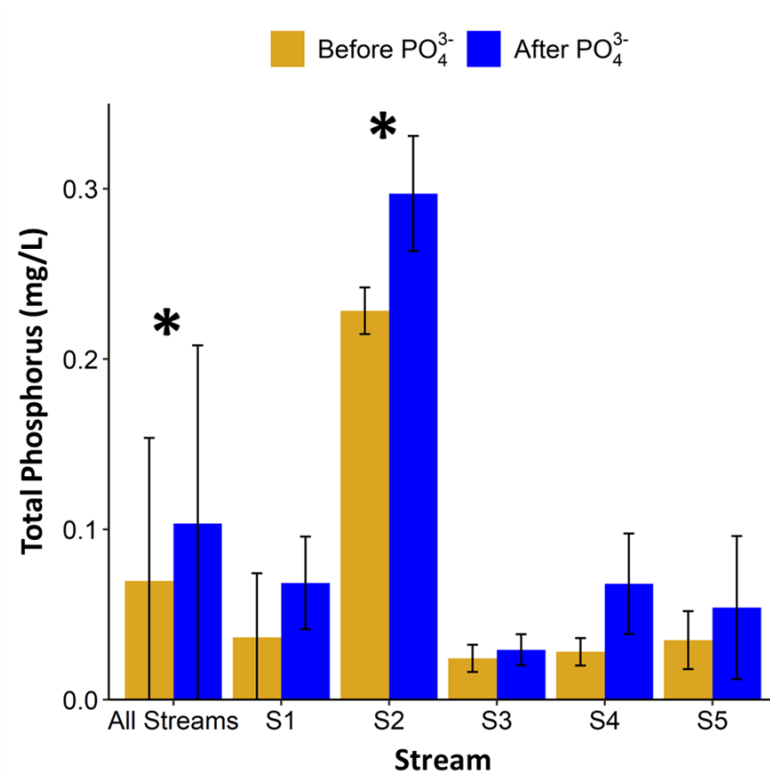


Figure 7: Average (n = 15) total phosphorus concentration in each urban stream before and after PO₄³⁻ addition into the DWDS. Error bars represent the standard deviation. Significant differences (p-value < 0.05) in concentration are indicated by an asterisk.

3.3.2 Impacts of PO₄³⁻ Addition on Urban Stream Microbial Community Composition

3.3.2.1 Non-Metric Multidimensional Scaling Analysis

NMDS and PERMANOVA analyses showed significant seasonal ($r^2 = 0.08$, p-value < 0.001) and pre- and post-PO₄³⁻ addition ($r^2 = 0.035$, p-value < 0.001) variation in the urban stream microbial community structures (Figures 8a, b). Interestingly, however, no significant differences were observed in the microbial community structure between the five urban streams (Appendix B Figure 3) despite differences in land development types, population densities, and chemistries. Previous work has observed seasonal differences in urban stream microbial community

composition^{150–152}, but this is the first work to the authors knowledge that has observed the impacts of DWDS PO_4^{3-} addition on stream microbial ecology.

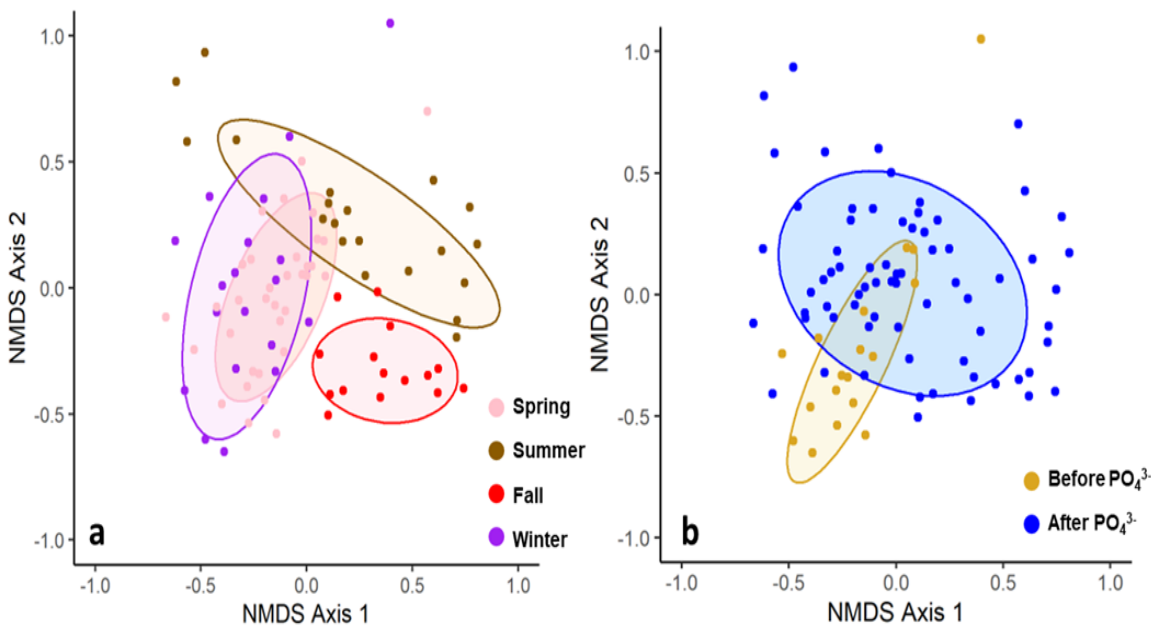


Figure 8: Nonmetric Multi-Dimensional Scaling plots of Bray-Curtis distances for the five urban stream sites sampled (a) seasonally and (b) before and after PO_4^{3-} corrosion control addition. The ellipses represent the 95% confidence interval of the distribution from the centroid of the cluster points.

3.3.2.2 Alpha Diversity and Relative Abundance Analysis

Microbial alpha diversity analysis revealed significant increases in the three alpha diversity indices measured in stream S4 and a significant increase in Chao's species richness in stream S5 after PO_4^{3-} addition into the DWDS (Table 4). This result is not surprising given the locations of streams S4 and S5, since one of these streams receives water from a neighboring suburb, and the other receives water from a neighboring golf course, and stream S4 has the second highest population density of all the streams studied (Table 2).

Table 4: Urban Stream alpha diversity indices before and after PO₄³⁻ addition into the DWDS

<i>Streams</i>	<i>Shannon Diversity</i>		<i>Chao's Richness</i>		<i>Pielou's Evenness</i>	
	<i>Before PO₄³⁻</i>	<i>After PO₄³⁻</i>	<i>Before PO₄³⁻</i>	<i>After PO₄³⁻</i>	<i>Before PO₄³⁻</i>	<i>After PO₄³⁻</i>
S1	5.92	6.48	460	805	.97	.98
S2	6.31	6.62	797	940	.98	.98
S3	6.44	6.34	773	738	.98	.98
S4	5.92	6.4*	456	756*	.97	.98*
S5	5.99	6.39	488	732*	.97	.97

* signifies a significant difference in the alpha diversity metric (p -value < 0.05)

Examining community membership, the collective urban stream network (all five streams) microbial community was primarily comprised of *Acidobacteria*, *Actinobacteria*, *Bacteroidetes*, *Epsilonbacteraeota*, *Firmicutes*, *Omnitrophicaeota*, *Patescibacteria*, *Planctomycetes*, *Proteobacteria*, and *Verrucomicrobia*, with *Proteobacteria* dominating in all urban stream networks, making up 52 to 66% of the community (Figure 9). The presence and abundances of these phyla are consistent with previous work which has highlighted their ubiquitous presence in both urbanized and forested stream networks^{153–155}. Previous studies of streams and rivers have found that in-stream microbial populations are related to taxa typically found in lakes and other freshwater environments^{154,156}. *Proteobacteria*, *Bacteroidetes*, *Verrucomicrobia*, and *Actinobacteria* are all considered typical freshwater lake phyla and have been studied extensively¹⁵⁶. Of the remaining phyla, members of the *Planctomycetes*, *Acidobacteria*, and *Firmicutes* phyla are commonly found in freshwater sediments¹⁵⁶, while more recent work has shown the abundance of both *Omnitrophicaeota* and *Patescibacteria* in fresh- and groundwater systems¹⁵⁷. Overall, significant changes in the relative abundances

of *Actinobacteria*, *Bacteroidetes*, *Omnitropicaeota*, *Planctomycetes*, *Verrucomicrobia*, and less-abundant phyla, such as *Chlamydiae*, were observed after PO_4^{3-} addition into the DWDS (Figure 9). Previous work has observed an association between each of these phyla and phosphorus uptake or utilization in sediment and marine environments¹⁵⁸⁻¹⁶⁰, however no study has detailed an association with phosphorus in freshwater environments. Future work should focus on assessing potential impacts of PO_4^{3-} addition on these six taxa given their importance in decomposition of organic matter and nutrient cycling as changes to their abundance may result in negative ecosystem impacts.

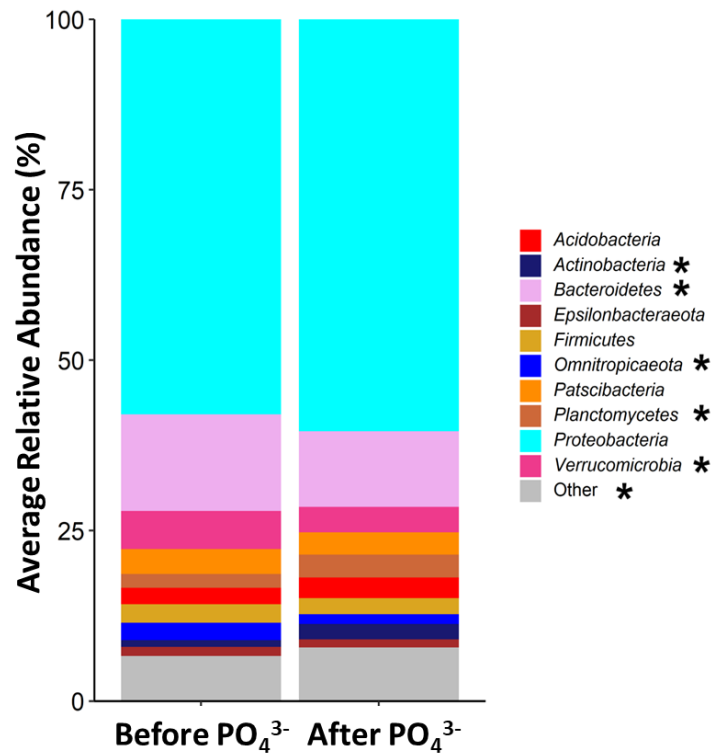


Figure 9: Top 10 most abundant phyla in all five urban streams before and after PO_4^{3-} addition in the distribution system. Proteobacteria dominated the urban stream microbial communities under both conditions. Significant differences (p-value < 0.05) in phyla after PO_4^{3-} addition in the DWDS are indicated by an asterisk.

Examining each stream individually, streams S1, S3, and S5 (Appendix B Figure B4) all had the same top ten phyla present over the course of the study, with limited significant differences in *Acidobacteria*, *Planctomycetes*, and *Verrucomicrobia* in S1 and none in S3 and S5. Both *Planctomycetes* and *Verrucomicrobia* belong to the Planctomycetes-Verrucomicrobia-Chlamydiae (PVC) superphylum which is an amalgamation of members of the three aforementioned phyla and four others, including *Omnitrophicaeota* (also known as OP3, Omnitrophica)¹⁶¹. Members of the PVC superphylum are widely distributed in the environment, occurring in soils, marine and freshwaters, and even human and animal intestinal tracks^{42,43}. Furthermore, previous works have observed an association between *Planctomycetes* and *Verrucomicrobia* abundance and phosphorus uptake or turnover in soils or algal masses^{158–160}. Similarly, previous work has also associated the abundance of members of the *Acidobacteria* phylum with phosphorus turnover in soil samples¹⁵⁹, however no study has examined the association between the aforementioned taxonomical abundances and phosphorus uptake in aquatic environments. The observed changes in PVC superphyla and *Acidobacteria* relative abundances could be indicative of phosphorus from the DWDS making its way into the urban stream networks, however further work would need to be done to confirm this.

Streams S2 and S4 differed in their top ten phyla (Appendix B Figure B5) with *Elusimicrobia* significantly increasing and replacing *Actinobacteria* in stream S2 and *Chlamydiae* replacing *Epsilonbacteraeota* in stream S4 after DWDS PO_4^{3-} addition. Limited studies^{162–164} have examined *Elusimicrobia* (now known as *Elusimicrobiota*), however they have been found in a variety of environments (e.g., groundwater, freshwater, intestinal tracts of animals and insects, sediments) and are predicted to possess nitrogenase (enzyme responsible for catalyzing biological nitrogen fixation) analogs that could be responsible for their nitrogen fixation abilities.

Furthermore, it is suggested that some lineages of *Elusimicrobiota* may have other nitrogen related enzymes (e.g., nitrite/nitrate oxidoreductase) that are used in energy conservation, but not much is known about this phylum in that case. As there were changes in nutrient limitation in the urban streams, the response and increased abundance of *Elusimicrobiota* may have been due to more favorable conditions for that taxa as opposed to *Actinobacteria*. *Chlamydiae* is a part of the PVC superphylum and contain both environmentally ubiquitous species and human pathogens¹⁶⁵, with recent studies in urban streams finding increased *Chlamydiae* after rainfall events driven by combined sewer overflow discharges¹⁶⁶. Although this phylum appeared in low proportions (1-4%) in S4, it is important to note that a combined sewer overflow outfall exists in the immediate vicinity of this stream and could be a potential source for this taxa, further highlighting the connection between the urban streams and urban water infrastructure. Furthermore, although not studied in the context of surface waters extensively, recent work in the marine space has identified one lineage of the *Chlamydiae* phylum that could uptake inorganic phosphate¹⁶⁷. As such, the prospect of phosphate impacts on the *Chlamydiae* phylum (and other members of the PVC-superphylum) are interesting for future consideration as potential eutrophication biomarkers in aquatic systems.

No significant changes in *Cyanobacteria* or *C. Accumulibacter* relative abundance were observed after PO_4^{3-} addition into the DS, nor were they present in the top ten taxa of any stream compared with urban stream samples collected before PO_4^{3-} addition into the DS. Members of the *C. Accumulibacter* genus are commonly found in wastewater treatment plants that perform enhanced biological phosphorus removal¹⁶⁸, so the low relative abundance in more dynamic freshwater systems, where parameters affecting their survival can vary depending on hydrologic conditions, is expected. The lack of significant changes in *Cyanobacteria* however was an

unexpected result as increased abundance of *Cyanobacteria* and other eutrophication- related taxa have been associated with an increase in the availability of phosphate due to its role in cell growth and maintenance^{125,126}. Certain *Cyanobacteria* are known to have a high affinity phosphate uptake system, called the “phosphate-specific transport system”¹⁶⁹, however, many of these functional traits are only induced under low phosphate concentration conditions (<0.1 mg/L¹⁷⁰); which were not displayed in the streams in this work. Collectively between the five urban streams studied, *Cyanobacteria* had an average relative abundance of 0.87% ± 1.1% before PO₄³⁻ addition into the DS, and 0.65% ± 0.62% after PO₄³⁻ addition. Combined with the results from the eutrophication assays¹⁴⁹, it is likely that the low abundance of *Cyanobacteria* is a combination of elevated phosphorus requirements and a natural occurrence in this set of urban streams. Likewise, the low abundance of *Cyanobacteria* could also be a result of the functional resiliency of the community (i.e., other organisms occupied the functional space that cyanobacteria usually do, therefore leaving it outcompeted) Future studies should include continued examination of *Cyanobacteria* and specific taxa including known contributors to harmful algal blooms such as *Microcystis*.

Overall, the lack of significant changes in the relative abundance of both *Cyanobacteria* and *C. accumulibacter* could be due to the dynamic nature of urban streams¹⁷¹. For example, seasonal changes in hydrologic conditions (e.g., streamflow, groundwater table) and environmental parameters can impact necessary (or inhibitory) nutrients for certain organisms¹⁷², which in turn would impact and shift microbial growth rates. As such, future studies should consider and explore the impacts of seasonal and event based hydrological dynamics on microbial nutrient availability. Furthermore, it is known that PO₄³⁻ binds with lead in pipe networks, so although DWDS pipe leaks could contribute additional phosphorus to urban stream networks, the

amount may not have been enough to cause significant changes in *Cyanobacterial* or *C. Accumulibacterial* abundance given other temporal and seasonal changes in the streams.

3.3.2.3 Absolute Abundance Analysis

No significant difference in the absolute abundance of total bacteria (Figure 10), *Cyanobacteria* (eutrophication indicator phylum), or *C. Accumulibacter* (polyphosphate accumulating genus) was observed in any urban stream after PO_4^{3-} addition into the DS (Appendix B Figures B6, B7). The lack of significant differences in absolute abundance combined with the significant changes in the relative abundance of different taxa in the urban streams suggests that PO_4^{3-} may be causing urban stream microbial communities to respond differently rather than changing the total number of organisms present in the urban streams. Different microorganisms have different nutrient requirements and as such, the amount of PO_4^{3-} reaching the streams from the DS may be enough for some members, while not enough for others. This conclusion is also supported by the observation of increased phosphorus requirements for *Cyanobacteria* in these urban streams from eutrophication assays conducted by Balangoda et al.¹⁴⁹. As such, it is imperative that future studies examine the impacts of long-term PO_4^{3-} addition on urban streams as lower dosages are used for scale maintenance in the DS and continued infiltration occurs.

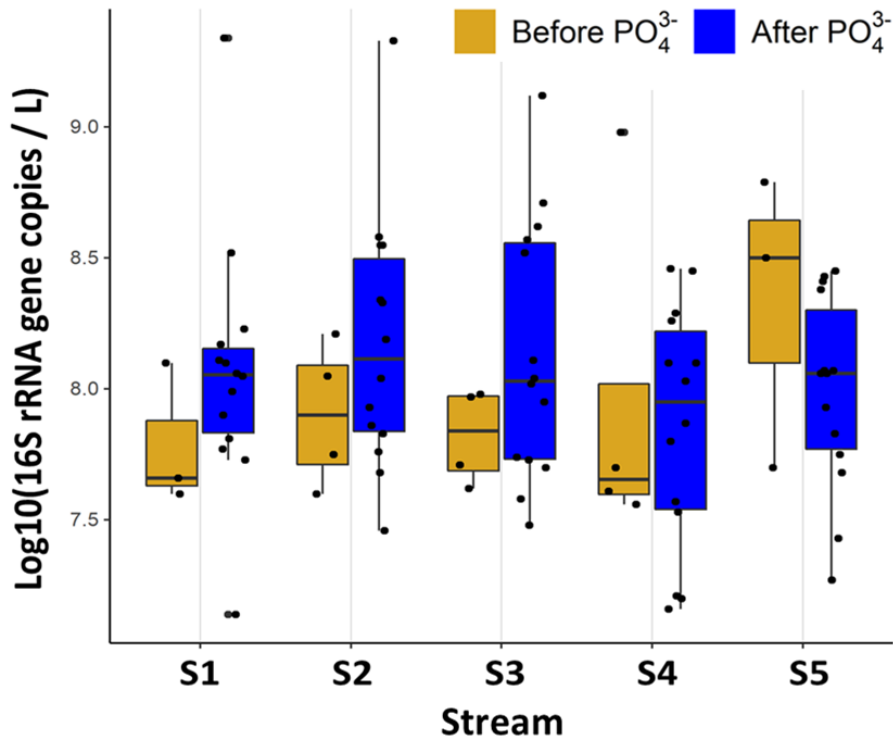


Figure 10: Total bacteria absolute density in urban streams before and after PO_4^{3-} addition into the DWDS. No significant differences were observed in any stream after PO_4^{3-} addition.

3.3.2.4 Impacts of Environmental Parameters on Urban Stream Microbial Community

Composition

Canonical correspondence analysis (CCA) of the urban streams microbial community composition revealed that 21% of the variance in composition could be explained by the geographic location of the streams, season, the presence, or absence of PO_4^{3-} addition into the DWDS, total and dissolved iron concentration, nitrogen concentration, phosphorous concentration, and human population density (Table 5). The presence or absence of PO_4^{3-} in the DWDS and the total phosphorus concentration of the streams were significant factors in explaining community composition likely due to these two parameters being related. Combined with the significant increase in the average total phosphorus concentrations after PO_4^{3-} addition into the

DWDS (Figure 7), this result provides further evidence that PO_4^{3-} may be reaching the urban streams via leaks from the DWDS. Additionally, iron is an important biogeochemical element that can serve as a co-factor in several biological processes^{171,172}, thus its significance in explaining variance in the microbial community is understandable. Microbial iron reduction has been shown to play a critical role in several nutrient cycles including nitrogen and phosphorus¹⁷³ and iron-oxidizing bacteria are often abundant in urban streams where groundwater infiltration occurs¹⁷⁴. Overall, with only 21% of the variance explained by parameters that were collected, there is still a large amount of variance unaccounted for in the microbial community. Other parameters that have been observed to be microbially relevant in urban stream systems include stream flow and residence time¹⁷², differences between community compositions of sediments and bulk stream waters^{175,176}, and climate and extreme weather impacts¹⁷⁷. Future studies of urban stream microbiomes should plan to include measurements for these parameters to better explain major drivers in community composition.

Table 5: Linear effect model for the stream community composition (OTUs) using all the stream water samples collected (n = 85) over the course of one year

Data Transformation	Model components^a	Explained by Model^b
<i>hellinger(x)</i>	Stream Location ^{6.37%} ± Season ^{5.18%} ± DWDS PO_4^{3-} Addition ^{1.70%} + Total Phosphorus ^{1.96%} - Total Nitrogen ^{1.68%} + Human Population Density ^{1.55%} + Total Iron ^{2.97%} -	21%

^aSuperscript numbers preceding each component in the models show their relative percent contribution to the overall model. ^bPercentage explained pertains to the adjusted R^2 for the overall model. All models were significant at p -values <0.001

3.3.3 Predicted Impacts of PO₄³⁻ Addition on Urban Stream Microbial Function

3.3.3.1 Default Phenotypes

Of the default phenotypes assessed by BugBase, there were no predicted significant changes observed after PO₄³⁻ addition into the DWDS, however, significant differences in phenotypic traits in urban stream have been observed seasonally^{178–180} and spatially¹⁵³.

3.3.3.2 Phosphorus Related Functional Traits

Predicted significant differences in phosphate uptake phenotypic traits including bacterial two-component regulatory systems (e.g., CreB-CreC, UhpB-UhpA) were observed in the urban streams after PO₄³⁻ addition (Figure 11, Appendix B Figures 8, 11, 12). Changes in two-component regulatory systems are not surprising given that they are bacterial response mechanisms to changes in environmental conditions¹⁸¹ and they result in a cascade of different gene expressions^{181,182}. A predicted significant decrease in the relative abundance of the CreC-CreB phosphate regulation system (CreBC) was observed in the urban streams S1, S4, and S5 (Figure 11 and Appendix B Figures 8, 11, 12, respectively). The CreBC system is a conserved regulatory system that has been observed in a myriad of gram-negative bacteria, including *Escherichia coli* and *Pseudomonas aeruginosa*¹⁸³. In these microorganisms, CreBC is responsible for the global regulation of gene expression¹⁸⁴ for nine genes dealing with mediation of growth, adaptation, and biofilm formation, however, in environmental conditions (i.e., limited nutrients) it is directly related to carbon source and energy metabolism¹⁸⁴. Additionally, a predicted significant increase in the relative abundance of the UhpB-UhpA hexose phosphate system was observed (Figure 11), which has been linked to the ability to uptake a broad range of organic phosphates¹⁸⁵. As temporal and spatial fluctuations occur in stream waters, it is expected that nutrient sources for microbial communities likewise

change, therefore as phosphorus concentrations in the urban streams were elevated after PO_4^{3-} introduction into the DWDS (Figure 7), it is possible that the Carbon:Nitrogen:Phosphorus (CNP) ratio changed impacting the relative abundance of microorganisms that express these systems and could be suggestive of PO_4^{3-} leaching from the DWDS. As such, total nitrogen – total phosphorus ratios (TN:TP) were calculated (Appendix B Table 13) and compared before and after PO_4^{3-} addition in the DS¹⁴⁹. No significant difference in TN:TP ratios were observed after PO_4^{3-} addition into the DS, however a seasonal pattern was observed. The lack of significant differences in TN:TP ratios could be due to the complex dynamics of phosphorus species in streams¹⁴⁹. As such future studies should also measure the carbon concentration to gain a better understanding of nutrient dynamics and the interactions between microbial communities as the CNP ratio can vary vastly in planktonic communities depending on a number of environmental factors^{186,187}.

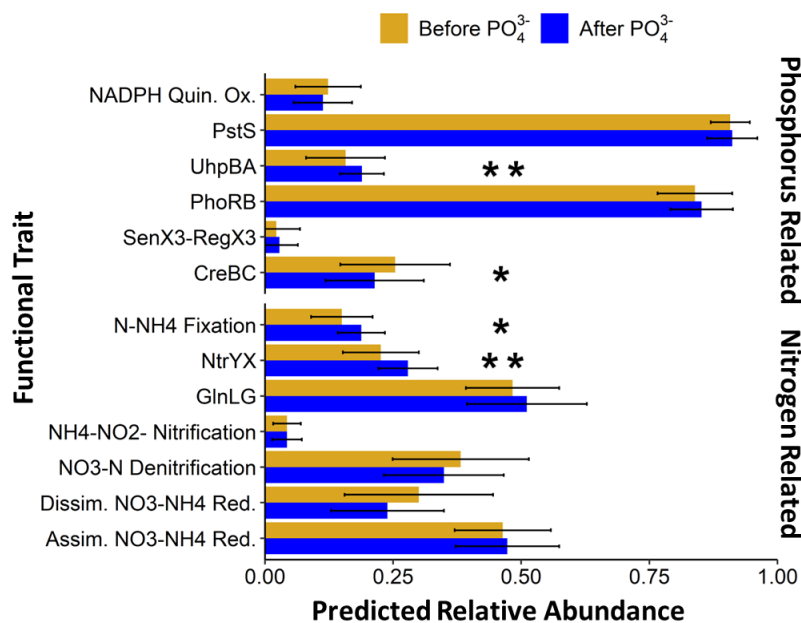


Figure 11: Predicted relative abundance of phosphorus- and nitrogen-related phenotypes in urban streams before and after PO_4^{3-} addition into the DWDS. Predicted significant differences in bacterial two-component regulatory systems and nitrogen fixation were observed across three of the five urban streams examined (*, $P < 0.05$; **, $P < 0.01$).

3.3.3.3 Nitrogen Related Functional Traits

Of the phenotypes relating to nitrogen utilization and uptake, there were predicted significant changes in the relative abundances of the NtrY-NtrX nitrogen two-component regulation system (NtrYX) and nitrogen-ammonia fixation after PO_4^{3-} addition into the DWDS (Figure 11), with overall predicted significant changes driven by stream S4 (Appendix B Figure 11). The NtrYX system is found in a variety of *Proteobacteria* and has been observed to be linked to several cellular processes including responses to oxygen stress, biofilm formation, and nitrogen fixation in the environment¹⁸⁸⁻¹⁹¹. This significant change in predicted functional profile alongside a significant increase in relative abundance of the nitrogen fixing taxa *Planctomycetes*¹⁹² (Figure 9), which have been observed to express the NtrYX system¹⁹¹ suggests the stream microbiome is responding to increased total phosphorus loading (Figure 7) This observation matches with the results from a previous study in which the NtrX gene was upregulated in an high phosphate environment¹⁹³, however, future studies should also confirm this change in the presence of extended PO_4^{3-} use in the DWDS.

Similarly, there was a predicted significant decrease in the functional trait for dissimilatory nitrate reduction, which could also be a response to the increased phosphorus loading in the urban streams. Furthermore, the predicted decrease in dissimilatory nitrate reduction could also be a result of a shift in nitrogen uptake in the urban stream network. Since there was an increase in the relative abundance of microorganisms that could fix atmospheric nitrogen and express the NtrYX system, there would be less of a need for those microorganisms who could reduce nitrate to satisfy overall nitrogen needs.

Overall, while predicted significant changes in both functional traits relating to phosphorus and nitrogen utilization were observed, these results should be interpreted with caution. To better

assess the active expression of functional traits in the urban stream microbial community, future studies should consider examining the impacts of prolonged PO_4^{3-} addition in the DWDS on the active microbial community by utilizing RNA-based approaches rather than DNA. Additionally, conducting RT-ddPCR on specific functional traits (e.g., *nifH* – indicator gene for nitrogen fixing bacteria) of interest over time would be a helpful addition to elucidating the impacts of PO_4^{3-} addition into the DWDS on urban stream microbial community functionality. Furthermore, as PO_4^{3-} continues to be added into the DWDS as a form of corrosion control, future studies should also examine the impacts of extended low dosages of PO_4^{3-} on urban stream microbial community functionality to ensure no adverse effects occur.

3.4 Conclusions

The addition of PO_4^{3-} as a DWDS lead corrosion control mechanism is a widely utilized and effective option, however the effects it can have on the microbial ecology of hydrologically connected urban streams were not previously documented. As many cities draw water from and release water to freshwater sources, this work examined the potential impacts of increasing the amount of phosphorus in the DWDS and its residual effects in surrounding urban stream networks. A significant increase in the total phosphorus concentration in the urban streams was observed after PO_4^{3-} addition into the DWDS and isotope analysis suggests the dominant source of nitrogen in these streams is urban wastewater. Collectively, these two observations suggest that the streams are hydrologically connected to the DWDS, and more generally urban water infrastructure. Additionally, varying changes in the urban stream's microbial community composition and predicted changes in nitrogen and phosphorus functional traits were observed after PO_4^{3-} addition

into the DWDS. The observations presented in this study suggest that while phosphate-based corrosion inhibitors are an effective tool in mitigating lead corrosion, their infiltration into local water bodies through leaks and breaks may result in changes in the existing stream microbial community. It should, however, be stressed that the impacts of such changes are unknown, but due to the degree of microbial functional redundancy in aquatic ecosystems it is possible that ecosystem impacts would not occur or would only be apparent over a longer timeframe than the year of study discussed here. Future work should carefully monitor how the microbial ecology of hydrologically connected urban streams change over longer periods of time when using phosphate-based corrosion inhibitors to ascertain the true urban stream impact.

4.0 Specific Aim 3.0: Examination of the Impacts of Drinking Water Distribution System Phosphate Corrosion Control Addition on the Distribution System Microbiome

Specific Aim 3.0 was partially funded by The National Science Foundation (grant number: 1929843). The results of Specific Aim 3.0 have been published in one journal publication and results shared in four conference proceedings:

Journal Article

Isaiah Spencer-Williams, Mitchell Meyer, William DePas, Emily Elliott, and Sarah-Jane Haig. Assessing the Impacts of Lead Corrosion Control on the Microbial Ecology and Abundance of Drinking-Water-Associated Pathogens in a Full-Scale Drinking Water Distribution System. *Environ. Sci. Technol.* 2023, 57, 48, 20360–20369. <https://doi.org/10.1021/acs.est.3c05272>

Peer Reviewed Conference Proceedings

Spencer-Williams, I., Meyers, M., DePas, W., Elliott, E., Haig, S.J. A Delicate Balance: Addressing Lead Contamination and Drinking Water-Associated Pathogen Abundance in a Full-Scale Drinking Water System. PA-American Water Works Association Southwest District Spring Meeting 2023. April 14, 2023

Spencer-Williams, I., Haig, S.J. Exploring the Impacts of Full-Scale Distribution System Lead Corrosion Control on Drinking Water-Associated Pathogens. Pennsylvania Water Environment Association Annual Technical Conference. June 7, 2022.

Conference Proceedings

Spencer-Williams, I., Meyers, M., DePas, W., Elliott, E., Haig, S.J. PO₄³⁻ Corrosion Control: The Unintended Consequences on Nontuberculous Mycobacteria in a Full-scale Drinking Water Distribution System. AEESP Annual Conference 2023. June 20 – 23, 2023.

Spencer-Williams, I., Mohammadshafie, N., Haig, S.J. Assessing the Impact of Orthophosphate Corrosion Control on Microbial Abundance in a Full-Scale Drinking Water Distribution System. AEESP Annual Conference 2019. May 14 – 16, 2019.

4.1 Introduction

As discussed in the introduction of the previous chapter, it is the responsibility of drinking water utilities to provide reliable access to potable drinking water. Therefore, it is vital that any operational changes made in the DWDS are holistically evaluated to ensure that negative public health impacts will not occur. Holistic evaluations of DWDS changes should include examinations of chemical contaminants that are already regulated (e.g., lead) and observations of contaminants on the CCLs, the impacts on total concentrations of different microorganisms connected to infrastructure issues (e.g., sulfur reducing bacteria), and any other risks that may be associated with the change. Many utilities often depend on microbial results obtained from standard organism measurements (i.e., fecal coliforms) or heterotrophic plate counts (HPCs) as their proxy for overall microbial water quality¹⁹⁴. However, previous work has shown that both standard fecal indicator organisms and HPCs often do not correlate with pathogen presence in aquatic systems⁸. Although useful methods in their respective rights, only relying on these types of measurements limit us from understanding other facets of microbial water quality risk assessment such as the presence of DWPIs. Pulmonary infections resulting from DWPIs that predominately cause infections in

immunocompromised individuals are a leading cause of morbidity and mortality¹⁹⁵⁻¹⁹⁸ in the United States¹⁹⁷ and are estimated to cost the United States economy 2.39 billion annually¹⁹⁹. Although all bacteria have the potential to cause human infection¹⁹⁸, DWPIs are typically referred to as organisms that pose little threat to healthy individuals but can cause infection in immunocompromised people (e.g., individuals with AIDS, cancer, cystic fibrosis¹²). Today, the incidence of waterborne disease outbreaks in the United States attributed to DWPIs that are not regulated by the U.S. EPA (e.g., *L. pneumophila*, and NTM) are increasing, far exceeding the traditionally monitored fecal-borne pathogens²⁰⁰⁻²⁰³. Furthermore, recent evidence has suggested that even otherwise healthy people can become infected with NTM after repeated exposure²⁰⁴.

DWDS's are a microbially diverse aquatic ecosystem that can be altered by several factors including source water quality, temperature, treatment processes, disinfection methods, piping materials, and nutrient limitations^{27,155,205}. Furthermore, the DWDS is an oligotrophic environment where diverse microbial communities containing DWPIs compete for limited nutrient availability. Thus, the introduction of up to 1.8 mg/L of PO_4^{3-} as a lead corrosion control agent into a DWDS which previously had non-detectable PO_4^{3-} will likely result in increased microbial growth and changes in microbial community composition in the DWDS. Specific Aim 2.0 examined the impacts of full-scale DWDS PO_4^{3-} lead corrosion control addition on hydrologically connected urban streams (which receive some of their water from the leaking and aging drinking water DS), with results suggesting that PO_4^{3-} addition impacted the microbial community composition of some urban streams, but this taxonomic change did not translate to immediate functional differences stressing the need for more long-term surveillance. Likewise, it is important to examine the impacts of prolonged PO_4^{3-} addition on the microbial ecology of the DWDS to

understand if excess phosphate will change nutrient limitation status in the DWDS and in turn lead to changes in the concentration and types of microbes present which could impact public health.

Despite the vast improvement in our understanding of the drinking water microbiome in the last decade^{206,207}, we still know relatively little about the impacts that large scale utility changes (e.g., the addition of PO_4^{3-} corrosion inhibitors) have on the drinking water microbiome. The addition of excess phosphorus into a DWDS with previously non-detectable phosphorus could potentially have various impacts on the DWDS microbial community composition (adverse for some microorganisms due to the change in nutrient availability and beneficial for others allowing increased microbial regrowth DWDS^{208,209}). In particular, recent metagenomics studies in a UK DS found an increase in microorganisms related to enhanced phosphate metabolism (e.g., *Candidatus Accumulibacter*)^{208,210,211} after increased phosphate addition. Furthermore, the importance of phosphate to the growth of DWPIs has been indicated in previous studies. For example, *L. pneumophila* have been shown to cause hypophosphatemia (low phosphate blood serum levels) during infections²¹², and phosphate water softeners have been shown to enrich for *Legionella*²¹³. Furthermore, drinking water appropriate levels of phosphate for corrosion control (1 – 3 mg/L) have been shown to reduce the biocidal effects of copper ions on culturable *Legionella*^{214,215}, increase the amount of *Legionella* and Mycobacteria present in source waters²¹⁶, and phosphorus presence in a model DWDS has been shown to correlate with *Mycobacterium* relative abundance^{217,218}. It is also important to note that DWPIs are often found in complex biofilm communities that can be affected by nutrient fluctuations and availability^{219,220}. Therefore, given that infections associated with DWPIs annually cause >145,000 infections¹², costing the economy >\$62 billion in losses due to deaths based on a value of statistical life calculation using the Department of Health and Human Services central value²²¹, and are resident microbes of the

DWDS, it is essential that any operational changes in the DWDS also involve proactive DWPI monitoring. The work presented in Aim 3 assesses the impacts of PO_4^{3-} corrosion control addition on the microbiome and DWPI density in the DS. It is *hypothesized* that the addition of excess PO_4^{3-} into a phosphorus limited DWDS will change both the total bacterial abundance and microbial ecology of the drinking water DWDS, with an increase in *L. pneumophila* and NTM density expected.

4.2 Research Approach

4.2.1 Sample Information and Orthophosphate Addition Details

From February 2019 to March 2020, samples were collected from seven routine monitoring sites in a DWDS in Pittsburgh, PA, USA, all of which received water from the same drinking water treatment plant (Figure 6). This plant treats surface water by using coagulation, sedimentation, filtration, and disinfection by chlorination. After disinfection, the treated water is pumped to a storage reservoir and then treated at a smaller treatment plant (microfiltration, UV light, and chlorination) before transport through the DWDS. The seven sites are in six different pressure districts representing residence times ranging from 59 to 229 h as estimated by a tracer study²²².

Prior to April 2019, soda ash was used as the corrosion control agent in the DWDS. After a year-long model pipe loop study conducted with the Pennsylvania Department of Environmental Protection, the drinking water utility decided to switch their corrosion control over to PO_4^{3-} , as it was the more effective option given the water chemistry of the system. Prior to PO_4^{3-} implementation, the utility conducted a 7-month DWDS flushing campaign beginning in

September of 2018. PO_4^{3-} was applied at three different locations throughout the DWDS: once directly after treatment in the treatment plant, once at a DWDS pump station, and once after treated water was distributed from one of the storage reservoirs. PO_4^{3-} was applied into the DWDS in a step-down methodology over the course of 6 months, with a starting dosage of 3.0 mg/L PO_4^{3-} in April 2019 to help ensure proper scale formation. As of September 2019, orthophosphate has been dosed at 1.8 mg/L PO_4^{3-} for scale maintenance (Appendix C Figure 1).

4.2.2 Sample Collection

1L water samples from the seven distribution system monitoring sites were collected after flushing the faucet for at least five minutes and waiting for both the temperature and chlorine residual to stabilize²²³. All samples were filtered within one hour of collection through a 0.2 μm polycarbonate filter (Isopore Membrane Filters, EMD Millipore, Billerica, MA, USA) and the resulting filters were stored at -20 °C for DNA extraction. In reviewing the preliminary results, we observed a significant 2-log₁₀ increase in NTM density and determined that further testing would need to be done to understand what caused this increase. As such, 12L water samples were collected at the treatment plant and used for our NTM bench-scale reactor assays. Two separate sampling bottles (Nalgene, Waltham, MA) were filled with 6L of water pre- and 6L post- PO_4^{3-} addition, stored on ice after collection and their chlorine residual was quenched using sodium thiosulfate before use.

4.2.3 Water Quality

Fourteen water quality parameters were measured (Appendix C Tables 1 and 2) following standard methods²²⁴. Temperature and pH were monitored on site using a portable pH and temperature meter (Hanna Instruments, Ann Arbor, MI, USA) (Appendix C Figures 1 and 2). Free and total chlorine, and PO₄³⁻ concentrations at the tap were measured onsite using a portable DR900 spectrophotometer (Hach, Loveland, CO, USA) (Appendix C Figure 2). ATP was also measured onsite using an AquaSnap Total ATP meter (Hygiena, California, USA). Total and dissolved concentrations of iron, manganese, copper, and lead were measured by inductively coupled plasma mass spectrometry (PerkinElmer NexION 300 ICP-MS, Waltham, MA). Prior to analysis, all dissolved metal samples were prepared by passing water through a 0.45 µm nylon syringe filter (ThermoFisher, Waltham, MA) primed with 5 mL of sample. All analyses, except pH, temperature, and ATP were performed in triplicate.

4.2.4 Microbial Analyses

4.2.4.1 Droplet Digital PCR

DNA was extracted from the stored filters using the FastDNA Spin Kit (MP Biomedicals, Solon, OH) and stored at -20 °C until use. The density (number of gene copies per unit volume of sample) of total bacteria and *Cyanobacteria* was determined using digital droplet PCR (ddPCR) as previously described²²⁵. Additional ddPCR assays for *L. pneumophila* (*Lmip* gene)²²⁶, *P. aeruginosa* (*Orpl* gene)²²⁷, and NTM (*atpE* gene)²²⁸ were conducted using previously published primers (Appendix C Table 3) following the approach outlined in [Section 3.2.4.1](#).

4.2.4.2 16S rRNA Amplicon Sequencing

16S rRNA gene amplicon (V4-V5 hypervariable region) library preparation and sequencing were performed on all samples (collected DWDS samples and negative controls) at Argonne National Laboratory following the Illumina Earth Microbiome Protocol¹⁴¹. Samples were processed following the procedures detailed in [Section 3.2.4.2](#).

4.2.4.3 Bench-Scale NTM Reactor Experiments

Eight 1.5L glass batch reactors (Fisherbrand, Houston, TX) were set up to contain 1L of drinking water obtained from the DWDS within an hour of sample collection. Four reactors contained DWDS water pre- PO_4^{3-} injection, and the remaining four contained DWDS water post- PO_4^{3-} injection. All reactors were kept in dark conditions and placed on individual stir plates (Corning, Corning, NY) set to 300rpm and run in parallel for 12 weeks until the reactors were out of water due to sample collection. To examine direct impacts on NTM growth, three different species of NTM that are found in the DWDS and have clinical or laboratory relevance were injected into the reactors: *Mycobacterium abscessus* (collected from a hospital ice machine, PA), *Mycobacterium avium* (collected from a monochloramine DWDS, MI²²³), and *Mycobacterium smegmatis* (strain mc²¹⁵⁵²²⁹, provided by the DePas lab, University of Pittsburgh). Each mycobacterial species was grown in liquid R2A media with growth measured via optical density and plate counts prior to inoculation. Once grown, equal concentrations of all three liquid cultures were mixed achieving a final concentration of 1×10^8 cfu/L (representative of the DWDS NTM average) which was injected into each reactor. Biweekly samples were collected from each reactor and processed for culturable NTM (evaluated by plate counts on Middlebrook 7H11, following standard procedures) and total NTM, *M. smegmatis*, *M. abscessus* and *M. avium* absolute density by ddPCR using previously published primers (Appendix C Table 4).

4.2.4.4 NTM Aggregation Assays

To determine the impacts of PO_4^{3-} addition on NTM aggregation (biofilm formation), an assay developed by DePas et al.²³⁰ was utilized to distinguish and quantify aggregated cells and planktonic cells over time. Briefly, NTM cultures were grown in Tryptone-Yeast-Extract-Magnesium Sulfate (TYEM) nutrient broth prior to starting the experiment to ensure the same starting concentration. Once grown, liquid culture replicates ($n = 3$ in each experiment, 3 total experiments for $n = 9$ for each NTM species) were grown in fresh TYEM nutrient broth for 35hr (as previous work²³⁰ shows peak NTM dispersal within 35hr) with different concentrations of PO_4^{3-} (0, 1, 20, and 100 μM). Cultures were then harvested by passing the culture through a 10 μm (*M. smegmatis*) or 5 μm cell strainer (*M. abscessus*, *M. avium*) and the optical density (OD600) of both the planktonic fraction (i.e., cells that passed through the strainer) and the aggregates collected on the strainer were recorded. The OD600 of the planktonic fraction was immediately recorded, while aggregates that collected on the strainer were resuspended in phosphate-buffered saline (PBS) with 6% Tween20 (Sigma-Aldrich, St. Louis, MO, USA). This suspension was then sonicated to resuspend remaining aggregates before recording the OD600. OD600 readings were used to calculate the planktonic to aggregate ratios. Average planktonic/aggregate ratios were then compared across phosphate concentrations using non-parametric Wilcoxon testing (significance denoted at $p\text{-value} < 0.05$).

4.2.5 Statistical Analyses

Taxonomic and OTU tables generated for the samples were transformed using the Hellinger transformation due to the dataset having many rare OTUs (present in a few samples), or low abundance OTUs (i.e., less than 10% relative abundances¹⁴⁴). The transformed OTU data was

then used to calculate pairwise dissimilarities between samples based on the Bray-Curtis dissimilarity index. Resulting matrices were examined for temporal and spatial patterns in the bacterial community structure by Non-metric Multidimensional Scaling as implemented in the Vegan package (version 2.5-7) in R (version 4.0.2)¹⁴⁵. Significant differences in the microbial community compositions (Hellinger transformed OTUs) before and after PO_4^{3-} addition were determined by nonparametric permutational multivariate analysis of variance (PERMANOVA) and differential abundance analysis using DESeq2²³¹. Relationships between environmental parameters and patterns in microbial community composition were examined by canonical correspondence analysis (CCA) with significance tested by ANOVA after removing collinear variables (variance inflation factor analysis value <10) and reducing the overall suite of environmental variables with a stepwise Akaike information criterion model. Additionally, significant differences in the relative and absolute bacterial density before and after PO_4^{3-} addition and differences in NTM species aggregation were determined by non-parametric Wilcoxon testing, while the functional relationships between water quality parameters and bacterial groups were analyzed by stepwise multivariate forward / reverse regression analysis. All statistical analyses were performed in R (version 4.0.2)¹⁴⁷ with significance set at a p-value < 0.05.

4.3 Results and Discussion

4.3.1 Impacts of PO₄³⁻ Addition on DWDS Microbial Community Composition

4.3.1.1 Non-Metric Multidimensional Scaling Analysis

For the 98 samples collected from the DWDS over the course of 1 year, NMDS (Figure 12a and 12b) and PERMANOVA analysis on the 16S rRNA gene amplicon sequencing data showed significant seasonal ($r^2 = 0.08$, p -value < 0.001) and pre- and post-PO₄³⁻ addition ($r^2 = 0.035$, p -value < 0.001) variation in the DWDS microbial community structures. The observed seasonal differences in microbial community composition in the DS are consistent with previous studies^{27,232} and the observed differences in communities based on PO₄³⁻ dosing corresponds with results found in Douerlo et al.²⁰⁸. Additionally, significant spatial differences were observed ($r^2 = 0.07$, p -value < 0.001), which is to be expected as each DWDS site has a different residence time and differing hydraulics and plumbing materials, however these spatial differences were only driven by temporary differences at one or two sites.

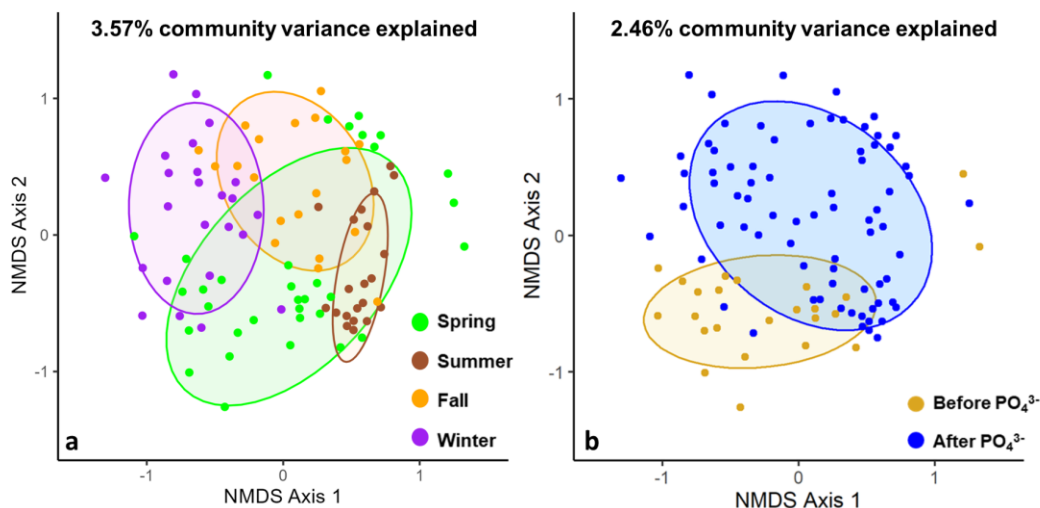


Figure 12: Non-metric Multi-Dimensional Scaling plots for all DS samples separated by a) season and b) orthophosphate addition into the DS (stress values = 0.26).

The percentage contribution of each parameter as determined by Canonical Correspondence Analysis is displayed at the top of each graph. The ellipses represent the 95% confidence interval of the distribution from the centroid of the cluster of points.

4.3.1.2 Alpha Diversity and Relative Abundance Analysis

Overall, few significant differences were found in community alpha diversity (e.g., Shannon diversity, Chao's richness, Pielou's evenness) one year after PO_4^{3-} addition despite the fact that previous work has found DS microbial communities to have temporal fluctuations due to differing flow patterns, season, location, and treatment processes^{27,205,232–234}. After one year of PO_4^{3-} addition, the average Chao's richness significantly increased (before: 52 ± 23 , after: 172 ± 190 , p-value = 0.037), which coincides with previous work detailing that environmental factors such as PO_4^{3-} concentration can act as a selective force in DWDS systems²⁰⁸. However, in Douterelo et al., they found that increased PO_4^{3-} decreased the richness of the microbial community. The contradiction in findings could be a result of DWDS differences including source water communities, DWDS pipe materials, and PO_4^{3-} dosing schemes. PO_4^{3-} was dosed into the

DWDS in Douterelo et al. at 1.2 mg/L, while in the DWDS examined here, the utility started dosing PO_4^{3-} into the DWDS at 3.0 mg/L and then lowered the concentration to 1.8 mg/L over time. The inclusion of a step-down approach for PO_4^{3-} dosing in the DWDS is likely a critical step in shaping the microbial membership within the pipe systems and its impact should be clarified in future studies. While richness significantly increased after one year of PO_4^{3-} addition, it is important to note that diversity is a combination of both richness and relative abundance of organisms. Therefore, while there can be an increase in the total number of organisms, if the relative abundances do not shift (i.e., in the case of an increase in a myriad of rare taxa at low abundances) then it is likely that community diversity will not change. Given this, the lack of significant differences in alpha diversity metrics could also be attributed to the shifting of functional or ecological niches, the varying C:N:P ratio requirements of different microorganisms^{186,187}, or a result of the duration of the study.

Examining community membership, the top ten phyla present in all DWDS sites were predominately composed of: *Acidobacteria*, *Actinobacteria*, *Bacteroidetes*, *Chloroflexi*, *Cyanobacteria*, *Dependentiae*, *Firmicutes*, *Planctomycetes*, *Proteobacteria*, and *Verrucomicrobia*. *Proteobacteria* and *Actinobacteria* dominated across all DS sites (Figure 13), comprising up to 98% of the community at times throughout the study. These results are consistent with other DWDS studies that examine community membership at the phylum level²³⁵⁻²³⁷. Furthermore, the *Acinetobacter*, *Pseudomonas* and *Sphingomonas* genera were the only three genera within the top 10 most abundant taxa present both before and after PO_4^{3-} addition (Figure 13), while a mix of smaller proportioned genera dominated across the sites.

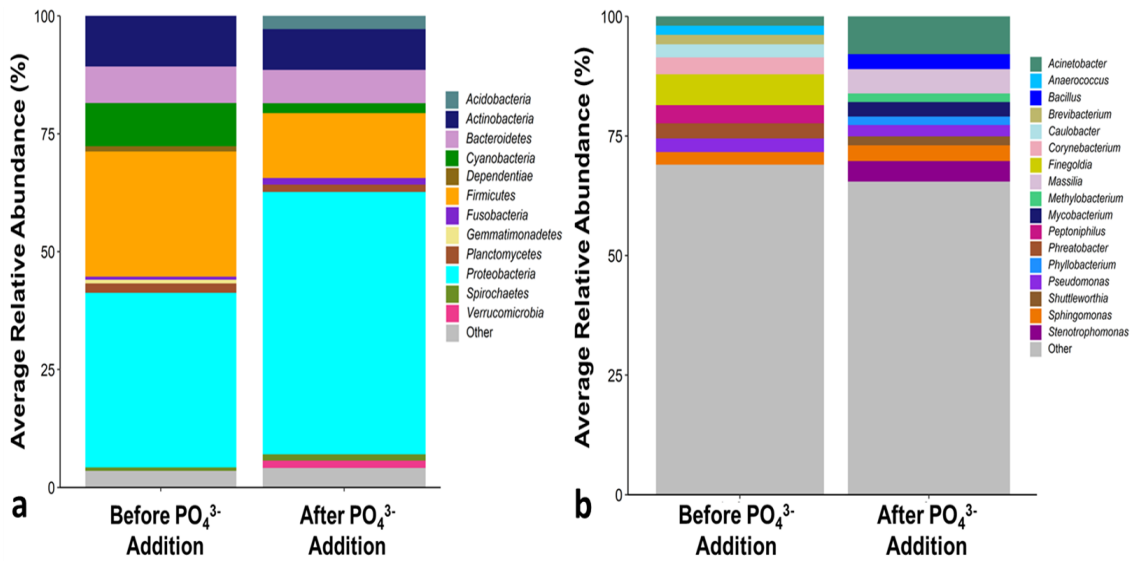


Figure 13: a) Top 10 most abundant phyla and b) top 10 most abundant genera across all DWDS sites before and 1-year after full-scale PO_4^{3-} addition (n = 14 in each condition).

To control for seasonality, only the matching months before and after PO_4^{3-} application were compared.

Apart from *Cyanobacteria*, differential abundance analysis revealed no other significant changes in the relative abundance of typical drinking water phyla. At the genus level, there were multiple significant changes in the abundance of rare drinking water taxa (e.g., *Nevskia*, *Stenotrophomonas*) and other uncultured organisms that could not be identified further. *Cyanobacteria* (particularly non-photosynthetic relatives such as *Melainabacteria*, which made up a third of the *Cyanobacteria* present in the DWDS) generally represented 10% or less of the DS microbial community and appeared to significantly decrease (9% before PO_4^{3-} addition, 2% one-year after PO_4^{3-} addition, p -value = 0.02) after PO_4^{3-} addition into the DWDS. This observed significant decrease in *Cyanobacteria* relative abundance is consistent with results from nutrient limitation assays conducted using water from the DWDS by Balangoda et al¹⁴⁹. Specifically, it was observed that green algae and *Cyanobacteria* grown in PO_4^{3-} treated DWDS waters collected a year after PO_4^{3-} addition only grew when provided with additional nitrogen treatment, as

compared green algae and *Cyanobacteria* in DWDS waters prior to PO_4^{3-} treatment that needed both phosphorus and nitrogen supplement. This observation suggests that nutrient limitations shifted for *Cyanobacteria* in the DWDS, going from nitrogen-phosphorus co-limitation to strict nitrogen limitation. In previous studies^{125,238} conducted in lake systems, similar observations of inhibited cyanobacterial growth in the presence of specific elevated nutrients have been observed, while a recent study suggests that inorganic phosphate can act as an inhibitor for energy storage enzymes, thus reducing the amount of energy available for use under nutrient limited conditions²³⁹. As such, the decrease in the relative abundance of *Cyanobacteria* in the DWDS could suggest a shift in the nutrient limitation in the DWDS and be used as a potential indicator to evaluate nutrient limitations in situ. However, further work is warranted to understand, evaluate, and better maintain nutrient limitations in the DWDS to control microbial presence and to better evaluate impacts on *Cyanobacteria* and related organisms abundance in drinking water such as *Melainiobacteria* like *Vampirovibrio spp.*,

The few significant changes in typical drinking water taxa observed in the DWDS microbial relative abundance in this study could be a result of the short duration of the study, as one year may not have been enough time to see any drastic impacts in microorganism abundance. Furthermore, although all DWDS monitoring sites receive water from the same treatment plant, the residence time varies widely between them, which could also have an impact on the types of organisms present²⁴⁰. The response in only a few typical taxa and many more rare (i.e., < 1% abundant or detected in a few samples) could also be indicative of shifts in microbial niches and function in response to elevated phosphate concentrations (and in turn, changes in nutrient limitations, C:N:P ratios, etc.), rather than shifts in taxonomic composition.

4.3.1.3 Impacts of Environmental Parameters

CCA revealed that 16.4% of the variance in the microbial community composition could be explained by a combination of factors including: the geographic location of the DWDS sites, the season samples were collected in, pH, total copper concentration, total iron concentration, and total phosphorus (Table 6). Spatiotemporal (i.e., season and site location) variation was expected as previous work has highlighted the impacts of spatial^{27,205,232}, temporal^{205,233}, and seasonal effects^{27,234} on the drinking water microbial community processes. Likewise the impacts of pH, phosphorus and dissolved metals have been shown to impact the DS microbiome^{208,210,211,213,219,232}. Other parameters that are important include water temperature, disinfectant residual, and residence time within the pipe. Water temperature was a significant confounding variable (determined by variable inflation factor analysis) when included in the model with season, which is expected as water temperature is often a function of the season. Similarly, residence time within the pipe was also a confounding factor with DWDS site location. Disinfectant residual not contributing to the variance in the community composition is interesting because it has been observed that both community composition and functional potential are impacted by the presence of disinfectants in a DWDS^{27,241,242}. Due to the relationships between disinfectant residual, residence time, water temperature, pipe material and corrosion, and inherent biofilm kinetics in the DWDS, it is likely that the impacts of disinfectant concentration were masked by site. Overall, to better examine this in the future, studies should consider collecting additional information including pipe material and disinfection byproduct measurements at the sampling point in the system, as well as conducting long terms studies at specific sites.

Table 6: Linear effect models for the whole distribution system community composition, and absolute density of NTM and *L. pneumophila* using all the distribution system water samples collected (n=98) over the course of one year

Taxa	Data Transformation ^a	Model components ^b	Explained by Model ^c
Community Composition (OTUs)	hellinger(x)	DWDS Site Location ^{6.38%} ± Season ^{3.57%} - pH ^{1.41%} + Total Copper ^{1.32%} + Total Iron ^{1.25%} - Total Phosphorus ^{2.46%}	16%
NTM	x ^{-0.3}	Season ^{29%} + Total Phosphorus ^{17%} - <i>L. pneumophila</i> ^{16%} - pH ^{6%} - Total Iron ^{3%} + Turbidity ^{3%} + <i>Cyanobacteria</i> ^{1%}	75%
<i>L. pneumophila</i>	x ^{0.2}	Season ^{36%} - NTM ^{16%} - Total Phosphorus ^{12%} + Total Iron ^{4%} - Total Chlorine ^{4%} + pH ^{3%} - Turbidity ^{1%}	76%

^aNTM and *L. pneumophila* concentrations were transformed using the Box-Cox method in R to ensure normal distributions of the data for the models. ^bSuperscript numbers proceeding each component in the models show their relative percent contribution to the overall model. ^cPercentage explained pertains to the adjusted R² for the overall model. All models were significant at p-values <0.001

4.3.2 Predicted Impacts of PO₄³⁻ Addition on DWDS Microbial Function

4.3.2.1 Default phenotypes

Throughout the DWDS, there were significant differences in the default phenotypic traits (e.g., aerobic, anaerobic, biofilm formation) at two of the seven monitoring sites after PO₄³⁻ addition into the DWDS. At site DS2 there was a decrease in the average predicted relative abundance of organisms that contained mobile genetic elements (MGEs), while at site DS6 there were increases in the predicted abundance of aerobic organisms and organisms capable of forming biofilms (Figure 14). MGEs (e.g., plasmids) are responsible for the mediation of horizontal gene transfer in bacteria, provide an important source of genetic diversity in microbial communities²⁴³, and are most often linked with the transmission of antibiotic resistance genes (ARGs)²⁴⁴. The observed

decrease in organisms containing mobile elements after PO_4^{3-} addition into the DWDS could be indicative of increased microbial community adaptation to the environment. Many DWDSs are phosphorus limited^{216,245} and often many organisms must utilize mechanisms like horizontal gene transfer to improve stress tolerance or gain a competitive advantage. In the presences of elevated phosphorus from PO_4^{3-} addition, it is possible that the C:N:P ratios at this site were favorable for organisms to not need to inherit genes or other mobile elements to keep a competitive advantage. However, more work over a longer period would need to be done to confirm this and identify if the increased MGEs correlates with increased ARGs. The increase of organisms capable of aerobic respiration and biofilm formation after PO_4^{3-} addition at site DS6 could be indicative of adaptive responses to keep the community stable. Specifically, it has been reported that increasing phosphorus concentrations can result in a reduction in extracellular polymeric substance (EPS) or an increase in the amount of pores present in the biofilm, thus weakening biofilms and making them more susceptible to detachment under drinking water pipe flows^{208,246}. If there were to be a huge detachment event, other organisms that may have been outcompeted in biofilm formation might have a new niche to fill in absence of those organisms lost to detachment; however, more work would need to be done to confirm this. Additionally, it is also important to mention that these differences were not observed site wide, suggesting that there may be more complex interactions at each specific site at play that were not captured in the sampling campaign. As such, it is imperative that long-term and site-specific monitoring be conducted to better understand the impacts of PO_4^{3-} on a per site basis to help inform what level of PO_4^{3-} dosing is needed to prevent lead leaching and adverse impacts to microbial communities.

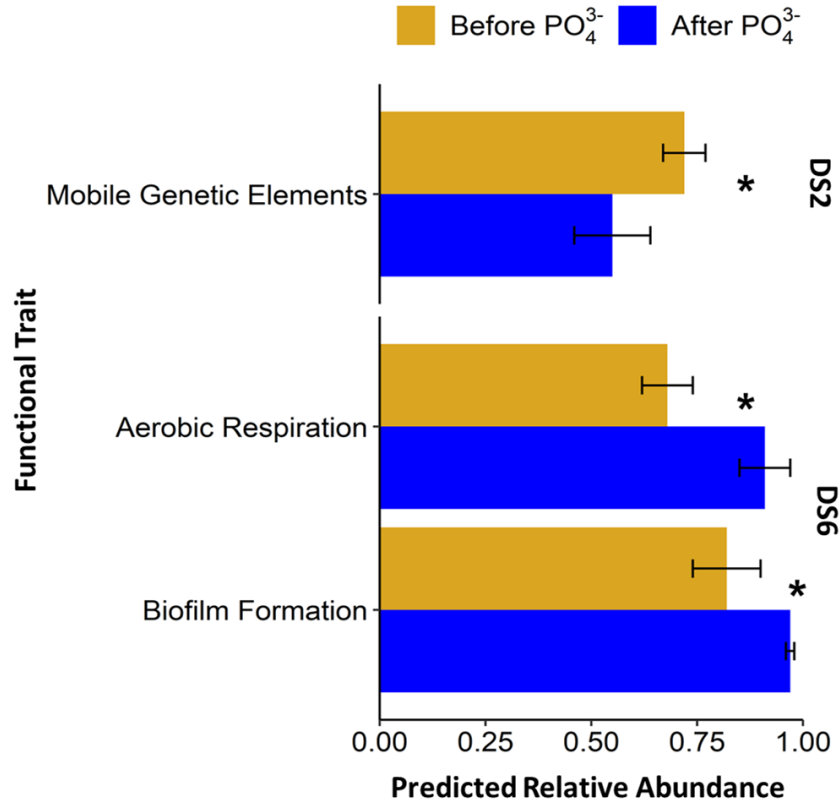


Figure 14: Significant changes in predicted relative abundance of default phenotypes at sites 710 and 773 in the DWDS, significant difference at a p-value < 0.05 are denoted by *

To control for seasonality, only the matching months before and after PO₄³⁻ application were compared.

4.3.2.2 Phosphate utilization phenotypes

Of the phenotypes relating to phosphate uptake, significant increases in the UhpBA two component regulatory system and the NAD(P)H quinone oxidoreductase were observed after PO₄³⁻ into the DWDS (Figure 15). The predicted significant increase in the UhpBA system is understandable as the UhpBA system has been linked to phosphate uptake¹⁸⁵. The increase could be indicative of a shift in microbial community function as the application of phosphate would apply a selective pressure to the current community, but further work using RNA-based or genomic approaches would need to be done to confirm this. Additionally, a predicted significant decrease in the NAD(P)H quinone oxidoreductase in chloroplasts and cyanobacteria was observed. The

NAD(P)H quinone oxidoreductase (NQR) is a flavoenzyme that helps in detoxifying water soluble quinones (i.e. ubiquinones) via two-electron reduction, preventing cell death from the oxidative stress that results from the single-electron reduction of quinones²⁴⁷. In cyanobacteria, NQR plays a role in the respiratory electron transport chain. Given the significant decrease in cyanobacteria and its non-photosynthetic relatives in the DWDS, a decrease in the NQR would be expected. The decrease in NQR could also be indicative of the downregulation of genes such as the *drgA* gene, which control cell resistance to bactericidal agents²⁴⁷. Furthermore, the decrease in NQR could simply be a result of the excess phosphorus present, and as such, the microorganisms have adapted to producing more NADH, rather than NAD(P)H.

4.3.2.3 Nitrogen utilization phenotypes

Of the phenotypes relating to nitrogen utilization, the observed decreases in ammonia nitrification and nitrate denitrification may be a result of the increased phosphorus concentration in the distribution system, and as such, an attempt to keep the N:P ratio stoichiometrically favorable in an already nutrient limited environment. Likewise, the observed decrease in ammonia nitrification and nitrate denitrification could be connected to the results from Balangoda et al, as the DWDS switched from N:P co-limitation to strict nitrogen limitation one year after PO_4^{3-} addition. Nitrogen utilization in the DWDS is often important in systems where chloramines are deployed as a supplementary disinfectant in response to poor free chlorine stability in the system. Chloramination can provide ammonia into the system which can then in turn promote the growth of nitrifying organisms, such as *Nitrosomonas spp*^{27,248}. Although not the case here, the observed changes in nitrogen utilization after PO_4^{3-} into the DWDS generate further questions about how PO_4^{3-} addition would impact the microbial communities of chloraminated systems. As such, future

studies should consider incorporating the examination of changes in community functional traits after making operational changes in a wide range of systems to ensure no adverse effects occur.

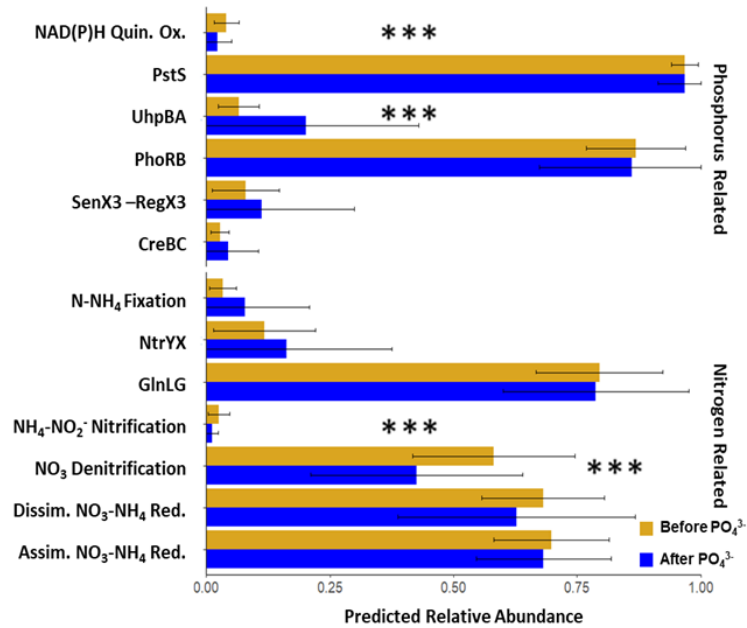


Figure 15: Predicted relative abundance of phosphorus & nitrogen related phenotypes in the DWDS, significant difference at a p-value < 0.001 are denoted by ***

A p-value of 0.001 was selected as the significance threshold because the functional trait prediction analysis was conducted on DNA samples rather than RNA samples. To control for seasonality, only the matching months before and after PO₄³⁻ application were compared.

4.3.3 Impacts of PO₄³⁻ on Bacterial density and DWPI density

As expected, the absolute density of total bacteria significantly increased one year after PO₄³⁻ addition into the DWDS with a 50-fold increase in observed density (Figure 16a, Appendix C Figure 3). This change was likely driven by a 2-log₁₀ increase in NTM density at all DWDS sites (Figure 16b). Interestingly, during this same timeframe a significant decrease in *L. pneumophila* density was observed across all DS sites (Figure 16a), likely due to a significant decrease in the

frequency of detection (100% detected before PO_4^{3-} , 62% detected after PO_4^{3-} , p-value < 0.001). Previous work has discussed the negative correlation between *Legionella* spp. and *Mycobacterium* spp.²³⁴ that may be due to both DWPIs competing for the same nutrients and niche. Further regression analysis revealed 76% of the variance in *L. pneumophila* density was explained by a combination of factors including NTM density (Table 5), further suggesting their proposed antagonistic relationship. However, it is also important to note that the significant decrease in the frequency of detection could be due to *L. pneumophila* density falling below the limit of detection of our method (this seems unlikely given the detection limit is one organism) or *L. pneumophila* entering protozoan hosts, which is often observed during times of stress^{249–251}.

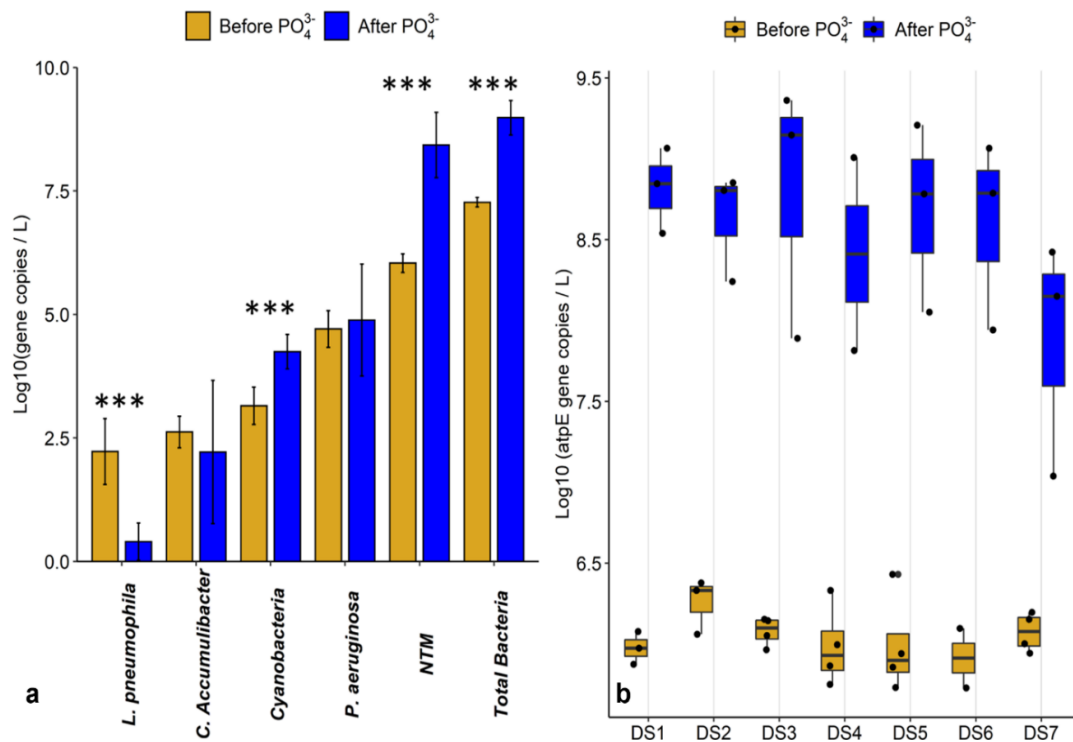


Figure 16: a) Geometric average (n = 14) of absolute density of DWPIs, total bacteria, *Cyanobacteria*, and *C. Accumulibacter* in the DWDS before and one year after PO_4^{3-} addition. Error bars represent the standard deviation. *** signifies a significant difference in measured density at p-value < 0.001. b) Boxplot of NTM absolute density at each DWDS site before and one-year after PO_4^{3-} addition.

In both graphs, the pairwise data (i.e., February & March 2019 - before and February & March 2020 - one-year after PO₄³⁻ addition) was used to control for seasonal fluctuations in density.

Interestingly, sequencing results (relative abundance) of both *Actinobacteria* (3% decrease, p -value = 0.073) and *Mycobacterium* (1.5% increase, p -value = 0.483) do not reflect this significant increase, suggesting that community changes were driven at the subgenus level as reflected by ddPCR results. It is also important to note that since our sequencing assays targeted the 16S rRNA gene which can vary between organisms, another possibility is that *Actinobacteria* and *Mycobacterium* differences may be masked by biasing towards changes in organisms with higher 16S rRNA copies (*Mycobacterium* have 1 copy of the 16S rRNA gene compared to the average 5.3 copies in bacteria in general). Possibly with metagenomics or more sampling, we may have observed changes in the *Mycobacterium* genus and future studies should take this into consideration when designing and planning to analyze these organisms. It is also important to note that the differences in assay target can make it challenging to analyze and compare these organisms. When doing amplicon sequencing (typically 16S rRNA), the data is generally reported as the relative abundance of the 16S rRNA gene copies present, while in ddPCR assays your gene target can be more specific (i.e., the *atpE* gene, the *hsp65* gene). This could also account for differences in assay results and should be considered when evaluating changes in taxa at lower order taxonomic levels (e.g., genus, species).

Previous work has detailed the ability of actinobacterial species to solubilize and uptake phosphorus in soil, freshwater, and marine environments^{252–254} and as such the observed significant increase in NTM density could result from the freshwater origins of the drinking water. Additionally, other work has shown a positive correlation between *Actinobacteria* abundance in drinking water systems and total phosphorus concentration²⁵⁵ while previous metagenomic work

has suggested that *Actinobacteria* may have a key role in phosphorus sequestration²⁵⁶ in the environment. Regression analysis on the NTM density data revealed that 74% of the variance in NTM density was explained by a combination of seasonality, total phosphorus concentration, *L. pneumophila* density, pH, total iron concentration, and turbidity (Table 5). Previous work has highlighted that NTM are impacted by factors such as season²⁵⁷, turbidity²⁵⁸, pH, nutrient availability, and metal concentrations^{259–261}. Interestingly, however, the observed increase in NTM (Figure 17) also coincided with a decrease in water temperature (Appendix C Figure 1). This observation was counterintuitive as previous NTM work has reported seasonal increases in NTM during warmer times of the year²⁵⁷ and positive correlations with warmer water temperatures²⁶². As such, the observed increase could have been due to a change in the biofilm population of NTM or potentially a response to a shift in ecological niches.

Similar to *Legionella*, the genus *Methylobacterium* is also thought to have an inverse relationship with *Mycobacterium*, as previous work has highlighted the absence of *Mycobacterium avium* in showerheads colonized with *Methylobacterium spp*^{200,263,264} and a more recent study highlights that *Methylobacterium spp.* presence can impact *Mycobacterium* biofilm formation²⁶⁵. In the DWDS examined, *Methylobacterium* had an average relative abundance of < 1% in samples collected before PO₄³⁻ addition and an average relative abundance of 2% in samples collected one year after PO₄³⁻ addition into the system. Furthermore, no significant relationship between *Methylobacterium* and *Mycobacteria* was observed in the examined system, so it is unlikely that changes in NTM were due to *Methylobacterium* presence. Given the observed increase in NTM density after PO₄³⁻ addition was not associated with other microbiome members it was important to determine whether the addition of PO₄³⁻ increased NTM growth or altered biofilm processes.

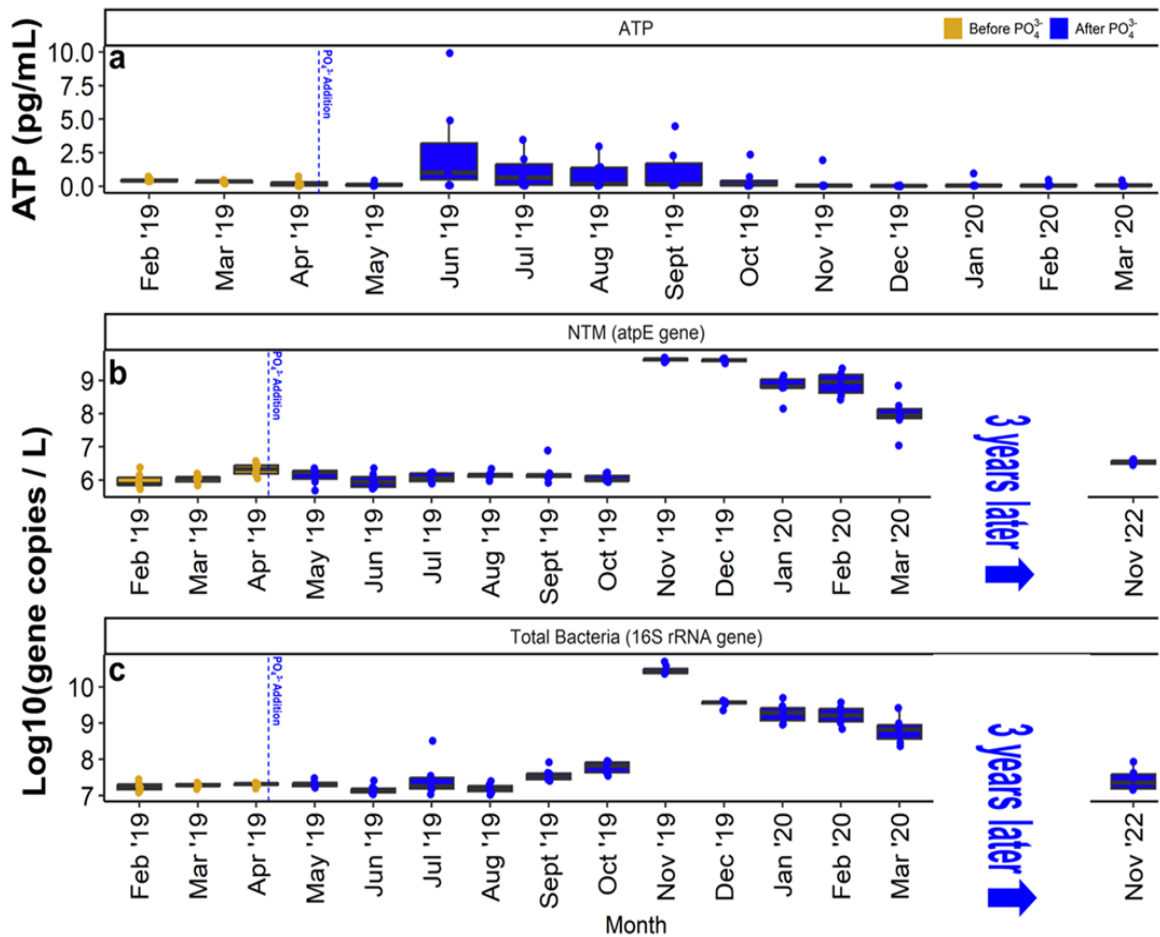


Figure 17: a) ATP, b) absolute NTM density and c) total bacterial density in the DWDS throughout the study duration and comparison three years later.

Note: only six samples were collected in 2022, as one of the routine monitoring sites has been shut down. No ATP measure was taken in the 2022 samples.

4.3.4 Impacts of PO_4^{3-} on NTM growth and aggregation potential

Since the two- \log_{10} increase in NTM density was observed suddenly across all DWDS sites seven months after PO_4^{3-} addition (November 2019; Figures 17, Appendix C Figure 4), further bench-scale experimentation to understand the mechanism driving this were performed. More specifically impacts on NTM growth and aggregation (biofilm formation) potential in the presence

and absence of PO_4^{3-} were assessed. Both viability (plate counts) and ddPCR analyses revealed no significant differences in total NTM or NTM species (*M. smegmatis*, *M. avium*, and *M. abscessus*) density between samples treated with or without PO_4^{3-} (Appendix C Figure 5). Interestingly, *M. smegmatis* was only detected in 9% of the samples taken, possibly because the laboratory mc²155 strain was outcompeted by the environmental *M. abscessus* and *M. avium* strains and other DWDS microbiota. It should also be noted that while all NTM were quantified (as identified by the *atpE* gene) in the DWDS, both *M. avium* and *M. abscessus* were present in the system at the time of the increase, albeit at lower densities (Appendix C, Figure 6). Given the sudden increase in the total NTM density in the DWDS and the lack of significant differences in batch reactor NTM growth (Figure 17, Appendix C Figure 5), it was unlikely that the PO_4^{3-} addition caused a significant impact on NTM growth. Instead, it is possible the PO_4^{3-} addition impacted NTM biofilm processes (formation and sloughing).

Biofilm formation is a complex, dynamic, and a continuous process that has several stages, some of which are dependent on nutrient concentrations^{266,267} and specific to the type of bacteria present²⁶⁸. Generally, the process is divided into three major stages: adherence, proliferation, and dispersal²⁶⁸. As nutrient concentrations shift and as biofilms begin to reach full maturity (i.e., maximum volume), it is possible for organisms within biofilms to disperse into the planktonic phase and recolonize in areas where conditions are more suited to biofilm growth²⁶⁷. Previous studies have shown the impact of phosphate concentration on the production of extracellular polymeric substance (EPS, an important component in bacterial adhesion in biofilms)^{210,269,270} and biofilm structural mechanics^{246,271,272}. Specifically, it has been reported that increasing phosphorus concentrations can result in a reduction in EPS or an increase in the amount of pores present in the

biofilm, thus weakening biofilms and making them more susceptible to detachment under drinking water pipe flows^{208,246}. With respect to *Mycobacteria*, previous work has suggested that a lack of phosphate triggers the expression of genes and metabolic pathways relating to mycobacterial cell aggregation²⁷³, while a clinical study mentioned use of PBS to keep mycobacterial cultures in suspension²⁷⁴. Given these considerations, it was hypothesized that increasing phosphate concentrations could impact the aggregation potential of NTM species and the stepdown in PO_4^{3-} dose in the DWDS (starting dose = 3.0 mg/L, scale maintenance dose = 1.8 mg/L) could likely be an explanation for the observed increase.

To elucidate the impact of phosphate on NTM aggregation, a comparison of planktonic and aggregate fractions of NTM cultures grown at varying phosphate concentrations was conducted following the protocol developed by Depas et al. In nutrient rich media (primarily C:N dominated), DePas et al. observed initial aggregation with aggregate dispersion and planktonic growth occurring around 35 hours and beyond²³⁰. In the presence of phosphate-augmented media, *M. smegmatis* behaved similarly to what was observed by DePas et al., however, *M. abscessus* and *M. avium* behaved differently (Figure 18).

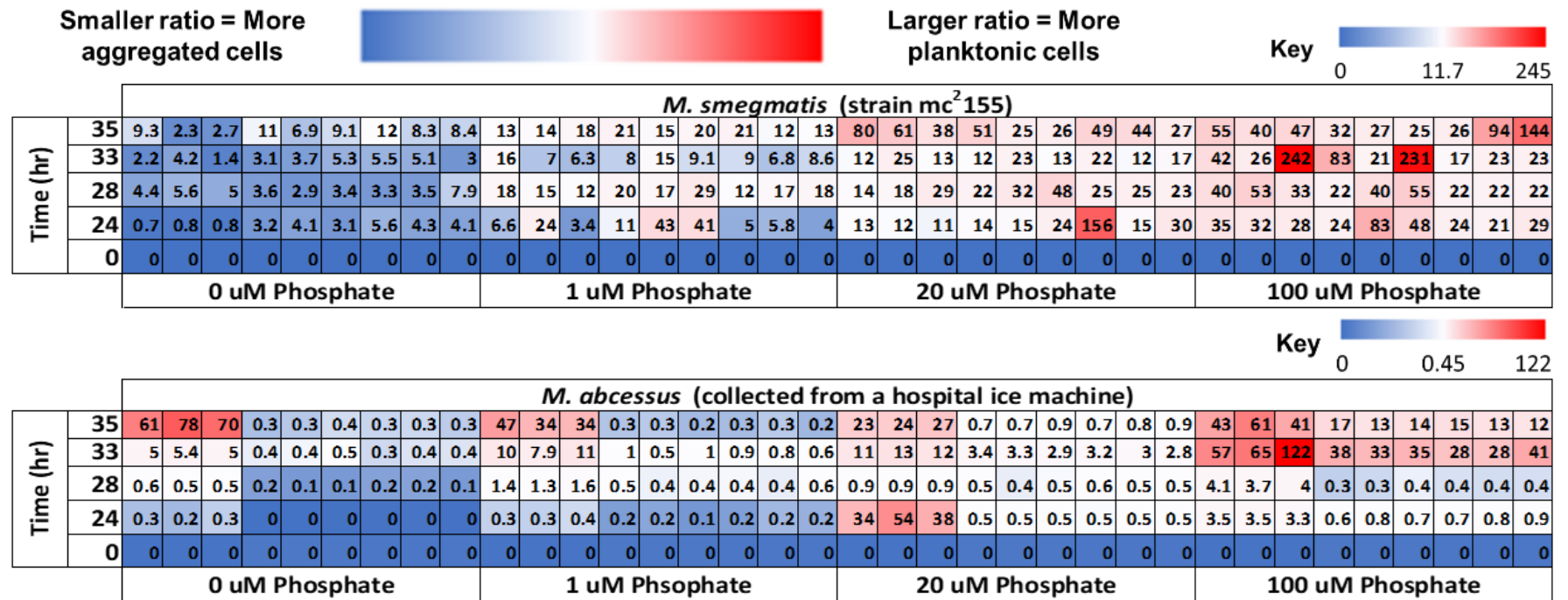


Figure 18: Planktonic vs aggregate NTM ratios (ranges in parentheses) for *M. smegmatis* (0 – 245) and *M. abscessus* (0 – 122) at different concentrations of phosphate (each tile is one technical replicate, for a total of n = 9 per species x phosphate concentration x time).

Blue colored cells represent a smaller ratio, signifying a larger proportion of aggregated NTM cells while white/red colored cells represent a higher ratio, signifying a larger proportion of planktonic NTM cells. The white cells represent the 50th percentile of each specific species dataset. The ratios were obtained by dividing the planktonic OD600 measurements by the aggregate OD600 measurements.

The impacts of different phosphate concentrations on NTM species dispersal seem to be species dependent, as the results of the NTM aggregation assay on *M. abscessus* revealed an increased ratio with higher phosphate concentrations, while the same trend was not observed with *M. avium*. The NTM aggregation assays for *M. abscessus* revealed significantly (p-value < 0.001) lower average ratios (more aggregate or fractions) in the 0 μ M and 1 μ M phosphate conditions compared to the 20 μ M and 100 μ M conditions (Figure 18, Appendix C Figures 7, 8). The increased ratio in the presence of elevated phosphate suggests that increased phosphate concentrations may cause disaggregation (potentially biofilm sloughing) for *M. abscessus*. In the *M. avium* assays, elevated ratios were present regardless of phosphate concentration (Figure 18), suggesting that phosphate concentration had less impact on *M. avium* than other NTM species.

The differences observed in NTM species could be attributed to differences in nutrient requirements between rapid- and slow-growing NTM, as one study posits that slow growing mycobacteria (e.g., *M. avium*) may not benefit from elevated phosphorus concentrations when compared with rapidly growing mycobacteria²⁷³. Additionally, previous spatial work has demonstrated NTM are late colonizers of biofilms in drinking water²⁷⁵. Therefore, it is possible that NTM could be on the outer surface of drinking water biofilms making detachment easier, however, more work is needed on the localization of NTM in drinking water biofilms. Furthermore, it is also possible that phosphate interacts with the constituents of the outer membrane of mycobacterial cells and causes a change in the cell hydrophobicity, however to the authors knowledge this has not been explored.

Given the data presented, it is possible the sudden increase in NTM in the DWDS was due to a large biofilm sloughing event, an interaction between phosphate and the NTM cell walls, or a

combination of both. Moreover, given what appears to be a gradual decrease to a new increased baseline NTM density (Figure 17), it is also important to consider the timescales of impact. Previous work has examined the impact of nutrient starvation on biofilm formation and suggests that prolonged nutrient starvation can lead to increased biofilm detachment²⁷⁶. In the presented system, the shift from excess PO_4^{3-} dosed in at 3.0 mg/L down to 1.8 mg/L could have been enough of a shift to trigger a starvation response from the biofilm. It could also be possible that the length of the elevated NTM concentrations were a delayed response to the change in DWDS PO_4^{3-} concentration (Figures 17, Appendix C Figure 5). Future studies should identify the drivers of NTM disaggregation in the presence of elevated phosphate concentrations, create a more normalized process for examining disaggregation that captures robust species dynamics and elucidate the species differences in biofilm formation potential, as well as determine the timescale of sloughing events in the DWDS. Additionally, connecting these results back to the sequencing results, future studies should also examine the potential antagonistic interactions with other organisms such as *Methylobacterium* to better understand how those interactions also shape and contribute to biofilm formation in a complex environment like the DWDS.

4.4 Conclusions

Overall, the results presented here suggest PO_4^{3-} addition into the DWDS temporarily increased the total number of bacteria present in the DWDS and altered community structure with respect to an increase in NTM and decrease in *L. pneumophila* density. The findings presented provide an interesting basis for the continued monitoring of DWPIs in nutrient-limited water treated with PO_4^{3-} corrosion control and demonstrated the need for surveillance during operational changes. Furthermore, as PO_4^{3-} addition has been shown to elicit a 2- \log_{10} increase in NTM density in a full-scale DWDS, likely driven by biofilm disaggregation from the results of the aggregation assays, more work is needed to understand the mechanisms driving this process. Future studies should consider using enhanced set-ups (e.g., pipe, continuous flow, or biofilm reactors with DWDS materials) to (1) conduct more targeted analysis (ddPCR and sequencing of different genes e.g., *hsp65*), (2) to determine what specific types of NTM or other DWPIs are present in a full scale DWDS, and (3) to continue to develop our understanding of the impacts of nutrients on these organisms and biofilm formation. Likewise, although no changes in NTM pulmonary disease incidence have been observed to date, additional longitudinal studies are required to ensure no adverse health impacts arise.

5.0 Specific Aim 4.0: Identification of Basement Floodwater Source and the Links to Resident Health

Specific Aim 4.0 was funded by The Pittsburgh Foundation (grant number: UN2021-121327) and the Center for Healthy Environments and Equity Research (CHEER) through the University of Pittsburgh's School of Public Health. At the time of writing, sample collection and water quality analysis for Specific Aim 4.0 is still ongoing. As such, only a subset of the data will be presented for the purposes of this document. Further commentary is given in Chapter 7 on future directions for this work. The presented results have been shared with faculty, staff, students, and community partners at university held forums. These results have not yet been published in any peer reviewed journals or presented at any conferences.

5.1 Introduction

Among all natural hazards (e.g., earthquakes, heat waves, etc.), flooding has the greatest economic and social impacts across the entire United States, with said impacts increasing with time²⁷⁷. Historically, most flooding research, mitigation strategies, and policies have been targeted at coastal regions threatened by rising sea levels, hurricanes, and climate change²⁷⁸. However, flooding in urbanized areas presents an emerging issue in urban water management. In particular, flooding due to heavy rainfall events can overwhelm aging and deteriorating water infrastructures, thus releasing pathogens and chemical contaminants from untreated wastewaters back into the environment^{279,280} by way of combined sewer systems. In the United States, approximately 40 million people are served by combined sewer systems in which stormwater and sewage are both conveyed in the same pipe²⁸¹.

In the City of Pittsburgh, recent shifts in precipitation patterns (15% increase in average annual rainfall levels from 2016-2020 compared to 2010-2015) combined with other geological, topographical, and environmental factors (e.g., percentage of impervious pavements) have contributed to increased flooding patterns and events (e.g., flash floods). As a result of increasing precipitation and stormwater volumes, Pittsburgh releases 34 billion liters of combined sewer overflow (mixed wastewater and stormwater) into local surface waters annually²⁸², which results in violations of the Clean Water Act and can result in complications in downstream water processing (e.g., drinking water treatment). Likewise, the increase in precipitation and subsequent flooding also has impacts on urban environments. Many urban residents often experience the effects of flooding through sewer backups and basement inundation²⁸³.

As such, it is imperative to identify and better understand the potential public health risks associated with basement floodwaters that could potentially contain untreated wastewater and

sewage. Urban floodwaters originating from backflow from combined sewer overflows may contain human enteric pathogens such as norovirus or other gastrointestinal (GI) pathogens. Non-foodborne gastroenteritis causes diarrheal disease, is most often associated with nausea and abdominal pain, and is estimated to cause 135 million infections each year in the United States, with *Salmonella* spp., *Campylobacter*, and norovirus as the leading causes of hospitalization^{284,285}. Previous studies^{286–289} have identified high levels of pathogenic waterborne microorganisms including *E. coli*, *Enterococci*, *Salmonella* spp., *Campylobacter*, *Cryptosporidium* spp., and norovirus after flooding or in contaminated water events, and recent work has suggested that stormwater exposure is related to an increase in GI-infection related hospital visits^{290–295}. Previous work has also explored the relationship between urban flooding events and microbial exposures^{286,289,296,297}, but there is still a relative lack of understanding about how infection risks can be attained from and incorporated into hydrologically based flood models. Recently an urban flooding study (sewage backflow)²⁹⁷ calculated the combined infection risk of *Campylobacter*, *Cryptosporidium*, *Giardia*, norovirus, and enterovirus using quantitative microbial risk assessment (QMRA) using the dose response approach described in de Man et al. (2014)²⁸⁶. In this study, assumptions of floodwater volume exposure, duration of exposure and homogeneous pathogen distribution were made and while this is a good start to addressing this issue, more information is needed regarding the pathogens present, distribution of pathogens, and exposure volumes²⁹⁸ to urban floodwaters).

Moreover, while more recent incorporations of QMRA into urban flooding models has resulted in more useful estimations of microbial risks associated with GI pathogens, there are still constraints with pathogen concentrations both for typical GI pathogens and other water relevant organisms not yet examined (e.g., DWPIs). Although human exposure to DWPIs can occur

through many pathways (e.g., ingestion of contaminated drinking water), inhalation of drinking water associated aerosols has been linked to pulmonary infections^{12,299,300} and studies have found that incidence of pulmonary infections caused by DWPIs are higher in rainy seasons^{301–303}. Despite these observations, DWPI transmission by aerosolization, aerosolization risks, and mitigation strategies are still poorly understood. Furthermore, the majority of DWPI outbreaks have not been linked back to specific water sources, further highlighting the need for both biogeographical surveys and quantitative risk assessments. Without both tools working in tandem, a more holistic understanding of exposure and risk assessments in our living spaces cannot be achieved and the development of proper mitigation strategies will be further delayed.

As much as it is important to identify and assess public health risks associated with basement flood waters in residential settings, it is equally important to evaluate and assess whether racial inequities exist with respect to said public health risks. In Pittsburgh, like many other cities around the nation, there are neighborhoods in which predominantly Black, indigenous, and people of color live where infrastructure maintenance has been deferred or delayed, potentially making cumulative flooding impacts more severe^{281,304,305}. To date, this is the first body of work that examines both non-disaster related basement floodwaters and floodwater related aerosols as a potential exposure route for these microorganisms. The work presented in Specific Aim 4 aims to determine the source of basement floodwaters in Pittsburgh and to characterize racial disparities in GI and DWPI exposure and incidence of basement flooding. It is *hypothesized* that residents in Black neighborhoods will be more exposed to GI pathogens and DWPIs due to increased sewage backup from dilapidated infrastructure.

5.2 Research Approach

5.2.1 Participant Recruitment and Survey Data Collection

Working alongside Women for a Healthy Environment (WHE), 25 residents who experience varying degrees of basement flooding were recruited to participate in the study. The 25 residents were distributed throughout the city of Pittsburgh, with samples collected from 13 homes of Black residents and 12 homes of White residents to compare differences in exposure by race. After successful recruitment, participants called the sampling team during basement flooding events and the sampling team responded within the hour. Upon arrival at the home, residents were administered a survey to collect information about the house, frequency of flooding, incidence of asthma and diarrheal events, and demographic information. Survey responses were then deidentified and stored in an encrypted online folder for later use. After sampling was completed, each resident was sent a \$50 to a store of their choosing as a token of appreciation for participating in the study. Each home was only sampled once, and the survey was only conducted once in each household.

5.2.2 Sample Collection

Water samples (up to 1L where applicable) were collected into sterile 1L sampling bottles (Nalgene, Waltham, MA) using a portable Masterflex peristaltic pump (Cole-Parmer, Vernon Hills, IL, USA). Directly after collection, the floodwater was filtered through a 0.2 μm polycarbonate filter (Isopore Membrane Filters, EMD Millipore, Billerica, MA, USA) for up to 20 minutes (to ensure maximum mRNA survival) and the resulting filters were stored at -80°C for

RNA extraction. Both the filtered water and remaining unfiltered water were saved and used for subsequent water quality analyses. Aerosol samples were collected for 20 minutes using the TE-BC251 NIOSH 2-stage Bioaerosol Cyclone sampler (Tisch Environmental, Cleves, OH) connected to a Gillian 5000 air pump (TISCH Environmental, Cleves, OH) running at the maximum speed of 2500 cc/min. The aerosol sampler and pump were set up on a stand at resident height at least six feet away from where water samples were being collected to minimize chances of human interference. Additionally, water fixtures or humidifiers in the space were turned off as source control for the aerosols. Directly after aerosol sample collection, RNAlater (Invitrogen, Waltham, Massachusetts, USA) was added to preserve RNA and the resulting samples were stored at -80°C until used for RNA extraction.

5.2.3 Water Quality

Ten water quality parameters were measured (Appendix D Table 1) following standard methods²²⁴. Temperature and pH were monitored on site using a portable pH and temperature meter (Hanna Instruments, Ann Arbor, MI, USA). Turbidity was measured using a Hach Portable Turbidimeter (HACH, Loveland, CO, USA). Nitrate/nitrite nitrogen (15N/14N) and oxygen (18O/16O) isotope ratios were measured using the denitrifier method described in Sigman et al. 2001 and Casciotti et al. 2002. Briefly, nitrate and nitrite were converted into nitrous oxide and the N and O isotopic composition was then measured using an IsoPrime isotope ratio mass spectrometer interfaced with a Micromass Trace Gas Pre-concentrator system (Thermo Fisher Scientific, Waltham, MA, USA). Total and dissolved concentrations of iron, manganese, copper, and lead were measured by inductively coupled plasma mass spectrometry (PerkinElmer NexION 300 ICP-MS, Waltham, MA, USA). Prior to analysis, all dissolved metal samples were prepared

by passing water through a 0.45 μm nylon syringe filter (Thermofisher, Waltham, MA, USA) primed with 5 mL of sample.

5.2.4 Microbial Analyses

5.2.4.1 Fecal Coliform Analysis

200 mL of unfiltered floodwaters were collected for fecal coliform analysis using the Colilert18 coliform test kit (IDEXX, Westbrook, ME, USA). Duplicate 100 mL samples were aliquoted into sterile bottles (IDEXX, Westbrook, ME, USA) and the Colilert18 Reagent (IDEXX, Westbrook, ME, USA) was added. Each sample was shaken until the reagent fully dissolved, poured into a QuantiTray2000 plate (IDEXX, Westbrook, ME, USA), and sealed using a Quanti-Tray Plate Sealer (IDEXX, Westbrook, ME, USA). Once sealed, the plates were incubated at 44.5°C for 18 hours and then examined against the control sample to determine fecal coliform presence. For the detection of fecal-borne *E. coli*, plates were examined in the dark using a 366nm UV light. The number of positive wells for both fecal coliforms and *E. coli* were then counted and compared against the included MPN table to determine concentrations of fecal coliforms and *E.coli* in the sample.

5.2.4.2 Droplet Digital PCR

RNA was extracted from the stored filters and aerosol samples using the PowerWater Kit (Qiagen, Germantown, Maryland) using methodology developed by Pitell et al.³⁰⁶ The resulting RNA extract was then DNase treated using TURBO DNase Treatment (Invitrogen, Waltham, Massachusetts, USA) and converted to cDNA using the iScript cDNA Synthesis kit (Bio-Rad Laboratories, Inc., Hercules, CA, USA) for downstream analyses. All cDNA was stored at -20 °C

until use. The density of total bacteria, *L. pneumophila*, *P. aeruginosa*, NTM, *Salmonella spp.*, and norovirus was determined using digital droplet PCR (ddPCR) as previously described²²⁵ using previously published primers (Appendix D Table 2) targeting the 16S rRNA¹³⁷, *Lmip*²²⁶, *OrpI*²²⁷, *atpE*²²⁸, *ttrC*²⁹⁶, and ORF1³⁰⁷ genes, respectively.

ddPCR reactions were performed for all cDNA samples (both water [n = 2] and aerosol [n = 5] to date), alongside negative controls (RNA extraction, ddPCR, and filtration controls) and positive controls (gblocks of the target amplicons provided by Integrated DNA Technologies, Inc., Coralville, IA, USA), both of which were negative and positive respectively. ddPCR was performed as described in Section 3.2.4.1 with specific assay reaction conditions and thresholding information presented in Appendix D Table 3 and Table 4.

5.3 Results and Discussion

5.3.1 Assessment of Racial Disparities through County Health Data

To assess the racial disparities in exposure and disease incidence in Pittsburgh, deidentified data from the Allegheny Health Department on the incidence of non-foodborne GI illness caused by *Salmonella*, *Campylobacter*, and *Cryptosporidium* from 2016 - 2018 were gathered. These data were then binned by neighborhood and each neighborhood was classified as either majority Black (Black was the biggest racial group in the neighborhood, regardless of percentage) or majority White (Table 7). The data suggests that there is a racial inequity in non-foodborne GI illness incidence in Pittsburgh as the average incidence in Black neighborhoods was nearly double that of the White neighborhoods, despite there only being three majority Black neighborhoods examined.

Additionally, the data were binned based on socioeconomic status (greater or less than the median household Pittsburgh income of \$42,500) of the neighborhood and compared. In this comparison, incidences of GI illness were comparable, suggesting that the driver of the differences in neighborhood incidences was likely race.

It is important to note however that using these data as a proxy for racial inequity in illness comes with several caveats. The Allegheny County Health Department only collects information on notifiable infections (i.e., infections that require healthcare workers to report them to public health officials), which means that infections from norovirus or the DWPIs are not tracked at the county level. Additionally, these data do not state whether the people from each neighborhood contracted the illness in their neighborhood nor does it state anything about where the patient was infected, making it difficult to ascertain if there are racial differences due to housing infrastructure design, maintenance, and age. Regardless, the stark difference in the incidence of reportable GI diseases provides enough context for future research to examine what drives the increased incidence in majority Black neighborhoods and populations.

Table 7: 2016-2018 Incidence of Notifiable non-foodborne GI infection caused by *Cryptosporidium*, *Campylobacter*, and *Salmonella* in the City of Pittsburgh

Neighborhood	Racial Breakdown		Incidence per 1000 people [95% CI]		
	%Black	%White	Cryptosporidium	Campylobacter	Salmonella
Homewood	95.3	4.16	0.16 [0, 0.001]	0.8 [0, 0.002]	1.2 [0, 0.002]
Perry South	64.6	26.54	0.00 [0, 0]	0.65 [0, 0.002]	0.91 [0, 0.003]
East Liberty	58.5	25	0.17 [0, 0.001]	0.51 [0, 0.002]	0.51 [0, 0.002]
Mount Oliver	40.6	40.4	0.00 [0, 0]	0.00 [0, 0]	0.4 [0, 0.002]
Perry North	39.9	62.67	0.15 [0, 0.002]	0.38 [0, 0.002]	0.38 [0, 0.002]
Sheraden	38.9	49.86	0.00 [0, 0]	0.19 [0, 0.001]	0.38 [0, 0.002]
Hazelwood	33.9	54.34	0.00 [0, 0]	0.00 [0,0]	0.93 [0, 0.002]
Bloomfield	25.2	81.57	0.00 [0, 0]	0.00 [0,0]	0.59 [0, 0.001]
Troy Hill	15.5	81.21	0.00 [0, 0]	0.37 [0, 0.003]	1.11 [0, 0.003]
Crafton	9.10	66.28	0.00 [0, 0]	0.00 [0,0]	0.36 [0, 0.002]
Downtown	9.00	74.57	0.00 [0, 0]	0.19 [0, 0.002]	0.56 [0, 0.002]
Mt. Washington	8.60	85.93	0.11 [0, 0.001]	0.23 [0, 0.001]	0.45 [0, 0.001]
Elliot	7.60	65.52	0.00 [0, 0]	0.23 [0, 0.003]	0.23 [0, 0.003]
Lawrenceville	6.60	86.17	0.00 [0, 0]	0.22 [0, 0.002]	0.89 [0, 0.002]
Banksville	5.30	88.10	0.21 [0, 0.002]	0.87 [0, 0.003]	1.20 [0, 0.003]
Brookline	4.10	91.43	0.00 [0, 0]	0.76 [0, 0.001]	0.23 [0, 0.001]
Squirrel Hill South	3.40	82.03	0.13 [0, 0.001]	0.40 [0, 0.001]	0.53 [0, 0.001]
Southside	3.30	88.54	0.00 [0, 0]	0.68 [0, 0.002]	0.68 [0, 0.002]
Averages	Combined Incidence		Cryptosporidium	Campylobacter	Salmonella
City of Pittsburgh	1.08 [0, 0.001]		0.07 [0, 0.0001]	0.41 [0, 0.001]	0.60 [0, 0.001]
Predominately Black	1.70 [0.001, 0.002]		0.12 [0, 0.0004]	0.69 [0, 0.001]	0.91 [0.001, 0.002]
Predominately White	0.96 [0, 0.001]		0.06 [0, 0.0001]	0.36 [0, 0.001]	0.54 [0, 0.001]

5.3.2 Absolute Abundance and Coliform Analysis

Examining the two water samples collected, NTM was detected in both with small amounts of *P. aeruginosa* also detected (Appendix D Figure 1). No viable *L. pneumophila*, *S. enterica*, or norovirus were detected in either of the water samples collected (Appendix D Figure 1). While there are not enough samples to make any representative conclusions, the presence and detection of NTM were expected in the water samples as the stormwater collected is presumed to have come through the walls in each residence. In general, NTM are ubiquitous in water and soil environments²⁵⁷, with positive associations with water quality parameters like turbidity and dissolved metal concentrations²⁵⁸ that can be increased from precipitation events. Likewise, not detecting *L. pneumophila*, *S. enterica*, or norovirus was also expected for these samples. Stormwaters are thought to have different microbial profiles from surface or treated drinking water, and while previous work³⁰⁸ has found *L. pneumophila* in harvested rainwaters, it was in low densities. Similarly, the absence of both *S. enterica* and norovirus - organisms associated with combined sewage overflows or fecal contamination^{296,307,309,310} is not a surprise given both water samples collected were reported to come from stormwater runoff through the walls and other openings in their basement rather than from sewage backup.

Fecal coliform analysis revealed an average of 2000 MPN / 100 mL, which is remarkably less than the average fecal coliform concentration in secondary clarification effluent from the three Pittsburgh WWTPs examined in Specific Aim 2 (Figure 19). The presence of fecal coliforms suggests that the floodwaters came in contact with a fecal source at some point, however, the true source of the floodwaters cannot be ascertained until isotope analysis is conducted.

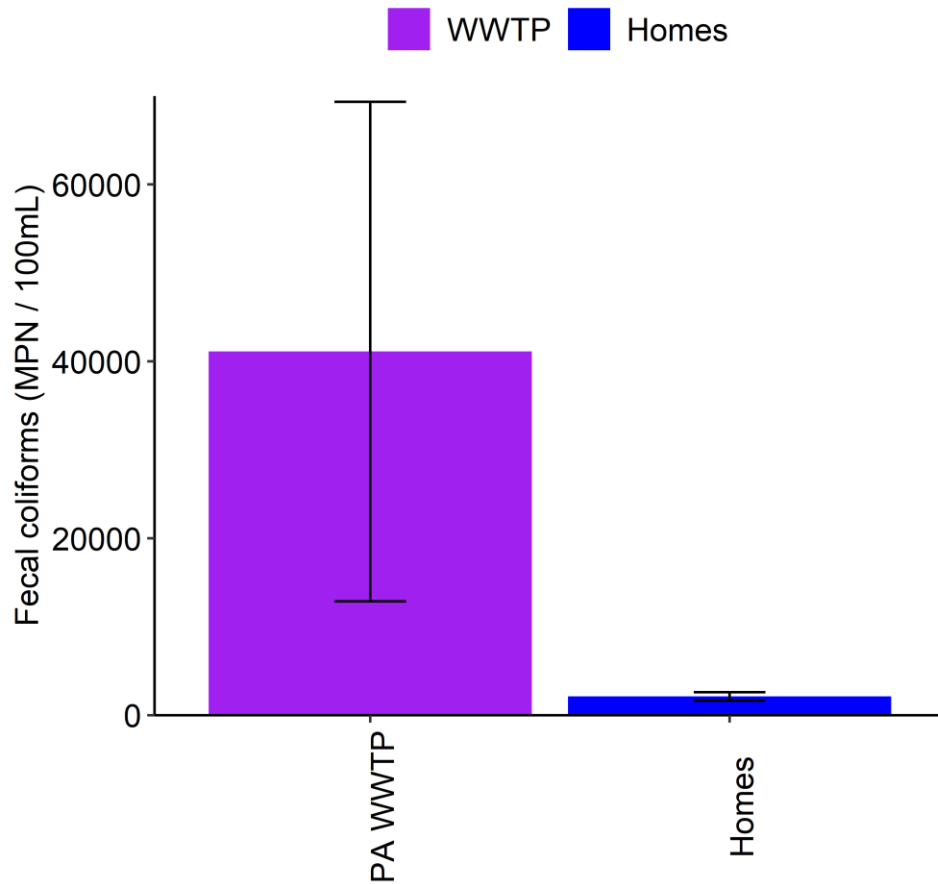


Figure 19: Average fecal coliform concentration from PA WWTPs in Specific Aim 1.0 and the stormwater samples (n = 2) collected for this study.

Like the water samples, the aerosol samples (n = 5) collected from each home had NTM and low concentrations of *P. aeruginosa*, with one home having detectable *L. pneumophila* (Figure 20). Additionally, neither *S. enterica* nor norovirus were detected in the aerosol samples collected from any of the homes. Generally, the assumed exposure route for both *S. enterica* and norovirus are thought to be ingestion of water, rather than inhalation, so being below the limit of detection in the aerosol samples makes sense. However, it's also important to note that occurrence of a hazard is often independent of inhalation likelihood in QRMA, so further work would need to be

done to identify the inhalation likelihood if found in aerosols. One potential reason for the lack of occurrence in the aerosol phase is that these two organisms do not partition into the aerosol phase (or survive less if they do) like many DWPIs do³¹¹, however more samples would need to be collected to justify this suggestion and further experimentation would need to be done to determine specific mechanisms that control the partitioning. To better understand and assess what a resident would be exposed to, the observed densities of each organism were normalized to the amount of time daily the average American spends in their basement to do laundry (10 minutes)³¹². Additionally, since all the residents who I collected aerosol samples from were Black women, I used the average at-rest inhalation rate of 11.3 m³/day for women³¹³ to better contextualize the data. On average, in a 10-minute laundry event these residents would be exposed to 10^{5.62} 16S rRNA gene copies with ~30% of the total microbial exposure being composed of potentially pathogenic NTM, and 100% of the exposure being respirable (< 5µm), viable organisms. This is comparable to the results of a study done in a library storage room and university dormitories³¹⁴. It is also noteworthy to mention that in one of the homes where there was standing floodwater, the density of total bacteria was higher than in the houses with little to not standing floodwater suggesting a possible interaction. However, while there is not enough data to say whether this is a statistically significant risk or increase in exposure, this observation provides further justification to continue to collect both water and aerosol samples in basements to better understand the potential exposures associated with going down into or spending time in those spaces. Particularly in the case of those who may use their basement for other purposes such as home office, home gym, or as is the case in some of the homes I sampled, a daycare / playroom for children, it is imperative to assess the linkages between floodwaters and over all indoor air exposures to ensure continued public health safety.

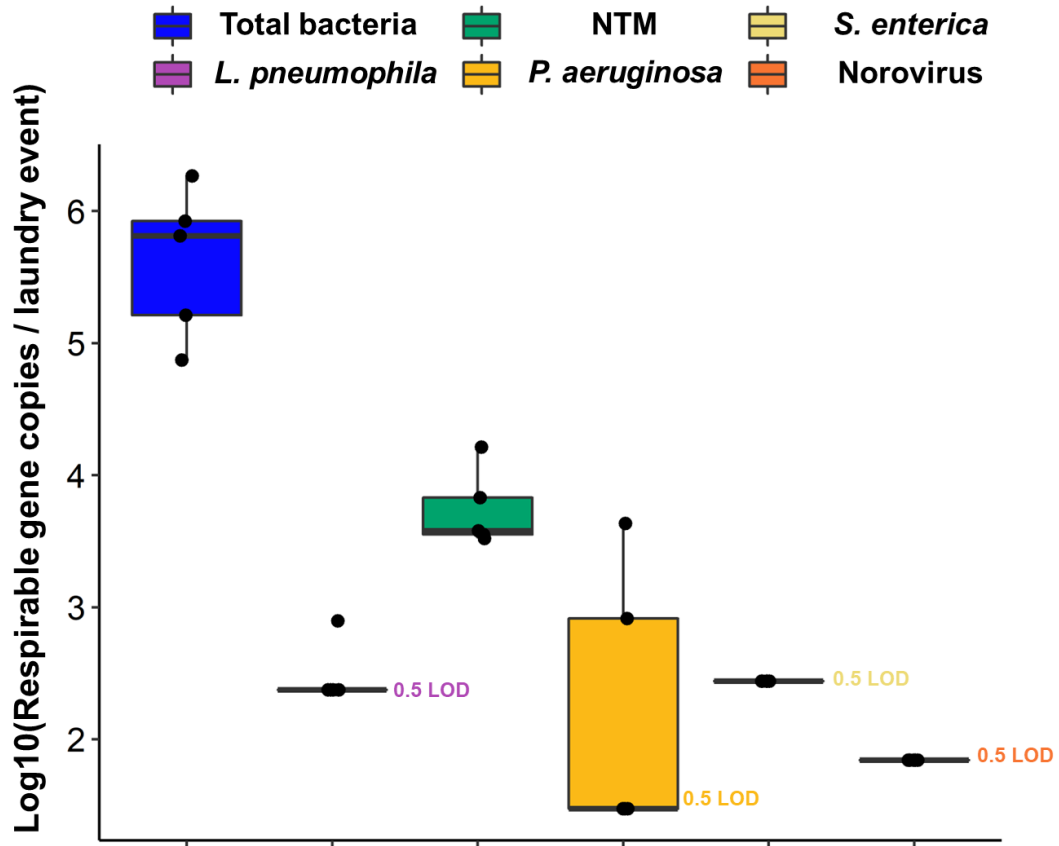


Figure 20: Boxplots of the log₁₀ transformed viable total bacteria, *L. pneumophila*, NTM, *P. aeruginosa*, *S. enterica*, and norovirus absolute gene copies within bio-respirable aerosols (< 5µm) that could be inhaled during a 10 minute laundry event (n = 5 homes). Samples with no detects had their densities set at half of the limit of detection for the assay prior to normalization. Absolute densities (calculated originally as gene copies / L of air) were normalized to an average time of 10 minutes per visit to the basement to do something like laundry. The average daily inhalation rate of a woman was used to calculate how much air would be inhaled during 10 minutes due to all the residents I samples from being Black women.

5.3.3 Lessons Learned and Future Considerations

5.3.3.1 Resident Participation and Recruitment

Conducting community based participatory research is rewarding, yet challenging because active participation can be difficult to obtain without the proper engagement strategies. From the onset, partnering with Women for a Healthy Environment and their community health workers lowered the entry barrier that many researchers face. However, there were still challenges faced in resident recruitment, which may be improved by the identification of additional community partners to extend the reach of the study. In future, a suite of community organizations should be approached and consulted to help recruitment go as smoothly as possible. Especially in neighborhoods that may have strained relationships with large research entities like a university, relying on more than one avenue to recruit and work with community members will be critical.

Likewise, when conducting research that requires community members to call a sampling team directly, it is important for future researchers to consider the lived experience of the community they are working with. Many people who experience basement flooding or generally wet basements typically have some process that they go through to alleviate the problem so that their space is usable again. To best consider this in future work, it is recommended that researchers themselves help with resident recruitment alongside any community organizations that they are working with to inform the residents of what exactly is needed for the sampling campaign. The presence of the researcher or research team in these spaces can help to turn that lived experience into an actionable outcome in favor of both parties. Of the five houses I have sampled, the likelihood of the resident calling me to come sample or in some cases referring me to another resident significantly increased when I was able to have direct conversation and connect with them beyond science. Beyond this, I was also able to glean much more information about the specific

impacts that their basement flooding had on the house, but also on them socially and emotionally. Few studies detail the social-emotional impacts of flooding^{315,316}, however, there is a need to better attune our scientific methods to incorporate lived experience and community capital, as they are the foundation for engaging and creating knowledge with community stakeholders.

5.3.3.2 Sample Collection

Thus far, only one fifth of the samples intended to be collected in this aim have been collected and analyzed. As such, no statistical analysis has been conducted as there is not enough statistical power to make any claims about the differences in microbial densities between homes. Likewise, with all the samples collected coming from the homes of Black residents, a fair comparison about the microbial densities experienced between racial groups cannot be made at this time. While average annual rainfall in Pittsburgh has increased over the last five years, 2023 marked a new record for the lowest total precipitation. A news article from the summer of 2023 remarked that in the first four months of 2023, Pittsburgh had received its lowest total rainfall since the first four months of 2019³¹⁷. As a result, even when it did rain, it either rained in small quantities or infrequently enough to saturate the groundwater table and cause the excessive flash flooding that many residents experience. Combined with the lived experience of those who consistently deal with wet basements, the lack of rainfall made the sampling campaign challenging and something noteworthy for others trying to conduct similar studies.

5.4 Expected Results and Preliminary Conclusions

Overall, though only a small number of samples have been collected to date, much was learned from the process of conducting community-based research like this. Namely, the best strategies for working with community partners and residents were identified through trial and error. From a scientific perspective, fecal coliforms NTM and *P. aeruginosa* were all identified in the water samples collected and the latter two in the aerosol phase. While no determination of the source of the floodwaters sampled can be made yet, the observations presented here provide preliminary evidence that basement floodwaters should be an area of future public health and environmental engineering research, especially when combined with the fact that climate change will continue to impact precipitation rate in urban areas. Also, with an almost doubled incidence of GI disease in Black neighborhoods in Pittsburgh where infrastructure maintenance is often delayed, it is imperative that future research addresses the reasons for this and highlights any influence that the built environment could play in making this a reality. Furthermore, I also believe that this work is necessary to ensure that all the spaces that people occupy are better understood from both a public health and engineering context so that overall quality of life can be improved. I expect that the completion of this work will provide the field with a foundation to build upon for future research in the intersections of public health and environmental engineering, particularly as shifts in housing trends and climate are pushing people to change how they view their basements and their use.

6.0 Specific Aim 5.0: Development of a Basement Indoor Air Quality Modeling Tool to Assess Physical, Chemical, and Biological Contaminant Pollution Exposure

Specific Aim 5.0 was conducted alongside the work done in Aim 4.0, which was funded by The Pittsburgh Foundation (grant number: UN2021-121327) and the Center for Healthy Environments and Equity Research (CHEER) through the University of Pittsburgh's School of Public Health. At the time of writing, results from Aim 5.0 have been submitted for review in a peer reviewed journal (Science of the Total Environment). Special acknowledgements are given to Joey Engelmeier, a MPH student in the School of Public Health who collaborated with me in the development of the indoor air quality (IAQ) tool, scenarios modeled in CONTAM, and for the expertise and discussion surrounding IAQ and exposure.

6.1 Introduction

Considering the discussion regarding potential exposure to pathogenic microorganisms originating from basement floodwaters and associated aerosols in the preceding chapter, it is imperative to incorporate an analysis of indoor air quality (IAQ) within basements (and other habitable spaces) to achieve a comprehensive evaluation of contaminant (physical, chemical, and biological) exposure and to delineate potential health outcomes. In the USA, many people spend upwards of 90% of their time in indoor environments^{318,319}. While about two thirds of this time is spent in residential settings, the bulk of our time is spent in primary living spaces (e.g., living rooms, bedrooms, kitchens)³²⁰. As such, much of the IAQ research conducted to date has focused on examining the important factors to maintain air quality in those spaces.

As public interests, building codes, and the housing market have changed over the last few decades, IAQ research has become more robust in the types of analyses available and in the parameters of interests. Namely, parameters such as ventilation, air exchange rates, and building location and layout have been studied^{321–324}. As well, target pollutants such as PM_{2.5}^{325–328}, radon^{329–331}, and mold spores^{323,332,333} have also been evaluated in common use spaces. While these analyses are important and necessary to uphold public health safety, it is important to recognize that there are other spaces within residential settings that could contribute to the overall IAQ and exposures to airborne contaminants that residents experience. Basements are important, but understudied residential microenvironments that fall into this category³³⁴. In recent years, basements have increasingly served as primary living spaces in the USA, with many homeowners converting these areas into functional rooms for various purposes such as bedrooms, home offices, or recreational spaces^{335,336}. This trend has been driven by factors such as rising housing costs and the desire for additional living space. In addition, the COVID-19 pandemic has prompted

significant shifts in basement use patterns³³⁷⁻³³⁹. With remote work becoming more prevalent, basements have seen heightened utilization as home offices and study areas. Additionally, the need for designated spaces for quarantine or isolation has led some households to repurpose basements to accommodate these requirements. Because historical IAQ research has primarily concentrated on traditional primary living spaces, neglecting basements³³⁴, it is imperative that IAQ analysis is performed in these dynamic spaces to inform amendments to basement building code and design to ensure public safety.

Basements are important yet challenging to model residential spaces due to their variable ventilation and air exchange rates (AERs), dynamic use patterns, and unique pollutant risks. In general, AERs depend on several building characteristics (e.g., number of floors, building envelope tightness, season), however few studies have quantified both the IAQ and airflows in basements despite their airflows being coupled with other residential spaces. In a 2009 study on three houses in Pennsylvania, basement AERs ranged from 0.03 to 0.36 h⁻¹³⁴⁰ while a more robust and recent study found AERs of 0.1 to 2.94 h⁻¹³²¹, with AERs being higher in the winter and lower in the summer. Seasonal variation in AERs is expected, particularly in residences that use natural ventilation techniques; whereas in residences that employ other ventilation strategies, AERs are more dependent on occupant activity³⁴¹. The variable use of basement spaces and occupant activities can also shape the IAQ of the basement itself, and subsequently other areas of the home. Occupant behavioral patterns have been shown to greatly impact factors such as building energy performance and the overall IAQ within personal spaces³⁴². Therefore, if basement use is an established and regular part of a resident's routine it is important to include it when trying to capture a resident's total home exposure.

Variable use patterns in basement settings can increase the variability in pollutant exposure. Trends in housing markets show that house-flipping older homes, particularly finishing peripheral spaces such as basements and garages, is becoming a popular method of increasing living space and real estate value³³⁵. By finishing spaces like basements, there is the potential for increased exposure to potent chemicals in construction that linger in basements as they off gas from the building materials^{343,344}. Furthermore, extreme shifts in precipitation have led to increased flood frequency and intensity, causing increased potential for water damage and microbial exposure, with basements being the first and most commonplace location for water damage. Homes affected by flooding exhibit elevated concentrations of bacterial endotoxins and mold spores, as documented in several studies³⁴⁵⁻³⁵², with these heightened levels being associated with respiratory issues such as allergies and asthma. As discussed in the previous chapter, the relationship between urban flooding events and microbial exposures^{286,289,296,297} has been studied, but rarely considered in basements, leaving microorganisms' influence on the basement IAQ under explored. In addition, radon, a naturally occurring radioactive gas which has a maximum contaminant level of 4pCi/L³⁵³ and is the second biggest cause of lung cancer in the USA^{329,330,354} is known to accumulate in basements due to its heavy density and tendency to seep through foundation cracks^{355,356}. While radon is typically assessed in basements, it has not been assessed in the context of new usage patterns. While housing markets in regions like the West Coast and the Gulf Coast are dominated by slab foundations, most single-family homes in areas such as the Northeast and Upper Midwest United States have some form of basement^{357,358}. Considering that extreme flooding is annually increasing in areas like the Northeast United States, microbial influenced IAQ will likely continue to be a research topic of interest, particularly in basements where there is an increased risk of water damage.

Given that a quarter of the new homes built in the United States in 2022 included a basement³⁵⁷, there is a need to update the current IAQ models and research to better represent exposures from all microenvironments, particularly inhalation exposures in basements. Improving the understanding of IAQ in basements will greatly help home assessors, policy and building code makers, researchers, and homeowners understand and ensure occupant safety and comfort. Thus, the work presented in Specific Aim 5.0 aims to develop an IAQ modelling tool to assess the exposure to physical, chemical, and biological pollutants in basements with different use patterns (e.g., home office, home gym, and tv / games space) outside of finishing material effects. It is *hypothesized* that different use patterns will impact the exposure levels and risks associated with each pollutant.

6.2 Research Approach

6.2.1 Physical, Chemical, and Biological Pollutant Selection

While there are numerous sub-types of pollutants that could exist in indoor spaces, much of the IAQ literature to date has focused on those pollutants that have correlation with human activity (e.g, PM2.5 generation from cooking)^{327,328,359} or environmental factors (e.g., increased mold spores after a flooding event)³⁵⁰. To best capture a range of realistic pollutants common to basements and other residential indoor spaces, PM2.5, radon, and mold spores were selected as pollutants of interest because of their known adverse health effects after chronic exposure^{326,329,330,332,333,360,361}.

6.2.2 CONTAM Multizone IAQ Modeling Overview and Residential Building Model

CONTAM³⁶² is a multizone IAQ and ventilation analysis program designed to evaluate the airflow rates, contaminant concentrations, and personal exposures in buildings. The CONTAM transport model treats a building as a system of interdependent, well-mixed zones that store air and contaminant mass and airflow elements that carry mass between them. Interzone airflows are a function of the pressure drop along each airflow path between two zones (Eq. 6-1).

$$F_{ji} = f(P_j - P_i) \quad (6-1)$$

where F_{ji} = airflow rate (kg/s) between zones j and i ; P_j, P_i = pressures in zones j and i in Pa, respectively. By the principle of conservation of mass, the transient mass-based solution across all airflow paths is as shown in Eq 6-2. The transient conservation of a contaminant species in each control volume is given by Eq. 6-3 and is used to calculate contaminant concentrations in each zone in the model using the linear skyline solver implemented in CONTAM. Upon calculation, all concentrations were converted to typical units (i.e., $\mu\text{g}/\text{m}^3$, pCi/L) using CONTAM's internal unit conversion system.

$$\frac{\partial m_i}{\partial t} \approx \frac{1}{\Delta t} \left[\left(\frac{P_i V_i}{RT_i} \right)_t - (m_i)_{t-\Delta t} \right] \approx \sum_j F_{ji} + F_n \quad (6-2)$$

$$\rho_i V_i C_i^\alpha |_{t+\Delta t} \approx \rho_i V_i C_i^\alpha |_t + \Delta t \times [G_i^\alpha + m_i \sum_\beta k^{\alpha\beta} C_i^\beta - \sum_j F_{i \rightarrow j} C_i^\alpha] \quad (6-3)$$

where m_i = mass of air in zone i in kg, P_i = zone pressure in Pa, V_i = zone volume in m^3 , T_i = zone temperature in K, $R = 287.055 \text{ J}/(\text{kg} \cdot \text{K})$, ρ_i = air density in zone i in kg/m^3 , C_i^α = mass ratio of contaminant species α in zone i in kg species per kg air in zone, G_i^α = contaminant species generation in kg/h, and $k^{\alpha\beta}$ = kinetic reaction rate constant for reactive contaminants in 1/h.

In this study only radon was considered to be reactive and followed the general exponential decay model (Eq. 6-4). For PM2.5 generation, a constant coefficient model without a removal rate

due to convergence issues was used (Eq. 6-5). Mold was applied as a constant concentration in each zone and concentrations only changes as a result of airflow.

$$G^{Rn}(t) = G_0 \times e^{-kt} \quad (6-4)$$

$$G^{PM2.5}(t + \Delta t) = G_t \quad (6-5)$$

where, G_0 is the initial generation rate of radon from concrete in pCi/hr taken from Chao et al.³⁵⁵, k is the first order decay constant for radon, and G_t is the generation rate of PM2.5 by a cooking source in $\mu\text{g/s}$ taken from Aquilina et al³²⁷.

It is important to note, the removal rates for PM2.5 by deposition and filtration (by a HVAC system) would have to be included to more accurately model exposures. Likewise, validation of this model design by real world data collection are needed to better design and model occupant exposure in highly variable residential settings. However, this modeling approach provides a foundation for future studies to build upon. In this study, CONTAM (v3.4) was used to simulate the contaminant transport and occupant exposure within a one story, single-family residential home with a subgrade basement.

6.2.2.1 Residential Building Model

A one-story single-family residence with a subgrade basement was chosen as the representative scenario for the IAQ modeling due to the unexplored nature of basement exposures and the large number of single-family residences with basements in the United States^{357,358}. The modeled residence was an 86 m² (926 ft²) residence with a basement, one occupiable floor, an attic, and a gable roof. All floors (basement, main, attic) were sized according to the 2015 International Residential Code³⁶³. The occupiable floor was comprised of six zones representing areas of standard residential occupancy: two bedrooms, a living room, a dining room, a kitchen, and a bathroom (Figure 21), with each zone sized based on the average American size³⁶⁴.

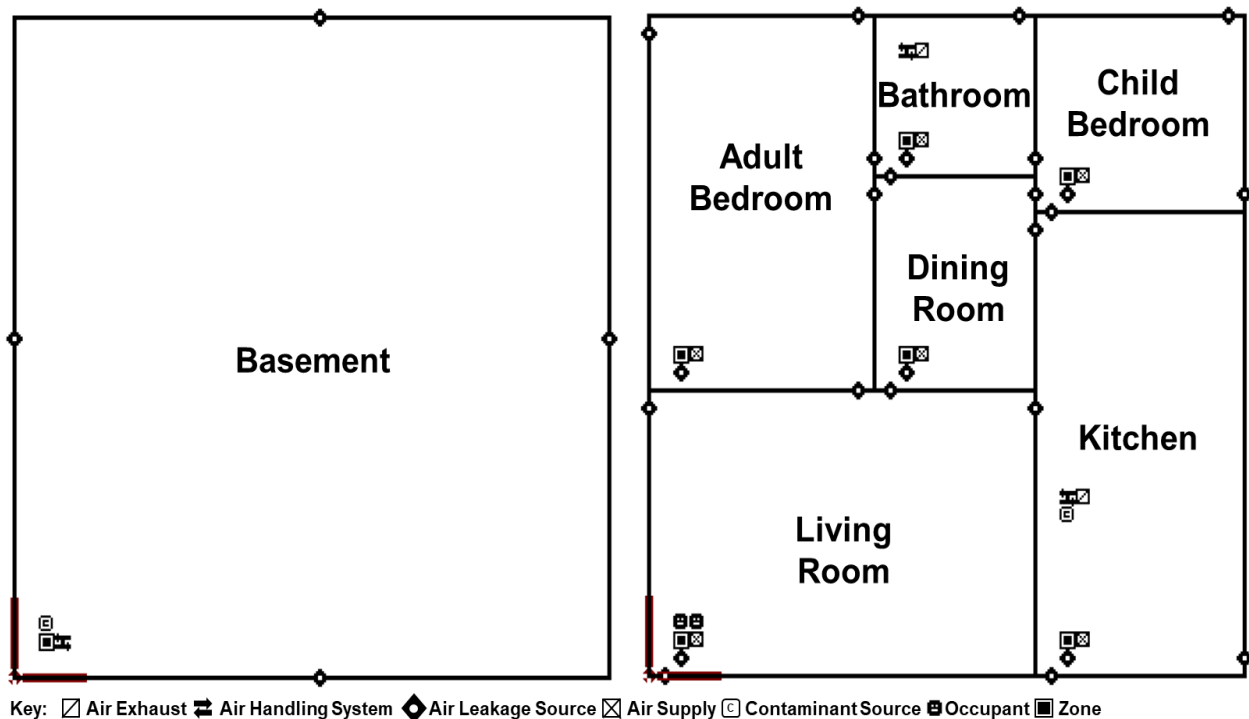


Figure 21: Single family residence modeled in CONTAM. The modeled residence was a one—story home with a subgrade basement that is used for laundry (control case scenario) and for a variety of other activities (test case scenarios).

Air flow leakage rates from the interior and exterior walls, basement walls, and floors in the residence were simulated using values from ASHRAE Standard 62.1³⁶⁵, which provides air leakage rates for residential buildings (Appendix E Table 1). To simplify the model design, I assumed that the air flow leakage would be distributed equally across the area of each wall and did not consider the impact of connection-based leakages (e.g., wall to ceiling, floor to wall). In the case of the floor airflow paths, I assumed that each zone had one passive floor vent that allowed for the movement of air between the basement and occupiable space. This floor vent was sized at 0.025 m² to simulate the size of the average floor vent in a home.

One HVAC unit was placed in the basement of the residence, with the outlet routed through the attic. The HVAC unit pulls in 100% outdoor air as the main supply source for each of the zones on the occupiable floor and in the basement under certain use conditions. The HVAC unit was simulated to operate on two separate schedules, one for average weekday home usage and one for average weekend usage. During the weekdays, the HVAC unit would operate at half capacity during sleeping hours (9PM – 7AM), full capacity from 7AM – 8 AM and from 5PM to 9PM, and off during working hours (8AM to 5PM). During the weekends, the HVAC unit would operate at half capacity during sleeping hours (9PM to 7AM) and at full capacity during the rest of the day. In residential spaces, average air flow rates are typically variable due to differences in home sizes, design, HVAC system specifications, and individual behaviors. As such, the rate required for a particular room is usually calculated based on the room size and the number of air changes per hour recommended for healthy IAQ. For the spaces on the occupiable floor, I assumed air supply flows to be the volume of the space multiplied by four air changes per hour (ACH) to meet the baseline suggestion of 12 m³/hr plus 5.1 m³/hr for every 9 m² from ASHRAE Standard 62.1. This resulted in airflow well beyond the suggested baseline, providing ample supply to each zone (Appendix E Table 2). Assuming that most people would not be able to renovate their HVAC system to incorporate a new supply into their basement setting, the three test scenarios were designed with a supply rate equal to a tenth of the space volume multiplied by four ACH to simulate having a small fan in the space for use while in the space. Similarly, ASHRAE Standard 62.1 was used to design exhaust airflow for kitchen and bathroom exhaust vents, which were set at 90 and 180 m³/hr, respectively.

6.2.2.2 Occupancy Schedule and Simulated Scenarios

Four different occupant use scenarios that represent a wide variety of uses and exposure conditions were modeled and simulated. In each scenario, an occupancy schedule (Appendix E Tables 3 and 4) was created for an adult (female) and child (ages 5 - 9) occupant to account for differences in inhalation and exposure rates. The control scenario consisted of the occupants following a standard schedule of going to work / school for 8 hours a day and then coming home and spending most of their time on the main floor in different spaces. On the weekends, both occupants remained on the main floor for most of the day, except for the adult going to the basement for 15 minutes each day to do laundry. In the other three scenarios (home office – HOF, home gym – HOG, and Den/Playroom – DG), both occupants spent varying amounts of time in the basement space and their exposure to each pollutant is measured as they move throughout the space (Appendix E Tables 3 and 4).

6.2.2.3 Contaminant and Exposure Modeling

Average ambient and indoor PM_{2.5}, radon, and mold spore concentrations were gathered from literature and government sources^{353,366–368} and imported into the simulation software to create as generalizable a model as possible. The average values used are listed in Appendix E Table 5. Additional sources were consulted for the average emanation rate of radon from concrete foundations³⁵⁵, average ratio of upstairs to downstairs radon concentration³⁵⁶, and PM_{2.5} generation during occupant activities like cooking³²⁷ and were included in the simulation (Appendix E Table 5). Because mold is either measured as spore equivalents or colony forming units per unit volume, the average concentrations were converted to mass-based concentrations for use in CONTAM. Using data from Sesartic et al. 2013³⁶⁹, it was assumed that the average weight of a mold spore was 33 picograms and that half of the average indoor mold concentration would

be airborne and respirable. Simulations were run for the course of a week at steady state weather conditions (20 °C, 101,325 Pa, 0 m/s wind speed) to remove both stack and wind effects on contaminant transport. Likewise, the effects of relative humidity which has been shown to impact these contaminants have been removed to simplify the model.

CONTAM presents exposure results for the occupants as the time dependent concentration of the selected contaminant over the simulated duration. Once the exposure data were obtained, the contaminant concentration profile was integrated to determine the exposure within a given timeframe. Then for each contaminant, all the exposures over the course of the week were summed and multiplied by the average breathing rate for a female adult and female child (ages 5 - 9) to determine the total contaminant mass inhaled over the course of the week. The average breathing rate for a female adult and child was chosen to try and describe the exposures faced by residents from the previous aim. These values were then averaged to determine an average exposure for the week. These data were then used alongside a designed exposure potential matrix to help homeowners qualitatively assess their potential exposures in their home and evaluate their behaviors (Section 6.2.3).

6.2.3 Exposure Potential Matrix

The importance of residential exposures has been explored for over 40 years, first gaining prominence through early exposure models put forth by Duan³⁷⁰ and Ott³⁷¹. The original Duan equation (Eqs 6-6 and 6-7) considers the cumulative effects of different concentrations of pollutant for different intervals of time:

$$E = \frac{1}{T} \sum C_{ijk} * t_k \quad (6-6)$$

$$E_i = C_{ijk} * t_k \quad (6-7)$$

where E = time-weighted integrated exposure, C = concentration, t = unit time, T = total time elapsed, i = the medium, j = the pathway and k = the microenvironment.

Despite being a generally used model for indoor residential exposures, this model assumes a constant intake rate which can greatly underestimate the true exposure within a space, particularly as different age groups and different activities will have different inhalation rates³⁷². To account for this, a factor for breathing rate was added to the original Duan microenvironmental model (Eq 6-8). This allows better insight into how much mass of an airborne pollutant reaches the sensitive tissues of the respiratory tract.

$$E_i = C_k * t_k * b_k \quad (6-8)$$

where E_i = exposure of an airborne pollutant, C_k = concentration of airborne pollutant in microenvironment k, t_k = time spent in microenvironment k, b_k = respiration rate (L/min) in microenvironment k, and k = the microenvironment.

Using the adjusted equations, a convenient and easy to understand exposure potential matrix was developed to help residents and home assessors understand residential occupancy patterns and its impacts on exposure to pollutants (Table 8).

Table 8: Relative Exposure Value (REV) questionnaire

Questionnaire	Value
How many days a week do you go to your basement?	
How many hours a day do you spend in your basement?	
What do you use your basement for? 1) bedroom, home office, laundry, storage 2) living room, workshop, storage area, playroom 3) home gym	
Do you have any children that spend time in the basement? If yes, select the age of the <i>youngest</i> child that regularly spends time in the basement and the value associated with that age range (listed to the left of the age range) 1) No children 1.4) 10 – 18 years old 1.9) 5 – 9 years old 2.4) 3 – 4 years old 2.8) 1 – 2 years old 3.3) <1 year old	
Multiply all values together, the product will be the relative exposure value (REV)	

Using Table 9, residents and home assessors alike could derive the t and b variables of equations 3 and 4. Questions 1 and 2 establish frequency and duration of time spent in a microenvironment; with the product of these two values equaling t . Questions 3 and 4 establish how breathing rate may increase through identifying the age and activity level of residents (Appendix E Tables 6 and 7). The multiplication factors in these two questions reflect the increase in breathing rate relative to resting female adult breathing rate of 4.8 L/min. To then help users make an informed decision about the products of the above equations and to integrate them into a model, a potential scale was created to elicit what qualifies as high or low potential for exposure based on an average of 10 hours spent in a single space at resting respiration³⁷³ for 7 days a week (70 unit hours) and assumed linear dose-response relationships for all three pollutants considered due to the assumed linear dose response for PM_{2.5}³⁷⁴. The REV scale was categorized into five

equal sized bins, each with a size of 14-unit hours at resting respiration and labeled from “Ultralow” to “Ultrahigh” (Table 9).

Table 9: Relative Exposure Value (REV) Bin Sizing

Rating	Relative Exposure Value
Ultralow	0-14
Low	15-28
Moderate	29-42
High	43-56
Ultrahigh	57+

6.2.4 Statistical Analysis of Exposure Data from CONTAM

Significant differences in the average pollutant exposure between the control (adult female following regular weekly schedule and using the basement for 15min each day at the weekend to do laundry) and different use case scenarios were determined by non-parametric Wilcoxon testing. All statistical analyses were performed in R (version 4.0.2)¹⁴⁷ with significance set at a p-value < 0.05.

6.3 Results and Discussion

6.3.1 Relative Exposure Calculation of Scenarios

Using the questionnaire, a REV score was calculated for each of the four scenarios and then assigned a rating according to Table 9. This resulted in the control scenario (15-minute laundry event 2 days a week) receiving an ultralow rating with a value of 0.5, and the other three

scenarios having higher ratings (Figure 22). In order from least REV to highest REV, the scenarios are as follows: home gym (REV = 21, low), home office (REV = 40.5, moderate), and den/playroom (REV = 46 for an adult, REV = 152 for a child aged 5 - 9).

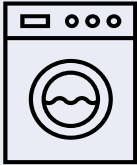

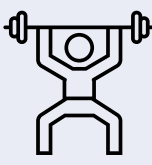
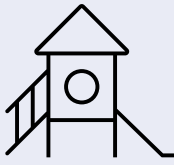
Relative Exposure Value (REV)	Scenarios			
	Control	Home Office	Home Gym	Playroom
0 – 14				
15 – 28				
29 – 42				
43 – 56	2 days a week, 15 min a day	5 days a week, 8 hours a day	7 days a week, 1 hour a day	7 days a week, 1 - 9 hours a day
57+				
REV =	0.5	40.5	21	46 (adult) 152 (child)

Figure 22: Relative Exposure Values (REVs) for each simulated scenario. The REV was calculated using the questionnaire presented in Table 8 and the activity and age of the occupant used in the simulation.

Without knowing the concentration of a certain pollutant or factoring the inhalation rate, residents and home assessors alike could get a sense of the amount of exposure in their space based on general occupancy information. Previous studies have detailed that people at either end of the age spectrum are generally more exposed to indoor pollutants and have examined the impacts of various pollutants in a variety of primary living spaces³⁷⁵⁻³⁷⁸. However, to the best of the author’s knowledge, very few studies in the building engineering space have holistically accounted for the impacts of occupant demographics and patterns in basements where controlled ventilation rates

are remarkably lower compared to other indoor spaces. Even in a recent review of the gaps in residential IAQ research, basements and crawl spaces are not listed as an area of priority research³²⁴. This is likely due to the global differences in the needs for IAQ research, as basements are much more common in the United States as opposed to places like Europe.

While localized to the US, research on the impact of occupant demography and activity on IAQ for secondary spaces like basements is critical. The exposure to pollutants of concern through indoor air is impacted by the type and frequency of activities carried out by occupants in the space (e.g., home office, gym) and what the collective uses are of the space (e.g., workshop, cooking), and as such these choices need to be accounted for more in IAQ tools. However, due to the large variety of these activities, it is difficult to quantify them and their possible interactions. This is where a tool such as the REV questionnaire could be used and further developed to capture this information for a multitude of spaces in homes. General factors could be created for common activities in household spaces based on average household use trends, with more specialized factors created for basement and crawl spaces depending on use and occupancy of the space.

Another important point to mention is the impacts on personal anxiety when it comes to self-assessments of exposure. It is possible that the dissemination of the REV questionnaire could cause increases in anxiety about a resident's space particularly if the resident was unaware of the exposure. However, the purpose of the REV is to help residents and assessors alike understand the context of the space so that mitigation strategies or further assessments of the space can be deployed. I would imagine this survey being conducted in the presence of a home assessor or community agency that would be able to provide a sense of relief to the resident and assure them that further interventions would be implemented.

6.3.2 Occupancy Exposure Results for Scenarios

Examining the average weekly exposures (i.e., the integrated contaminant profile for the occupant over time) in the control scenario, a larger proportion of the radon, PM2.5, and mold spores an occupant is exposed to comes from occupying the living room and other spaces in the house rather than the basement (Figure 23a). This is due to the occupant only going down into the basement for a total of 30 minutes per week in the control scenario. Comparing the control to the other scenarios, the percentage contributions for mold and PM2.5 vary but generally radon exposure from the basement increases (Figures 23b-d). This was to be expected as both the amount of time being spent in the basement and the concentration of radon are increasing. Previous work has detailed the ability for radon to become trapped in spaces with low ventilation like basements^{331,340}. Under the control scenario, the only ventilation that occurred in the basement was the passive ventilation from the exterior wall leakage. In the other three scenarios, a small amount of ventilation was added, but ultimately it made little to no difference in reducing the overall contribution from the basement as radon was constantly entering the house from the HVAC system due to its ambient presence.

For all the pollutants, the large percentage contribution from other spaces is likely due to model set up. In CONTAM, users can input ambient concentrations for their pollutants as well as starting concentrations within each zone. Based on ratios between upstairs and basement settings from Li et al³⁵⁶, a starting concentration of 0.624 pCi/L for radon was assigned to each first floor zone in CONTAM to simulate real world conditions. Likewise, starting concentrations were assumed for PM2.5 and mold spores (Appendix E Table 5). Users can also model removal mechanisms (e.g., deposition, radioactive decay). In this model, only the radioactive decay of radon was considered as a pollutant removal mechanism other than airflow leakage and air

circulation, as including filtration and deposition rates for PM2.5 prevented the model from converging upon a solution. In practical application, a filtration system and particle deposition would need to be considered to accurately estimate true pollutant exposure (and other particulate exposure). Similarly, the impacts of ventilation rate and the type of ventilation system are also important parameters to consider. A recent study³⁷⁹ shows that mechanical ventilation systems cannot be considered universal anti-radon measures as the rates needed to effectively remove radon from the residence increases negative environmental and energy impacts.

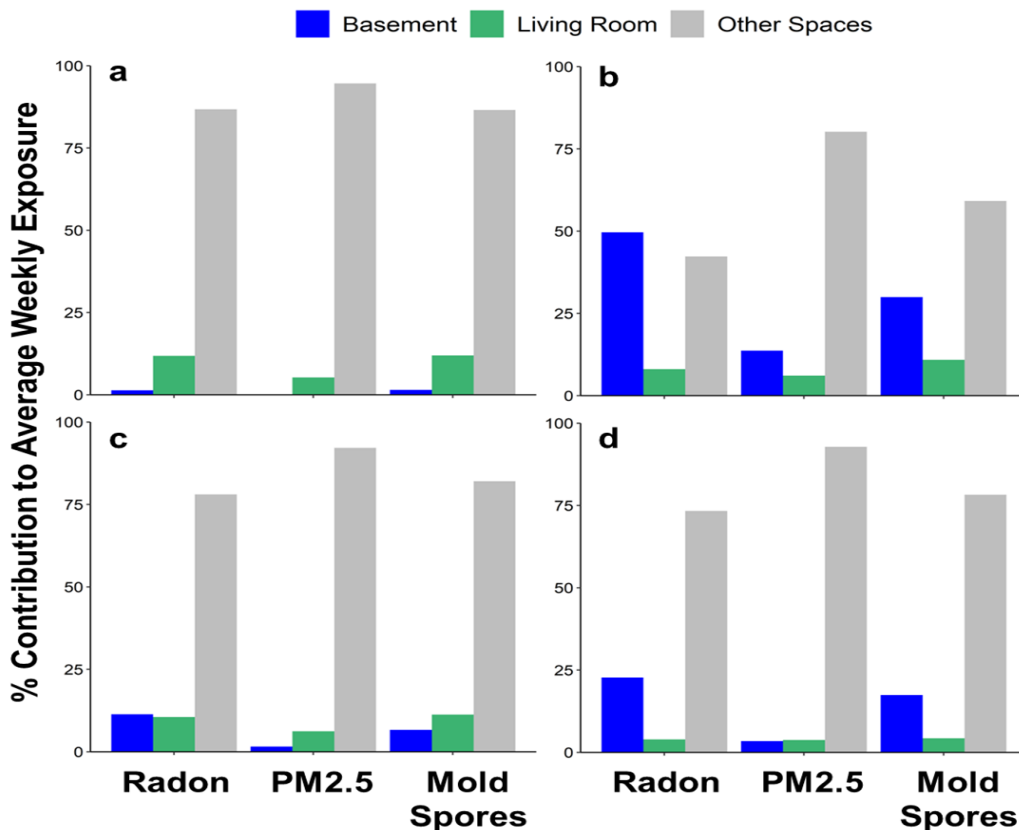


Figure 23: Percent contribution to average weekly exposure from the basement, living room, and other spaces in the home for the three pollutants examined under each scenario (a: Control, b: Home Office, c: Home Gym, d: Den / Play room).

The large percentage in the other category is due to the large amount of time spent either in outdoor spaces or in the bedroom for sleeping.

Significant differences ($p\text{-value} < 0.05$) in the average occupant exposure for radon, PM2.5, and mold spores in the basement were observed between the control and other scenarios (Figure 24). Factoring in the breathing rate and amount of air inhaled while in the basement for each scenario (Table 10) the home office and playroom scenarios had significantly higher masses of each pollutant compared to the control scenario, with the home office scenario having the highest masses inhaled. This is likely due to the increase in the frequency and duration spent in the basement in the home office and playroom scenarios. It is also noteworthy, that like the results from the REV calculations, the mass inhaled by a child in the tv/game room/ den scenario would be higher than that of an adult due to the difference in body mass between an adult and a child. A child's body is smaller than an adults and as such, a higher concentration relative to the exposure dose is inhaled. The difference in body weight could create an elevated chance for negative health outcomes in children, particularly if they were to spend large amounts of time in a space with lower ventilation rate compared to primary living spaces like living rooms and bedrooms.

Table 10: Total mass of pollutant inhaled per week while in the basement in each scenario

Pollutant	Control		HOF		HOG		DG	
	Adult	Child	Adult	Child	Adult	Child	Adult	Child
Radon (pCi)	19.6	37	8.1×10^4	1.5×10^5	2×10^4	37	1.1×10^4	2.2×10^4
PM2.5 (ug)	0.09	0.17	822	1550	137	0.17	75.9	143
# of Mold Spores	146	275	2.4×10^5	4.6×10^5	7.69×10^4	275	5.6×10^4	1.1×10^5

Control: 30 min of laundry per week; HOF: home office; HOG: home gym; DG: tv/game room/den. Control and HOF values were calculated using the average at rest inhalation rate of 4.8 L/min for the duration of time in the basement in each scenario. HOG and DG values were calculated using average inhalation rates based on activity from Pleil et al. 2021 For child values, the normalized factor based on body weight for a female child ages 5 -9 was used from Appendix E Table 5.

Like the increases in the mass of pollutant inhaled in the home office and tv/game room / den scenarios, the mass of pollutant inhaled in the home gym scenario also significantly increased from the control scenario, likely due to the increased inhalation rate used from Pleil et al.³⁷² (Appendix E Table 7) . However, an interesting point to note is that the values are on the same order of magnitude as in the tv/game room / den scenario, despite there being a higher rate of inhalation. Reviewing the occupancy schedule, it is likely that the schedules for both scenarios are similar enough that inhalation rate would not matter in terms of the inhaled pollutant. However, that is not to say that there could not be impacts on the dose-response relationships that would need to be calculated to assess true risk. Particularly in the case of basements where ventilation rates are often lower and pollutants like radon can be trapped, future work should evaluate the impacts of inhalation rate on the dose response relationships to ascertain any impacts to health risks.

Limited work has examined the impacts of inhalation rate on the exposure to indoor air pollutants of any kind³⁸⁰⁻³⁸², likely due to recommendations from regulatory agencies that suggest using the airborne concentration rather than incorporate the inhalation rate and body weight³⁸³. While necessary to assess the airborne concentration in a space, that alone is not a good indicator of how much pollutant could potentially reach the lungs.

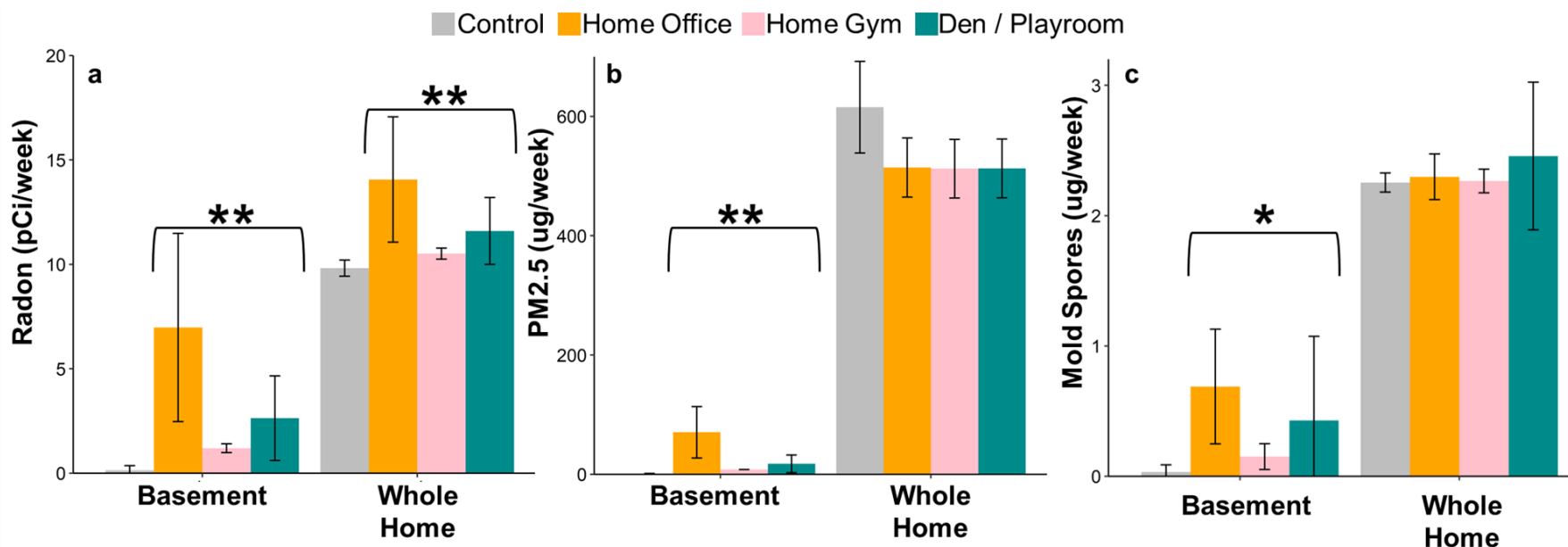


Figure 24: Average \pm standard deviation weekly ($n = 7$) basement and whole home exposure concentrations to a) radon, b) PM_{2.5}, and c) mold spores for each scenario. Significant differences were observed for all three pollutants between the control and each test scenario, while only a difference in whole home radon exposure was observed (due to basement contributions). * signifies a significant difference at <0.05 p-value and ** signifies a significant difference at a p-value < 0.01 .

6.3.3 Future Considerations and Limitations

The work done in this aim modeled and examined the exposure to physical, chemical, and biological pollutants in basements under a variety of use conditions and created an easy-to-understand tool to calculate relative exposure. While different use patterns had a significant impact on the exposure to pollutants in the modeled basement, there are several limitations and future considerations that should be addressed. First, for the REV scale it was assumed that the three pollutants studied followed a linear dose-response model. For PM_{2.5}, radon, and mold spore counts, there is no evidence that suggests that the dose-response relationships are nonlinear. Previous work suggests that PM_{2.5} concentrations above 2 µg/m³ follow a linear dose-response relationship³⁷⁴, while the dose-response relationships for both radon and mold are not accurate due to external influences in predicting cancer outcomes³⁸⁴ or are limited to a small number of studies with often contradicting results³⁸⁵. To accurately assess and develop tools that communities and researchers can use alike, future work will need to develop accurate dose-response relationships for a range of pollutants in multiple phases. There will also need to be more studies that accurately describe methods for detecting and reporting pollutant concentrations in confined spaces, particularly for biological pollutants like mold spores and their mycotoxins. Due to the numerous species and potential strains of mycotoxins produced from mold spores which may cause allergic reactions in individuals, there is no single standard for mold presence that can accurately predict acceptable levels for all members of a population; however, researchers can work to agree upon a standard method for detecting, measuring, and quantifying mold impacts for the most common species. Without standard methods to accurately quantify and identify relationships between

pollutant concentration and health outcomes, there will never be an accurate assessment of risk and exposure in indoor spaces, but particularly in basements.

Moreover, a better understanding of the impacts of building characteristics, renovations/retrofits, and occupancy activities on pollutant exposures to conduct better risk assessments in indoor environments. In this work, standard air leakage rates were assumed to conduct exposure modelling, however in reality these are all parameters that would have to be measured and assessed in real time and across a wide variety of residences. Additionally, only the radioactive decay of radon was considered as a pollutant removal mechanism other than airflow leakage and air circulation. Future works will need to incorporate filtration systems and particle deposition to accurately estimate pollutant exposure and understand the impacts of these systems indoors. Similarly, the impacts of ventilation rate and the type of ventilation system are also important parameters to consider alongside common use scenarios for basements. IAQ is closely related to the type of activities carried out by occupants. Therefore, the type, frequency and duration of activities performed by residents will influence the state and dynamics of the IAQ. Incorporating this will allow researchers to capture the variety in how different people occupy their residential spaces and work to build more generalizable models for others to build upon. Furthermore, conducting sensitivity analyses on the models created will help to inform how responsive the model outputs are given changes in input parameters, thus improving the overall functionality and reliability of the models.

Given the global impacts of climate change, more work will need to be done to assess how pollutant exposures are changing and to determine any interactions between the water and air phases. For instance, it is known that radon is geologic in nature and diffuses into the air from rock formations, soils, and building materials. A significant increase in precipitation could saturate the

groundwater table and further mobilize radon or other pollutants into basements that suffer from inundation. A recent study in India examined the annual effective dose for radon by both ingestion of water and inhalation of radon diffused from water³⁸⁶ and found no significant risk from exposure to water sources contaminated with low levels of radon; however, the authors conducted the study under dry conditions, so impacts from precipitation could not be determined. However, another study conducted simulated rainfall experiments to examine radon emanation from uranium mill tailings and found the radon emanation increases nonlinearly before decreasing and stabilizing due to changes in surface moisture content from rainfall³⁸⁷. This suggests that increased precipitation and changes in surface moisture content could likely impact radon emanation in other areas that experience increased precipitation, and it is recommended that studies on the diffusion rate of radon from foundations in flood prone areas are conducted. Likewise, as climate change impacts precipitation rates, it will also impact temperatures and seasonal effects on pollutant exposures. As such, future works should consider incorporating more long-term studies over multiple seasons to elucidate seasonal variations in pollutant exposure and IAQ in basements and other confined spaces. Finally, in practical application, zone-specific thresholds for different pollutants will need to be built off of existing indoor air quality data, the measurement of pollutants in a range of residences, and future modeling of indoor pollutant concentrations via simulation software like CONTAM. The work presented here provides a promising starting point for future work in the residential space and as such it will be imperative that as models are created, they are validated by real data collected from the environment to ensure the models are useful and accurate in predicting IAQ pollution and impacts.

6.4 Conclusions

Overall, there is need for better IAQ models that incorporate neglected microenvironments such as basements as changing housing market patterns and increased climate change impacts will continue to impact how residents use their spaces. The findings presented here provide an interesting basis for the continued modeling of basements for pollutant exposures. Exposures to radon, PM_{2.5}, and mold spores were significantly higher in each basement use scenario, as a result primarily of duration and frequency spent in the space. While the amount of pollutant inhaled was significantly higher under each basement use scenario, it is important to note that as of the time of writing, no further risk assessment work has been done to interpret what these results mean with respect to dose-response relationships and negative health outcomes. To ensure public health safety, it is recommended that future studies model and validate the scenarios they model with tangible data collected from residential basements. Moreover, improving the understanding of IAQ in basements will greatly help home assessors, researchers, and homeowners alike in increasing the comfort of residential spaces.

7.0 Concluding Remarks and Recommendations to Stakeholders

The world population is continually growing and so are the number of urban areas and systems needed to sustain society. Within those areas and systems, urban water infrastructures are currently unequipped to provide adequate water volume and quality due to the increasing number of challenges associated with water provision, public health, and environmental safety. In the coming years, regulations will become increasingly strict and new chemicals and microorganisms will become regulated to be treated for in all phases of urban water (wastewater, drinking water, and storm water). Likewise, with climate change impacts inevitably looming, impacts in the water treatment and infrastructure spaces will reverberate throughout other industries making it more difficult to sustainably advance society. As such, there is a need for us to better understand and evaluate how changes in the built environment, namely urban water infrastructure, impact microorganisms that are relevant to public and environmental health. Understanding these impacts will allow us to inform current and future design and operational choices (e.g., disinfection methods, corrosion control, etc.) allowing for proactive management and curation of the built environment to enhance the safety, reliability, and usability of our already limited water supply.

As an environmental engineer, it is important that I make my academic research findings translatable to a variety of people so that more informed decisions can be made at all levels. The following are a set of recommendations based on the work presented that I think should be considered as we all move forward to address the grand challenges, we have ahead of us in both the natural and built environments:

- Thoroughly examined alternative disinfection strategies for water treatment will be needed to aid society in meeting the global water demand. As our current water supplies

become more limited and emerging threats (e.g., enteric viruses, antibiotic resistance genes) to water continue to increase, solely depending on chlorination as our primary disinfectant will no longer be viable. Alternative physical, chemical, and biological treatment technologies will need to be employed and their impacts on a suite of parameters should be evaluated to uphold and advance the state of water treatment. Researchers and practitioners should collaborate in the development of these technologies to better design them for applicable use.

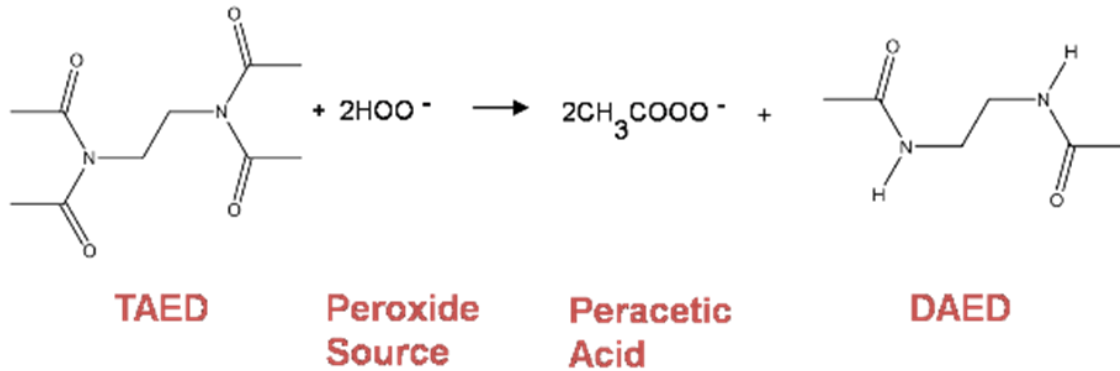
- The long-term links between operational changes in the built environment and impacts in the natural environment need to be further studied and elucidated. Changes in aging urban water pipes should be continuously monitored as a public and environmental safety measure. Whether pipes are replaced, or chemicals are added to maintain current pipe systems, future studies should consider conducting more in-situ long-term pipe studies to evaluate the scale of impact in both natural and engineered systems. Furthermore, researchers and practitioners should work together to identify priority areas of maintenance and to elucidate potential synergistic effects between both systems to ensure continual development and holistic protection of both systems.
- Intersectional and transdisciplinary evaluations of public health exposures from the interactions between water and indoor air will be imperative to understanding the true impacts of climate change on the built environment. Climate change impacts on our engineered systems will need to be examined using a transdisciplinary approach to identify, quantify, and assess the risk of threats to public and environmental health accurately and holistically. In particular, the impacts of floodwater mobilized pollutants in indoor spaces will need to be both modeled and examined in real world residential

settings to assess the pollutant exposures and risks. Moreover, new standard methods that incorporate fundamental science, community experience, and accessible communication across sectors will be a necessary component in assessing exposures to threats in the environment. Without these, siloed approaches to understanding the true impacts of climate change in urban water infrastructure will stymie the advancement of our systems, leaving them vulnerable to further degradation.

The next generations of scientists, engineers, and policymakers face a substantial task in safeguarding and advancing urban water infrastructure. By conducting comprehensive assessments of our existing systems and their interconnectivity, we can pave the way for the advancement of improved treatment technologies, enhanced management strategies, and the development and deployment of effective policy and legislation. Moreover, this endeavor will promote broader societal awareness and encourage proactive decision-making concerning public and environmental health.

Appendix A Aim 1.0 Supplementary Information

Appendix A.1 TAED-PAA Synthesis Information



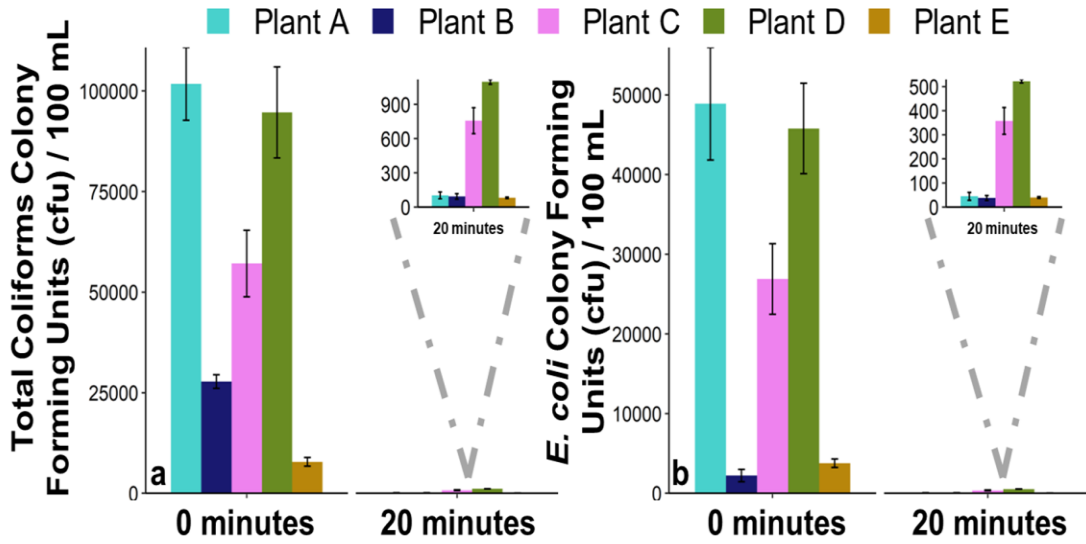
Appendix A Figure 1: TAED-PAA production schematic (provided by Lubrizol)

Sodium percarbonate (PCS) dissociates to sodium carbonate and hydrogen peroxide almost immediately in water. The hydrogen peroxide then reacts with TAED, hydrolysing it to triacetylenediamine (TriAED) and then diacetylenediamine (DAED). This process releases two moles of PAA and an end product, DAED. TAED-PAA synthesis differs from commercial PAA synthesis due to hydrogen peroxide and acetic acid not being present in the same way. Since the hydrogen peroxide is used to generate the peracetic acid rather than stabilize it, the hydrogen peroxide concentration in TAED generated PAA is significantly lower than that found in commercial PAA and so the total oxidant level is commensurately low also. The actual level will depend on the reaction conditions and the completeness of the reaction under those conditions.

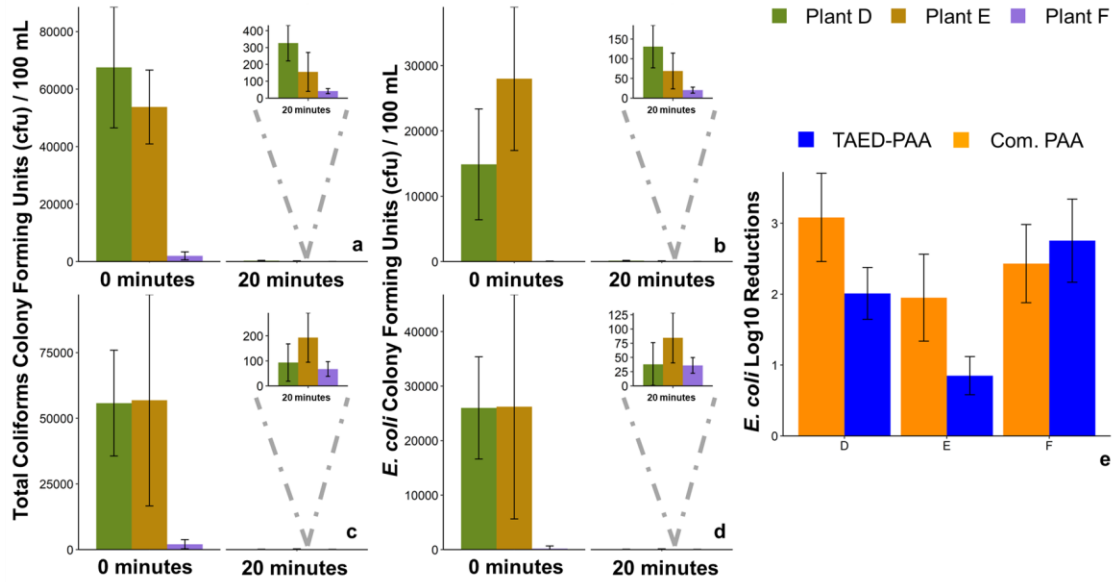
For example, under static mixing conditions, a maximum of 346 ppm peracetic acid is released (60 mins) from a 3.75g/l Jet Harvest 527 dose = 0.346g peracetic acid = **0.004 moles peracetic acid** (theoretical max peracetic acid release = 773ppm; max release achieved is

equivalent to 44.9% release). To generate the amount of peracetic acid using TAED, 0.002 moles of TAED and 0.004 moles of hydrogen peroxide. Assuming a total percarbonate level of **1.4657g/l @ 90.53% active = 1.327g/l sodium percarbonate (PCS), 0.0127 moles of hydrogen peroxide would be generated in solution.** Therefore, assuming no active degradation of peracid or peroxide during the 60 min peracid generation time (very unlikely), the remaining peroxide in solution would be = 0.0127 moles – 0.004 moles = **0.087 moles = 0.296g/l = 296 ppm.** After 60 min, the resulting solutions would contain a 346 ppm peracetic acid: 296ppm hydrogen peroxide ratio. The peroxide would decompose much more rapidly during dissolution and generation. This is compared to 15% commercial PAA which typically contains 26% peroxide. The nature of the in-situ reaction to generate PAA means that transport and handling hazards are greatly reduced compared to equilibrium, pre-formed PAA and only the amount of PAA required for the application is generated at the site. Both TAED and DAED are non-toxic and non-sensitizing compounds which biodegrade.

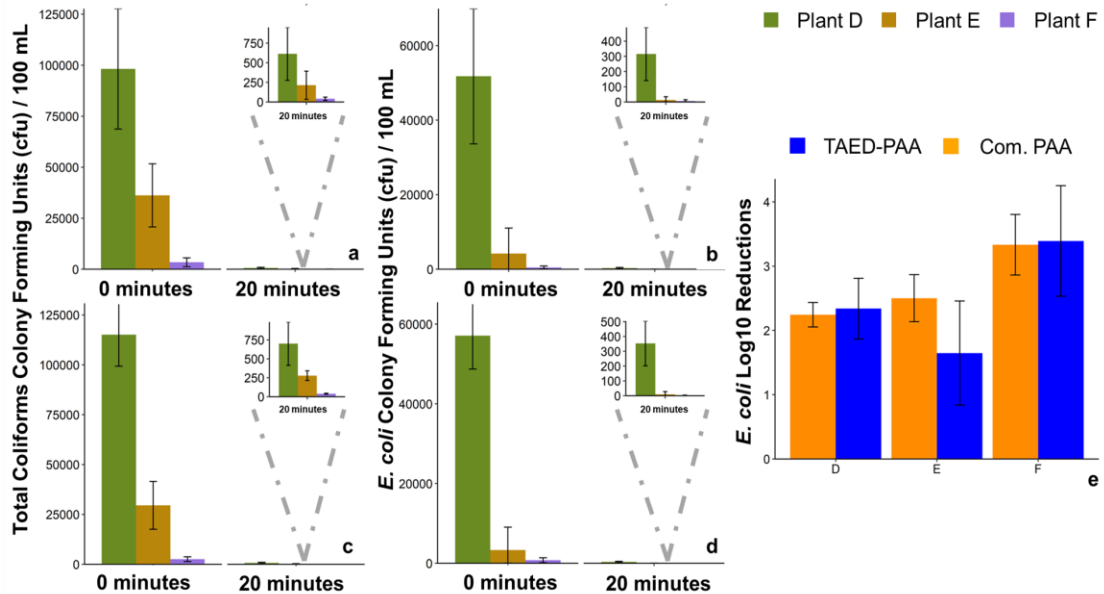
Appendix A.2 Water Quality Figures and Tables



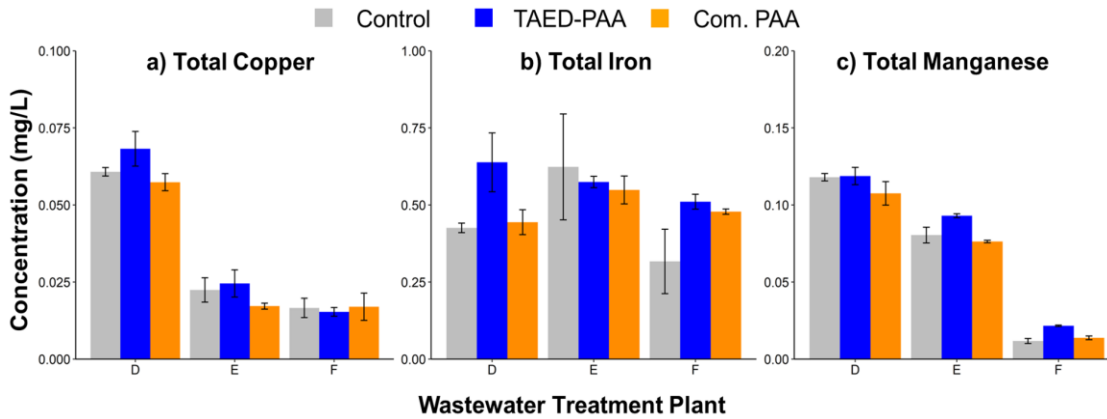
Appendix A Figure 2: Average (n = 9) a) total coliform and b) *E. coli* counts before and after TAED-PAA treatment for plants A – E



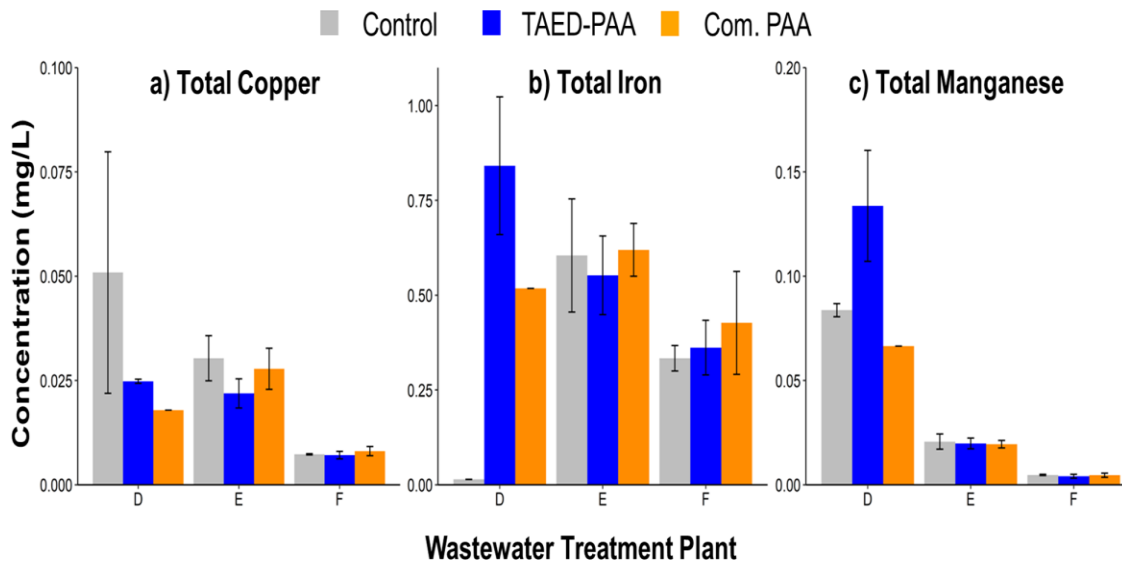
Appendix A Figure 3: Conventional Ct average (n = 9) a) TAED-PAA treated total coliform, b) TAED-PAA treated *E. coli*, c) Commercial PAA treated total coliform, d) Commercial PAA treated *E. coli* counts before and after treatment; e) *E. coli* log10 reductions under both PAA treatments



Appendix A Figure 4: Integral Ct average (n = 9) a) TAED-PAA treated total coliform, b) TAED-PAA treated *E. coli*, c) Commercial PAA treated total coliform, d) Commercial PAA treated *E. coli* counts before and after treatment; e) *E. coli* log10 reductions under both PAA treatments



Appendix A Figure 5: Average (n = 3) total transition metal concentrations with standard deviation before and after PAA application under conventional Ct approach. a) total copper, b) total iron, and c) total manganese across the three plants studied in section 2.3.2.



Appendix A Figure 6: Average (n = 3) total transition metal concentrations with standard deviation before and after PAA application under integral Ct approach. a) total copper, b) total iron, and c) total manganese across the three plants studied in section 2.3.2.

Appendix A Table 1: Average \pm s.d. water quality parameters pre- & post- conventional Ct PAA treatment

<i>Parameter</i>	Plant D			Plant E			Plant F		
	Control ^a	TAED-PAA	Com. PAA	Control	TAED-PAA	Com. PAA	Control	TAED-PAA	Com. PAA
<i>Total N (mg/L N)</i>	10.33 \pm 2.49	17.33 \pm 3.30	14.33 \pm 1.89	4.67 \pm 0.47	6.67 \pm 1.25	3.67 \pm 1.70	7.33 \pm 4.78	38.67 \pm 1.70	33.67 \pm 9.98
<i>Total P (mg/L P)</i>	3.50 ^b	3.50 ^b	3.50 ^b	5.32 \pm 0.02	3.55 \pm 0.07	3.50 \pm 0.07	2.12 \pm 0.20	3.26 \pm 0.31	3.50 \pm 0.27
<i>BOD₅ (mg/L O₂)</i>	37.31 \pm 10.07	42.83 \pm 9.87	28.28 \pm 9.02	23.33 \pm 6.78	26.74 \pm 9.04	29.40 \pm 11.63	38.81 \pm 14.29	33.19 \pm 8.70	30.26 \pm 14.14
<i>TDS (mg /L)</i>	235.33 \pm 204.13	86.00 \pm 2.37	85.56 \pm 2.06	464.00 \pm 43.20	318.67 \pm 13.19	276.00 \pm 33.94	480.00 \pm 3.27	433.33 \pm 13.19	434.67 \pm 4.99

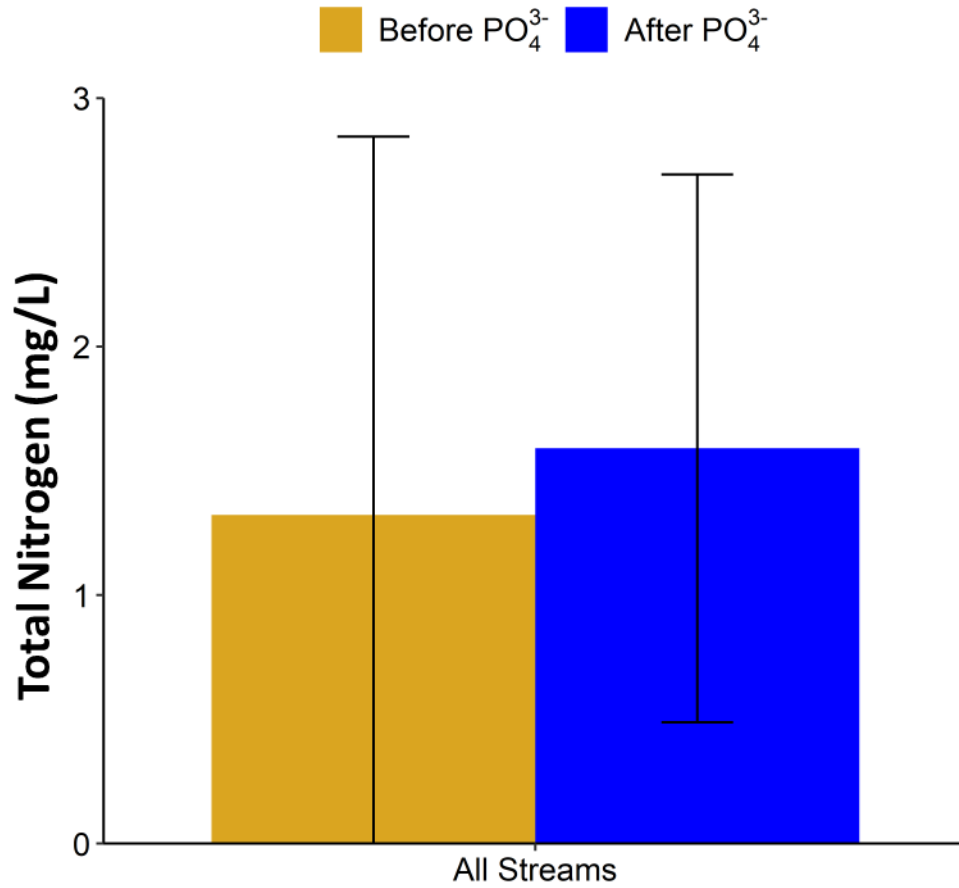
a) Negative controls consisted of wastewater without PAA addition

b) Samples reached method detection limit maximums. Was not able to reprocess.

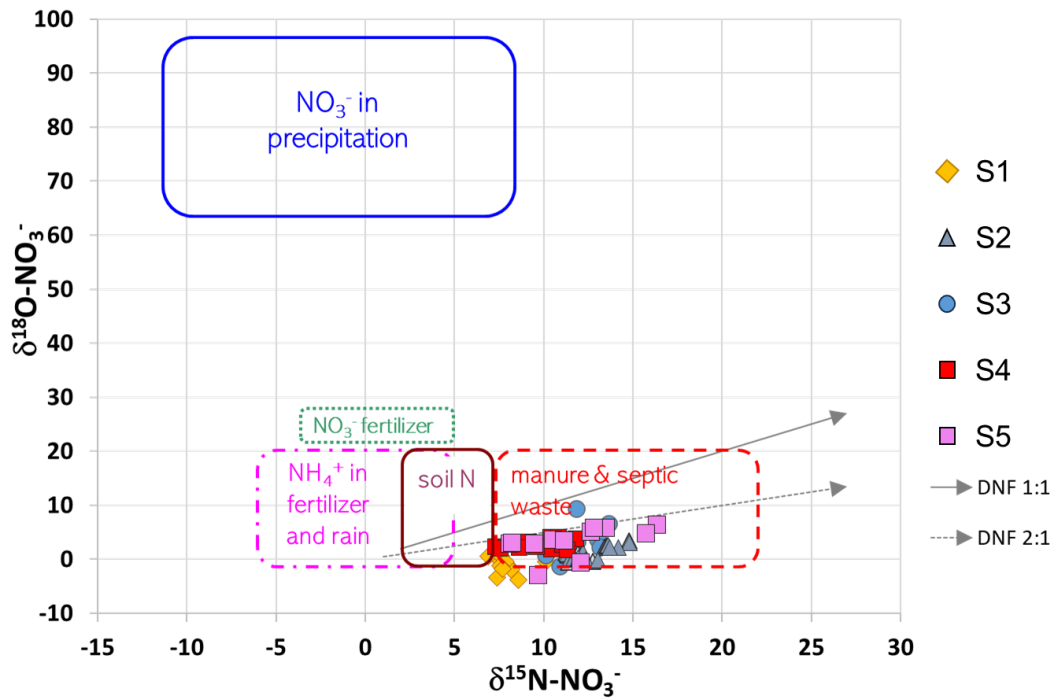
Appendix A Table 2: Average \pm s.d. water quality parameters pre- & post- integral Ct PAA treatment

<i>Parameter</i>	Plant D			Plant E			Plant F		
	Control	TAED-PAA	Com. PAA	Control	TAED-PAA	Com. PAA	Control	TAED-PAA	Com. PAA
<i>Total N (mg/L N)</i>	10.33 \pm 2.49	23.00 \pm 7.26	13.33 \pm 2.05	4.67 \pm 0.47	27.67 \pm 0.94	28.00 \pm 2.16	7.33 \pm 4.78	54.33 \pm 6.18	66.67 \pm 19.36
<i>Total P (mg/L P)</i>	3.50 \pm 0.00	3.97 \pm 0.07	0.17 \pm 0.16	5.32 \pm 0.02	6.47 \pm 0.17	3.50 \pm 0.83	2.12 \pm 0.20	2.08 \pm 0.07	3.50 \pm 0.04
<i>BOD₅ (mg/L O₂)</i>	74.25 \pm 13.88	87.94 \pm 19.76	86.10 \pm 26.50	30.53 \pm 8.73	43.54 \pm 5.84	20.55 \pm 10.18	52.88 \pm 15.92	46.76 \pm 11.95	43.73 \pm 15.80
<i>TDS (mg /L)</i>	230.67 \pm 207.56	70.89 \pm 5.77	77.78 \pm 2.74	420.00 \pm 21.42	398.67 \pm 13.60	401.33 \pm 15.43	464.00 \pm 22.86	413.33 \pm 37.85	438.67 \pm 40.84

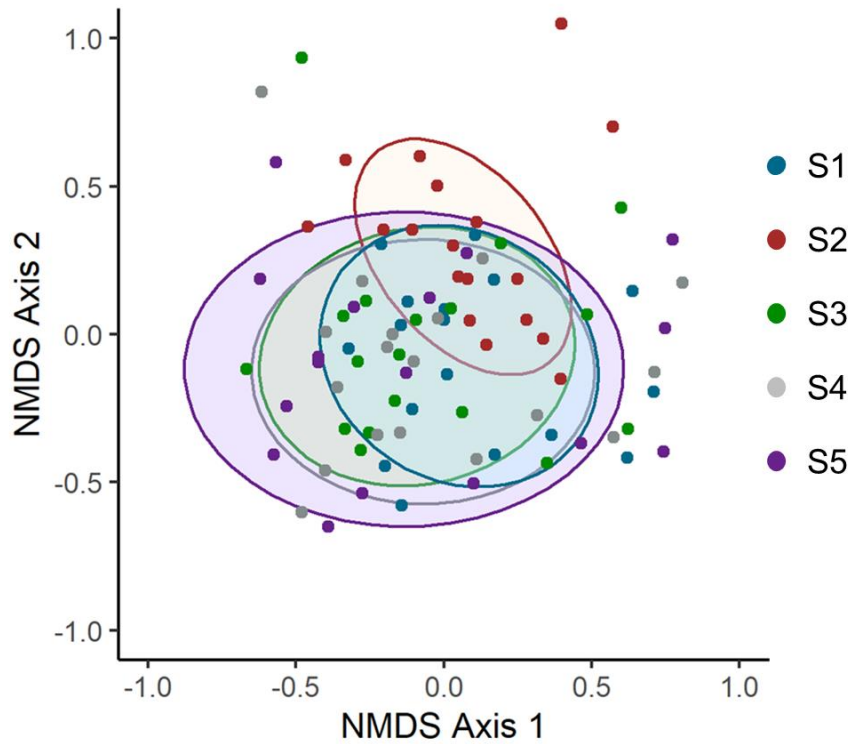
Appendix B Aim 2.0 Supplementary Information



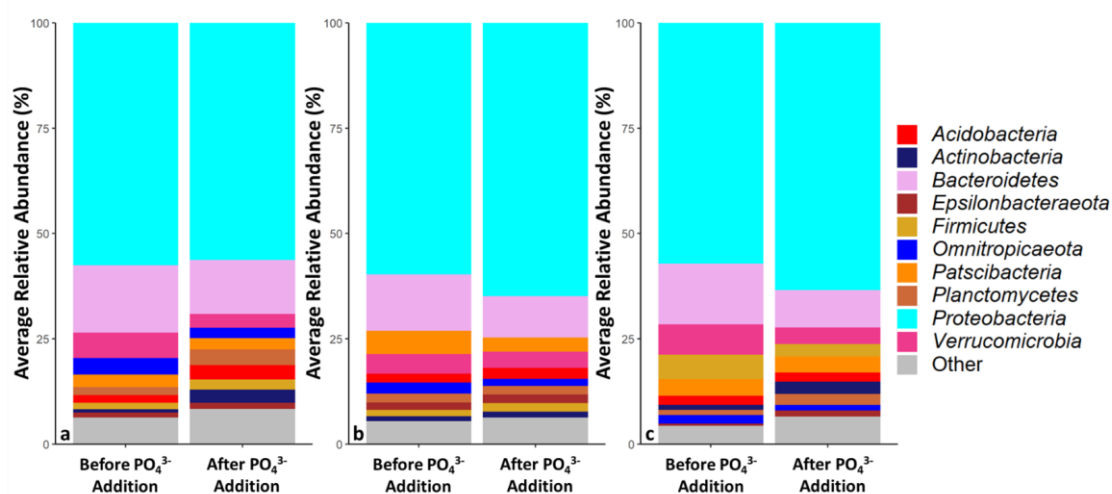
Appendix B Figure 1: Average (n = 15) total nitrogen concentration in each urban stream before and after PO_4^{3-} addition into the DWDS. Error bars represent the standard deviation.



Appendix B Figure 2: Average ($n = 15$) total nitrogen concentration in each urban stream before and after PO_4^{3-} addition into the DWDS. Error bars represent the standard deviation.

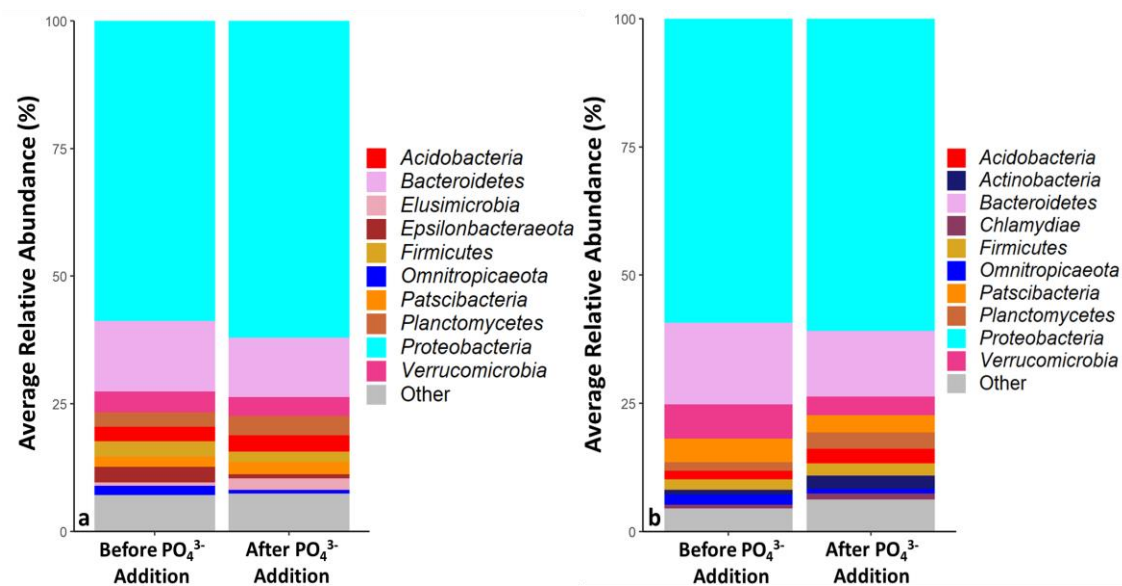


Appendix B Figure 3: Nonmetric multidimensional scaling (NMDS) plots of Bray-Curtis distances for the five urban stream sites sampled. The ellipses represent the 95% confidence interval of the distribution from the centroid of the cluster points.



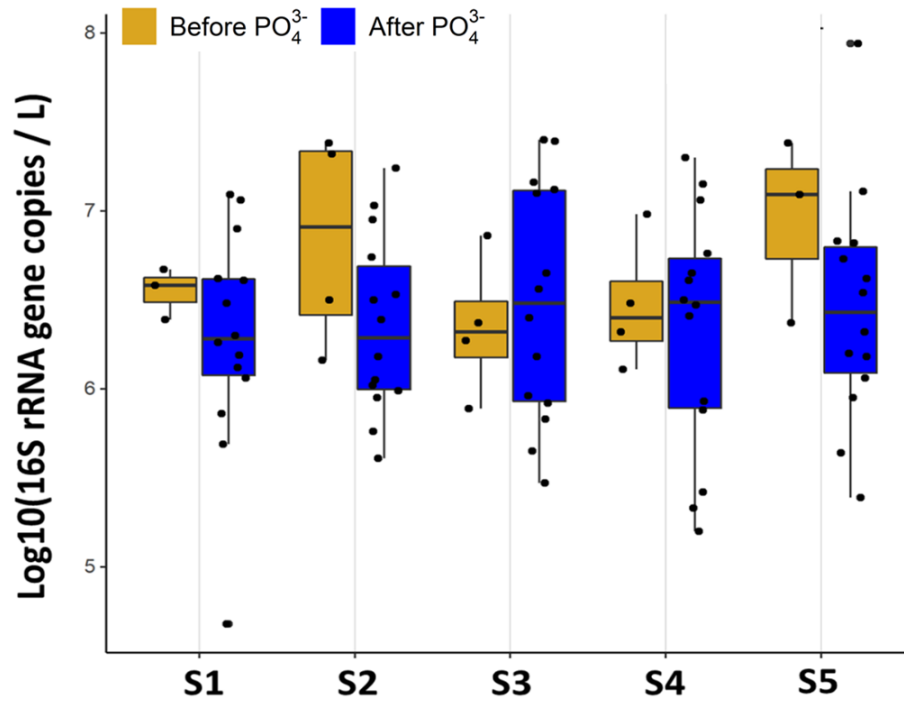
Appendix B Figure 4: Top 10 most abundant phyla in urban streams a) S1, b) S3, and c) S5 before and after PO_4^{3-} addition in the distribution system.

Streams S1, S3, and S5 all had the same top ten phyla represented. Significant changes in were observed in the relative abundances of *Acidobacteria*, *Planctomycetes*, and *Verrucomicrobia* in stream S1 while no significant differences were observed in streams S3 or S5.

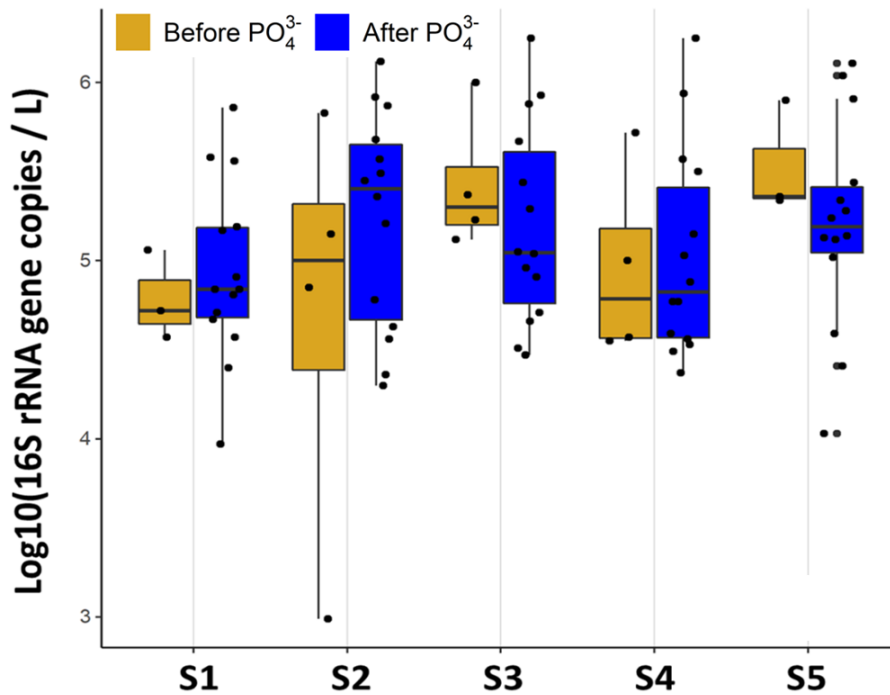


Appendix B Figure 5: Top 10 most abundant phyla in urban streams a) S2 and b) S4 before and after PO_4^{3-} addition in the distribution system.

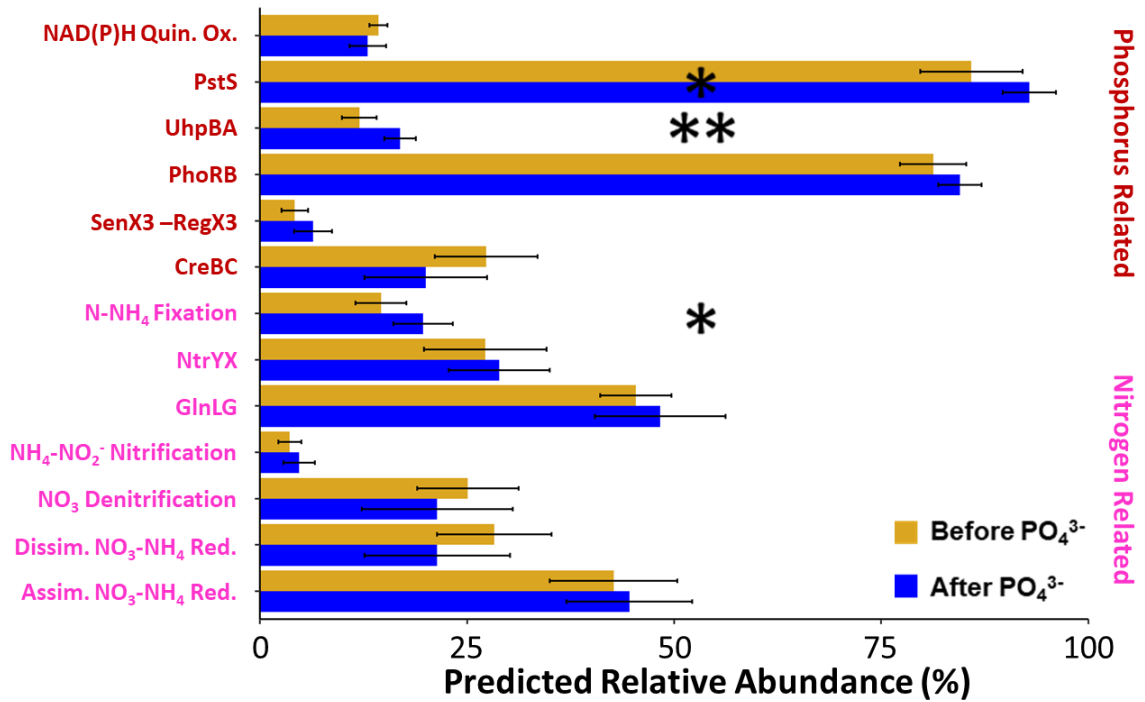
Significant changes in were observed in the relative abundances of *Elusimicrobia* and *Omnitropicaeota* in stream S2 while significant differences were observed in *Omnitropicaeota* and *Planctomycetes* in stream S4.



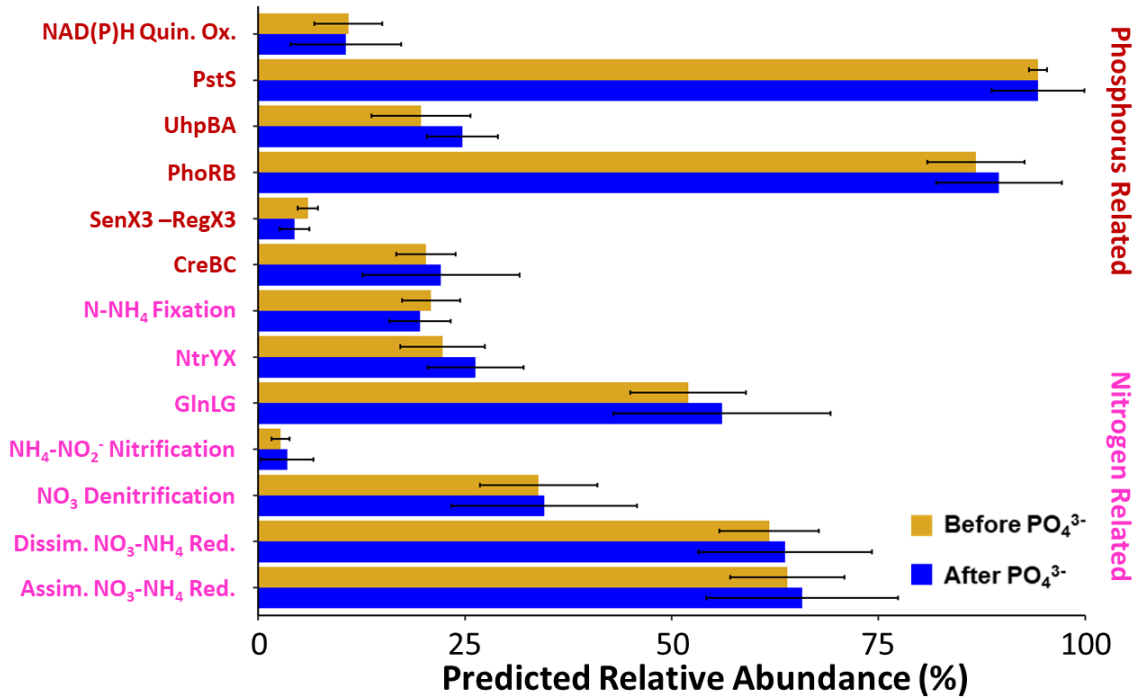
Appendix B Figure 6: Cyanobacteria absolute abundance in urban streams before and after PO₄³⁻ addition into the DWDS . No significant differences were observed in any stream after PO₄³⁻ addition.



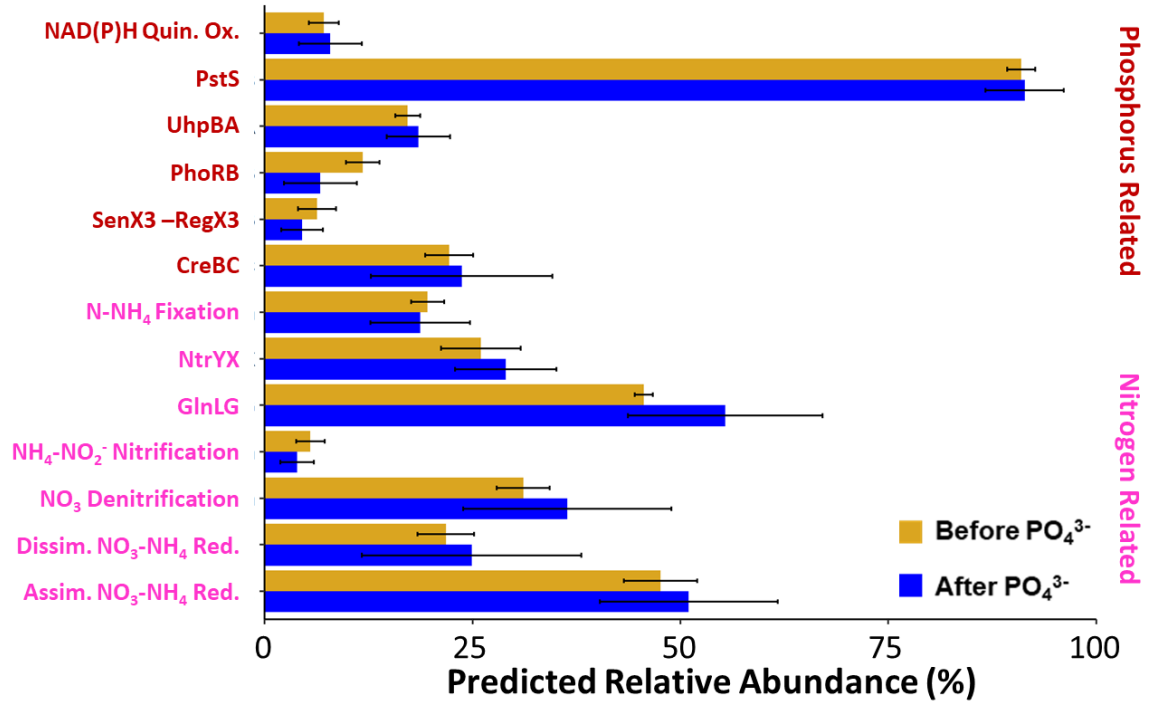
Appendix B Figure 7: *Candidatus Accumulibacter* absolute abundance in urban streams before and after PO₄³⁻ addition into the DWDS . No significant differences were observed in any stream after PO₄³⁻ addition.



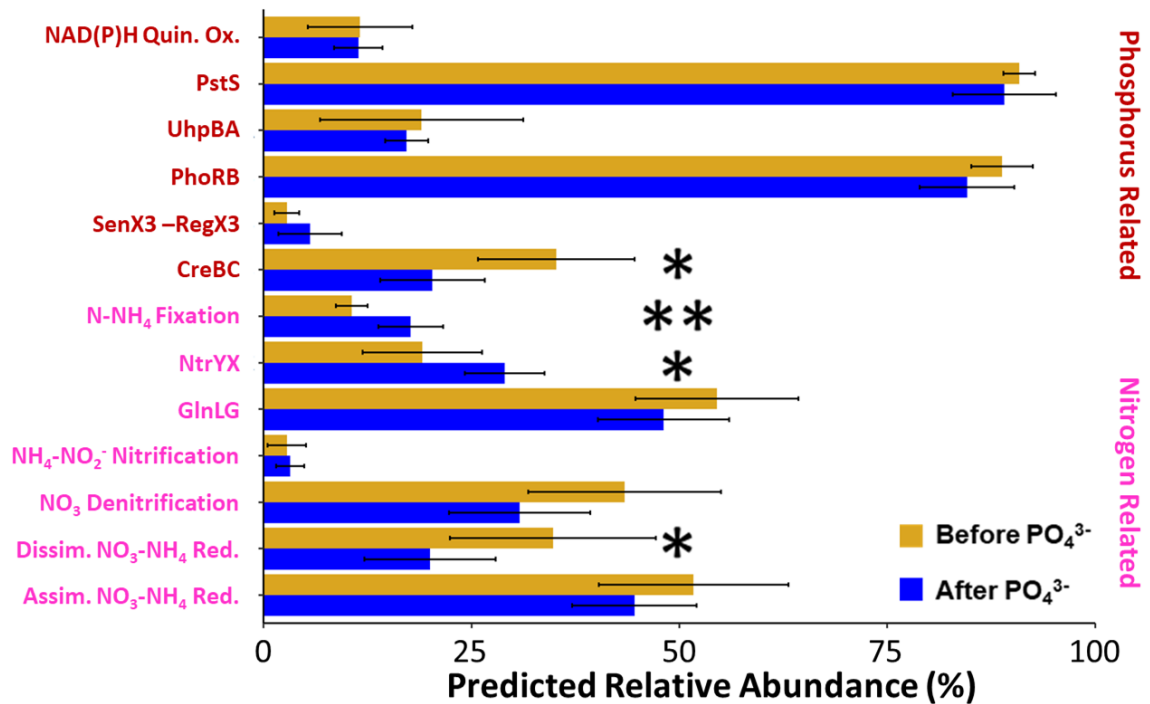
Appendix B Figure 8: Average phosphorus and nitrogen functional trait relative abundance of stream S1 before and after PO₄³⁻ addition into the DWDS. * represents a p-value < 0.05, ** represents a p-value < 0.01.



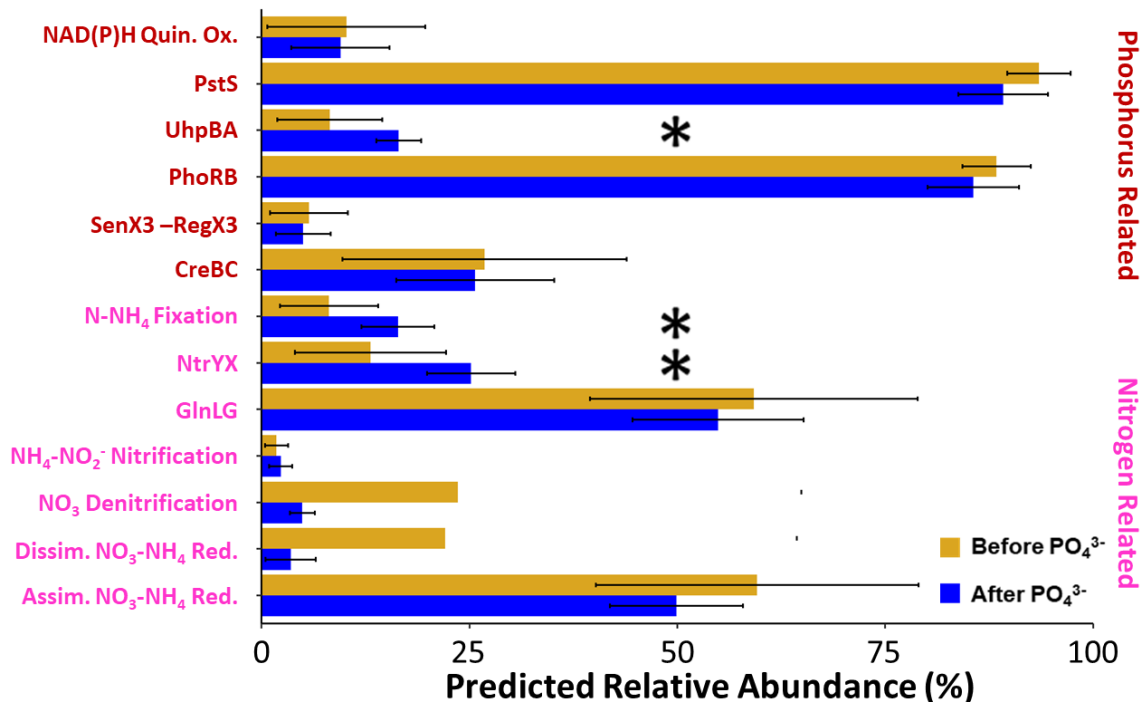
Appendix B Figure 9: Average phosphorus and nitrogen functional trait relative abundance of stream S2 before and after PO₄³⁻ addition into the DWDS.



Appendix B Figure 10: Average phosphorus and nitrogen functional trait relative abundance of stream S3 before and after PO₄³⁻ addition into the DWDS.



Appendix B Figure 11: Average phosphorus and nitrogen functional trait relative abundance of stream S4 before and after PO₄³⁻ addition into the DWDS. * represents a p-value < 0.05, ** represents a p-value < 0.01.



Appendix B Figure 12: Average phosphorus and nitrogen functional trait relative abundance of stream S5 before and after PO₄³⁻ addition into the DWDS. * represents a p-value < 0.05, ** represents a p-value < 0.01.

Appendix B Table 1: Different water quality parameters measured in this study and the method / apparatus

Parameter	Unit	Method / Apparatus
<i>Temperature</i>	°C	YSI multiparameter sonde
<i>pH</i>	--	YSI multiparameter sonde
<i>Dissolved Oxygen</i>	mg/L O ₂	YSI multiparameter sonde
<i>Total Reactive Phosphorus</i>	µg/L P	Lachat QuikChem Analyzer
<i>Soluble Reactive Phosphorus</i>	µg/L P	Lachat QuikChem Analyzer
<i>Total Phosphorus</i>	µg/L P	Lachat QuikChem Analyzer
<i>Ammonia</i>	mg/L N	Lachat QuikChem Analyzer
<i>Nitrate & Nitrite</i>	mg/L N	Lachat QuikChem Analyzer
<i>Chloride</i>	mg/L	Lachat QuikChem Analyzer
<i>Sulfate</i>	mg/L	Lachat QuikChem Analyzer
<i>Bromide</i>	mg/L	Lachat QuikChem Analyzer
<i>Phosphate (IC)</i>	mg/L	Dionex Ion Chromatograph
<i>Nitrogen Dioxide (IC)</i>	mg/L	Dionex Ion Chromatograph
<i>Nitrate (IC)</i>	mg/L	Dionex Ion Chromatograph
<i>Total & Dissolved Iron</i>	mg/L	ICP-MS
<i>Total & Dissolved Copper</i>	mg/L	ICP-MS
<i>Total & Dissolved Manganese</i>	mg/L	ICP-MS
<i>Total & Dissolved Lead</i>	mg/L	ICP-MS

Appendix B Table 2: Average ± standard deviation (s.d.) measured water quality parameters before and after full-scale PO₄³⁻ addition into the DWDS. Dissolved concentrations are in parentheses.

Parameter	Average ± s.d. Before PO₄³⁻ (n = 15)	Average ± s.d. After PO₄³⁻ (n = 15)
Temperature	4.24 ± 1.19	7.76 ± 2.27
pH	8.40 ± 0.17	7.82 ± 0.11
Dissolved Oxygen	0.001 ± 0.002	1.71 ± 0.364
Total Phosphorus	0.069 ± 0.084	0.103 ± 0.105
Total Nitrogen	1.32 ± 1.52	1.59 ± 1.10
Total (& Dissolved) Iron	0.028 ± 0.027 (0.017 ± 0.017)	0.013 ± 0.016 (0.001 ± 0.001)
Total (& Dissolved) Copper	0.005 ± 0.006 (0.004 ± 0.005)	0.009 ± 0.004 (0.008 ± 0.003)
Total (& Dissolved) Manganese	0.006 ± 0.013	0.001 ± 0.001

Total (& Dissolved) Lead	(0.001 ± 0.002)	(0.0001 ± 0.0001)
	0.3 ± 1.0	0.051 ± 0.043
	(0.057 ± 0.062)	(0.01 ± 0.01)

Appendix B Table 3: ddPCR target genes, amplicon size, annealing temperature, and primer sequences

Target Taxa	Target gene	Approx. Amplicon Size (bp)	Annealing Temp. (°C)	Sequence (5' to 3')
Total Bacteria	16S rRNA	200	57	F: ACTCCTACGGGAGGCAG R: ATTACCGCGGCTGCTGG
<i>Cyanobacteria</i>	16S rRNA	422	60	F: GGGGAATCTTCCGCAATGGG R: GACTACTGGGGTATCTAATCCCATT
<i>Candidatus Accumulibacter</i>	16S rRNA	351	60	F: CCAGCAGCCGCGGTAAT R: GTTAGCTACGGCACTAAAAGG

Appendix B Table 4: ddPCR reaction conditions

Target taxa (gene)	Temperatures and Times	# of cycles
Total Bacteria	95°C, 5:00, Ramp 2/s	45
	95°C, 0:30, Ramp 2/s	
	57°C, 1:00, Ramp 2/s	
	72°C, 1:00, Ramp 2/s	
	4°C, 5:00, Ramp 2/s	
	90°C, 5:00, Ramp 2/s	
	12°C, --, Ramp 2/s	
<i>Cyanobacteria</i> , <i>Candidatus Accumulibacter</i>	95°C, 5:00, Ramp 2/s	44
	95°C, 0:30, Ramp 2/s	
	60°C, 1:00, Ramp 2/s	
	72°C, 1:00, Ramp 2/s	
	4°C, 5:00, Ramp 2/s	
	90°C, 5:00, Ramp 2/s	
	12°C, --, Ramp 2/s	

Appendix B Table 5: ddPCR assay thresholds, LOD, and LOQ

Target taxa (gene)	ddPCR Threshold	Limit of Detection	Limit of Quantification
Total Bacteria	12900	5.3 gene copies / 20 µL	53 gene copies / 20 µL
<i>Cyanobacteria</i>	9567	7.9 gene copies / 20 µL	7.9 gene copies / 20 µL
<i>Candidatus Accumulibacter</i>	7632	1.1 gene copies / 20 µL	116 gene copies / 20 µL

Thresholds were determined experimentally by spiking target taxa's gblock at different concentrations into water DNA matrix and adjusting threshold until expected concentration was read out.

Appendix B Table 6: Module list of functional traits relating to phosphate or nitrogen metabolism

BugBase Module ID	Module Name
M00145	NADPH Quinone Oxidoreductase in Chloroplasts and Cyanobacteria
M00175	Nitrogen Fixation: Nitrogen-Ammonia
M00222	Phosphate Transport System
M00434	PhoRB Phosphate Starvation Response
M00438	Nitrate-Nitrite Transport System
M00443	SenX3-RegX3 Phosphate Starvation Response
M00449	CreBC Phosphate Regulation
M00473	UhpBA Hexose Phosphate Uptake
M00497	GlnLG Nitrogen Regulation
M00498	NtrYX Nitrogen Regulation
M00524	FixLJ Nitrogen Fixation
M00528	Ammonia-Nitrite Nitrification
M00529	Nitrate-Nitrogen Denitrification
M00530	Dissimilatory Nitrate Reduction: Nitrate-Ammonia
M00531	Assimilatory Nitrate Reduction: Nitrate-Ammonia

Appendix B Table 7: Significant responses ($p < 0.05$) of green algae and Cyanobacteria biomass to various nutrient treatments (N as mg N/L and P as mg P/L) before PO_4^{3-} addition, two months, and twelve months after PO_4^{3-} addition in S1

Algae Type	Before PO_4^{3-} Addition	Two months after PO_4^{3-} Addition	One year after PO_4^{3-} Addition
Green Algae	0.05P, 0.1P, 0.2P, 0.5P, 0.05P+5N, 0.1P+1N, 0.2P+2N, 0.5P+5N	0.05P+0.5N, 0.1P+0.1N, 0.2P+0.2N, 0.5P+0.5N	0.2P+2N, 0.5P+5
Cyanobacteria	0.05P, 0.1P, 0.2P, 0.5P 0.05P+0.5N, 0.1P+1N, 0.2P+2N, 0.5P+5N	0.2P+2N, 0.5P+5N	0.2P+2N, 0.5P+5N

Appendix B Table 8: Significant responses ($p < 0.05$) of green algae and Cyanobacteria biomass to various nutrient treatments (N as mg N/L and P as mg P/L) before PO_4^{3-} addition, two months, and twelve months after PO_4^{3-} addition in S2

Algae Type	Before PO_4^{3-} Addition	Two months after PO_4^{3-} Addition	One year after PO_4^{3-} Addition
Green Algae	No response	No response	No response
<i>Cyanobacteria</i>	No response	No response	No response

Appendix B Table 9: Significant responses ($p < 0.05$) of green algae and Cyanobacteria biomass to various nutrient treatments (N as mg N/L and P as mg P/L) before PO_4^{3-} addition, two months, and twelve months after PO_4^{3-} addition in S3

Algae Type	Before PO_4^{3-} Addition	Two months after PO_4^{3-} Addition	One year after PO_4^{3-} Addition
Green Algae	0.05P+5N, 0.1P+1N, 0.2P+2N, 0.5P+5N	1N, 2N, 5N, 0.05P+0.5N, 0.1P+1N, 0.2P+2N, 0.5P+5N	0.1P+1N, 0.2P+2N, 0.5P+5N
<i>Cyanobacteria</i>	0.05P, 0.1P, 0.2P, 0.5P 0.05P+0.5N, 0.1P+1N, 0.2P+2N, 0.5P+5N	0.2P+2N, 0.5P+5N	0.5P+5N

Appendix B Table 10: Significant responses ($p < 0.05$) of green algae and Cyanobacteria biomass to various nutrient treatments (N as mg N/L and P as mg P/L) before PO_4^{3-} addition, two months, and twelve months after PO_4^{3-} addition in S4

Algae Type	Before PO_4^{3-} Addition	Two months after PO_4^{3-} Addition	One year after PO_4^{3-} Addition
Green Algae	0.05P, 0.1P, 0.2P, 0.5P, 0.05P+5N, 0.1P+1N, 0.2P+2N, 0.5P+5N	2N, 5N, 0.1P+1N, 0.2P+2N, 0.5P+5N	0.05P, 0.1P, 0.2P, 0.5P, 0.05P+0.5N, 0.1P+1N, 0.2P+2N, 0.5P+5N
<i>Cyanobacteria</i>	0.05P, 0.1P, 0.2P, 0.5P 0.05P+0.5N, 0.1P+1N, 0.2P+2N, 0.5P+5N	0.2P+2N, 0.5P+5N	0.2P, 0.5P, 0.1P+1N, 0.2P+2N, 0.5P+5N

Appendix B Table 11: Significant responses ($p < 0.05$) of green algae and Cyanobacteria biomass to various nutrient treatments (N as mg N/L and P as mg P/L) before PO_4^{3-} addition, two months, and twelve months after PO_4^{3-} addition in S5

Algae Type	Before PO_4^{3-} Addition	Two months after PO_4^{3-} Addition	One year after PO_4^{3-} Addition
<i>Green Algae</i>	0.05P, 0.1P, 0.2P, 0.5P, 0.05P+5N, 0.1P+1N, 0.2P+2N, 0.5P+5N	0.05P+0.5N, 0.1P+1N, 0.2P+2N, 0.5P+5N	0.05P, 0.1P, 0.2P, 0.5P, 0.05P+0.5N, 0.1P+1N, 0.2P+2N, 0.5P+5
<i>Cyanobacteria</i>	0.05P, 0.1P, 0.2P, 0.5P 0.05P+0.5N, 0.1P+1N, 0.2P+2N, 0.5P+5N	0.2P, 0.5P, 0.2P+2N, 0.5P+5N	0.1P, 0.2P, 0.5P, 0.05P+0.5N, 0.1P+1N, 0.2P+2N, 0.5P+5N

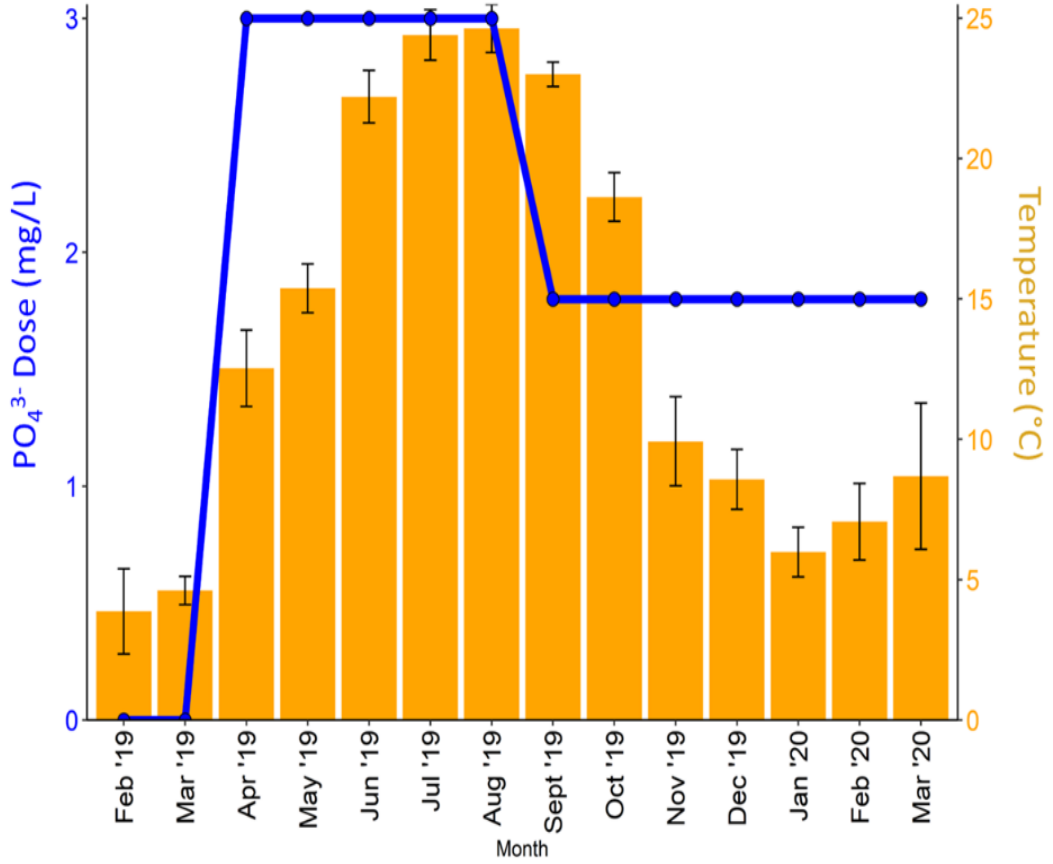
Appendix B Table 12: Significant responses ($p < 0.05$) of green algae and Cyanobacteria biomass to various nutrient treatments (N as mg N/L and P as mg P/L) before PO_4^{3-} addition, two months, and twelve months after PO_4^{3-} addition in tap water (DWDS)

Algae Type	Before PO_4^{3-} Addition	Two months after PO_4^{3-} Addition	One year after PO_4^{3-} Addition
<i>Green Algae</i>	0.05P+5N	0.2P+2N, 0.5P+5N	1N, 2N, 5N, 0.2P+2N, 0.5P+5
<i>Cyanobacteria</i>	No response	No response	2N

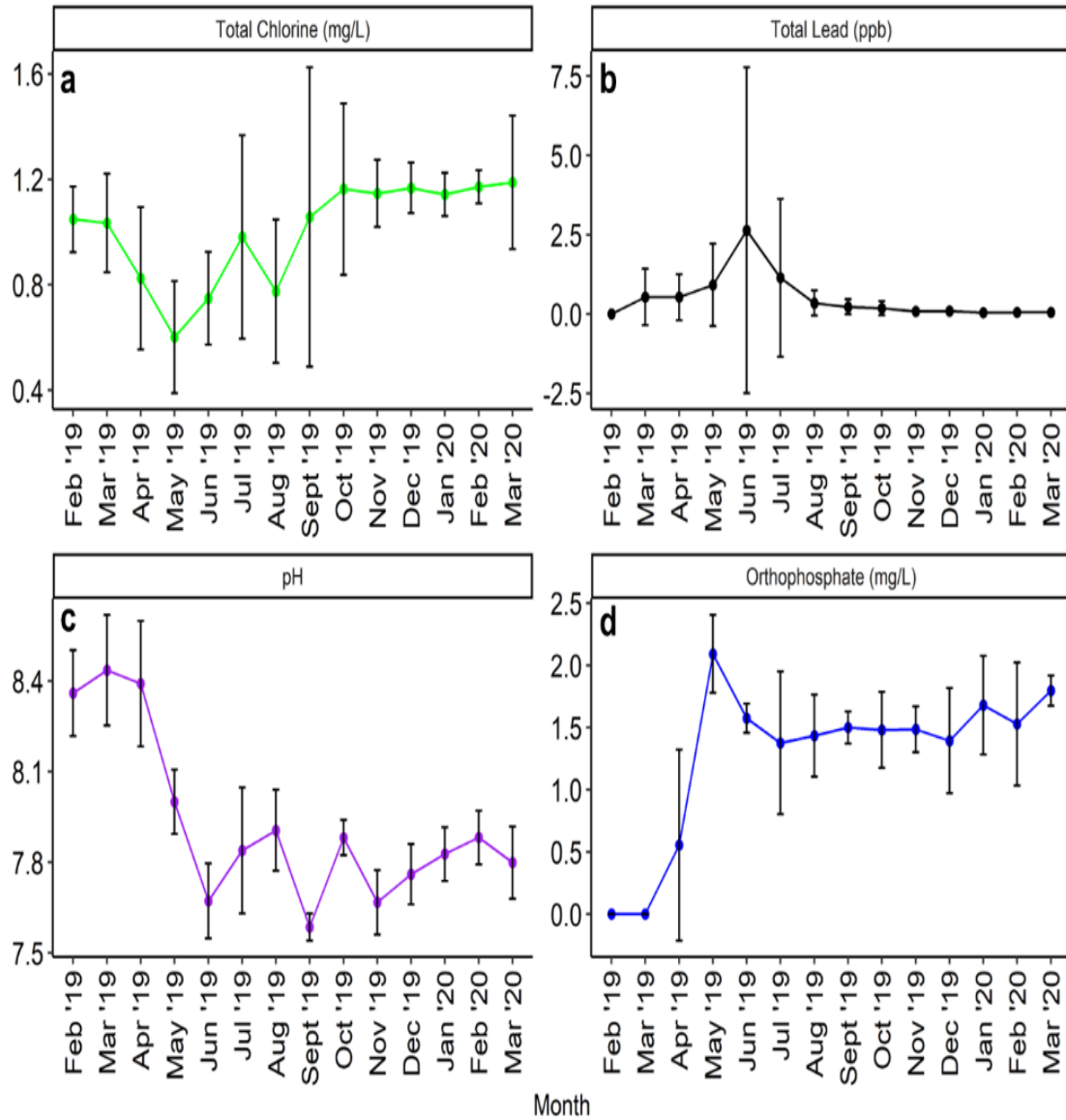
Appendix B Table 13: Urban stream TN:TP ratios before and one year after PO_4^{3-} addition into the DWDS

Stream	Before PO_4^{3-} Addition	One year after PO_4^{3-} Addition
Shades Run (S1)	40.1	34.9
Negley Run (S2)	20.2	12.8
Fern Hollow (S3)	31.2	34.1
Panther Hollow (S4)	60.2	24.9
Phipps Run (S5)	40.3	22.6

Appendix C Aim 3.0 Supplementary Information

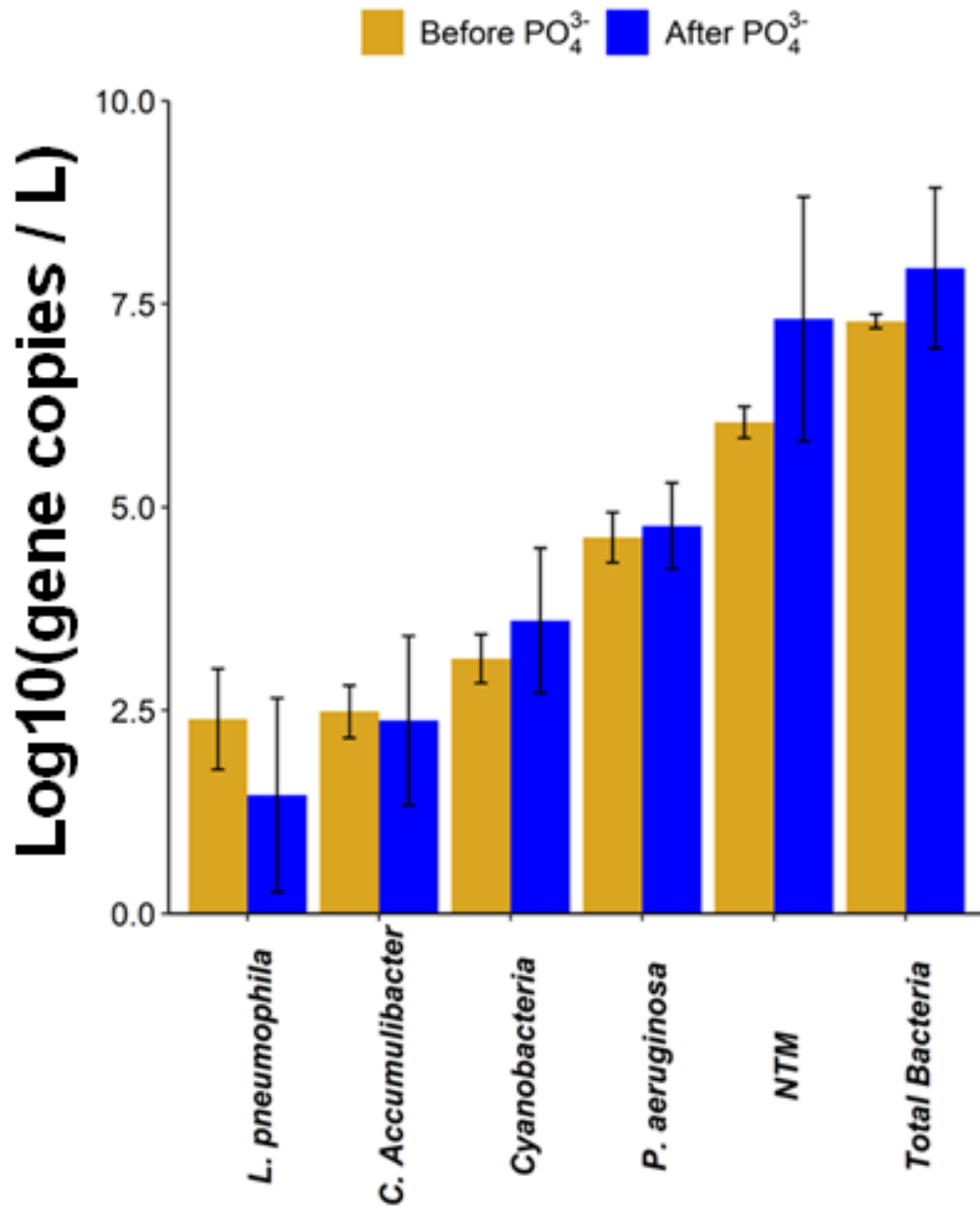


Appendix C Figure 1: PO₄³⁻ dosing (left scale, in blue) and water temperature (right scale, in orange) over the duration of the one-year study. Water temperature was averaged between the seven distribution sites and error bars represent the standard deviation.

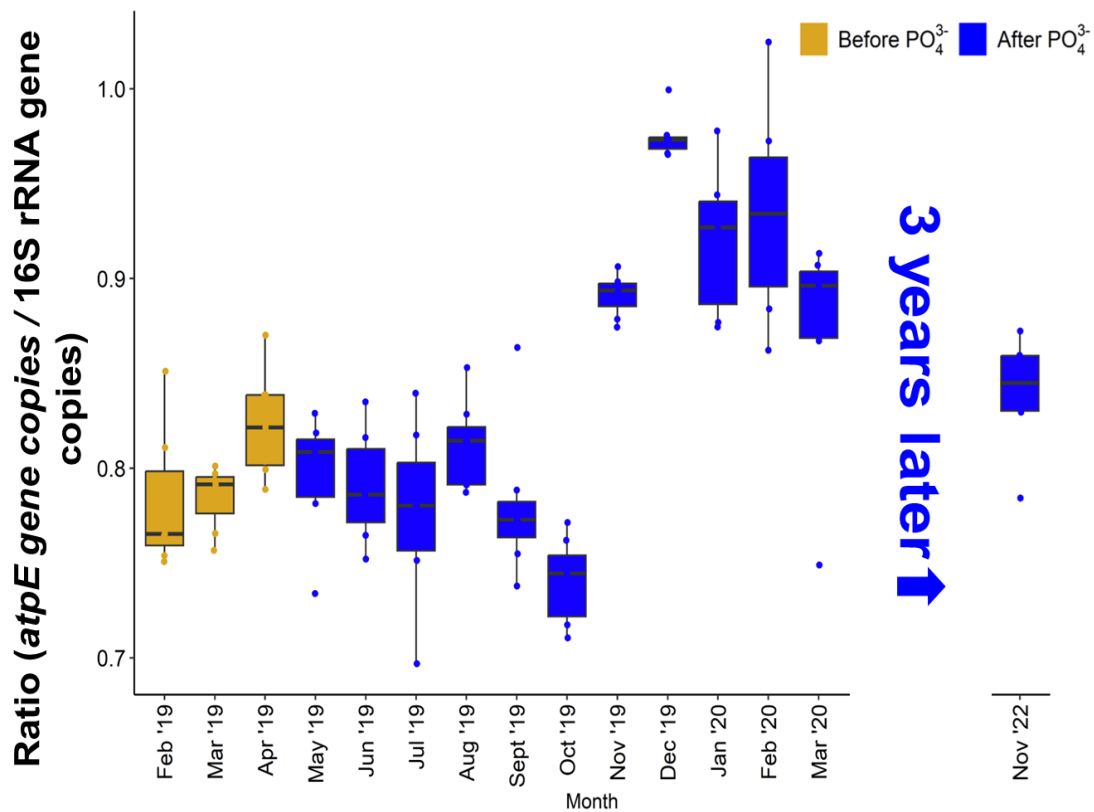


Appendix C Figure 2: (a) Total chlorine, (b) total lead, (c) pH, and (d) PO_4^{3-} concentration across the seven distribution system sites over the duration of the one-year study.

The PO_4^{3-} concentration measured in the distribution system differs from the dose in Figure C1 due to scale formation.

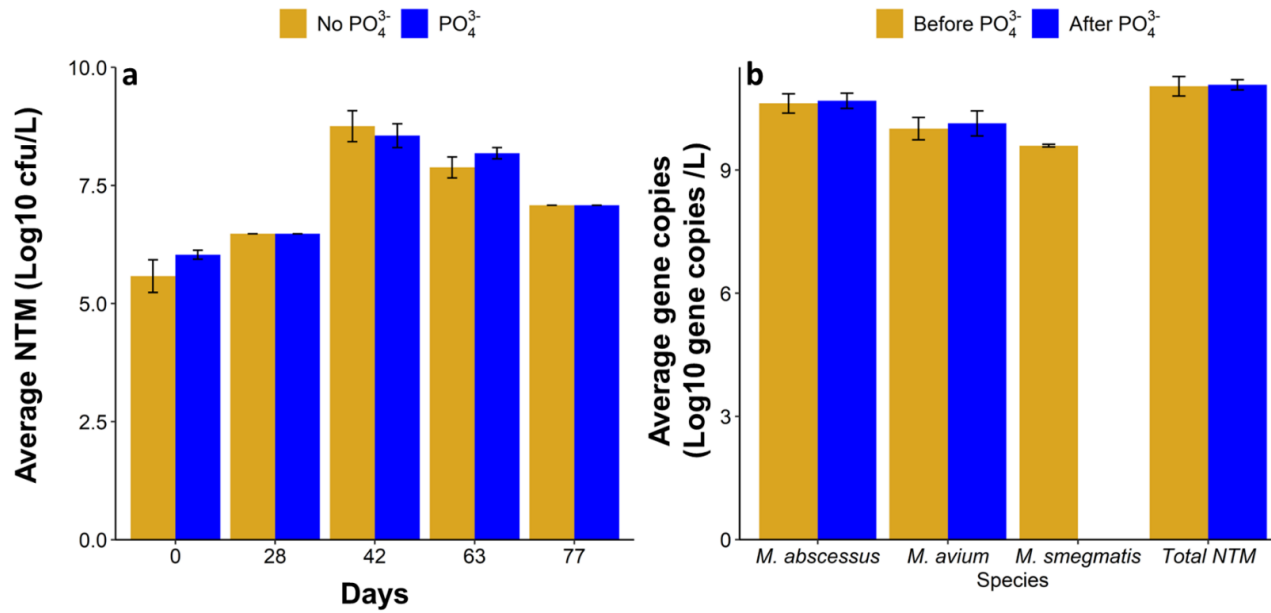


Appendix C Figure 3: Average \pm standard deviation of absolute density of DWPIs, total bacteria, and Cyanobacteria in the DWDS before ($n = 21$) and after PO_4^{3-} addition ($n = 77$). The after category contains data from 9 months of sample collection.



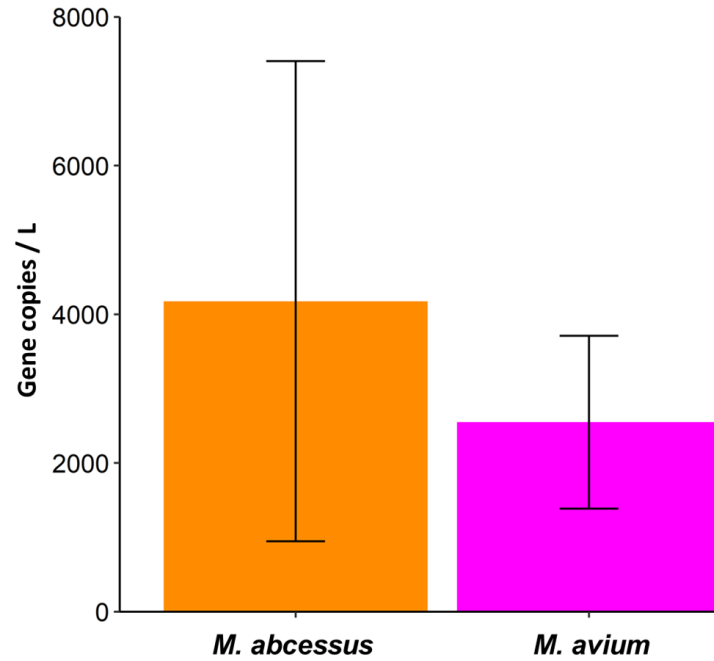
Appendix C Figure 4: Ratio of NTM (as measured by the *atpE* gene) to total bacteria (as measured by the 16S rRNA gene) across the seven distribution system sites over the course of the study duration and three years later.

Note: only six samples were collected in 2022, as one of the routine monitoring sites has been shut down

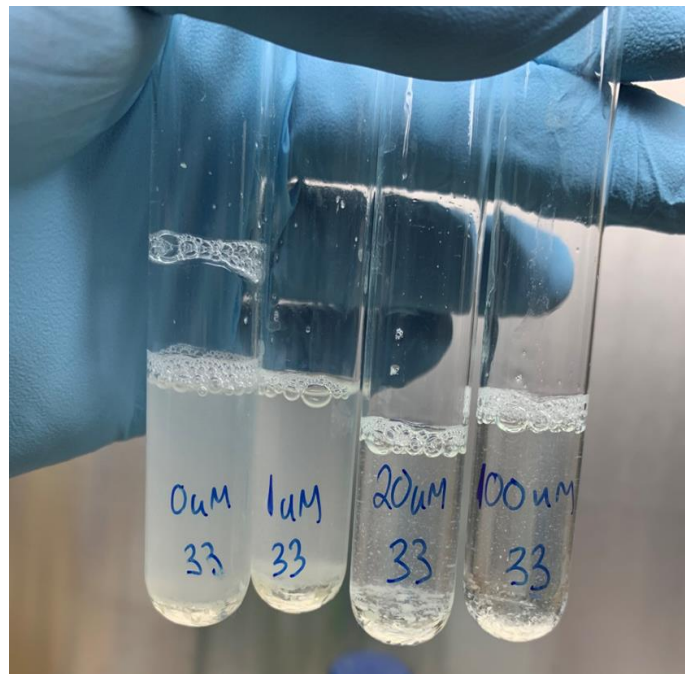


Appendix C Figure 5: a) NTM concentration over the batch reactor study duration and b) absolute density of NTM species in batch reactors.

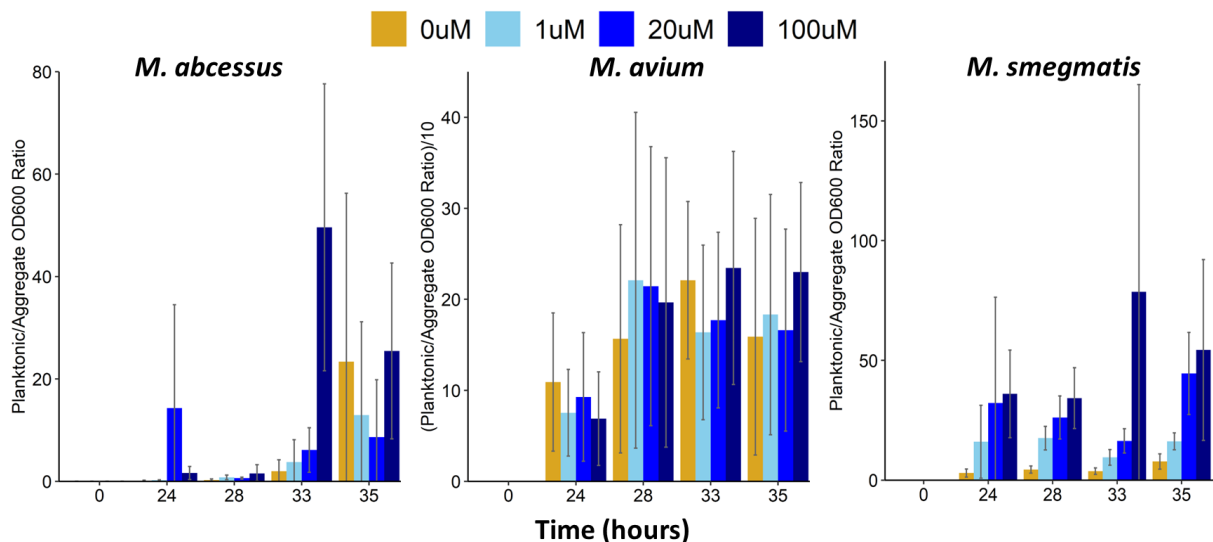
Over the duration of the experiment (~ 3 months), a significant difference in *M. smegmatis* density was observed, likely due to competition with the environmental *M. avium*, *M. abscessus*, and other microorganisms present in the water.



Appendix C Figure 6: Average densities of *M. abscessus* and *M. avium* in the DWDS at the time of the significant increase in 2019

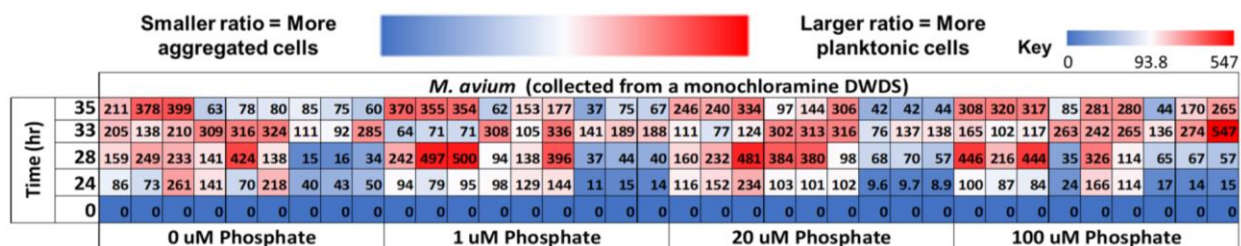


Appendix C Figure 7: Aggregate fraction of *M. abscessus* cultures suspended in phosphate buffered saline mixed with 6% Tween20. As phosphate level increased, the number of suspended aggregates decreased



Appendix C Figure 8: Average (n = 9 for each species, at each timepoint, at each phosphorus concentration) ± standard deviation of planktonic vs aggregate NTM ratios for *M. abscessus* (left), *M. avium* (middle), and *M. smegmatis* (right).

Ratios were obtained by dividing the planktonic OD600 measurements by the aggregate OD600 measurements. A larger ratio signifies a larger amount of NTM in the planktonic phase.



Appendix C Figure 9: Planktonic vs aggregate NTM ratios (ranges in parentheses) for *M. avium* (0 – 547) at different concentrations of phosphate (each tile is one technical replicate, for a total of n = 9 per species x phosphate concentration x time).

Blue colored cells represent a smaller ratio, signifying a larger proportion of aggregated NTM cells while white/red colored cells represent a higher ratio, signifying a larger proportion of planktonic NTM cells. The white cells represent the 50th percentile of each specific species dataset. The ratios were obtained by dividing the planktonic OD600 measurements by the aggregate OD600 measurements.

Appendix C Table 1: Different water quality parameters measured in this study and the method / apparatus used

Parameter	Unit	Method / Apparatus
<i>Temperature</i>	°C	Temperature probe
<i>pH</i>	--	pH electrode
<i>Orthophosphate</i>	mg/L PO ₄ ³⁻	PhosVer3 Ascorbic Acid Method
<i>Total & Dissolved Iron</i>	mg/L	ICPMS (dissolved 0.45 µm filtered)
<i>Total & Dissolved Copper</i>	mg/L	ICPMS (dissolved 0.45 µm filtered)
<i>Total & Dissolved Manganese</i>	mg/L	ICPMS (dissolved 0.45 µm filtered)
<i>Total & Dissolved Lead</i>	µg/L	ICPMS (dissolved 0.45 µm filtered)
<i>Total Chlorine</i>	mg/L Cl ₂	DPD Method
<i>Free Chlorine</i>	mg/L Cl ₂	DPD Method
<i>Turbidity</i>	NTU	Turbidimeter
<i>ATP</i>	mg/L	AquaSnap Total ATP meter

Appendix C Table 2: Average ± standard deviation (s.d.) measured water quality parameters before and after full-scale PO₄³⁻ addition into the DWDS. Dissolved concentrations are in parentheses.

Parameter	Average ± s.d. Before PO₄³⁻ (n = 14)	Average ± s.d. After PO₄³⁻ (n = 14)
Temperature	4.24 ± 1.19	7.76 ± 2.27
pH	8.40 ± 0.17	7.82 ± 0.11
Orthophosphate	0.001 ± 0.002	1.71 ± 0.364
Total (& Dissolved) Iron	0.028 ± 0.027 (0.017 ± 0.017)	0.013 ± 0.016 (0.001 ± 0.001)
Total (& Dissolved) Copper	0.005 ± 0.006 (0.004 ± 0.005)	0.009 ± 0.004 (0.008 ± 0.003)
Total (& Dissolved) Manganese	0.006 ± 0.013 (0.001 ± 0.002)	0.001 ± 0.001 (0.0001 ± 0.0001)
Total (& Dissolved) Lead	0.3 ± 1.0 (0.057 ± 0.062)	0.051 ± 0.043 (0.01 ± 0.01)
Total Chlorine	1.04 ± 0.16	1.17 ± 0.19
Free Chlorine	0.94 ± 0.16	1.06 ± 0.18
Turbidity	0.068 ± 0.031	0.102 ± 0.065
ATP	4.1x10 ⁻⁷ ± 1.3x10 ⁻⁷	1.2x10 ⁻⁷ ± 1.4x10 ⁻⁷

Appendix C Table 3: ddPCR target genes, amplicon size, annealing temperature, and primer sequences

Target Taxa	Target gene	Approx. Amplicon Size (bp)	Annealing Temp. (°C)	Sequence (5' to 3')
Total Bacteria	16S rRNA	200	57	F: ACTCCTACGGGAGGCAG R: ATTACCGCGGCTGCTGG
<i>Legionella pneumophila</i>	<i>Lmip</i>	150	57	F: CCGATGCCACATCATTAGC R: CCAATTGAGCGCCACTCATAG
<i>Pseudomonas aeruginosa</i>	<i>Orpl</i>	117	57	F: CGAGTACAACATGGCTCTGG R: ACCGGACGCTCTTTACCATA
Nontuberculous mycobacteria	<i>atpE</i>	164	57	F: CGGYGCCGGTATCGGYGA R: CGAAGACGAACARSGCCAT
<i>Mycobacterium abscessus</i>	<i>rpoB</i>	77	56.5	F: CGATAGAGGACTTCGCCTAACC R: TCGAGCACGTAAACTCCCTTC
<i>Mycobacterium avium</i>	16S rRNA	97	55.5	F: GGGTGAGTAACACGTGTGCAA R: CCAGAAGACATGCGTCGTGA
<i>Mycobacterium smegmatis</i>	<i>rrnB</i>	75	60.7	F: ATCCTCGCTGCCACTAGAGA R: AAACAACACGCCCGACTTTG
<i>Cyanobacteria</i>	16S rRNA	422	60	F: GGGGAATCTTCCGCAATGGG R: GACTACTGGGGTATCTAATCCCATT

Appendix C Table 4: ddPCR reaction conditions

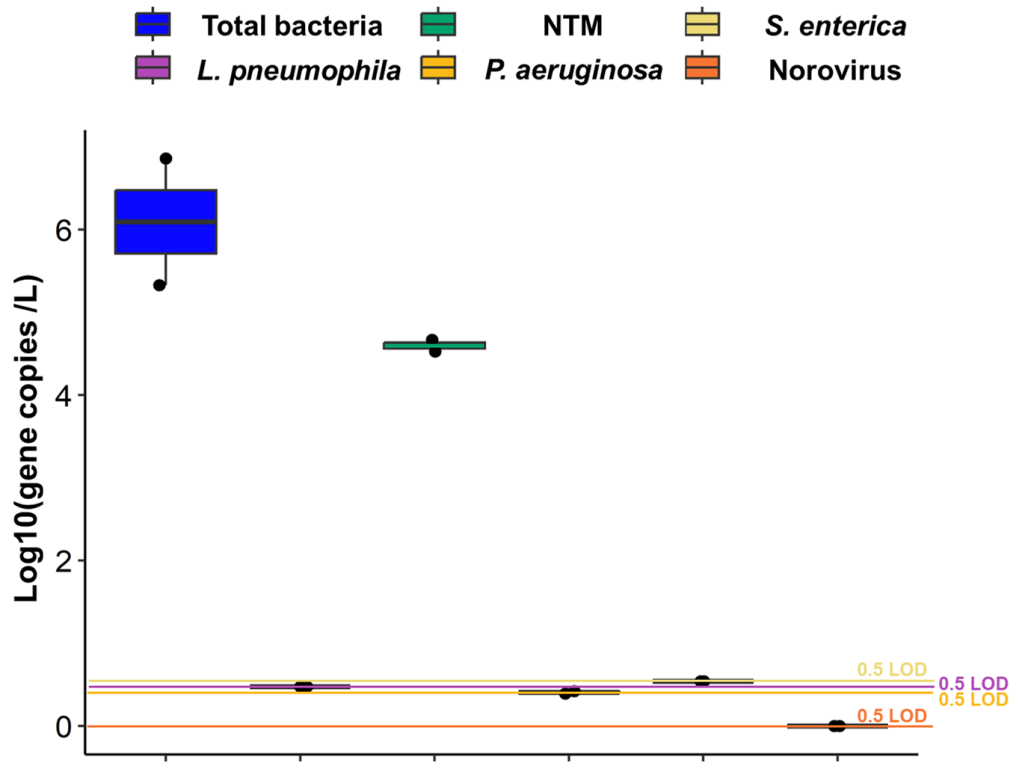
Target taxa (gene)	Temperatures and Times	# of cycles
Total Bacteria, <i>L. pneumophila</i> , <i>P. aeruginosa</i> , NTM	95°C, 5:00, Ramp 2/s	45
	95°C, 0:30, Ramp 2/s	
	57°C, 1:00, Ramp 2/s	
	72°C, 1:00, Ramp 2/s	
	4°C, 5:00, Ramp 2/s	
	90°C, 5:00, Ramp 2/s	
	12°C, --, Ramp 2/s	
<i>M. abscessus</i>	95°C, 5:00, Ramp 2/s	45
	95°C, 0:30, Ramp 2/s	
	56.5°C, 1:00, Ramp 2/s	
	72°C, 1:00, Ramp 2/s	
	4°C, 5:00, Ramp 2/s	
	90°C, 5:00, Ramp 2/s	
	12°C, --, Ramp 2/s	
<i>M. avium</i>	95°C, 5:00, Ramp 2/s	45
	95°C, 0:30, Ramp 2/s	
	55.5°C, 1:00, Ramp 2/s	
	72°C, 1:00, Ramp 2/s	
	4°C, 5:00, Ramp 2/s	
	90°C, 5:00, Ramp 2/s	
	12°C, --, Ramp 2/s	
<i>M. smegmatis</i>	95°C, 5:00, Ramp 2/s	45
	95°C, 0:30, Ramp 2/s	
	60.7°C, 1:00, Ramp 2/s	
	72°C, 1:00, Ramp 2/s	
	4°C, 5:00, Ramp 2/s	
	90°C, 5:00, Ramp 2/s	
	12°C, --, Ramp 2/s	
Cyanobacteria	95°C, 5:00, Ramp 2/s	44
	95°C, 0:30, Ramp 2/s	
	60°C, 1:00, Ramp 2/s	
	72°C, 1:00, Ramp 2/s	
	4°C, 5:00, Ramp 2/s	
	90°C, 5:00, Ramp 2/s	
12°C, --, Ramp 2/s		

Appendix C Table 5: ddPCR assay thresholds, LOD, and LOQ

Target taxa (gene)	ddPCR Threshold	Limit of Detection	Limit of Quantification
Total Bacteria	12900	5.3 gene copies / 20 µL	53 gene copies / 20 µL
<i>L. pneumophila</i>	8800	6.08 gene copies / 20 µL	6.08 gene copies / 20 µL
<i>P. aeruginosa</i>	4500	7.3 gene copies / 20 µL	7.3 gene copies / 20 µL
NTM	10600	5.6 gene copies / 20 µL	5.6 gene copies / 20 µL
<i>M. abscessus</i>	9093	6.62 gene copies / 20 µL	6.62 gene copies / 20 µL
<i>M. avium</i>	9431	6.62 gene copies / 20 µL	66 gene copies / 20 µL
<i>M. smegmatis</i>	11643	5.8 gene copies / 20 µL	5.8 gene copies / 20 µL
<i>Cyanobacteria</i>	9567	7.9 gene copies / 20 µL	7.9 gene copies / 20 µL

Thresholds were determined experimentally by spiking target taxa's gblock at different concentrations into water DNA matrix and adjusting threshold until expected concentration was read out.

Appendix D Aim 4.0 Supplementary Information



Appendix D Figure 1: Boxplots of the log₁₀ transformed viable total bacteria, *L. pneumophila*, NTM, *P. aeruginosa*, *S. enterica*, and norovirus absolute gene copies within floodwaters. Samples with no detects had their densities set at half of the limit of detection for the assay prior to normalization.

Appendix D Table 1: Different water quality parameters measured in this study and the method / apparatus used

Parameter	Unit	Method / Apparatus
Temperature	°C	Temperature probe
pH	--	pH electrode
Turbidity	NTU	PhosVer3 Ascorbic Acid Method
Total & Dissolved Iron	mg/L	ICPMS (dissolved 0.45 µm filtered)
Total & Dissolved Copper	mg/L	ICPMS (dissolved 0.45 µm filtered)
Total & Dissolved Manganese	mg/L	ICPMS (dissolved 0.45 µm filtered)
Nitrate & Nitrite	mg/L N	Lachat QuikChem Analyzer

Appendix D Table 2: ddPCR target genes, amplicon size, annealing temperature, and primer sequences

Target Taxa	Target gene	Approx. Amplicon Size (bp)	Annealing Temp. (°C)	Sequence (5' to 3')
Total Bacteria	16S rRNA	200	54	F: ACTCCTACGGGAGGCAG R: ATTACCGCGGCTGCTGG
<i>Legionella pneumophila</i>	<i>Lmip</i>	150	56	F: CCGATGCCACATCATTAGC R: CCAATTGAGCGCCACTCATAG
<i>Pseudomonas aeruginosa</i>	<i>Orpl</i>	117	56	F: CGAGTACAACATGGCTCTGG R: ACCGGACGCTCTTTACCATA
Nontuberculous mycobacteria	<i>atpE</i>	164	59	F: CGGYGCCGGTATCGGYGA R: CGAAGACGAACARSGCCAT
<i>Salmonella enterica</i>	<i>ttrC</i>	127	61.6	F: GCCTTACAGGCGTTCTTCG R: ATTTTTGGCAGCCTTACCG
Norovirus	ORF1	498	48	F: TTATTGAAATGTGGGATGGAG R: CTGCGAAGCTCCAATCAC

Appendix D Table 3: ddPCR reaction conditions

Target taxa	Temperatures and Times	# of cycles
Total Bacteria	95°C, 5:00, Ramp 2/s	45
	95°C, 1:00, Ramp 2/s	
	54°C, 1:00, Ramp 2/s	
	72°C, 2:00, Ramp 2/s	
	4°C, 5:00, Ramp 2/s	
	90°C, 5:00, Ramp 2/s	
	12°C, --, Ramp 2/s	
<i>L. pneumophila</i> , <i>P. aeruginosa</i>	95°C, 5:00, Ramp 2/s	45
	95°C, 1:00, Ramp 2/s	
	56°C, 1:00, Ramp 2/s	
	72°C, 2:00, Ramp 2/s	
	4°C, 5:00, Ramp 2/s	
	90°C, 5:00, Ramp 2/s	
	12°C, --, Ramp 2/s	
NTM	95°C, 5:00, Ramp 2/s	45
	95°C, 1:00, Ramp 2/s	
	59°C, 1:00, Ramp 2/s	
	72°C, 2:00, Ramp 2/s	
	4°C, 5:00, Ramp 2/s	
	90°C, 5:00, Ramp 2/s	
	12°C, --, Ramp 2/s	
<i>S. enterica</i>	95°C, 5:00, Ramp 2/s	45
	95°C, 0:30, Ramp 2/s	
	61.6°C, 1:00, Ramp 2/s	
	72°C, 1:00, Ramp 2/s	
	4°C, 5:00, Ramp 2/s	
	90°C, 5:00, Ramp 2/s	
	12°C, --, Ramp 2/s	
Norovirus	95°C, 5:00, Ramp 2/s	45
	95°C, 1:00, Ramp 2/s	
	48°C, 1:00, Ramp 2/s	
	72°C, 2:00, Ramp 2/s	
	4°C, 5:00, Ramp 2/s	
	90°C, 5:00, Ramp 2/s	
	12°C, --, Ramp 2/s	

Appendix D Table 4: ddPCR assay thresholds, LOD, and LOQ

Target taxa (gene)	ddPCR Threshold	Limit of Detection	Limit of Quantification
Total Bacteria	8000	1.5 gene copies / 20 µL	1.5 gene copies / 20 µL
<i>L. pneumophila</i>	10600	5.91 gene copies / 20 µL	5.91 gene copies / 20 µL
<i>P. aeruginosa</i>	10000	1 gene copies / 20 µL	7.13 gene copies / 20 µL
NTM	4000	1 gene copies / 20 µL	5.4 gene copies / 20 µL
<i>S. enterica</i>	3150	7 gene copies / 20 µL	70 gene copies / 20 µL
Norovirus	5600	1.77 gene copies / 20 µL	1.77 gene copies / 20 µL

Thresholds were determined experimentally by spiking target taxa's gblock at different concentrations into water DNA matrix and adjusting threshold until expected concentration was read out.

Appendix E Aim 5.0 Supplementary Information

Appendix E Table 1: Assumed residential structure airflow path leakage areas used in CONTAM model from ASHRAE 62.1

Component	Effective Leakage Area (at reference pressure 4 Pa – cm²/m²)
Basement exterior walls	25
Main floor exterior walls	0.138
Main floor interior walls	2.01
Floor vent leakage	3.68
Attic floor leakage	2.01

Appendix E Table 2: Zone design air supply rates

Zone	Design Air Supply Rate (m³/hr)
Basement	18.26
Living Room	234
Bedroom Adult	179.2
Bedroom Child	87.16
Dining Room	73.152
Kitchen	206.04
Bathroom	54.86

Appendix E Table 3: Adult occupancy schedule used in the CONTAM simulation for all case scenarios

Time	Control		HOF		HOG		DG			
	Weekday	Weekend	Weekday	Weekend	Weekday	Weekend	Weekday	Weekend		
00:00 AM	Bedroom	Bedroom	Bedroom	Bedroom	Bedroom	Bedroom	Bedroom	Bedroom		
6:00					Basement					
7:00	Kitchen	Kitchen	Kitchen	Kitchen	Kitchen	Kitchen	Kitchen	Kitchen		
8:00	Work	Living room	Basement	Living room	Work	Living room	Work	Living room		
9:00										
10:00										
11:00		Kitchen Dining room		Kitchen Dining room		Kitchen Dining room		Kitchen Dining room	Kitchen Dining room	Kitchen Dining room
12:00 PM										
13:00		Basement (15min)		Basement (15min)		Basement (15min)		Basement (15min)	Basement	Basement
14:00										
15:00	Living room	Living room	Living room	Living room	Living room	Living room				
16:00										
17:00	Living room	Living room	Living room	Living room	Living room	Living room	Basement			
18:00	Kitchen	Kitchen	Kitchen	Kitchen	Kitchen	Kitchen	Kitchen	Kitchen		
19:00	Dining room	Dining room	Dining room	Dining room	Dining room	Dining room	Dining room	Dining room		
20:00										
21:00	Bedroom	Bedroom	Bedroom	Bedroom	Bedroom	Bedroom	Bedroom	Bedroom		
22:00										
23:00										

Appendix E Table 4: Child occupancy schedule used in the CONTAM simulation for all case scenarios

Time	Control		HOF		HOG		DG			
	Weekday	Weekend	Weekday	Weekend	Weekday	Weekend	Weekday	Weekend		
00:00 AM	Bedroom	Bedroom	Bedroom	Bedroom	Bedroom	Bedroom	Bedroom	Bedroom		
6:00			Bedroom		Bedroom					
7:00	Dining room	Dining room	Dining room	Dining room	Dining room	Dining room	Dining room	Dining room		
8:00	School		Dining room		Home School (Basement)		Dining room		School	Dining room
9:00		Living room	Living room	Living room		Living room	Living room	Basement		
10:00										Dining room
11:00		Living room	Living room	Living room		Living room	Living room	Basement		
12:00 PM										Living room
13:00		Living room	Living room	Living room		Living room	Living room	Basement		
14:00	Living room				Living room				Living room	Living room
15:00		Living room	Living room	Living room		Living room	Living room	Basement		
16:00	Living room				Living room				Living room	Living room
17:00		Living room	Living room	Living room		Living room	Living room	Basement		
18:00	Living room				Living room				Living room	Living room
19:00		Dining room	Dining room	Dining room		Dining room	Dining room	Dining room		
20:00	Dining room				Dining room				Dining room	Dining room
21:00		Dining room	Dining room	Dining room		Dining room	Dining room	Dining room		
22:00	Bedroom				Bedroom				Bedroom	Bedroom
23:00		Bedroom	Bedroom	Bedroom		Bedroom	Bedroom	Bedroom		

Appendix E Table 5: Assumed Ambient and starting zone pollutant concentrations or mass flow rate

Pollutant	Concentration or mass flow rate	Reference
PM2.5 (Ambient)	8 ug/m ³	US EPA 2023
PM2.5 Generation (Cooking)	16.14 ug/s	Aquilina et al. 2022
Radon (Ambient)	0.4 pCi/L	US EPA 2023
Radon (Basement)	1.3 pCi/L	US EPA 2023
Radon (Main Floor Zones)	0.624 pCi/L	Li et al. 2022
Radon Emanation	235 pCi /m ² hr	Chao et al. 1997
Mold Spores (Ambient)	2775 spores/m ³	Haas et al. 2023
Mold Spores (Basement)	33000 spores/m ³	Afanou et al. 2019
Mold Spores (Main Floor Zones)	330 spores/m ³	Reponen et al. 2010

Appendix E Table 6: Age-based intake factors for children ages 0 – 18 years

Gender	<1 year	1 – 2 years	3 – 4 years	5 – 9 years	10 – 14 years	15 – 18 years
Male	3.31	2.75	2.36	1.87	1.39	1.4
Female	3.24	2.82	2.35	1.89	1.39	1.41

Appendix E Table 7: Activity-based intake factors from Pleil et al. 2021

Condition	Breathing Rate (breath/min)	Tidal Volume (L/breath)	Ventilation Rate (L/min)
Nominal At-Rest	12	0.5	6
Normal Activity	16	1	16
Moderate Exercise	20	2	40

Bibliography

- (1) Rozos, E.; Makropoulos, C. Source to Tap Urban Water Cycle Modelling. *Environ. Model. Softw.* **2013**, *41*, 139–150. <https://doi.org/10.1016/j.envsoft.2012.11.015>.
- (2) McGrane, S. J. Impacts of Urbanisation on Hydrological and Water Quality Dynamics, and Urban Water Management: A Review. *Hydrol. Sci. J.* **2016**, *61* (13), 2295–2311. <https://doi.org/10.1080/02626667.2015.1128084>.
- (3) Carstens, D.; Amer, R. Spatio-Temporal Analysis of Urban Changes and Surface Water Quality. *J. Hydrol.* **2019**, *569*, 720–734. <https://doi.org/10.1016/j.jhydrol.2018.12.033>.
- (4) Boretti, A.; Rosa, L. Reassessing the Projections of the World Water Development Report. *Npj Clean Water* **2019**, *2* (1), 1–6. <https://doi.org/10.1038/s41545-019-0039-9>.
- (5) Burek, P.; Satoh, Y.; Fischer, G.; Kahil, M. T.; Scherzer, A.; Tramberend, S.; Nava, L. F.; Wada, Y.; Eisner, S.; Flörke, M.; Hanasaki, N.; Magnuszewski, P.; Cosgrove, B.; Wiberg, D. *Water Futures and Solution - Fast Track Initiative (Final Report)*; Monograph; WP-16-006: IIASA, Laxenburg, Austria, 2016. <https://iiasa.dev.local/> (accessed 2023-08-30).
- (6) UNESCO World Water Assessment Programme. *The United Nations World Water Development Report 2018: Nature-Based Solutions for Water*; France, 2018.
- (7) American Society of Civil Engineers. *2021 Report Card for America's Infrastructure*; 2021. https://infrastructurereportcard.org/wp-content/uploads/2020/12/National_IRC_2021-report.pdf (accessed 2024-02-05).
- (8) Ortega, C.; Solo-Gabriele, H. M.; Abdelzaher, A.; Wright, M.; Deng, Y.; Stark, L. M. Correlations between Microbial Indicators, Pathogens, and Environmental Factors in a Subtropical Estuary. *Mar. Pollut. Bull.* **2009**, *58* (9), 1374–1381. <https://doi.org/10.1016/j.marpolbul.2009.04.015>.
- (9) Xiao, R.; Ou, T.; Ding, S.; Fang, C.; Xu, Z.; Chu, W. Disinfection By-Products as Environmental Contaminants of Emerging Concern: A Review on Their Occurrence, Fate and Removal in the Urban Water Cycle. *Crit. Rev. Environ. Sci. Technol.* **2023**, *53* (1), 19–46. <https://doi.org/10.1080/10643389.2022.2043101>.
- (10) Kasonga, T. K.; Coetzee, M. A. A.; Kamika, I.; Ngole-Jeme, V. M.; Benteke Momba, M. N. Endocrine-Disruptive Chemicals as Contaminants of Emerging Concern in Wastewater and

Surface Water: A Review. *J. Environ. Manage.* **2021**, *277*, 111485. <https://doi.org/10.1016/j.jenvman.2020.111485>.

- (11) Khan, S.; Naushad, Mu.; Govarathanan, M.; Iqbal, J.; Alfadul, S. M. Emerging Contaminants of High Concern for the Environment: Current Trends and Future Research. *Environ. Res.* **2022**, *207*, 112609. <https://doi.org/10.1016/j.envres.2021.112609>.
- (12) Proctor, C.; Garner, E.; Hamilton, K. A.; Ashbolt, N. J.; Caverly, L. J.; Falkinham, J. O.; Haas, C. N.; Prevost, M.; Prevots, D. R.; Pruden, A.; Raskin, L.; Stout, J.; Haig, S.-J. Tenets of a Holistic Approach to Drinking Water-Associated Pathogen Research, Management, and Communication. *Water Res.* **2022**, *211*, 117997. <https://doi.org/10.1016/j.watres.2021.117997>.
- (13) Henze, M.; Loosdrecht, M. C. M. van; Ekama, G. A.; Brdjanovic, D. *Biological Wastewater Treatment*; IWA Publishing, 2008.
- (14) Nguyen, A. Q.; Vu, H. P.; Nguyen, L. N.; Wang, Q.; Djordjevic, S. P.; Donner, E.; Yin, H.; Nghiem, L. D. Monitoring Antibiotic Resistance Genes in Wastewater Treatment: Current Strategies and Future Challenges. *Sci. Total Environ.* **2021**, *783*, 146964. <https://doi.org/10.1016/j.scitotenv.2021.146964>.
- (15) Wang, J.; Chu, L.; Wojnárovits, L.; Takács, E. Occurrence and Fate of Antibiotics, Antibiotic Resistant Genes (ARGs) and Antibiotic Resistant Bacteria (ARB) in Municipal Wastewater Treatment Plant: An Overview. *Sci. Total Environ.* **2020**, *744*, 140997. <https://doi.org/10.1016/j.scitotenv.2020.140997>.
- (16) Pazda, M.; Kumirska, J.; Stepnowski, P.; Mulkiwicz, E. Antibiotic Resistance Genes Identified in Wastewater Treatment Plant Systems – A Review. *Sci. Total Environ.* **2019**, *697*, 134023. <https://doi.org/10.1016/j.scitotenv.2019.134023>.
- (17) Rout, P. R.; Shahid, M. K.; Dash, R. R.; Bhunia, P.; Liu, D.; Varjani, S.; Zhang, T. C.; Surampalli, R. Y. Nutrient Removal from Domestic Wastewater: A Comprehensive Review on Conventional and Advanced Technologies. *J. Environ. Manage.* **2021**, *296*, 113246. <https://doi.org/10.1016/j.jenvman.2021.113246>.
- (18) Bivins, A.; North, D.; Ahmad, A.; Ahmed, W.; Alm, E.; Been, F.; Bhattacharya, P.; Bijlsma, L.; Boehm, A. B.; Brown, J.; Buttiglieri, G.; Calabro, V.; Carducci, A.; Castiglioni, S.; Cetecioglu Gurol, Z.; Chakraborty, S.; Costa, F.; Curcio, S.; de los Reyes, F. L. I.; Delgado Vela, J.; Farkas, K.; Fernandez-Casi, X.; Gerba, C.; Gerrity, D.; Girones, R.; Gonzalez, R.; Haramoto, E.; Harris, A.; Holden, P. A.; Islam, Md. T.; Jones, D. L.; Kasprzyk-Hordern, B.; Kitajima, M.; Kotlarz, N.; Kumar, M.; Kuroda, K.; La Rosa, G.; Malpei, F.; Mautus, M.;

- McLellan, S. L.; Medema, G.; Meschke, J. S.; Mueller, J.; Newton, R. J.; Nilsson, D.; Noble, R. T.; van Nuijs, A.; Peccia, J.; Perkins, T. A.; Pickering, A. J.; Rose, J.; Sanchez, G.; Smith, A.; Stadler, L.; Stauber, C.; Thomas, K.; van der Voorn, T.; Wigginton, K.; Zhu, K.; Bibby, K. Wastewater-Based Epidemiology: Global Collaborative to Maximize Contributions in the Fight Against COVID-19. *Environ. Sci. Technol.* **2020**, *54* (13), 7754–7757. <https://doi.org/10.1021/acs.est.0c02388>.
- (19) Ahmed, W.; Angel, N.; Edson, J.; Bibby, K.; Bivins, A.; O'Brien, J. W.; Choi, P. M.; Kitajima, M.; Simpson, S. L.; Li, J.; Tschärke, B.; Verhagen, R.; Smith, W. J. M.; Zaugg, J.; Dierens, L.; Hugenholtz, P.; Thomas, K. V.; Mueller, J. F. First Confirmed Detection of SARS-CoV-2 in Untreated Wastewater in Australia: A Proof of Concept for the Wastewater Surveillance of COVID-19 in the Community. *Sci. Total Environ.* **2020**, *728*, 138764. <https://doi.org/10.1016/j.scitotenv.2020.138764>.
- (20) Huang, Y.; Zhou, N.; Zhang, S.; Yi, Y.; Han, Y.; Liu, M.; Han, Y.; Shi, N.; Yang, L.; Wang, Q.; Cui, T.; Jin, H. Norovirus Detection in Wastewater and Its Correlation with Human Gastroenteritis: A Systematic Review and Meta-Analysis. *Environ. Sci. Pollut. Res. Int.* **2022**, *29* (16), 22829–22842. <https://doi.org/10.1007/s11356-021-18202-x>.
- (21) USEPA. *Wastewater Technology Fact Sheet: Chlorine Disinfection*; Fact Sheet; Office of Water: Washington DC, 1999. <https://www3.epa.gov/npdes/pubs/chlo.pdf> (accessed 2020-12-14).
- (22) Miklos, D. B.; Remy, C.; Jekel, M.; Linden, K. G.; Drewes, J. E.; Hübner, U. Evaluation of Advanced Oxidation Processes for Water and Wastewater Treatment – A Critical Review. *Water Res.* **2018**, *139*, 118–131. <https://doi.org/10.1016/j.watres.2018.03.042>.
- (23) United States. *Safe Drinking Water Act*; 1974; Vol. Volume 88, pp 1660–1694. <https://www.govinfo.gov/content/pkg/STATUTE-88/pdf/STATUTE-88-Pg1660-2.pdf> (accessed 2022-08-08).
- (24) US EPA. Regulation Timeline: Contaminants Regulated Under the Safe Drinking Water Act, 2015.
- (25) US EPA, O. *Basic Information on the CCL and Regulatory Determination*. <https://www.epa.gov/ccl/basic-information-ccl-and-regulatory-determination> (accessed 2022-08-10).
- (26) M. Byrne, D.; C. Lohman, H. A.; M. Cook, S.; M. Peters, G.; S. Guest, J. Life Cycle Assessment (LCA) of Urban Water Infrastructure: Emerging Approaches to Balance

Objectives and Inform Comprehensive Decision-Making. *Environ. Sci. Water Res. Technol.* **2017**, 3 (6), 1002–1014. <https://doi.org/10.1039/C7EW00175D>.

- (27) Potgieter, S.; Pinto, A.; Sigudu, M.; du Preez, H.; Ncube, E.; Venter, S. Long-Term Spatial and Temporal Microbial Community Dynamics in a Large-Scale Drinking Water Distribution System with Multiple Disinfectant Regimes. *Water Res.* **2018**, 139, 406–419. <https://doi.org/10.1016/j.watres.2018.03.077>.
- (28) Proctor, C. R.; Hammes, F. Drinking Water Microbiology—from Measurement to Management. *Curr. Opin. Biotechnol.* **2015**, 33, 87–94. <https://doi.org/10.1016/j.copbio.2014.12.014>.
- (29) El-Chakhtoura, J.; Prest, E.; Saikaly, P.; van Loosdrecht, M.; Hammes, F.; Vrouwenvelder, H. Dynamics of Bacterial Communities before and after Distribution in a Full-Scale Drinking Water Network. *Water Res.* **2015**, 74, 180–190. <https://doi.org/10.1016/j.watres.2015.02.015>.
- (30) McCoy, S. T.; VanBriesen, J. M. Comparing Spatial and Temporal Diversity of Bacteria in a Chlorinated Drinking Water Distribution System. *Environ. Eng. Sci.* **2014**, 31 (1), 32–41. <https://doi.org/10.1089/ees.2013.0174>.
- (31) Antonelli, M.; Turolla, A.; Mezzanotte, V.; Nurizzo, C. Peracetic Acid for Secondary Effluent Disinfection: A Comprehensive Performance Assessment. *Water Sci. Technol.* **2013**, 68 (12), 2638–2644. <https://doi.org/10.2166/wst.2013.542>.
- (32) Antonelli, M.; Mezzanotte, V.; Panouillères, M. Assessment of Peracetic Acid Disinfected Effluents by Microbiotests. *Environ. Sci. Technol.* **2009**, 43 (17), 6579–6584. <https://doi.org/10.1021/es900913t>.
- (33) Saddiqi, M. M.; Zhao, W.; Cotterill, S.; Dereli, R. K. Smart Management of Combined Sewer Overflows: From an Ancient Technology to Artificial Intelligence. *WIREs Water* **2023**, 10 (3), e1635. <https://doi.org/10.1002/wat2.1635>.
- (34) Tibbetts, J. Combined Sewer Systems: Down, Dirty, and Out of Date. *Environ. Health Perspect.* **2005**, 113 (7), A464–A467.
- (35) Ahmed, W.; Hamilton, K.; Toze, S.; Cook, S.; Page, D. A Review on Microbial Contaminants in Stormwater Runoff and Outfalls: Potential Health Risks and Mitigation Strategies. *Sci. Total Environ.* **2019**, 692, 1304–1321. <https://doi.org/10.1016/j.scitotenv.2019.07.055>.

- (36) Hofstra, N. Quantifying the Impact of Climate Change on Enteric Waterborne Pathogen Concentrations in Surface Water. *Curr. Opin. Environ. Sustain.* **2011**, 3 (6), 471–479. <https://doi.org/10.1016/j.cosust.2011.10.006>.
- (37) USEPA. *Disinfection of Wastewater: Task Force Report*; Washington DC, 1976; p 65. <https://nepis.epa.gov/Exe/ZyNET.exe/9101F9QT.TXT?ZyActionD=ZyDocument&Client=EPA&Index=1976+Thru+1980&Docs=&Query=&Time=&EndTime=&SearchMethod=1&TocRestrict=n&Toc=&TocEntry=&QField=&QFieldYear=&QFieldMonth=&QFieldDay=&IntQFieldOp=0&ExtQFieldOp=0&XmlQuery=&File=D%3A%5Czyfiles%5CIndex%20Data%5C76thru80%5CTxt%5C00000029%5C9101F9QT.txt&User=ANONYMOUS&Password=anonymous&SortMethod=h%7C-&MaximumDocuments=1&FuzzyDegree=0&ImageQuality=r75g8/r75g8/x150y150g16/i425&Display=hpfr&DefSeekPage=x&SearchBack=ZyActionL&Back=ZyActionS&BackDesc=Results%20page&MaximumPages=1&ZyEntry=1&SeekPage=x&ZyPURL#> (accessed 2020-11-04).
- (38) USEPA. 2012 Guidelines for Water Reuse. **2012**, 643.
- (39) USEPA. National Pollution Discharge Elimination System - Water Quality Based Permits for Recreational Water Criteria, 2015.
- (40) USEPA. *Quality Criteria for Water*; Office of Water Regulations and Standards, Washington DC, 1986.
- (41) Lofrano, G.; Brown, J. Wastewater Management through the Ages: A History of Mankind. *Sci. Total Environ.* **2010**, 408 (22), 5254–5264. <https://doi.org/10.1016/j.scitotenv.2010.07.062>.
- (42) Water Environment Federation. *Peracetic Acid Disinfection: Implementation Considerations for Water Resource Recovery Facilities*, 1st ed.; Water Environment Federation, 2020.
- (43) Monarca, S. MUTAGENICITY AND DISINFECTION BY-PRODUCTS IN SURFACE DRINKING WATER DISINFECTED WITH PERACETIC ACID. *Environ. Toxicol. Chem.* **2002**, 21 (2), 309–318.
- (44) Richardson, S. D.; Ternes, T. A. Water Analysis: Emerging Contaminants and Current Issues. *Anal. Chem.* **2014**, 86 (6), 2813–2848. <https://doi.org/10.1021/ac500508t>.
- (45) Richardson, S. D.; Plewa, M. J.; Wagner, E. D.; Schoeny, R.; DeMarini, D. M. Occurrence, Genotoxicity, and Carcinogenicity of Regulated and Emerging Disinfection by-Products in

- Drinking Water: A Review and Roadmap for Research. *Mutat. Res. Mutat. Res.* **2007**, 636 (1), 178–242. <https://doi.org/10.1016/j.mrrev.2007.09.001>.
- (46) Kitis, M. Disinfection of Wastewater with Peracetic Acid: A Review. *Environ. Int.* **2004**, 30 (1), 47–55. [https://doi.org/10.1016/S0160-4120\(03\)00147-8](https://doi.org/10.1016/S0160-4120(03)00147-8).
- (47) Baldry, M. G. C. The Bactericidal, Fungicidal and Sporicidal Properties of Hydrogen Peroxide and Peracetic Acid. *J. Appl. Bacteriol.* **1983**, 54, 417–423.
- (48) Baldry, M. G. C.; French, M. S.; Slater, D. The Activity of Peracetic Acid on Sewage Indicator Bacteria and Viruses. *Water Sci. Technol.* **1991**, 24 (2), 353–357. <https://doi.org/10.2166/wst.1991.0089>.
- (49) Baldry, M. G. C.; Cavdore, A.; French, M. S.; Rodrigues, L. M.; Schirch, P. F. T.; Threadgold, T. L. Effluent Disinfection in Warm Climates with Peracetic Acid. *Water Sci. Technol.* **1995**, 31 (5–6), 161–164.
- (50) Koivunen, J.; Heinonen-Tanski, H. Peracetic Acid (PAA) Disinfection of Primary, Secondary and Tertiary Treated Municipal Wastewaters. *Water Res.* **2005**, 39 (18), 4445–4453. <https://doi.org/10.1016/j.watres.2005.08.016>.
- (51) Luukkonen, T.; Teeriniemi, J.; Prokkola, H.; Ramo, J.; Lassi, U. Chemical Aspects of Peracetic Acid Based Wastewater Disinfection. *Water SA* **2014**, 40 (1), 73-.
- (52) Bauermeister, L. J.; Bowers, J. W. J.; Townsend, J. C.; McKee, S. R. The Microbial and Quality Properties of Poultry Carcasses Treated with Peracetic Acid as an Antimicrobial Treatment. *Poult. Sci.* **2008**, 87 (11), 2390–2398. <https://doi.org/10.3382/ps.2008-00087>.
- (53) Shen, X.; Sheng, L.; Gao, H.; Hanrahan, I.; Suslow, T. V.; Zhu, M.-J. Enhanced Efficacy of Peroxyacetic Acid Against *Listeria Monocytogenes* on Fresh Apples at Elevated Temperature. *Front. Microbiol.* **2019**, 10. <https://doi.org/10.3389/fmicb.2019.01196>.
- (54) Carrasco, G.; Urrestarazu, M. Green Chemistry in Protected Horticulture: The Use of Peroxyacetic Acid as a Sustainable Strategy. *Int. J. Mol. Sci.* **2010**, 11 (5), 1999–2009. <https://doi.org/10.3390/ijms11051999>.
- (55) Yoganasimha, S.; Trahan, W. R.; Best, A. M.; Bowlin, G. L.; Kitten, T. O.; Moon, P. C.; Madurantakam, P. A. Peracetic Acid: A Practical Agent for Sterilizing Heat-Labile

Polymeric Tissue-Engineering Scaffolds. *Tissue Eng. Part C Methods* **2014**, *20* (9), 714–723. <https://doi.org/10.1089/ten.tec.2013.0624>.

- (56) Liu, T.; Liu, S.; Zheng, M.; Chen, Q.; Ni, J. Performance Assessment of Full-Scale Wastewater Treatment Plants Based on Seasonal Variability of Microbial Communities via High-Throughput Sequencing. *PLOS ONE* **2016**, *11* (4), e0152998. <https://doi.org/10.1371/journal.pone.0152998>.
- (57) Pedersen, L.-F.; Pedersen, P. B.; Nielsen, J. L.; Nielsen, P. H. Peracetic Acid Degradation and Effects on Nitrification in Recirculating Aquaculture Systems. *Aquaculture* **2009**, *296* (3), 246–254. <https://doi.org/10.1016/j.aquaculture.2009.08.021>.
- (58) Lee, W.-N.; Huang, C.-H. Formation of Disinfection Byproducts in Wash Water and Lettuce by Washing with Sodium Hypochlorite and Peracetic Acid Sanitizers. *Food Chem. X* **2019**, *1*, 100003. <https://doi.org/10.1016/j.fochx.2018.100003>.
- (59) Sun, P.; Zhang, T.; Mejia-Tickner, B.; Zhang, R.; Cai, M.; Huang, C.-H. Rapid Disinfection by Peracetic Acid Combined with UV Irradiation. *Environ. Sci. Technol. Lett.* **2018**, *5* (6), 400–404. <https://doi.org/10.1021/acs.estlett.8b00249>.
- (60) Crebelli, R.; Conti, L.; Monarca, S.; Feretti, D.; Zerbini, I.; Zani, C.; Veschetti, E.; Cutilli, D.; Ottaviani, M. Genotoxicity of the Disinfection By-Products Resulting from Peracetic Acid- or Hypochlorite-Disinfected Sewage Wastewater. *Water Res.* **2005**, *39* (6), 1105–1113. <https://doi.org/10.1016/j.watres.2004.12.029>.
- (61) Dell'Erba, A.; Falsanisi, D.; Liberti, L.; Notarnicola, M.; Santoro, D. Disinfection By-Products Formation during Wastewater Disinfection with Peracetic Acid. *Desalination* **2007**, *215* (1–3), 177–186. <https://doi.org/10.1016/j.desal.2006.08.021>.
- (62) Kumar, S.; Singh, M.; Cosby, D. E.; Cox, N. A.; Thippareddi, H. Efficacy of Peroxy Acetic Acid in Reducing Salmonella and Campylobacter Spp. Populations on Chicken Breast Fillets. *Poult. Sci.* **2020**, *99* (5), 2655–2661. <https://doi.org/10.1016/j.psj.2019.12.045>.
- (63) Kataria, J.; Vaddu, S.; Rama, E. N.; Sidhu, G.; Thippareddi, H.; Singh, M. Evaluating the Efficacy of Peracetic Acid on Salmonella and Campylobacter on Chicken Wings at Various pH Levels. *Poult. Sci.* **2020**, *99* (10), 5137–5142. <https://doi.org/10.1016/j.psj.2020.06.070>.
- (64) Otterspoor, S.; Farrell, J. An Evaluation of Buffered Peracetic Acid as an Alternative to Chlorine and Hydrogen Peroxide Based Disinfectants. *Infect. Dis. Health* **2019**, *24* (4), 240–243. <https://doi.org/10.1016/j.idh.2019.06.003>.

- (65) Chhetri, R. K.; Baun, A.; Andersen, H. R. Acute Toxicity and Risk Evaluation of the CSO Disinfectants Performic Acid, Peracetic Acid, Chlorine Dioxide and Their by-Products Hydrogen Peroxide and Chlorite. *Sci. Total Environ.* **2019**, *677*, 1–8. <https://doi.org/10.1016/j.scitotenv.2019.04.350>.
- (66) Fraisse, A.; Temmam, S.; Deboosere, N.; Guillier, L.; Delobel, A.; Maris, P.; Vialette, M.; Morin, T.; Perelle, S. Comparison of Chlorine and Peroxyacetic-Based Disinfectant to Inactivate Feline Calicivirus, Murine Norovirus and Hepatitis A Virus on Lettuce. *Int. J. Food Microbiol.* **2011**, *151* (1), 98–104. <https://doi.org/10.1016/j.ijfoodmicro.2011.08.011>.
- (67) Kiejza, D.; Kotowska, U.; Polińska, W.; Karpińska, J. Peracids - New Oxidants in Advanced Oxidation Processes: The Use of Peracetic Acid, Peroxymonosulfate, and Persulfate Salts in the Removal of Organic Micropollutants of Emerging Concern – A Review. *Sci. Total Environ.* **2021**, *790*, 148195. <https://doi.org/10.1016/j.scitotenv.2021.148195>.
- (68) Maurício, R.; Jorge, J.; Dias, R.; Noronha, J. P.; Amaral, L.; Daam, M. A.; Mano, A. P.; Diniz, M. S. The Use of Peracetic Acid for Estrogen Removal from Urban Wastewaters: E2 as a Case Study. *Environ. Monit. Assess.* **2020**, *192* (2), 114. <https://doi.org/10.1007/s10661-020-8079-7>.
- (69) Deng, J.; Wang, H.; Fu, Y.; Liu, Y. Phosphate-Induced Activation of Peracetic Acid for Diclofenac Degradation: Kinetics, Influence Factors and Mechanism. *Chemosphere* **2022**, *287*, 132396. <https://doi.org/10.1016/j.chemosphere.2021.132396>.
- (70) Kim, J.; Zhang, T.; Liu, W.; Du, P.; Dobson, J. T.; Huang, C.-H. Advanced Oxidation Process with Peracetic Acid and Fe(II) for Contaminant Degradation. *Environ. Sci. Technol.* **2019**, *53* (22), 13312–13322. <https://doi.org/10.1021/acs.est.9b02991>.
- (71) Kim, J.; Du, P.; Liu, W.; Luo, C.; Zhao, H.; Huang, C.-H. Cobalt/Peracetic Acid: Advanced Oxidation of Aromatic Organic Compounds by Acetylperoxyl Radicals. *Environ. Sci. Technol.* **2020**, *54* (8), 5268–5278. <https://doi.org/10.1021/acs.est.0c00356>.
- (72) Li, R.; Manoli, K.; Kim, J.; Feng, M.; Huang, C.-H.; Sharma, V. K. Peracetic Acid–Ruthenium(III) Oxidation Process for the Degradation of Micropollutants in Water. *Environ. Sci. Technol.* **2021**, *55* (13), 9150–9160. <https://doi.org/10.1021/acs.est.0c06676>.
- (73) Sun, P.; Zhang, T.; Mejia-Tickner, B.; Zhang, R.; Cai, M.; Huang, C.-H. Rapid Disinfection by Peracetic Acid Combined with UV Irradiation. *Environ. Sci. Technol. Lett.* **2018**, *5* (6), 400–404. <https://doi.org/10.1021/acs.estlett.8b00249>.

- (74) Zhang, T.; Wang, T.; Mejia-Tickner, B.; Kissel, J.; Xie, X.; Huang, C.-H. Inactivation of Bacteria by Peracetic Acid Combined with Ultraviolet Irradiation: Mechanism and Optimization. *Environ. Sci. Technol.* **2020**, *54* (15), 9652–9661. <https://doi.org/10.1021/acs.est.0c02424>.
- (75) Luukkonen, T.; Heyninck, T.; Rämö, J.; Lassi, U. Comparison of Organic Peracids in Wastewater Treatment: Disinfection, Oxidation and Corrosion. *Water Res.* **2015**, *85*, 275–285. <https://doi.org/10.1016/j.watres.2015.08.037>.
- (76) Luukkonen, T.; Pehkonen, S. O. Peracids in Water Treatment: A Critical Review. *Crit. Rev. Environ. Sci. Technol.* **2017**, *47* (1), 1–39. <https://doi.org/10.1080/10643389.2016.1272343>.
- (77) Sun, Y. Control Effect of Peracetic Acid on Chlorinated DBP Formation and the Application of PAA Pre-Oxidation in Drinking Water Treatment. 57.
- (78) Bettenhausen, C. A. How Peracetic Acid Is Changing Wastewater Treatment. *Chemical & Engineering News*. April 20, 2020. <https://cen.acs.org/environment/water/peracetic-acid-changing-wastewater-treatment/98/i15> (accessed 2021-12-02).
- (79) USEPA. *EPA 600/4-79-020 Methods for Chemical Analysis of Water and Wastes*. https://www.wbdg.org/FFC/EPA/EPACRIT/epa600_4_79_020.pdf (accessed 2019-10-02).
- (80) USEPA. Total Chlorine DPD Method, 2018.
- (81) USEPA. Method 1604: Total Coliforms and Escherichia Coli in Water by Membrane Filtration Using a Simultaneous Detection Technique (MI Medium), 2002.
- (82) Block, P. The Decomposition Kinetics of Peracetic Acid and Hydrogen Peroxide in Municipal Wastewaters. *Proc. Water Environ. Fed.* **2016**, *2016* (10), 555–563. <https://doi.org/10.2175/193864716819707265>.
- (83) Veschetti, E.; Cutilli, D.; Bonadonna, L.; Briancesco, R.; Martini, C.; Cecchini, G.; Anastasi, P.; Ottaviani, M. Pilot-Plant Comparative Study of Peracetic Acid and Sodium Hypochlorite Wastewater Disinfection. *Water Res.* **2003**, *37* (1), 78–94. [https://doi.org/10.1016/S0043-1354\(02\)00248-8](https://doi.org/10.1016/S0043-1354(02)00248-8).
- (84) Zanetti, F.; De Luca, G.; Sacchetti, R.; Stampi, S. Disinfection Efficiency of Peracetic Acid (PAA): Inactivation of Coliphages and Bacterial Indicators in a Municipal Wastewater Plant. *Environ. Technol.* **2007**, *28*, 1265–1271. <https://doi.org/10.1080/09593332808618886>.

- (85) Lefevre, F.; Audic, J. M.; Ferrand, F. Peracetic Acid Disinfection of Secondary Effluents Discharged off Coastal Seawater. *Water Sci. Technol.* **1992**, *25* (12), 155–164. <https://doi.org/10.2166/wst.1992.0347>.
- (86) Stampi, S.; Luca, G. D.; Zanetti, F. Evaluation of the Efficiency of Peracetic Acid in the Disinfection of Sewage Effluents. *J. Appl. Microbiol.* **2001**, *91* (5), 833–838. <https://doi.org/10.1046/j.1365-2672.2001.01451.x>.
- (87) Domínguez Henao, L.; Cascio, M.; Turolla, A.; Antonelli, M. Effect of Suspended Solids on Peracetic Acid Decay and Bacterial Inactivation Kinetics: Experimental Assessment and Definition of Predictive Models. *Sci. Total Environ.* **2018**, *643*, 936–945. <https://doi.org/10.1016/j.scitotenv.2018.06.219>.
- (88) Domínguez Henao, L.; Delli Compagni, R.; Turolla, A.; Antonelli, M. Influence of Inorganic and Organic Compounds on the Decay of Peracetic Acid in Wastewater Disinfection. *Chem. Eng. J.* **2018**, *337*, 133–142. <https://doi.org/10.1016/j.cej.2017.12.074>.
- (89) Pedersen, P. O.; Brodersen, E.; Cecil, D. Disinfection of Tertiary Wastewater Effluent Prior to River Discharge Using Peracetic Acid; Treatment Efficiency and Results on by-Products Formed in Full Scale Tests. *Water Sci. Technol.* **2013**, *68* (8), 1852–1856. <https://doi.org/10.2166/wst.2013.436>.
- (90) Mattle, M. J.; Crouzy, B.; Brennecke, M.; R. Wigginton, K.; Perona, P.; Kohn, T. Impact of Virus Aggregation on Inactivation by Peracetic Acid and Implications for Other Disinfectants. *Environ. Sci. Technol.* **2011**, *45* (18), 7710–7717. <https://doi.org/10.1021/es201633s>.
- (91) Wagner, M.; Brumelis, D.; Gehr, R. Disinfection of Wastewater by Hydrogen Peroxide or Peracetic Acid: Development of Procedures for Measurement of Residual Disinfectant and Application to a Physicochemically Treated Municipal Effluent. *Water Environ. Res.* **2002**, *74* (1), 33–50.
- (92) Cavallini, G. S.; de Campos, S. X.; de Souza, J. B.; Vidal, C. M. de S. Evaluation of the Physical-Chemical Characteristics of Wastewater after Disinfection with Peracetic Acid. *Water. Air. Soil Pollut.* **2013**, *224* (10).
- (93) Amerian, T.; Farnood, R.; Sarathy, S.; Santoro, D. Effects of Total Suspended Solids, Particle Size, and Effluent Temperature on the Kinetics of Peracetic Acid Decomposition in Municipal Wastewater. *Water Sci. Technol.* **2019**, *80* (12), 2299–2309. <https://doi.org/10.2166/wst.2020.047>.

- (94) Falsanisi, D.; Gehr, R.; Liberti, L.; Notarnicola, M. Effect of Suspended Particles on Disinfection of a Physicochemical Municipal Wastewater with Peracetic Acid. *Water Qual. Res. J.* **2008**, *43* (1), 47–54. <https://doi.org/10.2166/wqrj.2008.006>.
- (95) McFadden, M.; Loconsole, J.; Schockling, A. J.; Nerenberg, R.; Pavissich, J. P. Comparing Peracetic Acid and Hypochlorite for Disinfection of Combined Sewer Overflows: Effects of Suspended-Solids and pH. *Sci. Total Environ.* **2017**, *599–600*, 533–539. <https://doi.org/10.1016/j.scitotenv.2017.04.179>.
- (96) Rothbart, S.; Ember, E. E.; Eldik, R. van. Mechanistic Studies on the Oxidative Degradation of Orange II by Peracetic Acid Catalyzed by Simple Manganese(II) Salts. Tuning the Lifetime of the Catalyst. *New J. Chem.* **2012**, *36* (3), 732–748. <https://doi.org/10.1039/C2NJ20852K>.
- (97) Yuan, Z.; Ni, Y.; Heiningen, A. R. P. V. Kinetics of the Peracetic Acid Decomposition: Part II: pH Effect and Alkaline Hydrolysis. *Can. J. Chem. Eng.* **1997**, *75* (1), 42–47. <https://doi.org/10.1002/cjce.5450750109>.
- (98) Zhao, X.; Cheng, K.; Hao, J.; Liu, D. Preparation of Peracetic Acid from Hydrogen Peroxide, Part II: Kinetics for Spontaneous Decomposition of Peracetic Acid in the Liquid Phase. *J. Mol. Catal. Chem.* **2008**, *284* (1), 58–68. <https://doi.org/10.1016/j.molcata.2008.01.003>.
- (99) USEPA. Recreational Water Quality Criteria, 2012.
- (100) *Emerging Trends In Disinfection: Peracetic Acid*. <https://www.wateronline.com/doc/emerging-trends-in-disinfection-peracetic-acid-0001> (accessed 2024-02-05).
- (101) Manoli, K.; Sarathy, S.; Maffettone, R.; Santoro, D. Detailed Modeling and Advanced Control for Chemical Disinfection of Secondary Effluent Wastewater by Peracetic Acid. *Water Res.* **2019**, *153*, 251–262. <https://doi.org/10.1016/j.watres.2019.01.022>.
- (102) Levin, R. B.; Epstein, P. R.; Ford, T. E.; Harrington, W.; Olson, E.; Reichard, E. G. U.S. Drinking Water Challenges in the Twenty-First Century. *Environ. Health Perspect.* **2002**, *110* (Suppl 1), 43–52.
- (103) Turner, S. W. D.; Rice, J. S.; Nelson, K. D.; Vernon, C. R.; McManamay, R.; Dickson, K.; Marston, L. Comparison of Potential Drinking Water Source Contamination across One Hundred U.S. Cities. *Nat. Commun.* **2021**, *12*, 7254. <https://doi.org/10.1038/s41467-021-27509-9>.

- (104)Rabin, R. The Lead Industry and Lead Water Pipes “A MODEST CAMPAIGN.” *Am. J. Public Health* **2008**, 98 (9), 1584–1592. <https://doi.org/10.2105/AJPH.2007.113555>.
- (105)Troesken, W. *The Great Lead Water Pipe Disaster*; MIT Press, 2006.
- (106)Kirkwood, J. P. COLLECTION OF REPORTS, (CONDENSED), OPINIONS OF CHEMISTS IN REGARD TO THE USE OF LEAD PIPE POR SERVICE PIPE, DISTRIBUTION OF WATER SUPPLY OP CITIES, 1859. <https://collections.nlm.nih.gov/ext/mhl/63150830R/PDF/63150830R.pdf> (accessed 2022-08-08).
- (107)Swann, A. On Lead-Poisoning from Service Pipes, in Relation to Sterility and Abortion. *Br. Med. J.* **1889**, 1 (1468), 352.
- (108)Stainthorpe, W. W. OBSERVATIONS ON 120 CASES OF LEAD ABSORPTION FROM DRINKING-WATER. *The Lancet* **1914**, 184 (4743), 213–215. [https://doi.org/10.1016/S0140-6736\(01\)08571-3](https://doi.org/10.1016/S0140-6736(01)08571-3).
- (109)Goovaerts, P. The Drinking Water Contamination Crisis in Flint: Modeling Temporal Trends of Lead Level since Returning to Detroit Water System. *Sci. Total Environ.* **2017**, 581, 66–79. <https://doi.org/10.1016/j.scitotenv.2016.09.207>.
- (110)Olson, T. M.; Wax, M.; Yonts, J.; Heidecorn, K.; Haig, S.-J.; Yeoman, D.; Hayes, Z.; Raskin, L.; Ellis, B. R. Forensic Estimates of Lead Release from Lead Service Lines during the Water Crisis in Flint, Michigan. *Environ. Sci. Technol. Lett.* **2017**, 4 (9), 356–361. <https://doi.org/10.1021/acs.estlett.7b00226>.
- (111)Pieper, K. J.; Tang, M.; Edwards, M. A. Flint Water Crisis Caused By Interrupted Corrosion Control: Investigating “Ground Zero” Home. *Environ. Sci. Technol.* **2017**, 51 (4), 2007–2014. <https://doi.org/10.1021/acs.est.6b04034>.
- (112)Morrison, O. *The main cause of Pittsburgh’s lead crisis wasn’t corporate management*. PublicSource. <http://www.publicsource.org/pwsa-pittsburgh-lead-water-corrosion-soda-ash-caustic-soda-orthophosphate/> (accessed 2022-07-22).
- (113)Bae, Y.; Pasteris, J. D.; Giammar, D. E. The Ability of Phosphate To Prevent Lead Release from Pipe Scale When Switching from Free Chlorine to Monochloramine. *Environ. Sci. Technol.* **2020**, 54 (2), 879–888. <https://doi.org/10.1021/acs.est.9b06019>.

- (114)Becker, A. The Effect of Corrosion Inhibitors in Drinking Water Installations of Copper. *Mater. Corros.* **2002**, *53* (8), 560–567. [https://doi.org/10.1002/1521-4176\(200208\)53:8<560::AID-MACO560>3.0.CO;2-C](https://doi.org/10.1002/1521-4176(200208)53:8<560::AID-MACO560>3.0.CO;2-C).
- (115)Cantor, A. F.; Denig-Chakroff, D.; Vela, R. R.; Oleinik, M. G.; Lynch, D. L. Use of Polyphosphate in Corrosion Control. *J. AWWA* **2000**, *92* (2), 95–102. <https://doi.org/10.1002/j.1551-8833.2000.tb08820.x>.
- (116)Comber, S.; Cassé, F.; Brown, B.; Martin, J.; Hillis, P.; Gardner, M. Phosphate Treatment to Reduce Plumbosolvency of Drinking Water Also Reduces Discharges of Copper into Environmental Surface Waters. *Water Environ. J.* **2011**, *25* (2), 266–270. <https://doi.org/10.1111/j.1747-6593.2010.00219.x>.
- (117)Edwards, M.; McNeill, L. S. Effect of PHOSPHATE Inhibitors on Lead Release from Pipes. *J. AWWA* **2002**, *94* (1), 79–90. <https://doi.org/10.1002/j.1551-8833.2002.tb09383.x>.
- (118)McNeill, L. S.; Edwards, M. Phosphate Inhibitor Use at US Utilities. *J. AWWA* **2002**, *94* (7), 57–63. <https://doi.org/10.1002/j.1551-8833.2002.tb09506.x>.
- (119)Schock, M. Corrosion Inhibitor Applications in Drinking Water Treatment: Conforming to the Lead and Copper Rule. **1996**.
- (120)Yohai, L.; Schreiner, W. H.; Vázquez, M.; Valcarce, M. B. Phosphate Ions as Inhibiting Agents for Copper Corrosion in Chlorinated Tap Water. *Mater. Chem. Phys.* **2013**, *139* (2), 817–824. <https://doi.org/10.1016/j.matchemphys.2013.02.037>.
- (121)US EPA. Optimal Corrosion Control Treatment Evaluation Technical Recommendations for Primacy Agencies and Public Water Systems, 2016. <https://www.epa.gov/sites/default/files/2016-03/documents/occtmarch2016.pdf> (accessed 2022-08-08).
- (122)Alawadhi, A.; Tartakovsky, D. Bayesian Update and Method of Distributions: Application to Leak Detection in Transmission Mains. *Water Resour. Res.* **2020**, *56*. <https://doi.org/10.1029/2019WR025879>.
- (123)Kaushal, S. S.; Belt, K. T. The Urban Watershed Continuum: Evolving Spatial and Temporal Dimensions. *Urban Ecosyst.* **2012**, *15* (2), 409–435. <https://doi.org/10.1007/s11252-012-0226-7>.

- (124) Welty, C.; Miller, A. J.; Belt, K. T.; Smith, J. A.; Band, L. E.; Groffman, P. M.; Scanlon, T. M.; Warner, J.; Ryan, R. J.; Shedlock, R. J.; McGuire, M. P. Design of an Environmental Field Observatory for Quantifying the Urban Water Budget. *Novotny Vladimir Brown Paul Eds Cities Future Integr. Sustain. Water Landsc. Manag. Lond. Int. Water Assoc.* 72-88 **2007**.
- (125) Jankowiak, J.; Hattenrath-Lehmann, T.; Kramer, B. J.; Ladds, M.; Gobler, C. J. Deciphering the Effects of Nitrogen, Phosphorus, and Temperature on Cyanobacterial Bloom Intensification, Diversity, and Toxicity in Western Lake Erie. *Limnol. Oceanogr.* **2019**, *64* (3), 1347–1370. <https://doi.org/10.1002/lno.11120>.
- (126) Tiwari, B.; Singh, S.; Kaushik, M. S.; Mishra, A. K. Regulation of Organophosphate Metabolism in Cyanobacteria. A Review. *Microbiology* **2015**, *84* (3), 291–302. <https://doi.org/10.1134/S0026261715030200>.
- (127) Akbari, A.; Wang, Z.; He, P.; Wang, D.; Lee, J.; Han, I.; Li, G.; Gu, A. Z. Unrevealed Roles of Polyphosphate-accumulating Microorganisms. *Microb. Biotechnol.* **2021**, *14* (1), 82–87. <https://doi.org/10.1111/1751-7915.13730>.
- (128) Appenzeller, B. M. R.; Batté, M.; Mathieu, L.; Block, J. C.; Lahoussine, V.; Cavard, J.; Gatel, D. Effect of Adding Phosphate to Drinking Water on Bacterial Growth in Slightly and Highly Corroded Pipes. *Water Res.* **2001**, *35* (4), 1100–1105. [https://doi.org/10.1016/S0043-1354\(00\)00337-7](https://doi.org/10.1016/S0043-1354(00)00337-7).
- (129) Batté, M.; Koudjonou, B.; Laurent, P.; Mathieu, L.; Coallier, J.; Prévost, M. Biofilm Responses to Ageing and to a High Phosphate Load in a Bench-Scale Drinking Water System. *Water Res.* **2003**, *37* (6), 1351–1361. [https://doi.org/10.1016/S0043-1354\(02\)00476-1](https://doi.org/10.1016/S0043-1354(02)00476-1).
- (130) Camacho, A.; De Wit, R. Effect of Nitrogen and Phosphorus Additions on a Benthic Microbial Mat from a Hypersaline Lake. *Aquat. Microb. Ecol. - AQUAT MICROB ECOL* **2003**, *32*, 261–273. <https://doi.org/10.3354/ame032261>.
- (131) Carpenter, S. R. Phosphorus Control Is Critical to Mitigating Eutrophication. *Proc. Natl. Acad. Sci.* **2008**, *105* (32), 11039–11040. <https://doi.org/10.1073/pnas.0806112105>.
- (132) Elser, J. J.; Bracken, M. E. S.; Cleland, E. E.; Gruner, D. S.; Harpole, W. S.; Hillebrand, H.; Ngai, J. T.; Seabloom, E. W.; Shurin, J. B.; Smith, J. E. Global Analysis of Nitrogen and Phosphorus Limitation of Primary Producers in Freshwater, Marine and Terrestrial Ecosystems. *Ecol. Lett.* **2007**, *10* (12), 1135–1142. <https://doi.org/10.1111/j.1461-0248.2007.01113.x>.

- (133)Schindler, D. W. Evolution of Phosphorus Limitation in Lakes. *Science* **1977**, *195* (4275), 260–262. <https://doi.org/10.1126/science.195.4275.260>.
- (134)Thingstad, T. F.; Zweifel, U. L.; Rassoulzadegan, F. P Limitation of Heterotrophic Bacteria and Phytoplankton in the Northwest Mediterranean. *Limnol. Oceanogr.* **1998**, *43* (1), 88–94. <https://doi.org/10.4319/lo.1998.43.1.0088>.
- (135)US EPA, O. *Nutrient Pollution: The Issue*. US EPA. <https://www.epa.gov/nutrientpollution/issue> (accessed 2021-01-08).
- (136)Barbiero, R. P.; Lesht, B. M.; Warren, G. J.; Rudstam, L. G.; Watkins, J. M.; Reavie, E. D.; Kovalenko, K. E.; Karatayev, A. Y. A Comparative Examination of Recent Changes in Nutrients and Lower Food Web Structure in Lake Michigan and Lake Huron. *J. Gt. Lakes Res.* **2018**, *44* (4), 573–589. <https://doi.org/10.1016/j.jglr.2018.05.012>.
- (137)Fierer, N.; Jackson, J. A.; Vilgalys, R.; Jackson, R. B. Assessment of Soil Microbial Community Structure by Use of Taxon-Specific Quantitative PCR Assays. *Appl. Environ. Microbiol.* **2005**, *71* (7), 4117–4120. <https://doi.org/10.1128/AEM.71.7.4117-4120.2005>.
- (138)Nübel, U.; Garcia-Pichel, F.; Muyzer, G. PCR Primers to Amplify 16S rRNA Genes from Cyanobacteria. *Appl. Environ. Microbiol.* **1997**, *63* (8), 3327–3332.
- (139)He, S.; Gall, D. L.; McMahon, K. D. “Candidatus Accumulibacter” Population Structure in Enhanced Biological Phosphorus Removal Sludges as Revealed by Polyphosphate Kinase Genes. *Appl. Environ. Microbiol.* **2007**, *73* (18), 5865–5874. <https://doi.org/10.1128/AEM.01207-07>.
- (140)Lievens, A.; Jacchia, S.; Kagkli, D.; Savini, C.; Querci, M. Measuring Digital PCR Quality: Performance Parameters and Their Optimization. *PLOS ONE* **2016**, *11* (5), e0153317. <https://doi.org/10.1371/journal.pone.0153317>.
- (141)Caporaso, J. G.; Lauber, C. L.; Walters, W. A.; Berg-Lyons, D.; Huntley, J.; Fierer, N.; Owens, S. M.; Betley, J.; Fraser, L.; Bauer, M.; Gormley, N.; Gilbert, J. A.; Smith, G.; Knight, R. Ultra-High-Throughput Microbial Community Analysis on the Illumina HiSeq and MiSeq Platforms. *ISME J.* **2012**, *6* (8), 1621–1624. <https://doi.org/10.1038/ismej.2012.8>.
- (142)Bolyen, E.; Rideout, J. R.; Dillon, M. R.; Bokulich, N. A.; Abnet, C. C.; Al-Ghalith, G. A.; Alexander, H.; Alm, E. J.; Arumugam, M.; Asnicar, F.; Bai, Y.; Bisanz, J. E.; Bittinger, K.; Brejnrod, A.; Brislawn, C. J.; Brown, C. T.; Callahan, B. J.; Caraballo-Rodríguez, A. M.; Chase, J.; Cope, E. K.; Da Silva, R.; Diener, C.; Dorrestein, P. C.; Douglas, G. M.; Durall,

D. M.; Duvallet, C.; Edwardson, C. F.; Ernst, M.; Estaki, M.; Fouquier, J.; Gauglitz, J. M.; Gibbons, S. M.; Gibson, D. L.; Gonzalez, A.; Gorlick, K.; Guo, J.; Hillmann, B.; Holmes, S.; Holste, H.; Huttenhower, C.; Huttley, G. A.; Janssen, S.; Jarmusch, A. K.; Jiang, L.; Kaehler, B. D.; Kang, K. B.; Keefe, C. R.; Keim, P.; Kelley, S. T.; Knights, D.; Koester, I.; Kosciulek, T.; Kreps, J.; Langille, M. G. I.; Lee, J.; Ley, R.; Liu, Y.-X.; Lofffield, E.; Lozupone, C.; Maher, M.; Marotz, C.; Martin, B. D.; McDonald, D.; McIver, L. J.; Melnik, A. V.; Metcalf, J. L.; Morgan, S. C.; Morton, J. T.; Naimey, A. T.; Navas-Molina, J. A.; Nothias, L. F.; Orchanian, S. B.; Pearson, T.; Peoples, S. L.; Petras, D.; Preuss, M. L.; Pruesse, E.; Rasmussen, L. B.; Rivers, A.; Robeson, M. S.; Rosenthal, P.; Segata, N.; Shaffer, M.; Shiffer, A.; Sinha, R.; Song, S. J.; Spear, J. R.; Swafford, A. D.; Thompson, L. R.; Torres, P. J.; Trinh, P.; Tripathi, A.; Turnbaugh, P. J.; Ul-Hasan, S.; van der Hooft, J. J. J.; Vargas, F.; Vázquez-Baeza, Y.; Vogtmann, E.; von Hippel, M.; Walters, W.; Wan, Y.; Wang, M.; Warren, J.; Weber, K. C.; Williamson, C. H. D.; Willis, A. D.; Xu, Z. Z.; Zaneveld, J. R.; Zhang, Y.; Zhu, Q.; Knight, R.; Caporaso, J. G. Reproducible, Interactive, Scalable and Extensible Microbiome Data Science Using QIIME 2. *Nat. Biotechnol.* **2019**, *37* (8), 852–857. <https://doi.org/10.1038/s41587-019-0209-9>.

(143)Ward, T.; Larson, J.; Meulemans, J.; Hillmann, B.; Lynch, J.; Sidiropoulos, D.; Spear, J. R.; Caporaso, G.; Blekhman, R.; Knight, R.; Fink, R.; Knights, D. *BugBase Predicts Organism-Level Microbiome Phenotypes*; 2017; p 133462. <https://doi.org/10.1101/133462>.

(144)Pierre; Legendre, G. Ecologically Meaningful Transformations for Ordination of Species Data. **2001**, *129*, 271–280.

(145)Oksanen, J.; Guillaume Blanchet, F.; Friendly, M.; Kindt, R.; Legendre, P.; McGlenn, D.; Minchin, P. R.; O’Hara, R. B.; Simpson, G. L.; Solymos, P.; H. Stevens, M. H.; Szoecs, E.; Helene Wagner. *Vegan: Community Ecology Package*, 2020. <https://cran.r-project.org/web/packages/vegan/vegan.pdf> (accessed 2021-10-11).

(146)Haig, S.-J.; Quince, C.; Davies, R. L.; Dorea, C. C.; Collins, G. The Relationship between Microbial Community Evenness and Function in Slow Sand Filters. *mBio* *6* (5), e00729-15. <https://doi.org/10.1128/mBio.00729-15>.

(147)R Core Team. R: The R Project for Statistical Computing, 2020. <https://www.r-project.org/> (accessed 2021-10-11).

(148)Hopkins, K. G.; Bain, D. J. Research Note: Mapping Spatial Patterns in Sewer Age, Material, and Proximity to Surface Waterways to Infer Sewer Leakage Hotspots. *Landsc. Urban Plan.* **2018**, *170*, 320–324. <https://doi.org/10.1016/j.landurbplan.2017.04.011>.

- (149)Balangoda, A.; Elliott, E. M.; Dabundo, R.; Spencer-Williams, I.; Haig, S.-J. Assessing Nutrient Limitation in Urban Streams Following the Addition of Orthophosphate-Based Corrosion Control to Drinking Water. *Sci. Total Environ.* **2023**, *In Review*.
- (150)Vignale, F. A.; Bernal Rey, D.; Pardo, A. M.; Almasqué, F. J.; Ibarra, J. G.; Fernández Do Porto, D.; Turjanski, A. G.; López, N. I.; Helman, R. J. M.; Raiger Iustman, L. J. Spatial and Seasonal Variations in the Bacterial Community of an Anthropogenic Impacted Urban Stream. *Microb. Ecol.* **2022**. <https://doi.org/10.1007/s00248-022-02055-z>.
- (151)Xiao, Z.; Li, G.; Zhao, Y.; Xiao, K.; Chen, Q.; Bao, P.; Tang, J.; Ruan, T.; Zama, E. F.; Xu, Y. Bacterioplankton Richness and Composition in a Seasonal Urban River. *Front. Environ. Sci.* **2021**, *9*.
- (152)Fang, W.; Fan, T.; Wang, S.; Yu, X.; Lu, A.; Wang, X.; Zhou, W.; Yuan, H.; Zhang, L. Seasonal Changes Driving Shifts in Microbial Community Assembly and Species Coexistence in an Urban River. *Sci. Total Environ.* **2023**, *905*, 167027. <https://doi.org/10.1016/j.scitotenv.2023.167027>.
- (153)Hosen, J. D.; Febria, C. M.; Crump, B. C.; Palmer, M. A. Watershed Urbanization Linked to Differences in Stream Bacterial Community Composition. *Front. Microbiol.* **2017**, *8*.
- (154)Hassell, N.; Tinker, K. A.; Moore, T.; Ottesen, E. A. Temporal and Spatial Dynamics in Microbial Community Composition within a Temperate Stream Network. *Environ. Microbiol.* **2018**, *20* (10), 3560–3572. <https://doi.org/10.1111/1462-2920.14311>.
- (155)Staley, C.; Gould, T. J.; Wang, P.; Phillips, J.; Cotner, J. B.; Sadowsky, M. J. Species Sorting and Seasonal Dynamics Primarily Shape Bacterial Communities in the Upper Mississippi River. *Sci. Total Environ.* **2015**, *505*, 435–445. <https://doi.org/10.1016/j.scitotenv.2014.10.012>.
- (156)Newton, R. J.; Jones, S. E.; Eiler, A.; McMahon, K. D.; Bertilsson, S. A Guide to the Natural History of Freshwater Lake Bacteria. *Microbiol. Mol. Biol. Rev. MMBR* **2011**, *75* (1), 14–49. <https://doi.org/10.1128/MMBR.00028-10>.
- (157)Fiedler, C. J.; Schönher, C.; Proksch, P.; Kerschbaumer, D. J.; Mayr, E.; Zunabovic-Pichler, M.; Domig, K. J.; Perfler, R. Assessment of Microbial Community Dynamics in River Bank Filtrate Using High-Throughput Sequencing and Flow Cytometry. *Front. Microbiol.* **2018**, *9*.

- (158)Faria, M.; Bordin, N.; Kizina, J.; Harder, J.; Devos, D.; Lage, O. M. Planctomycetes Attached to Algal Surfaces: Insight into Their Genomes. *Genomics* **2018**, *110* (5), 231–238. <https://doi.org/10.1016/j.ygeno.2017.10.007>.
- (159)Bergkemper, F.; Schöler, A.; Engel, M.; Lang, F.; Krüger, J.; Schloter, M.; Schulz, S. Phosphorus Depletion in Forest Soils Shapes Bacterial Communities towards Phosphorus Recycling Systems. *Environ. Microbiol.* **2016**, *18* (6), 1988–2000. <https://doi.org/10.1111/1462-2920.13188>.
- (160)Hu, Y.; Duan, C.; Fu, D.; Wu, X.; Yan, K.; Fernando, E.; Karunarathna, S. C.; Promputtha, I.; Mortimer, P. E.; Xu, J. Structure of Bacterial Communities in Phosphorus-Enriched Rhizosphere Soils. *Appl. Sci.* **2020**, *10* (18), 6387. <https://doi.org/10.3390/app10186387>.
- (161)Fuerst, J. A. The PVC Superphylum: Exceptions to the Bacterial Definition? *Antonie Van Leeuwenhoek* **2013**, *104* (4), 451–466. <https://doi.org/10.1007/s10482-013-9986-1>.
- (162)Méheust, R.; Castelle, C. J.; Matheus Carnevali, P. B.; Farag, I. F.; He, C.; Chen, L.-X.; Amano, Y.; Hug, L. A.; Banfield, J. F. Groundwater Elusimicrobia Are Metabolically Diverse Compared to Gut Microbiome Elusimicrobia and Some Have a Novel Nitrogenase Paralog. *ISME J.* **2020**, *14* (12), 2907–2922. <https://doi.org/10.1038/s41396-020-0716-1>.
- (163)Uzun, M.; Koziyeva, V.; Dziuba, M.; Alekseeva, L.; Krutkina, M.; Sukhacheva, M.; Baslerov, R.; Grouzdev, D. Recovery and Genome Reconstruction of Novel Magnetotactic Elusimicrobiota from Bog Soil. *ISME J.* **2023**, *17* (2), 204–214. <https://doi.org/10.1038/s41396-022-01339-z>.
- (164)Cremer, F.; Serra Moncadas, L.; Andrei, A.-S. Complete Genome Sequence from an Uncultivated Freshwater Elusimicrobiota Lineage. *Microbiol. Resour. Announc.* **2022**, *11* (9), e00426-22. <https://doi.org/10.1128/mra.00426-22>.
- (165)Collingro, A.; Köstlbacher, S.; Horn, M. Chlamydiae in the Environment. *Trends Microbiol.* **2020**, *28* (11), 877–888. <https://doi.org/10.1016/j.tim.2020.05.020>.
- (166)Chaudhary, A.; Kauser, I.; Ray, A.; Poretsky, R. Taxon-Driven Functional Shifts Associated with Storm Flow in an Urban Stream Microbial Community. *mSphere* **2018**, *3* (4). <https://doi.org/10.1128/mSphere.00194-18>.
- (167)Dharamshi, J. E.; Tamarit, D.; Eme, L.; Stairs, C. W.; Martijn, J.; Homa, F.; Jørgensen, S. L.; Spang, A.; Ettema, T. J. G. Marine Sediments Illuminate Chlamydiae Diversity and

- (168) Welles, L.; Abbas, B.; Sorokin, D. Y.; Lopez-Vazquez, C. M.; Hooijmans, C. M.; van Loosdrecht, M. C. M.; Brdjanovic, D. Metabolic Response of “Candidatus Accumulibacter Phosphatis” Clade II C to Changes in Influent P/C Ratio. *Front. Microbiol.* **2017**, 7, 2121. <https://doi.org/10.3389/fmicb.2016.02121>.
- (169) Dignum, M.; Matthijs, H. C.; Pel, R.; Laanbroek, H. J.; Mur, L. R. Nutrient Limitation of Freshwater Cyanobacteria. In *Harmful cyanobacteria*; Springer, 2005; pp 65–86.
- (170) Litke, D. W. *Review of Phosphorus Control Measures in the United States and Their Effects on Water Quality*; 1999. <https://doi.org/10.3133/wri994007>.
- (171) Zeglin, L. H. Stream Microbial Diversity in Response to Environmental Changes: Review and Synthesis of Existing Research. *Front. Microbiol.* **2015**, 6. <https://doi.org/10.3389/fmicb.2015.00454>.
- (172) Jones, E. F.; Griffin, N.; Kelso, J. E.; Carling, G. T.; Baker, M. A.; Aanderud, Z. T. Stream Microbial Community Structured by Trace Elements, Headwater Dispersal, and Large Reservoirs in Sub-Alpine and Urban Ecosystems. *Front. Microbiol.* **2020**, 11, 3005. <https://doi.org/10.3389/fmicb.2020.491425>.
- (173) Li, Y.; Yu, S.; Strong, J.; Wang, H. Are the Biogeochemical Cycles of Carbon, Nitrogen, Sulfur, and Phosphorus Driven by the “FeIII–FeII Redox Wheel” in Dynamic Redox Environments? *J. Soils Sediments* **2012**, 12 (5), 683–693. <https://doi.org/10.1007/s11368-012-0507-z>.
- (174) Paul, M. J.; Meyer, J. L. Streams in the Urban Landscape. *Annu. Rev. Ecol. Syst.* **2001**, 32 (1), 333–365. <https://doi.org/10.1146/annurev.ecolsys.32.081501.114040>.
- (175) Wang, H.; Liu, X.; Wang, Y.; Zhang, S.; Zhang, G.; Han, Y.; Li, M.; Liu, L. Spatial and Temporal Dynamics of Microbial Community Composition and Factors Influencing the Surface Water and Sediments of Urban Rivers. *J. Environ. Sci.* **2023**, 124, 187–197. <https://doi.org/10.1016/j.jes.2021.10.016>.
- (176) Ouyang, L.; Chen, H.; Liu, X.; Wong, M. H.; Xu, F.; Yang, X.; Xu, W.; Zeng, Q.; Wang, W.; Li, S. Characteristics of Spatial and Seasonal Bacterial Community Structures in a River under Anthropogenic Disturbances. *Environ. Pollut.* **2020**, 264, 114818. <https://doi.org/10.1016/j.envpol.2020.114818>.

- (177)Mishra, A.; Alnahit, A.; Campbell, B. Impact of Land Uses, Drought, Flood, Wildfire, and Cascading Events on Water Quality and Microbial Communities: A Review and Analysis. *J. Hydrol.* **2021**, *596*, 125707. <https://doi.org/10.1016/j.jhydrol.2020.125707>.
- (178)Wilhelm, S. W.; LeCleir, G. R.; Bullerjahn, G. S.; McKay, R. M.; Saxton, M. A.; Twiss, M. R.; Bourbonniere, R. A. Seasonal Changes in Microbial Community Structure and Activity Imply Winter Production Is Linked to Summer Hypoxia in a Large Lake. *FEMS Microbiol. Ecol.* **2014**, *87* (2), 475–485. <https://doi.org/10.1111/1574-6941.12238>.
- (179)Samad, M. S.; Bertilsson, S. Seasonal Variation in Abundance and Diversity of Bacterial Methanotrophs in Five Temperate Lakes. *Front. Microbiol.* **2017**, *8*.
- (180)Hullar, M. A. J.; Kaplan, L. A.; Stahl, D. A. Recurring Seasonal Dynamics of Microbial Communities in Stream Habitats. *Appl. Environ. Microbiol.* **2006**, *72* (1), 713–722. <https://doi.org/10.1128/AEM.72.1.713-722.2006>.
- (181)Ibrahim, I. M.; Puthiyaveetil, S.; Allen, J. F. A Two-Component Regulatory System in Transcriptional Control of Photosystem Stoichiometry: Redox-Dependent and Sodium Ion-Dependent Phosphoryl Transfer from Cyanobacterial Histidine Kinase Hik2 to Response Regulators Rre1 and RppA. *Front. Plant Sci.* **2016**, *7*, 137. <https://doi.org/10.3389/fpls.2016.00137>.
- (182)Stock, A. M.; Robinson, V. L.; Goudreau, P. N. Two-Component Signal Transduction. *Annu. Rev. Biochem.* **2000**, *69*, 183–215.
- (183)Huang, H.-H.; Chen, W.-C.; Lin, C.-W.; Lin, Y.-T.; Ning, H.-C.; Chang, Y.-C.; Yang, T.-C. Relationship of the CreBC Two-Component Regulatory System and Inner Membrane Protein CreD with Swimming Motility in *Stenotrophomonas maltophilia*. *PLOS ONE* **2017**, *12* (4), e0174704. <https://doi.org/10.1371/journal.pone.0174704>.
- (184)Avison, M. B.; Horton, R. E.; Walsh, T. R.; Bennett, P. M. *Escherichia coli* CreBC Is a Global Regulator of Gene Expression That Responds to Growth in Minimal Media. *J. Biol. Chem.* **2001**, *276* (29), 26955–26961. <https://doi.org/10.1074/jbc.M011186200>.
- (185)Verhamme, D. L. T.; Arents, J. C.; Postma, P. W.; Crielaard, W.; Hellingwerf, K. J. Printed in Great Britain Glucose-6-Phosphate-Dependent Phosphoryl.
- (186)Cleveland, C. C.; Liptzin, D. C:N:P Stoichiometry in Soil: Is There a “Redfield Ratio” for the Microbial Biomass? *Biogeochemistry* **2007**, *85* (3), 235–252. <https://doi.org/10.1007/s10533-007-9132-0>.

- (187)They, N. H.; Amado, A. M.; Cotner, J. B. Redfield Ratios in Inland Waters: Higher Biological Control of C:N:P Ratios in Tropical Semi-Arid High Water Residence Time Lakes. *Front. Microbiol.* **2017**, *8*.
- (188)Lemmer, K. C.; Alberge, F.; Myers, K. S.; Dohnalkova, A. C.; Schaub, R. E.; Lenz, J. D.; Imam, S.; Dillard, J. P.; Noguera, D. R.; Donohue, T. J. The NtrYX Two-Component System Regulates the Bacterial Cell Envelope. *mBio* **2020**, *11* (3). <https://doi.org/10.1128/mBio.00957-20>.
- (189)Carrica, M. del C.; Fernandez, I.; Martí, M. A.; Paris, G.; Goldbaum, F. A. The NtrY/X Two-Component System of *Brucella* Spp. Acts as a Redox Sensor and Regulates the Expression of Nitrogen Respiration Enzymes. *Mol. Microbiol.* **2012**, *85* (1), 39–50. <https://doi.org/10.1111/j.1365-2958.2012.08095.x>.
- (190)Carrica, M. del C.; Fernandez, I.; Sieira, R.; Paris, G.; Goldbaum, F. A. The Two-Component Systems PrrBA and NtrYX Co-Ordinately Regulate the Adaptation of *Brucella Abortus* to an Oxygen-Limited Environment. *Mol. Microbiol.* **2013**, *88* (2), 222–233. <https://doi.org/10.1111/mmi.12181>.
- (191)Calatrava-Morales, N.; Nogales, J.; Amezttoy, K.; van Steenberg, B.; Soto, M. J. The NtrY/NtrX System of *Sinorhizobium Meliloti* GR4 Regulates Motility, EPS I Production, and Nitrogen Metabolism but Is Dispensable for Symbiotic Nitrogen Fixation. *Mol. Plant-Microbe Interactions*® **2017**, *30* (7), 566–577. <https://doi.org/10.1094/MPMI-01-17-0021-R>.
- (192)Delmont, T. O.; Quince, C.; Shaiber, A.; Esen, Ö. C.; Lee, S. T.; Rappé, M. S.; McLellan, S. L.; Lückner, S.; Eren, A. M. Nitrogen-Fixing Populations of Planctomycetes and Proteobacteria Are Abundant in Surface Ocean Metagenomes. *Nat. Microbiol.* **2018**, *3* (7), 804–813. <https://doi.org/10.1038/s41564-018-0176-9>.
- (193)Fernández, I.; Sycz, G.; Goldbaum, F. A.; Carrica, M. del C. Acidic pH Triggers the Phosphorylation of the Response Regulator NtrX in Alphaproteobacteria. *PLOS ONE* **2018**, *13* (4), e0194486. <https://doi.org/10.1371/journal.pone.0194486>.
- (194)Vital, M.; Dignum, M.; Magic-Knezev, A.; Ross, P.; Rietveld, L.; Hammes, F. Flow Cytometry and Adenosine Tri-Phosphate Analysis: Alternative Possibilities to Evaluate Major Bacteriological Changes in Drinking Water Treatment and Distribution Systems. *Water Res.* **2012**, *46* (15), 4665–4676. <https://doi.org/10.1016/j.watres.2012.06.010>.
- (195)El Bcheraoui, C.; Mokdad, A. H.; Dwyer-Lindgren, L.; Bertozzi-Villa, A.; Stubbs, R. W.; Morozoff, C.; Shirude, S.; Naghavi, M.; Murray, C. J. L. Trends and Patterns of Differences

- in Infectious Disease Mortality Among US Counties, 1980-2014. *JAMA* **2018**, *319* (12), 1248–1260. <https://doi.org/10.1001/jama.2018.2089>.
- (196)Lopez, A. D.; Mathers, C. D.; Ezzati, M.; Jamison, D. T.; Murray, C. J. L. Global and Regional Burden of Disease and Risk Factors, 2001: Systematic Analysis of Population Health Data. *Lancet Lond. Engl.* **2006**, *367* (9524), 1747–1757. [https://doi.org/10.1016/S0140-6736\(06\)68770-9](https://doi.org/10.1016/S0140-6736(06)68770-9).
- (197)Masur, H.; Read, S. W. Opportunistic Infections and Mortality: Still Room for Improvement. *J. Infect. Dis.* **2015**, *212* (9), 1348–1350. <https://doi.org/10.1093/infdis/jiv236>.
- (198)Pirofski, L.; Casadevall, A. Q&A: What Is a Pathogen? A Question That Begs the Point. *BMC Biol.* **2012**, *10* (1), 6. <https://doi.org/10.1186/1741-7007-10-6>.
- (199)Collier, S. A.; Deng, L.; Adam, E. A.; Benedict, K. M.; Beshearse, E. M.; Blackstock, A. J.; Bruce, B. B.; Derado, G.; Edens, C.; Fullerton, K. E.; Gargano, J. W.; Geissler, A. L.; Hall, A. J.; Havelaar, A. H.; Hill, V. R.; Hoekstra, R. M.; Reddy, S. C.; Scallan, E.; Stokes, E. K.; Yoder, J. S.; Beach, M. J. Estimate of Burden and Direct Healthcare Cost of Infectious Waterborne Disease in the United States. *Emerg. Infect. Dis.* **2021**, *27* (1), 140–149. <https://doi.org/10.3201/eid2701.190676>.
- (200)Feazel, L. M.; Baumgartner, L. K.; Peterson, K. L.; Frank, D. N.; Harris, J. K.; Pace, N. R. Opportunistic Pathogens Enriched in Showerhead Biofilms. *Proc. Natl. Acad. Sci.* **2009**, *106* (38), 16393–16399. <https://doi.org/10.1073/pnas.0908446106>.
- (201)Benedict, K. M. Surveillance for Waterborne Disease Outbreaks Associated with Drinking Water — United States, 2013–2014. *MMWR Morb. Mortal. Wkly. Rep.* **2017**, *66*. <https://doi.org/10.15585/mmwr.mm6644a3>.
- (202)Adjemian, J.; Frankland, T. B.; Daida, Y. G.; Honda, J. R.; Olivier, K. N.; Zelazny, A.; Honda, S.; Prevots, D. R. Epidemiology of Nontuberculous Mycobacterial Lung Disease and Tuberculosis, Hawaii, USA. *Emerg. Infect. Dis.* **2017**, *23* (3), 439–447. <https://doi.org/10.3201/eid2303.161827>.
- (203)Cunha, B. A.; Burillo, A.; Bouza, E. Legionnaires' Disease. *The Lancet* **2016**, *387* (10016), 376–385. [https://doi.org/10.1016/S0140-6736\(15\)60078-2](https://doi.org/10.1016/S0140-6736(15)60078-2).
- (204)Falkinham, J. O. Nontuberculous Mycobacteria from Household Plumbing of Patients with Nontuberculous Mycobacteria Disease. *Emerg. Infect. Dis.* **2011**, *17* (3), 419–424. <https://doi.org/10.3201/eid1703.101510>.

- (205) Lin, W.; Yu, Z.; Zhang, H.; Thompson, I. P. Diversity and Dynamics of Microbial Communities at Each Step of Treatment Plant for Potable Water Generation. *Water Res.* **2014**, *52*, 218–230. <https://doi.org/10.1016/j.watres.2013.10.071>.
- (206) Zhang, Y.; Liu, W.-T. The Application of Molecular Tools to Study the Drinking Water Microbiome – Current Understanding and Future Needs. *Crit. Rev. Environ. Sci. Technol.* **2019**, *49* (13), 1188–1235. <https://doi.org/10.1080/10643389.2019.1571351>.
- (207) Douterelo, I.; Boxall, J. B.; Deines, P.; Sekar, R.; Fish, K. E.; Biggs, C. A. Methodological Approaches for Studying the Microbial Ecology of Drinking Water Distribution Systems. *Water Res.* **2014**, *65*, 134–156. <https://doi.org/10.1016/j.watres.2014.07.008>.
- (208) Douterelo, I.; Dutilh, B. E.; Calero, C.; Rosales, E.; Martin, K.; Husband, S. Impact of Phosphate Dosing on the Microbial Ecology of Drinking Water Distribution Systems: Fieldwork Studies in Chlorinated Networks. *Water Res.* **2020**, *187*, 116416. <https://doi.org/10.1016/j.watres.2020.116416>.
- (209) Jang, H.-J.; Choi, Y.-J.; Ro, H.-M.; Ka, J.-O. Effects of Phosphate Addition on Biofilm Bacterial Communities and Water Quality in Annular Reactors Equipped with Stainless Steel and Ductile Cast Iron Pipes. *J. Microbiol.* **2012**, *50* (1), 17–28. <https://doi.org/10.1007/s12275-012-1040-x>.
- (210) Del Olmo, G.; Ahmad, A.; Jensen, H.; Karunakaran, E.; Rosales, E.; Calero Preciado, C.; Gaskin, P.; Douterelo, I. Influence of Phosphate Dosing on Biofilms Development on Lead in Chlorinated Drinking Water Bioreactors. *NPJ Biofilms Microbiomes* **2020**, *6*. <https://doi.org/10.1038/s41522-020-00152-w>.
- (211) Rosales, E.; Del Olmo, G.; Calero Preciado, C.; Douterelo, I. Phosphate Dosing in Drinking Water Distribution Systems Promotes Changes in Biofilm Structure and Functional Genetic Diversity. *Front. Microbiol.* **2020**, *11*.
- (212) Wada, M.; Kawashima, A. Lower Serum Phosphate Levels in Patients with Legionella Pneumonia Relative to Patients with Non-Legionella Pneumonia. *J. Fam. Med. Prim. Care* **2021**, *10* (11), 4272–4276. https://doi.org/10.4103/jfmmpc.jfmmpc_728_21.
- (213) Jereb, G.; Eržen, I.; Oder, M.; Poljšak, B. Phosphate Drinking Water Softeners Promote Legionella Growth. *J. Water Health* **2022**, *20* (7), 1084–1090. <https://doi.org/10.2166/wh.2022.055>.

- (214) Song, Y.; Pruden, A.; Edwards, M. A.; Rhoads, W. J. Natural Organic Matter, Orthophosphate, pH, and Growth Phase Can Limit Copper Antimicrobial Efficacy for *Legionella* in Drinking Water. *Environ. Sci. Technol.* **2021**, *55* (3), 1759–1768. <https://doi.org/10.1021/acs.est.0c06804>.
- (215) Song, Y.; Pruden, A.; Rhoads, W. J.; Edwards, M. A. Pilot-Scale Assessment Reveals Effects of Anode Type and Orthophosphate in Governing Antimicrobial Capacity of Copper for *Legionella Pneumophila* Control. *Water Res.* **2023**, *242*, 120178. <https://doi.org/10.1016/j.watres.2023.120178>.
- (216) Kimbell, L. K.; LaMartina, E. L.; Kohls, S.; Wang, Y.; Newton, R. J.; McNamara, P. J. Impact of Corrosion Inhibitors on Antibiotic Resistance, Metal Resistance, and Microbial Communities in Drinking Water. *mSphere* **2023**, *8* (5), e00307-23. <https://doi.org/10.1128/msphere.00307-23>.
- (217) Zhu, J.; Liu, R.; Cao, N.; Yu, J.; Liu, X.; Yu, Z. Mycobacterial Metabolic Characteristics in a Water Meter Biofilm Revealed by Metagenomics and Metatranscriptomics. *Water Res.* **2019**, *153*, 315–323. <https://doi.org/10.1016/j.watres.2019.01.032>.
- (218) Garner, E.; McLain, J.; Bowers, J.; Engelthaler, D. M.; Edwards, M. A.; Pruden, A. Microbial Ecology and Water Chemistry Impact Regrowth of Opportunistic Pathogens in Full-Scale Reclaimed Water Distribution Systems. *Environ. Sci. Technol.* **2018**, *52* (16), 9056–9068. <https://doi.org/10.1021/acs.est.8b02818>.
- (219) Salgar-Chaparro, S. J.; Lepkova, K.; Pojtanabuntoeng, T.; Darwin, A.; Machuca, L. L. Nutrient Level Determines Biofilm Characteristics and Subsequent Impact on Microbial Corrosion and Biocide Effectiveness. *Appl. Environ. Microbiol.* **2020**, *86* (7), e02885-19. <https://doi.org/10.1128/AEM.02885-19>.
- (220) Fang, W.; Hu, J. y.; Ong, S. I. Influence of Phosphorus on Biofilm Formation in Model Drinking Water Distribution Systems. *J. Appl. Microbiol.* **2009**, *106* (4), 1328–1335. <https://doi.org/10.1111/j.1365-2672.2008.04099.x>.
- (221) ASPE. *Appendix D: Updating Value per Statistical Life (VSL) Estimates for Inflation and Changes in Real Income*. <https://aspe.hhs.gov/reports/updating-vsl-estimates> (accessed 2022-07-14).
- (222) Daley, C. R. PITTSBURGH WATER AND SEWER AUTHORITY COMPREHENSIVE DISTRIBUTION SYSTEM FLUORIDE TRACER STUDY, University of Pittsburgh, Pittsburgh, PA, 2007.

- (223)Haig, S.-J.; Kotlarz, N.; Kalikin, L. M.; Chen, T.; Guikema, S.; LiPuma, J. J.; Raskin, L. Emerging Investigator Series: Bacterial Opportunistic Pathogen Gene Markers in Municipal Drinking Water Are Associated with Distribution System and Household Plumbing Characteristics. *Environ. Sci. Water Res. Technol.* **2020**, *6* (11), 3032–3043. <https://doi.org/10.1039/D0EW00723D>.
- (224)Cleseri, L. S.; Greenberg, A. E.; Eaton, A. D. *Standard Methods for the Examination of Water and Wastewater*, 20th ed.; American Public Health Association, 2005.
- (225)Spencer-Williams, I.; Balangoda, A.; Dabundo, R.; Elliott, E.; Haig, S.-J. Exploring the Impacts of Full-Scale Distribution System Orthophosphate Corrosion Control Implementation on the Microbial Ecology of Hydrologically Connected Urban Streams. *Microbiol. Spectr.* **2022**, *10* (6), e02158-22. <https://doi.org/10.1128/spectrum.02158-22>.
- (226)Wullings, B. A.; Bakker, G.; van der Kooij, D. Concentration and Diversity of Uncultured Legionella Spp. in Two Unchlorinated Drinking Water Supplies with Different Concentrations of Natural Organic Matter. *Appl. Environ. Microbiol.* **2011**, *77* (2), 634–641. <https://doi.org/10.1128/AEM.01215-10>.
- (227)Feizabadi, M. M.; Majnooni, A.; Nomanpour, B.; Fatolahzadeh, B.; Raji, N.; Delfani, S.; Habibi, M.; Asadi, S.; Parvin, M. Direct Detection of Pseudomonas Aeruginosa from Patients with Healthcare Associated Pneumonia by Real Time PCR. *Infect. Genet. Evol.* **2010**, *10* (8), 1247–1251. <https://doi.org/10.1016/j.meegid.2010.08.008>.
- (228)Radomski, N.; Roguet, A.; Lucas, F. S.; Veyrier, F. J.; Cambau, E.; Accrombessi, H.; Moilleron, R.; Behr, M. A.; Moulin, L. atpE Gene as a New Useful Specific Molecular Target to Quantify Mycobacterium in Environmental Samples. *BMC Microbiol.* **2013**, *13*, 277. <https://doi.org/10.1186/1471-2180-13-277>.
- (229)Snapper, S. B.; Melton, R. E.; Mustafa, S.; Kieser, T.; Jacobs, W. R. Isolation and Characterization of Efficient Plasmid Transformation Mutants of Mycobacterium Smegmatis. *Mol. Microbiol.* **1990**, *4* (11), 1911–1919. <https://doi.org/10.1111/j.1365-2958.1990.tb02040.x>.
- (230)DePas, W. H.; Bergkessel, M.; Newman, D. K. Aggregation of Nontuberculous Mycobacteria Is Regulated by Carbon-Nitrogen Balance. *mBio* **2019**, *10* (4), e01715-19. <https://doi.org/10.1128/mBio.01715-19>.
- (231)Love, M. I.; Huber, W.; Anders, S. Moderated Estimation of Fold Change and Dispersion for RNA-Seq Data with DESeq2. *Genome Biol.* **2014**, *15* (12), 550. <https://doi.org/10.1186/s13059-014-0550-8>.

- (232)Pinto, A. J.; Schroeder, J.; Lunn, M.; Sloan, W.; Raskin, L. Spatial-Temporal Survey and Occupancy-Abundance Modeling To Predict Bacterial Community Dynamics in the Drinking Water Microbiome. *mBio* **2014**, *5* (3), e01135-14. <https://doi.org/10.1128/mBio.01135-14>.
- (233)Thom, C.; Smith, C. J.; Moore, G.; Weir, P.; Ijaz, U. Z. *Microbiome in Drinking Water Treatment and Distribution: A Critical Review and Meta-Analysis from Source to Tap*; 2021; p 2021.08.30.457654. <https://doi.org/10.1101/2021.08.30.457654>.
- (234)J. Ley, C.; R. Proctor, C.; Singh, G.; Ra, K.; Noh, Y.; Odimayomi, T.; Salehi, M.; Julien, R.; Mitchell, J.; Pouyan Nejadhashemi, A.; J. Whelton, A.; Gim Aw, T. Drinking Water Microbiology in a Water-Efficient Building: Stagnation, Seasonality, and Physicochemical Effects on Opportunistic Pathogen and Total Bacteria Proliferation. *Environ. Sci. Water Res. Technol.* **2020**, *6* (10), 2902–2913. <https://doi.org/10.1039/D0EW00334D>.
- (235)Zhang, C.; Qin, K.; Struewing, I.; Buse, H.; Santo Domingo, J.; Lytle, D.; Lu, J. The Bacterial Community Diversity of Bathroom Hot Tap Water Was Significantly Lower Than That of Cold Tap and Shower Water. *Front. Microbiol.* **2021**, *12*, 625324. <https://doi.org/10.3389/fmicb.2021.625324>.
- (236)Santos, Q. M. B. los; L. Schroeder, J.; C. Sevillano-Rivera, M.; Sungthong, R.; Z. Ijaz, U.; T. Sloan, W.; J. Pinto, A. Emerging Investigators Series: Microbial Communities in Full-Scale Drinking Water Distribution Systems – a Meta-Analysis. *Environ. Sci. Water Res. Technol.* **2016**, *2* (4), 631–644. <https://doi.org/10.1039/C6EW00030D>.
- (237)Van Assche, A.; Crauwels, S.; De Brabanter, J.; Willems, K. A.; Lievens, B. Characterization of the Bacterial Community Composition in Water of Drinking Water Production and Distribution Systems in Flanders, Belgium. *MicrobiologyOpen* **2018**, *8* (5), e00726. <https://doi.org/10.1002/mbo3.726>.
- (238)Dolman, A. M.; Rücker, J.; Pick, F. R.; Fastner, J.; Rohrlack, T.; Mischke, U.; Wiedner, C. Cyanobacteria and Cyanotoxins: The Influence of Nitrogen versus Phosphorus. *PLoS ONE* **2012**, *7* (6), e38757. <https://doi.org/10.1371/journal.pone.0038757>.
- (239)Ferretti, M. V.; Hussien, R. A.; Ballicora, M. A.; Iglesias, A. A.; Figueroa, C. M.; Asencion Diez, M. D. The ADP-Glucose Pyrophosphorylase from Melainabacteria: A Comparative Study between Photosynthetic and Non-Photosynthetic Bacterial Sources. *Biochimie* **2022**, *192*, 30–37. <https://doi.org/10.1016/j.biochi.2021.09.011>.
- (240)Wang, H.; Masters, S.; Edwards, M. A.; Falkinham, J. O.; Pruden, A. Effect of Disinfectant, Water Age, and Pipe Materials on Bacterial and Eukaryotic Community Structure in Drinking

Water Biofilm. *Environ. Sci. Technol.* **2014**, 48 (3), 1426–1435. <https://doi.org/10.1021/es402636u>.

- (241) Dai, Z.; Sevillano-Rivera, M. C.; Calus, S. T.; Bautista-de los Santos, Q. M.; Eren, A. M.; van der Wielen, P. W. J. J.; Ijaz, U. Z.; Pinto, A. J. Disinfection Exhibits Systematic Impacts on the Drinking Water Microbiome. *Microbiome* **2020**, 8 (1), 42. <https://doi.org/10.1186/s40168-020-00813-0>.
- (242) Waak, M. B.; Hozalski, R. M.; Hallé, C.; LaPara, T. M. Comparison of the Microbiomes of Two Drinking Water Distribution Systems—with and without Residual Chloramine Disinfection. *Microbiome* **2019**, 7 (1), 87. <https://doi.org/10.1186/s40168-019-0707-5>.
- (243) Rodríguez-Beltrán, J.; Sørum, V.; Toll-Riera, M.; de la Vega, C.; Peña-Miller, R.; San Millán, Á. Genetic Dominance Governs the Evolution and Spread of Mobile Genetic Elements in Bacteria. *Proc. Natl. Acad. Sci.* **2020**, 117 (27), 15755–15762. <https://doi.org/10.1073/pnas.2001240117>.
- (244) Inda-Díaz, J. S.; Lund, D.; Parras-Moltó, M.; Johnning, A.; Bengtsson-Palme, J.; Kristiansson, E. Latent Antibiotic Resistance Genes Are Abundant, Diverse, and Mobile in Human, Animal, and Environmental Microbiomes. *Microbiome* **2023**, 11 (1), 44. <https://doi.org/10.1186/s40168-023-01479-0>.
- (245) LeChevallier, M. W.; Shaw, N. J.; Smith, D. B. *Factors Limiting Microbial Growth in Distribution Systems: Full-Scale Experiments*; American Water Works Association, 1996.
- (246) Huang, C.; Clark, G. G.; Zaki, F. R.; Won, J.; Ning, R.; Boppart, S. A.; Elbanna, A. E.; Nguyen, T. H. Effects of Phosphate and Silicate on Stiffness and Viscoelasticity of Mature Biofilms Developed with Simulated Drinking Water. *Biofouling* **2023**, 39 (1), 36–46. <https://doi.org/10.1080/08927014.2023.2177538>.
- (247) Elanskaya, I. V.; Grivennikova, V. G.; Groshev, V. V.; Kuznetsova, G. V.; Semina, M. E.; Timofeev, K. N. Role of NAD(P)H:Quinone Oxidoreductase Encoded by drgA Gene in Reduction of Exogenous Quinones in Cyanobacterium *Synechocystis* Sp. PCC 6803 Cells. *Biochem. Biokhimiia* **2004**, 69 (2), 137–142. <https://doi.org/10.1023/b:biry.0000018943.21179.ba>.
- (248) Hossain, S.; Chow, C. W. K.; Cook, D.; Sawade, E.; Hewa, G. A. Review of Nitrification Monitoring and Control Strategies in Drinking Water System. *Int. J. Environ. Res. Public Health* **2022**, 19 (7), 4003. <https://doi.org/10.3390/ijerph19074003>.

- (249)Delafont, V.; Rodier, M.-H.; Maisonneuve, E.; Cateau, E. Vermamoeba Vermiformis: A Free-Living Amoeba of Interest. *Microb. Ecol.* **2018**, *76* (4), 991–1001. <https://doi.org/10.1007/s00248-018-1199-8>.
- (250)Buse, H. Y.; Ji, P.; Gomez-Alvarez, V.; Pruden, A.; Edwards, M. A.; Ashbolt, N. J. Effect of Temperature and Colonization of Legionella Pneumophila and Vermamoeba Vermiformis on Bacterial Community Composition of Copper Drinking Water Biofilms. *Microb. Biotechnol.* **2017**, *10* (4), 773–788. <https://doi.org/10.1111/1751-7915.12457>.
- (251)Buse, H. Y.; Ashbolt, N. J. Differential Growth of Legionella Pneumophila Strains within a Range of Amoebae at Various Temperatures Associated with In-premise Plumbing. *Lett. Appl. Microbiol.* **2011**, *53* (2), 217–224. <https://doi.org/10.1111/j.1472-765X.2011.03094.x>.
- (252)Boubekri, K.; Soumare, A.; Mardad, I.; Lyamlouli, K.; Hafidi, M.; Ouhdouch, Y.; Kouisni, L. The Screening of Potassium- and Phosphate-Solubilizing Actinobacteria and the Assessment of Their Ability to Promote Wheat Growth Parameters. *Microorganisms* **2021**, *9* (3), 470. <https://doi.org/10.3390/microorganisms9030470>.
- (253)Rofner, C.; Sommaruga, R.; Teresa Pérez, M. Phosphate and ATP Uptake by Lake Bacteria: Does Taxonomical Identity Matter? *Environ. Microbiol.* **2016**, *18* (12), 4782–4793. <https://doi.org/10.1111/1462-2920.13368>.
- (254)Dastager, S. G.; Damare, S. Marine Actinobacteria Showing Phosphate-Solubilizing Efficiency in Chora Island, Goa, India. *Curr. Microbiol.* **2013**, *66* (5), 421–427. <https://doi.org/10.1007/s00284-012-0288-z>.
- (255)Zhang, H.; Ma, M.; Huang, T.; Miao, Y.; Li, H.; Liu, K.; Yang, W.; Ma, B. Spatial and Temporal Dynamics of Actinobacteria in Drinking Water Reservoirs: Novel Insights into Abundance, Community Structure, and Co-Existence Model. *Sci. Total Environ.* **2022**, *814*, 152804. <https://doi.org/10.1016/j.scitotenv.2021.152804>.
- (256)Ghai, R.; Mizuno, C. M.; Picazo, A.; Camacho, A.; Rodriguez-Valera, F. Key Roles for Freshwater Actinobacteria Revealed by Deep Metagenomic Sequencing. *Mol. Ecol.* **2014**, *23* (24), 6073–6090. <https://doi.org/10.1111/mec.12985>.
- (257)Blanc, S. M.; Robinson, D.; Fahrenfeld, N. L. Potential for Nontuberculous Mycobacteria Proliferation in Natural and Engineered Water Systems Due to Climate Change: A Literature Review. *City Environ. Interact.* **2021**, *11*, 100070. <https://doi.org/10.1016/j.cacint.2021.100070>.

- (258) Falkinham, J. O.; Norton, C. D.; LeChevallier, M. W. Factors Influencing Numbers of Mycobacterium Avium, Mycobacterium Intracellulare, and Other Mycobacteria in Drinking Water Distribution Systems. *Appl. Environ. Microbiol.* **2001**, *67* (3), 1225–1231. <https://doi.org/10.1128/AEM.67.3.1225-1231.2001>.
- (259) Dowdell, K.; Haig, S.-J.; Caverly, L. J.; Shen, Y.; LiPuma, J. J.; Raskin, L. Nontuberculous Mycobacteria in Drinking Water Systems – the Challenges of Characterization and Risk Mitigation. *Curr. Opin. Biotechnol.* **2019**, *57*, 127–136. <https://doi.org/10.1016/j.copbio.2019.03.010>.
- (260) Wang, J.; Sui, M.; Yuan, B.; Li, H.; Lu, H. Inactivation of Two Mycobacteria by Free Chlorine: Effectiveness, Influencing Factors, and Mechanisms. *Sci. Total Environ.* **2019**, *648*, 271–284. <https://doi.org/10.1016/j.scitotenv.2018.07.451>.
- (261) Wang, H.; Masters, S.; Falkinham, J. O.; Edwards, M. A.; Pruden, A. Distribution System Water Quality Affects Responses of Opportunistic Pathogen Gene Markers in Household Water Heaters. *Environ. Sci. Technol.* **2015**, *49* (14), 8416–8424. <https://doi.org/10.1021/acs.est.5b01538>.
- (262) Revetta, R. P.; Gomez-Alvarez, V.; Gerke, T. L.; Santo Domingo, J. W.; Ashbolt, N. J. Changes in Bacterial Composition of Biofilm in a Metropolitan Drinking Water Distribution System. *J. Appl. Microbiol.* **2016**, *121* (1), 294–305. <https://doi.org/10.1111/jam.13150>.
- (263) Szwetkowski, K. J.; Falkinham, J. O. Methylobacterium Spp. as Emerging Opportunistic Premise Plumbing Pathogens. *Pathogens* **2020**, *9* (2), 149. <https://doi.org/10.3390/pathogens9020149>.
- (264) Muñoz Egea, M. C.; Ji, P.; Pruden, A.; Falkinham III, J. O. Inhibition of Adherence of Mycobacterium Avium to Plumbing Surface Biofilms of Methylobacterium Spp. *Pathogens* **2017**, *6* (3), 42. <https://doi.org/10.3390/pathogens6030042>.
- (265) Pradal, I.; Esteban, J.; Mediero, A.; García-Coca, M.; Aguilera-Correa, J. J. Contact Effect of a Methylobacterium Sp. Extract on Biofilm of a Mycobacterium Chimaera Strain Isolated from a 3T Heater-Cooler System. *Antibiotics* **2020**, *9* (8), 474. <https://doi.org/10.3390/antibiotics9080474>.
- (266) Faria, S.; Joao, I.; Jordao, L. General Overview on Nontuberculous Mycobacteria, Biofilms, and Human Infection. *J. Pathog.* **2015**, *2015*, 809014. <https://doi.org/10.1155/2015/809014>.

- (267)Martínez, L. C.; Vadyvaloo, V. Mechanisms of Post-Transcriptional Gene Regulation in Bacterial Biofilms. *Front. Cell. Infect. Microbiol.* **2014**, *4*, 38. <https://doi.org/10.3389/fcimb.2014.00038>.
- (268)Funari, R.; Shen, A. Q. Detection and Characterization of Bacterial Biofilms and Biofilm-Based Sensors. *ACS Sens.* **2022**, *7* (2), 347–357. <https://doi.org/10.1021/acssensors.1c02722>.
- (269)Fang, W.; Hu, J.; Ong, S. L. Effects of Phosphorus on Biofilm Disinfections in Model Drinking Water Distribution Systems. *J. Water Health* **2009**, *8* (3), 446–454. <https://doi.org/10.2166/wh.2009.303>.
- (270)Noh, J. H.; Yoo, S. H.; Son, H.; Fish, K. E.; Douterelo, I.; Maeng, S. K. Effects of Phosphate and Hydrogen Peroxide on the Performance of a Biological Activated Carbon Filter for Enhanced Biofiltration. *J. Hazard. Mater.* **2020**, 388, 121778. <https://doi.org/10.1016/j.jhazmat.2019.121778>.
- (271)Shen, Y.; Huang, P. C.; Huang, C.; Sun, P.; Monroy, G. L.; Wu, W.; Lin, J.; Espinosa-Marzal, R. M.; Boppart, S. A.; Liu, W.-T.; Nguyen, T. H. Effect of Divalent Ions and a Polyphosphate on Composition, Structure, and Stiffness of Simulated Drinking Water Biofilms. *Npj Biofilms Microbiomes* **2018**, *4* (1), 1–9. <https://doi.org/10.1038/s41522-018-0058-1>.
- (272)Clark, G. G.; Geisler, D.; Coey, E. J.; Pollitz, L. J.; Zaki, F. R.; Huang, C.; Boppart, S. A.; Nguyen, T. H. Influence of Phosphate on Bacterial Release from Activated Carbon Point-of-Use Filters and on Biofilm Characteristics. *Sci. Total Environ.* **2024**, 169932. <https://doi.org/10.1016/j.scitotenv.2024.169932>.
- (273)Torvinen, E.; Lehtola, M. J.; Martikainen, P. J.; Miettinen, I. T. Survival of Mycobacterium Avium in Drinking Water Biofilms as Affected by Water Flow Velocity, Availability of Phosphorus, and Temperature. *Appl. Environ. Microbiol.* **2007**, *73* (19), 6201–6207. <https://doi.org/10.1128/AEM.00828-07>.
- (274)Elguezabal, N.; Bastida, F.; Sevilla, I. A.; González, N.; Molina, E.; Garrido, J. M.; Juste, R. A. Estimation of Mycobacterium Avium Subsp. Paratuberculosis Growth Parameters: Strain Characterization and Comparison of Methods. *Appl. Environ. Microbiol.* **2011**, *77* (24), 8615–8624. <https://doi.org/10.1128/AEM.05818-11>.
- (275)Revetta, R. P.; Gomez-Alvarez, V.; Gerke, T. L.; Curioso, C.; Santo Domingo, J. W.; Ashbolt, N. J. Establishment and Early Succession of Bacterial Communities in Monochloramine-Treated Drinking Water Biofilms. *FEMS Microbiol. Ecol.* **2013**, *86* (3), 404–414. <https://doi.org/10.1111/1574-6941.12170>.

- (276)Hunt, S. M.; Werner, E. M.; Huang, B.; Hamilton, M. A.; Stewart, P. S. Hypothesis for the Role of Nutrient Starvation in Biofilm Detachment. *Appl. Environ. Microbiol.* **2004**, *70* (12), 7418–7425. <https://doi.org/10.1128/AEM.70.12.7418-7425.2004>.
- (277)Medicine, N. A. of S., Engineering, and; Studies, D. on E. and L.; Board, W. S. and T.; Affairs, P. and G.; Events, P. on R., Resilience, and Extreme; States, C. on U. F. in the U. *Framing the Challenge of Urban Flooding in the United States*; National Academies Press, 2019.
- (278)Rosenzweig, B. R.; McPhillips, L.; Chang, H.; Cheng, C.; Welty, C.; Matsler, M.; Iwaniec, D.; Davidson, C. I. Pluvial Flood Risk and Opportunities for Resilience. *WIREs Water* **2018**, *5* (6), e1302. <https://doi.org/10.1002/wat2.1302>.
- (279)Mailhot, A.; Talbot, G.; Lavallée, B. Relationships between Rainfall and Combined Sewer Overflow (CSO) Occurrences. *J. Hydrol.* **2015**, *523*, 602–609. <https://doi.org/10.1016/j.jhydrol.2015.01.063>.
- (280)Madoux-Humery, A.-S.; Dorner, S.; Sauvé, S.; Aboufadi, K.; Galarneau, M.; Servais, P.; Prévost, M. Temporal Variability of Combined Sewer Overflow Contaminants: Evaluation of Wastewater Micropollutants as Tracers of Fecal Contamination. *Water Res.* **2013**, *47* (13), 4370–4382. <https://doi.org/10.1016/j.watres.2013.04.030>.
- (281)Sampson, N. R.; Price, C. E.; Kassem, J.; Doan, J.; Hussein, J. “We’re Just Sitting Ducks”: Recurrent Household Flooding as An Underreported Environmental Health Threat in Detroit’s Changing Climate. *Int. J. Environ. Res. Public. Health* **2019**, *16* (1), 6. <https://doi.org/10.3390/ijerph16010006>.
- (282)Fischbach, J. R.; Siler-Evans, K.; Tierney, D.; Wilson, M. T.; Cook, L. M.; Warren May, L. Robust Stormwater Management in the Pittsburgh Region: A Pilot Study. **2017**.
- (283)Ford, A.; Mizikar, R.; Mulholland, T.; Sayles, M.; Bowers, R.; Kramer, L. Grounded Strategies 6587 Hamilton Ave Pittsburgh, PA 15206 Groundedpgh.Org. 109.
- (284)Fletcher, S. M.; McLaws, M.-L.; Ellis, J. T. Prevalence of Gastrointestinal Pathogens in Developed and Developing Countries: Systematic Review and Meta-Analysis. *J. Public Health Res.* **2013**, *2* (1), e9–e9. <https://doi.org/10.4081/jphr.2013.e9>.
- (285)Hall, A. J.; Rosenthal, M.; Gregoricus, N.; Greene, S. A.; Ferguson, J.; Henao, O. L.; Vinjé, J.; Lopman, B. A.; Parashar, U. D.; Widdowson, M.-A. Incidence of Acute Gastroenteritis

and Role of Norovirus, Georgia, USA, 2004–2005 - Volume 17, Number 8—August 2011 - Emerging Infectious Diseases Journal - CDC. <https://doi.org/10.3201/eid1708.101533>.

- (286)de Man, H.; van den Berg, H. H. J. L.; Leenen, E. J. T. M.; Schijven, J. F.; Schets, F. M.; van der Vliet, J. C.; van Knapen, F.; de Roda Husman, A. M. Quantitative Assessment of Infection Risk from Exposure to Waterborne Pathogens in Urban Floodwater. *Water Res.* **2014**, *48*, 90–99. <https://doi.org/10.1016/j.watres.2013.09.022>.
- (287)Katukiza, A. y.; Ronteltap, M.; van der Steen, P.; Foppen, J. w. a.; Lens, P. n. l. Quantification of Microbial Risks to Human Health Caused by Waterborne Viruses and Bacteria in an Urban Slum. *J. Appl. Microbiol.* **2014**, *116* (2), 447–463. <https://doi.org/10.1111/jam.12368>.
- (288)Mark, O.; Jørgensen, C.; Hammond, M.; Khan, D.; Tjener, R.; Erichsen, A.; Helwich, B. A New Methodology for Modelling of Health Risk from Urban Flooding Exemplified by Cholera: Case Dhaka, Bangladesh. *J. Flood Risk Manag.* **2018**, *11* (51), S28–S42. <https://doi.org/10.1111/jfr3.12182>.
- (289)Andersen, S. T.; Mark, O.; Albrechtsen, H.-J. Quantitative Microbial Risk Assessment of the Impacts of Flooded Basements in Urban Areas by Combining Quantitative Microbial Data with Hydrological Software. **2014**, *8*.
- (290)Lin, C. J.; Wade, T. J.; Hilborn, E. D. Flooding and Clostridium Difficile Infection: A Case-Crossover Analysis. *Int. J. Environ. Res. Public Health* **2015**, *12* (6), 6948–6964. <https://doi.org/10.3390/ijerph120606948>.
- (291)Wade, T. J.; Lin, C. J.; Jagai, J. S.; Hilborn, E. D. Flooding and Emergency Room Visits for Gastrointestinal Illness in Massachusetts: A Case-Crossover Study. *PLOS ONE* **2014**, *9* (10), e110474. <https://doi.org/10.1371/journal.pone.0110474>.
- (292)Mulder, A. C.; Pijnacker, R.; de Man, H.; van de Kasstele, J.; van Pelt, W.; Mughini-Gras, L.; Franz, E. “Sickenin’ in the Rain” – Increased Risk of Gastrointestinal and Respiratory Infections after Urban Pluvial Flooding in a Population-Based Cross-Sectional Study in the Netherlands. *BMC Infect. Dis.* **2019**, *19*, 377. <https://doi.org/10.1186/s12879-019-3984-5>.
- (293)Wang, P.; Asare, E. O.; Pitzer, V. E.; Dubrow, R.; Chen, K. Floods and Diarrhea Risk in Young Children in Low- and Middle-Income Countries. *JAMA Pediatr.* **2023**, *177* (11), 1206–1214. <https://doi.org/10.1001/jamapediatrics.2023.3964>.
- (294)Luo, P.; Chen, M.; Kuang, W.; Ni, H.; Zhao, J.; Dai, H.; Ren, X.; Yi, S.; Hong, X.; Zha, W.; Lv, Y. Hysteresis Effects of Different Levels of Storm Flooding on Susceptible Enteric

Infectious Diseases in a Central City of China. *BMC Public Health* **2023**, *23* (1), 1874. <https://doi.org/10.1186/s12889-023-16754-w>.

- (295)Liu, Q.; Yuan, J.; Yan, W.; Liang, W.; Liu, M.; Liu, J. Association of Natural Flood Disasters with Infectious Diseases in 168 Countries and Territories from 1990 to 2019: A Worldwide Observational Study. *Glob. Transit.* **2023**, *5*, 149–159. <https://doi.org/10.1016/j.glt.2023.09.001>.
- (296)Mao, Y.; Zeineldin, M.; Usmani, M.; Uprety, S.; Shisler, J. L.; Jutla, A.; Unnikrishnan, A.; Nguyen, T. H. Distribution and Antibiotic Resistance Profiles of Salmonella Enterica in Rural Areas of North Carolina After Hurricane Florence in 2018. *GeoHealth* **2021**, *5* (2), e2020GH000294. <https://doi.org/10.1029/2020GH000294>.
- (297)Van Bijnen, M.; Korving, H.; Langeveld, J.; Clemens, F. Quantitative Impact Assessment of Sewer Condition on Health Risk. *Water* **2018**, *10* (3), 245. <https://doi.org/10.3390/w10030245>.
- (298)Addison-Atkinson, W.; Chen, A. S.; Memon, F. A.; Chang, T.-J. Modelling Urban Sewer Flooding and Quantitative Microbial Risk Assessment: A Critical Review. *J. Flood Risk Manag.* **2022**, *15* (4), e12844. <https://doi.org/10.1111/jfr3.12844>.
- (299)Angenent, L. T.; Kelley, S. T.; St Amand, A.; Pace, N. R.; Hernandez, M. T. Molecular Identification of Potential Pathogens in Water and Air of a Hospital Therapy Pool. *Proc. Natl. Acad. Sci. U. S. A.* **2005**, *102* (13), 4860–4865. <https://doi.org/10.1073/pnas.0501235102>.
- (300)Falkinham, J. O.; Hilborn, E. D.; Arduino, M. J.; Pruden, A.; Edwards, M. A. Epidemiology and Ecology of Opportunistic Premise Plumbing Pathogens: Legionella Pneumophila, Mycobacterium Avium, and Pseudomonas Aeruginosa. *Environ. Health Perspect.* **2015**, *123* (8), 749–758. <https://doi.org/10.1289/ehp.1408692>.
- (301)Alarcon Falconi, T. M.; Cruz, M. S.; Naumova, E. N. The Shift in Seasonality of Legionellosis in the USA. *Epidemiol. Infect.* **2018**, *146* (14), 1824–1833. <https://doi.org/10.1017/S0950268818002182>.
- (302)Gleason, J. A.; Kratz, N. R.; Greeley, R. D.; Fagliano, J. A. Under the Weather: Legionellosis and Meteorological Factors. *EcoHealth* **2016**, *13* (2), 293–302. <https://doi.org/10.1007/s10393-016-1115-y>.
- (303)Halsby, K. D.; Joseph, C. A.; Lee, J. V.; Wilkinson, P. The Relationship between Meteorological Variables and Sporadic Cases of Legionnaires' Disease in Residents of

- England and Wales. *Epidemiol. Infect.* **2014**, *142* (11), 2352–2359. <https://doi.org/10.1017/S0950268813003294>.
- (304)Hale, R. L.; Flint, C. G.; Jackson-Smith, D.; Endter-Wada, J. Social Dimensions of Urban Flood Experience, Exposure, and Concern. *JAWRA J. Am. Water Resour. Assoc.* **2018**, *54* (5), 1137–1150. <https://doi.org/10.1111/1752-1688.12676>.
- (305)Hossain, M. K.; Meng, Q. A Multi-Decadal Spatial Analysis of Demographic Vulnerability to Urban Flood: A Case Study of Birmingham City, USA. *Sustainability* **2020**, *12* (21), 9139. <https://doi.org/10.3390/su12219139>.
- (306)Pitell, S.; Haig, S.-J. A Breath of Fresh Air: Assessing Anti-Microbial Showerheads for the Reduction of Aerosolized Opportunistic Pathogen Exposure In Preparation. *Prep.* **2024**.
- (307)Rockey, N.; Young, S.; Kohn, T.; Pecson, B.; Wobus, C. E.; Raskin, L.; Wigginton, K. R. UV Disinfection of Human Norovirus: Evaluating Infectivity Using a Genome-Wide PCR-Based Approach. *Environ. Sci. Technol.* **2020**, *54* (5), 2851–2858. <https://doi.org/10.1021/acs.est.9b05747>.
- (308)Ahmed, W.; Vieritz, A.; Goonetilleke, A.; Gardner, T. Health Risk from the Use of Roof-Harvested Rainwater in Southeast Queensland, Australia, as Potable or Nonpotable Water, Determined Using Quantitative Microbial Risk Assessment. *Appl. Environ. Microbiol.* **2010**, *76* (22), 7382–7391. <https://doi.org/10.1128/AEM.00944-10>.
- (309)Liang, L.; Goh, S. G.; Vergara, G. G. R. V.; Fang, H. M.; Rezaeinejad, S.; Chang, S. Y.; Bayen, S.; Lee, W. A.; Sobsey, M. D.; Rose, J. B.; Gin, K. Y. H. Alternative Fecal Indicators and Their Empirical Relationships with Enteric Viruses, Salmonella Enterica, and Pseudomonas Aeruginosa in Surface Waters of a Tropical Urban Catchment. *Appl. Environ. Microbiol.* **2015**, *81* (3), 850–860. <https://doi.org/10.1128/AEM.02670-14>.
- (310)Lodder, W. J.; Husman, A. M. de R. Presence of Noroviruses and Other Enteric Viruses in Sewage and Surface Waters in The Netherlands. *Appl. Environ. Microbiol.* **2005**, *71* (3), 1453–1461. <https://doi.org/10.1128/AEM.71.3.1453-1461.2005>.
- (311)Pitell, S.; Haig, S.-J. Assessing the Impact of Anti-Microbial Showerheads on the Prevalence and Abundance of Opportunistic Pathogens in Shower Water and Shower Water-Associated Aerosols. *Front. Microbiomes* **2023**, *2*.
- (312)U.S. Bureau of Labor Statistics. *American Time Use Survey 2022*; Table A-1. Time spent in detailed primary activities and percent of the civilian population engaging in each activity,

averages per day by sex, 2022 annual averages; Data Tables; United States Department of Labor; p 4.

- (313)Exposure Factors Handbook - Chapter 6: Inhalation Rates. **2011**.
- (314)Chang, C.-W.; Lin, M.-H. Optimization of PMA-qPCR for Staphylococcus Aureus and Determination of Viable Bacteria in Indoor Air. *Indoor Air* **2018**, 28 (1), 64–72. <https://doi.org/10.1111/ina.12404>.
- (315)Campbell, L.; Cheng, H.; Svendsen, E.; Kochnowier, D.; Bunting-Howarth, K.; Wapnitsky, P. Living with Water: Documenting Lived Experience and Social-Emotional Impacts of Chronic Flooding for Local Adaptation Planning. *Cities Environ. CATE* **2021**, 14 (1). <https://doi.org/10.15365/cate.2021.140104>.
- (316)Silva, S. Down Then Out: Basement Apartments and Housing Insecurity in the Face of Flood Risks. Thesis, Massachusetts Institute of Technology, 2022. <https://dspace.mit.edu/handle/1721.1/145169> (accessed 2024-02-07).
- (317)Panizzi, T. *Quarter-inch of rain breaks 3-week dry spell; more coming*. TribLIVE.com. <https://triblive.com/local/regional/quarter-inch-of-rain-breaks-3-week-dry-spell-more-coming/> (accessed 2024-02-06).
- (318)Klepeis, N. E.; Nelson, W. C.; Ott, W. R.; Robinson, J. P.; Tsang, A. M.; Switzer, P.; Behar, J. V.; Hern, S. C.; Engelmann, W. H. The National Human Activity Pattern Survey (NHAPS): A Resource for Assessing Exposure to Environmental Pollutants. *J. Expo. Sci. Environ. Epidemiol.* **2001**, 11 (3), 231–252. <https://doi.org/10.1038/sj.jea.7500165>.
- (319)Wallace, L. *Document Display | NEPIS | US EPA*. EPA National Service Center for Environmental Publications. <https://nepis.epa.gov/Exe/ZyNET.exe/2000UC5T.TXT?ZyActionD=ZyDocument&Client=EPA&Index=1986+Thru+1990&Docs=&Query=&Time=&EndTime=&SearchMethod=1&TocRestrict=n&Toc=&TocEntry=&QField=&QFieldYear=&QFieldMonth=&QFieldDay=&IntQFieldOp=0&ExtQFieldOp=0&XmlQuery=&File=D%3A%5Czyfiles%5CIndex%20Data%5C86thru90%5CTxt%5C00000013%5C2000UC5T.txt&User=ANONYMOUS&Password=anonymous&SortMethod=h%7C-&MaximumDocuments=1&FuzzyDegree=0&ImageQuality=r75g8/r75g8/x150y150g16/i425&Display=hpfr&DefSeekPage=x&SearchBack=ZyActionL&Back=ZyActionS&BackDesc=Results%20page&MaximumPages=1&ZyEntry=1&SeekPage=x&ZyPURL> (accessed 2023-10-05).

- (320)Marć, M.; Śmiełowska, M.; Namieśnik, J.; Zabiegała, B. Indoor Air Quality of Everyday Use Spaces Dedicated to Specific Purposes-a Review. *Environ. Sci. Pollut. Res. Int.* **2018**, *25* (3), 2065–2082. <https://doi.org/10.1007/s11356-017-0839-8>.
- (321)Du, L.; Batterman, S.; Godwin, C.; Rowe, Z.; Chin, J.-Y. Air Exchange Rates and Migration of VOCs in Basements and Residences. *Indoor Air* **2015**, *25* (6), 598–609. <https://doi.org/10.1111/ina.12178>.
- (322)Francisco, P. W.; Jacobs, D. E.; Targos, L.; Dixon, S. L.; Breyse, J.; Rose, W.; Cali, S. Ventilation, Indoor Air Quality, and Health in Homes Undergoing Weatherization. *Indoor Air* **2017**, *27* (2), 463–477. <https://doi.org/10.1111/ina.12325>.
- (323)Holme, J. A.; Øya, E.; Afanou, A. K. J.; Øvrevik, J.; Eduard, W. Characterization and Pro-Inflammatory Potential of Indoor Mold Particles. *Indoor Air* **2020**, *30* (4), 662–681. <https://doi.org/10.1111/ina.12656>.
- (324)Baeza_Romero, M. T.; Dudzinska, M. R.; Amouei Torkmahalleh, M.; Barros, N.; Coggins, A. M.; Ruzgar, D. G.; Kildsgaard, I.; Naseri, M.; Rong, L.; Saffell, J.; Scutaru, A. M.; Staszowska, A. A Review of Critical Residential Buildings Parameters and Activities When Investigating Indoor Air Quality and Pollutants. *Indoor Air* **2022**, *32* (11), e13144. <https://doi.org/10.1111/ina.13144>.
- (325)Xing, Y.-F.; Xu, Y.-H.; Shi, M.-H.; Lian, Y.-X. The Impact of PM_{2.5} on the Human Respiratory System. *J. Thorac. Dis.* **2016**, *8* (1), E69–E74. <https://doi.org/10.3978/j.issn.2072-1439.2016.01.19>.
- (326)Yang, S.; Fang, D.; Chen, B. Human Health Impact and Economic Effect for PM_{2.5} Exposure in Typical Cities. *Appl. Energy* **2019**, *249*, 316–325. <https://doi.org/10.1016/j.apenergy.2019.04.173>.
- (327)Aquilina, N. J.; Camilleri, S. F. Impact of Daily Household Activities on Indoor PM_{2.5} and Black Carbon Concentrations in Malta. *Build. Environ.* **2022**, *207*, 108422. <https://doi.org/10.1016/j.buildenv.2021.108422>.
- (328)Chu, M. T.; Gillooly, S. E.; Levy, J. I.; Vallarino, J.; Reyna, L. N.; Cedeño Laurent, J. G.; Coull, B. A.; Adamkiewicz, G. Real-Time Indoor PM_{2.5} Monitoring in an Urban Cohort: Implications for Exposure Disparities and Source Control. *Environ. Res.* **2021**, *193*, 110561. <https://doi.org/10.1016/j.envres.2020.110561>.

- (329)Ngoc, L. T. N.; Park, D.; Lee, Y.-C. Human Health Impacts of Residential Radon Exposure: Updated Systematic Review and Meta-Analysis of Case–Control Studies. *Int. J. Environ. Res. Public Health* **2023**, *20* (1), 97. <https://doi.org/10.3390/ijerph20010097>.
- (330)Nunes, L. J. R.; Curado, A.; Graça, L. C. C. da; Soares, S.; Lopes, S. I. Impacts of Indoor Radon on Health: A Comprehensive Review on Causes, Assessment and Remediation Strategies. *Int. J. Environ. Res. Public Health* **2022**, *19* (7), 3929. <https://doi.org/10.3390/ijerph19073929>.
- (331)Yarmoshenko, I. V.; Onishchenko, A. D.; Malinovsky, G. P.; Vasilyev, A. V.; Zhukovsky, M. V. MODELING and Justification of Indoor Radon Prevention and Remediation Measures in Multi-Storey Apartment Buildings. *Results Eng.* **2022**, *16*, 100754. <https://doi.org/10.1016/j.rineng.2022.100754>.
- (332)Du, C.; Li, B.; Yu, W. Indoor Mould Exposure: Characteristics, Influences and Corresponding Associations with Built Environment—A Review. *J. Build. Eng.* **2021**, *35*, 101983. <https://doi.org/10.1016/j.jobe.2020.101983>.
- (333)Hughes, K. M.; Price, D.; Torriero, A. A. J.; Symonds, M. R. E.; Suphioglu, C. Impact of Fungal Spores on Asthma Prevalence and Hospitalization. *Int. J. Mol. Sci.* **2022**, *23* (8), 4313. <https://doi.org/10.3390/ijms23084313>.
- (334)Vardoulakis, S.; Giagloglou, E.; Steinle, S.; Davis, A.; Smeuwenhoek, A.; Galea, K. S.; Dixon, K.; Crawford, J. O. Indoor Exposure to Selected Air Pollutants in the Home Environment: A Systematic Review. *Int. J. Environ. Res. Public Health* **2020**, *17* (23), 8972. <https://doi.org/10.3390/ijerph17238972>.
- (335)Ruml, D.; Clarkin, D. Characteristic Analysis of Flipped Homes in Upper Arlington, Ohio: Average Square Footage, Duration and Year Built.
- (336)Garcia, J. *Home Renovation Facts and Statistics (2024)*. Architectural Digest. <https://www.architecturaldigest.com/reviews/home-improvement/home-renovation-facts-statistics> (accessed 2024-02-15).
- (337)Capolongo, S.; Rebecchi, A.; Buffoli, M.; Appolloni, L.; Signorelli, C.; Fara, G. M.; D'Alessandro, D. COVID-19 and Cities: From Urban Health Strategies to the Pandemic Challenge. A Decalogue of Public Health Opportunities. *Acta Bio Medica Atenei Parm.* **2020**, *91* (2), 13–22. <https://doi.org/10.23750/abm.v91i2.9515>.

- (338)D'Alessandro, D.; Gola, M.; Appolloni, L.; Dettori, M.; Fara, G. M.; Rebecchi, A.; Settimo, G.; Capolongo, S. COVID-19 and Living Space Challenge. Well-Being and Public Health Recommendations for a Healthy, Safe, and Sustainable Housing. *Acta Bio-Medica Atenei Parm.* **2020**, *91* (9-S), 61–75. <https://doi.org/10.23750/abm.v91i9-S.10115>.
- (339)D'Alessandro, D.; Rebecchi, A.; Appolloni, L.; Brambilla, A.; Brusaferrero, S.; Buffoli, M.; Carta, M.; Casuccio, A.; Coppola, L.; Corazza, M. V.; D'Elia, R.; Dell'Ovo, M.; Dettori, M.; Fara, G. M.; Ferrante, M.; Giammanco, G.; Gola, M.; Gori, D.; Lauria, A.; Mosca, E. I.; Nagyova, I.; Raffo, M.; Signorelli, C.; Spinato, C.; Sun, T.; Vitale, F.; Capolongo, S.; on behalf of the Attendees of the LVII Course "Re-Think Cities and Living Spaces for Public Health Purposes, according with the C.-19 L. of the S. of E. and P. M. "Giuseppe D. Re-Thinking the Environment, Cities, and Living Spaces for Public Health Purposes, According with the COVID-19 Lesson: The LVII Erice Charter. *Land* **2023**, *12* (10), 1863. <https://doi.org/10.3390/land12101863>.
- (340)Turk, B.; Hughes, J. *Movement and Sources of Basement Ventilation Air and Moisture During ASD Radon Control*; Contractor Report; 2009. https://www.epa.gov/sites/default/files/2014-08/documents/moisturestudy_analysis.pdf (accessed 2024-02-12).
- (341)Bekö, G.; Gustavsen, S.; Frederiksen, M.; Bergsøe, N. C.; Kolarik, B.; Gunnarsen, L.; Toftum, J.; Clausen, G. Diurnal and Seasonal Variation in Air Exchange Rates and Interzonal Airflows Measured by Active and Passive Tracer Gas in Homes. *Build. Environ.* **2016**, *104*, 178–187. <https://doi.org/10.1016/j.buildenv.2016.05.016>.
- (342)Muroni, A.; Gaetani, I.; Hoes, P.-J.; Hensen, J. L. M. Occupant Behavior in Identical Residential Buildings: A Case Study for Occupancy Profiles Extraction and Application to Building Performance Simulation. *Build. Simul.* **2019**, *12* (6), 1047–1061. <https://doi.org/10.1007/s12273-019-0573-x>.
- (343)Huang, L.; Fantke, P.; Ritscher, A.; Jolliet, O. Chemicals of Concern in Building Materials: A High-Throughput Screening. *J. Hazard. Mater.* **2022**, *424*, 127574. <https://doi.org/10.1016/j.jhazmat.2021.127574>.
- (344)Weschler, C. J. Changes in Indoor Pollutants since the 1950s. *Atmos. Environ.* **2009**, *43* (1), 153–169. <https://doi.org/10.1016/j.atmosenv.2008.09.044>.
- (345)Deborah N Barbeau; Barbeau, D. N.; L. Faye Grimsley; Grimsley, L. F.; Grimsley, L. F.; LuAnn White; White, L. E.; LuAnn White; J.M. El-Dahr; El-Dahr, J. M.; Maureen Y. Lichtveld; Lichtveld, M. Y. Mold Exposure and Health Effects Following Hurricanes Katrina

and Rita. *Annu. Rev. Public Health* **2010**, *31* (1), 165–178. <https://doi.org/10.1146/annurev.publhealth.012809.103643>.

- (346)Gina Solomon; Solomon, G.; Mervi Hjelmroos-Koski; Hjelmroos-Koski, M. K.; Miriam Rotkin-Ellman; Rotkin-Ellman, M.; S. Katharine Hammond; Hammond, S. K. Airborne Mold and Endotoxin Concentrations in New Orleans, Louisiana, after Flooding, October through November 2005. *Environ. Health Perspect.* **2006**, *114* (9), 1381–1386. <https://doi.org/10.1289/ehp.9198>.
- (347)Margaret A. Riggs; Riggs, M. A.; Carol Y. Rao; Rao, C. Y.; Clive Brown; Brown, C.; David Van Sickle; Van Sickle, D.; Kristin J. Cummings; Cummings, K. J.; Dunn, K. M.; Kevin H. Dunn; Dunn, K. H.; James A. Deddens; Deddens, J. A.; Jill Ferdinands; Ferdinands, J. M.; David B. Callahan; Callahan, D.; Ronald L. Moolenaar; Moolenaar, R. L.; Lynne E. Pinkerton; Pinkerton, L. E. Resident Cleanup Activities, Characteristics of Flood-Damaged Homes and Airborne Microbial Concentrations in New Orleans, Louisiana, October 2005. *Environ. Res.* **2008**, *106* (3), 401–409. <https://doi.org/10.1016/j.envres.2007.11.004>.
- (348)Carol Y. Rao; Rao, C. Y.; Changa Kurukularatne; Kurukularatne, C.; Julia Garcia-Diaz; Garcia-Diaz, J.; Sandra A. Kemmerly; Kemmerly, S. A.; Deoine Reed; Reed, D.; Scott K. Fridkin; Fridkin, S. K.; Juliette Morgan; Morgan, J. Implications of Detecting the Mold *Syncephalastrum* in Clinical Specimens of New Orleans Residents after Hurricanes Katrina and Rita. *J. Occup. Environ. Med.* **2007**, *49* (4), 411–416. <https://doi.org/10.1097/jom.0b013e31803b94f9>.
- (349)Erica Bloom; Bloom, E.; L. Faye Grimsley; Grimsley, L. F.; Christina Pehrson; Pehrson, C.; John L. Lewis; Lewis, J.; Lennart Larsson; Larsson, L. Molds and Mycotoxins in Dust from Water-Damaged Homes in New Orleans after Hurricane Katrina. *Indoor Air* **2009**, *19* (2), 153–158. <https://doi.org/10.1111/j.1600-0668.2008.00574.x>.
- (350)Emerson, J. B.; Keady, P. B.; Brewer, T. E.; Clements, N.; Morgan, E. E.; Awerbuch, J.; Miller, S. L.; Fierer, N. Impacts of Flood Damage on Airborne Bacteria and Fungi in Homes after the 2013 Colorado Front Range Flood. *Environ. Sci. Technol.* **2015**, *49* (5), 2675–2684. <https://doi.org/10.1021/es503845j>.
- (351)Daniela Jakšić; Jakšić, D.; Miranda Sertić; Sertić, M.; Sándor Kocsubé; Kocsubé, S.; Ivana Kovačević; Kovačević, I.; Domagoj Kifer; Kifer, D.; Ana Mornar; Mornar, A.; Biljana Nigović; Nigović, B.; Maja Šegvić Klarić; Klarić, M. Š. Post-Flood Impacts on Occurrence and Distribution of Mycotoxin-Producing Aspergilli from the Sections *Circumdati*, *Flavi*, and *Nigri* in Indoor Environment. *J. Fungi* **2020**, *6* (4), 282. <https://doi.org/10.3390/jof6040282>.

- (352)Lorraine N. Vélez-Torres; Lorraine N. Vélez-Torres; Bolaños-Rosero, B.; Benjamín Bolaños-Rosero; Filipa Godoy-Vitorino; Filipa Godoy-Vitorino; Rivera-Mariani, F. E.; Félix E. Rivera-Mariani; Juan P. Maestre; Juan P. Maestre; Kerry Kinney; Kerry A. Kinney; Humberto Cavallin; Humberto Cavallín. Hurricane María Drives Increased Indoor Proliferation of Filamentous Fungi in San Juan, Puerto Rico: A Two-Year Culture-Based Approach. *PeerJ* **2022**, *10*, e12730–e12730. <https://doi.org/10.7717/peerj.12730>.
- (353)US EPA, O. *What is EPA's Action Level for Radon and What Does it Mean?* <https://www.epa.gov/radon/what-epas-action-level-radon-and-what-does-it-mean> (accessed 2024-01-24).
- (354)Organization, W. H. *WHO Handbook on Indoor Radon: A Public Health Perspective*; World Health Organization, 2009.
- (355)Chao, C. Y. H.; Tung, T. C. W.; Chan, D. W. T.; Burnett, J. Determination of Radon Emanation and Back Diffusion Characteristics of Building Materials in Small Chamber Tests. *Build. Environ.* **1997**, *32* (4), 355–362. [https://doi.org/10.1016/S0360-1323\(96\)00071-6](https://doi.org/10.1016/S0360-1323(96)00071-6).
- (356)Li, L.; Stern, R. A.; Blomberg, A. J.; Kang, C.-M.; Wei, Y.; Liu, M.; Peralta, A. A.; Lawrence, J.; Vieira, C. L. Z.; Koutrakis, P. Ratios between Radon Concentrations in Upstairs and Basements: A Study in the Northeastern and Midwestern United States. *Environ. Sci. Technol. Lett.* **2022**, *9* (2), 191–197. <https://doi.org/10.1021/acs.estlett.1c00989>.
- (357)Bureau, U. C. *CHARS - Current Data*. <https://www.census.gov/construction/chars/current.html> (accessed 2023-10-31).
- (358)Bureau, U. C. *SOC - About the Survey*. <https://www.census.gov/construction/soc/about.html> (accessed 2024-01-31).
- (359)Militello-Hourigan, R. E.; Miller, S. L. The Impacts of Cooking and an Assessment of Indoor Air Quality in Colorado Passive and Tightly Constructed Homes. *Build. Environ.* **2018**, *144*, 573–582. <https://doi.org/10.1016/j.buildenv.2018.08.044>.
- (360)MI, B.; undefined. Assessment of the Health Impacts of Particulate Matter Characteristics. *Res. Rep. Health Eff. Inst.* **2012**, No. 161, 5–38.
- (361)Norbäck, D.; Cai, G.-H. Microbial Agents in the Indoor Environment: Associations with Health. In *Indoor Environmental Quality and Health Risk toward Healthier Environment for All*; Kishi, R., Norbäck, D., Araki, A., Eds.; Current Topics in Environmental Health and

- Preventive Medicine; Springer: Singapore, 2020; pp 179–198. https://doi.org/10.1007/978-981-32-9182-9_9.
- (362)Dols, W. S.; Polidoro, B. J. *CONTAM User Guide and Program Documentation Version 3.4*; National Institute of Standards and Technology, 2020. <https://doi.org/10.6028/NIST.TN.1887r1>.
- (363)*CHAPTER 3 BUILDING PLANNING, 2015 International Residential Code (IRC) | ICC Digital Codes.* https://codes.iccsafe.org/content/IRC2015P3/chapter-3-building-planning#IRC2015P3_Pt03_Ch03_SecR304 (accessed 2024-01-31).
- (364)*Standard Size of Rooms in Residential Building and their Locations.* The Constructor. <https://theconstructor.org/building/size-room-location-building/13269/> (accessed 2024-02-15).
- (365)American National Standards Institute; American Society of Heating, Refrigerating, and Air-Conditioning Engineers. ANSI/ASHRAE Standard 62.1-2022: Ventilation and Acceptable Indoor Air Quality, 2022.
- (366)US EPA, O. *Particulate Matter (PM_{2.5}) Trends.* <https://www.epa.gov/air-trends/particulate-matter-pm25-trends> (accessed 2024-01-24).
- (367)Reponen, T.; Singh, U.; Schaffer, C.; Vesper, S.; Johansson, E.; Adhikari, A.; Grinshpun, S. A.; Indugula, R.; Ryan, P.; Levin, L.; LeMasters, G. Visually Observed Mold and Moldy Odor versus Quantitatively Measured Microbial Exposure in Homes. *Sci. Total Environ.* **2010**, 408 (22), 5565–5574. <https://doi.org/10.1016/j.scitotenv.2010.07.090>.
- (368)Haas, D.; Ilieva, M.; Fritz, T.; Galler, H.; Habib, J.; Kriso, A.; Kropsch, M.; Ofner-Kopeinig, P.; Reinthaler, F. F.; Strasser, A.; Zentner, E.; Schalli, M. Background Concentrations of Airborne, Culturable Fungi and Dust Particles in Urban, Rural and Mountain Regions. *Sci. Total Environ.* **2023**, 892, 164700. <https://doi.org/10.1016/j.scitotenv.2023.164700>.
- (369)Sesartic, A.; Lohmann, U.; Storelvmo, T. Modelling the Impact of Fungal Spore Ice Nuclei on Clouds and Precipitation. *Environ. Res. Lett.* **2013**, 8 (1), 014029. <https://doi.org/10.1088/1748-9326/8/1/014029>.
- (370)Duan, N. Models for Human Exposure to Air Pollution. *Environ. Int.* **1982**, 8 (1), 305–309. [https://doi.org/10.1016/0160-4120\(82\)90041-1](https://doi.org/10.1016/0160-4120(82)90041-1).

- (371)Ott, W. R. Concepts of Human Exposure to Air Pollution. *Environ. Int.* **1982**, 7 (3), 179–196. [https://doi.org/10.1016/0160-4120\(82\)90104-0](https://doi.org/10.1016/0160-4120(82)90104-0).
- (372)Pleil, J. D.; Wallace, M. A. G.; Davis, M. D.; Matty, C. M. The Physics of Human Breathing: Flow, Timing, Volume, and Pressure Parameters for Normal, on-Demand, and Ventilator Respiration. *J. Breath Res.* **2021**, 15 (4), 10.1088/1752-7163/ac2589. <https://doi.org/10.1088/1752-7163/ac2589>.
- (373)Dincer, D.; Tietz, C.; Dalci, K. An Investigation into Sleep Environment as a Multi-Functional Space. *Buildings* **2023**, 13 (2), 406. <https://doi.org/10.3390/buildings13020406>.
- (374)Schwartz, J.; Laden, F.; Zanobetti, A. The Concentration-Response Relation between PM(2.5) and Daily Deaths. *Environ. Health Perspect.* **2002**, 110 (10), 1025–1029.
- (375)Mata, T. M.; Felgueiras, F.; Martins, A. A.; Monteiro, H.; Ferraz, M. P.; Oliveira, G. M.; Gabriel, M. F.; Silva, G. V. Indoor Air Quality in Elderly Centers: Pollutants Emission and Health Effects. *Environments* **2022**, 9 (7), 86. <https://doi.org/10.3390/environments9070086>.
- (376)Pickett, A. R.; Bell, M. L. Assessment of Indoor Air Pollution in Homes with Infants. *Int. J. Environ. Res. Public Health* **2011**, 8 (12), 4502–4520. <https://doi.org/10.3390/ijerph8124502>.
- (377)Genjo, K. Assessment of Indoor Climate for Infants in Nursery School Classrooms in Mild Climatic Areas in Japan. *Buildings* **2022**, 12 (7), 1054. <https://doi.org/10.3390/buildings12071054>.
- (378)Gabriel, M. F.; Felgueiras, F.; Batista, R.; Ribeiro, C.; Ramos, E.; Mourão, Z.; de Oliveira Fernandes, E. Indoor Environmental Quality in Households of Families with Infant Twins under 1 Year of Age Living in Porto. *Environ. Res.* **2021**, 198, 110477. <https://doi.org/10.1016/j.envres.2020.110477>.
- (379)Felicioni, L.; Jiránek, M.; Vlasatá, B.; Lupíšek, A. An Environmental Evaluation of Ventilation Systems Aimed at Reducing Indoor Radon Concentration. *Buildings* **2023**, 13 (11), 2706. <https://doi.org/10.3390/buildings13112706>.
- (380)Fu, Y.; Liu, S.; Guo, W.; He, Q.; Chen, W.; Ruan, G.; Qian, H.; Wang, Y.; Liu, L. Inhalation Exposure Assessment Techniques on Ventilation Dilution of Infectious Respiratory Particles in a Retrofitted Hospital Lung Function Room. *Build. Environ.* **2023**, 242, 110544. <https://doi.org/10.1016/j.buildenv.2023.110544>.

- (381)Asikainen, A.; Carrer, P.; Kephelopoulos, S.; Fernandes, E. de O.; Wargocki, P.; Hänninen, O. Reducing Burden of Disease from Residential Indoor Air Exposures in Europe (HEALTHVENT Project). *Environ. Health* **2016**, *15* (1), S35. <https://doi.org/10.1186/s12940-016-0101-8>.
- (382)Koivisto, A. J.; Kling, K. I.; Hänninen, O.; Jayjock, M.; Löndahl, J.; Wierzbicka, A.; Fonseca, A. S.; Uhrbrand, K.; Boor, B. E.; Jiménez, A. S.; Hämeri, K.; Maso, M. D.; Arnold, S. F.; Jensen, K. A.; Viana, M.; Morawska, L.; Hussein, T. Source Specific Exposure and Risk Assessment for Indoor Aerosols. *Sci. Total Environ.* **2019**, *668*, 13–24. <https://doi.org/10.1016/j.scitotenv.2019.02.398>.
- (383)US EPA, O. *Exposure Assessment Tools by Routes - Inhalation*. <https://www.epa.gov/expobox/exposure-assessment-tools-routes-inhalation> (accessed 2024-01-31).
- (384)Scott, B. R. Epidemiologic Studies Cannot Reveal the True Shape of the Dose–Response Relationship for Radon-Induced Lung Cancer. *Dose-Response* **2019**, *17* (1), 1559325819828617. <https://doi.org/10.1177/1559325819828617>.
- (385)Hsu, N.-Y.; Wang, J.-Y.; Su, H.-J. A Dose-Dependent Relationship between the Severity of Visible Mold Growth and IgE Levels of Pre-School-Aged Resident Children in Taiwan. *Indoor Air* **2010**, *20* (5), 392–398. <https://doi.org/10.1111/j.1600-0668.2010.00663.x>.
- (386)Rani, S.; Kansal, S.; Singla, A. K.; Mehra, R. Radiological Risk Assessment to the Public Due to the Presence of Radon in Water of Barnala District, Punjab, India. *Environ. Geochem. Health* **2021**, *43* (12), 5011–5024. <https://doi.org/10.1007/s10653-021-01012-y>.
- (387)Wang, H.; Wang, W.; He, R.; Hong, C.; Wang, J.; Li, X.; Liu, Y. Experimental Study on Unsteady Radon Exhalation from the Overburden Layer of the Uranium Mill Tailings Pond under Rainfall. *Sci. Technol. Nucl. Install.* **2022**, *2022*, e9366056. <https://doi.org/10.1155/2022/9366056>.